Genetics of Functional AcrAB-TolC Tripartite Complex Assembly

by

Jon William Weeks

A Dissertation Presented in Partial Fulfillment
of the Requirements for the Degree
Doctor of Philosophy

Approved April 2012 by the
Graduate Committee:

Rajeev Misra, Chair
Valerie Stout
Yixin Shi
Josephine Clark-Curtiss

ARIZONA STATE UNIVERSITY

August 2012

ABSTRACT

Intrinsic antibiotic resistance is of growing concern in modern medical treatment. The primary action of multidrug resistant strains is through over-expression of active transporters which recognize a broad range of antibiotics. In *Escherichia coli,* the TolC-AcrAB complex has become a model system to understand antibiotic efflux. While the structures of these three proteins (and many of their homologs) are known, the exact mechanisms of interaction are still poorly understood. By mutational analysis of the TolC turn 1 residues, a drug hypersensitive mutant has been identified which is defective in functional interactions with AcrA and AcrB. Antibiotic resistant revertants carry alterations in both TolC and AcrA act by stabilizing functional complex assembly and opening of the TolC aperture, as monitored by stability of a labile TolC mutant and sensitivity to vancomycin, respectively. Alterations in the AcrB periplasmic hairpin loops lead to a similar antibiotic hypersensitivity phenotype and destabilized complex assembly. Likewise, alterations in TolC which constitutively open the aperture suppress this antibiotic sensitivity. Suppressor alterations in AcrA and AcrB partially restore antibiotic resistance by mediating stability of the complex. The AcrA suppressor alterations isolated in these studies map to the three crystallized domains and it is concluded they alter the AcrA conformation such that it is permanently fixed in an active state, which wild type only transiently goes through when activated by AcrB. Through this genetic evidence, a direct interaction between TolC and AcrB which is stabilized by AcrA has been

i

proposed. In addition to stabilizing the interactions between TolC and AcrB, AcrA is also responsible for triggering opening of the TolC aperture by mediating energy flow from AcrB to TolC. By permanently altering the conformation of AcrA, suppressor mutants allow defective TolC or AcrB mutants to regain functional interactions lost by the initial mutations. The data provide the genetic proof for direct interaction between AcrB and that AcrA mediated opening of TolC requires AcrB as a scaffold.

I dedicate this to my family and friends, without whom I would not have been able to succeed. Thank you for your support and guidance through the years. Also to my mentor, Dr. Rajeev Misra, who has taken me from the beginnings of research and seen me through to the end of this work. I could never have completed this work without his help, guidance, patience, and friendship. Finally, to my lab colleagues and committee members, who have given me guidance and helped me through times of frustration and have been there to celebrate the milestones. I will always cherish the times we have spent together.

TABLE OF CONTENTS

LIST OF TABLES

LIST OF FIGURES

x

xi

Introduction

Gram-Negative Bacteria

Gram-negative bacteria contain two lipid membranes, separated by the periplasmic space. The outer membrane has two layers; the inner layer contains phospholipids while the outer layer contains primarily lipopolysaccharides (LPS). This LPS layer helps to act as an initial permeability barrier. It does this by its amphipathic nature, the polysaccharide portion is negatively charged to create a barrier to help prevent the entry of hydrophilic antibiotics from entering the cell, whereas the lipid portion (Lipid A) of LPS molecule is highly hydrophobic, which helps to prevent hydrophobic antibiotics from crossing the outer membrane (Raetz, 1990; Raetz and Whitfield, 2002). The inner membrane is a phospholipid bilayer, which acts as a final permeability barrier to prevent toxic molecules from entering into the cytoplasm and allowing desired molecules to be selectively transported into the cell.

Outer Membrane

As stated above, the outer membrane is a bilayer comprised of primarily two different types of lipid molecules. The outer leaflet of the outer membrane is primarily composed of LPS molecules (Takeuchi and Nikaido, 1984). The lipid portion, lipid A, contains between 4 and 6 lipid molecules, depending on bacterial species and strain. The inner leaflet is composed of phospholipids, primarily phosphatidylethanolamine and secondarily, phosphatidylglycerol and

diphosphatidylglycerol (Lugtenberg and Peters, 1976; Harwood and Russell, 1984). Many studies have been performed to look at protein interactions with various phospholipids. In particular, the β-barrel outer membrane proteins OmpF and OmpT show preferential interaction with phosphatidylethanolamine, the more abundant phospholipid head group (O'Keefe et al., 2000; Brandenburg et al., 2004). In contrast, the outer membrane protein OmpA shows little distinction between phosphatidylethanolamine and phosphatidylglycerol (Kleinschmidt, 2003; Ramakrishnan et al., 2004). All three OMPs show increased interaction with hydrocarbon chains in the range of 14 to 18 carbons, which is typical of the composition of bacterial membranes (Kleinschmidt, 2003, O'Keefe et al., 2000, Brandenburg et al., 2004). Taken together, the interactions between both the polar head groups and the hydrophobic acyl chains act to form a seam between outer membrane proteins and lipid molecules. It has also been found that some lipoproteins bind to phospholipid head groups. For example, the non-essential BamE lipoprotein binds to phosphatidylglycerol (Knowles et al., 2011). However, unlike the aforementioned interactions, these interactions are thought to primarily anchor lipoproteins to specific regions of the outer membrane.

The majority of proteins embedded in the outer membrane are β-barrel proteins. These β-barrel proteins typically have an even number of anti-parallel sheets which circle around to form pore proteins. The β-barrels have a hydrophilic core and a hydrophobic exterior. The length of the hydrophobic exterior of β-barrel is such that it limits the hydrophobic mismatch between them and the

hydrocarbon chain of the lipids (O'Keefe *et al.*, 2000). Additionally, the exterior surface contains a ring of charged or polar residues at the outer limits of the hydrophobic core in order to properly align with the phospholipid head groups. In several cases, the exterior loops act to gate the pore from allowing molecules to freely diffuse into the periplasm. Therefore the β-barrel proteins act in many ways as the initial barrier for hydrophobic molecules to enter into the cell.

It is the gated outer membrane proteins and the amphipathic nature of the LPS/phospholipid bilayer that prevents noxious chemicals from freely entering the cell. Commonly, mutations affecting the outer membrane, either through the LPS or OMPs, typically cause hypersensitivity to a wide array of antibiotics and detergents. Additionally, mutations which alter the charge of the outer membrane surface or decrease the permeability of the outer membrane can increase resistance to certain antimicrobial agents.

Inner Membrane

Unlike the outer membrane, the inner membrane is composed of a phospholipid bilayer. However, this bilayer is enriched with phosphatidylethanolamine. The inner membrane is often characterized by its abundance of cytochromes, which are atypical of the outer membrane. The integral proteins of the inner membrane are typically α-helical bundles, which typically lie at a tilt to the membrane instead of being perpendicular. This allows the helices to shift their orientation as the membrane thickness changes. This

movement prevents drastic changes in the hydrophobic mismatch (O'Keefe *et al.*, 2000; Deol *et al.*, 2004; Sansom *et al.*, 2005). While these changes allow for stabilization of the hydrophobic mismatch, in some cases, it also allows the protein to function properly. Many of these α-helical bundle proteins function as transporters which must be energized for functionality. In the case of secondary transporters, which are energized by a proton gradient, the proper alignment of charged and polar residues within the membrane must be properly aligned. While minor changes in the tilt of the α-helices can cause little change, these small changes can drastically influence the functioning of the protein.

Besides allowing nutrients to enter into the cell, the transporters of the inner membrane also allow for the removal of toxic molecules from the cytoplasm or inner membrane. This important function is performed by various classes of efflux systems, the majority of which are secondary transporters.

Periplasmic Space

The periplasmic space is an aqueous environment which separates the inner and outer membranes. This region is home to the peptidoglycan, which gives rigidity to the cell. As this cell wall is unique to bacteria, many antibiotics target the peptidoglycan and cause cell death. There are many types of proteins within the periplasmic space, varying in nature from chaperones to assist in OMP assembly to enzymes which assist in cell wall synthesis and maintaining nutrients within the cell. Chaperones, such as SurA, act to sequester the greasy OMPs on

their way to the Bam (β-barrel assembly machinery) complex and prevent aggregation of these proteins. In cells lacking SurA, there is an abundance of mis-folded OMPs which cause toxicity in the cell. The periplasmic protease DegP acts to degrade mis-folded OMPs and potentially as a chaperone at low temperatures. While mis-folded OMPs are a major substrate for DegP, DegP is also responsible for the degradation of other periplasmic proteins, such as AcrA. Gerken and Misra showed that the stability of the mutant $AcrA_{L222Q}$ is dependent on the presence of DegP; without DegP, $AcrA_{L222Q}$ is stable (2004).

In addition to the aforementioned chaperones and proteases, the periplasm is home to enzymes such as maltose binding protein (MBP). MBP helps in the transport of maltodextrins from LamB (the OMP which allows uptake of maltodextrins into the cell) to inner membrane transporter proteins MalG and MalF (Duplay *et al*., 1984). The periplasm is also home to other enzymes such as β-lactamase. β-lactamase is encoded by the *ampC* and is responsible for intrinsic resistance of *E. coli* to many β-lactam antibiotics. Clinical and zoological isolates of extended spectrum β-lactam resistant enteric bacteria have become an epidemic plaguing current medical treatments.

Antibiotics and Their Resistance

Antibiotics are compounds which are either naturally produced by one microorganism to kill or inhibit the growth of other microorganisms, or synthesized with the active portion of a naturally occurring chemical. Bacteria and

other microorganisms have evolved many ways of combating these antibiotics either by inactivating the antibiotic, preventing their entry into the cell, or actively transporting them out of the cell. As the focus of this study will be on active transport of the antibiotics from the cell, the other mechanisms of resistance will only be briefly discussed.

In order to inactivate the antibiotic, specific enzymes must be present in the bacteria which physically alter the antibiotic so as to disrupt its natural function. An example of this would be β-lactamase, which acts to destroy the lactam ring in the β-lactam antibiotics. This then prevents this class of antibiotics from inhibiting cell wall synthesis. To prevent entry of the antibiotic into the cell, LPS can be modified to change its overall net charge. These modifications are set in motion by the activation of the PmrAB two-component system (Herrera *et al*., 2010). While inactivation of antibiotics and modification of the cell wall are two important means of obtaining antibiotic resistance, active transport of antibiotics from the cell is of major importance. Many clinical isolates of antibiotic resistant strains increase the expression of efflux pumps (Bratu *et al*., 2009; Fralick 1996; Dastidar *et al*., 2007; Fabrega *et al*., 2010; Pages and Amaral, 2009; Srikumar *et al*., 1998; Swick *et al*., 2011; Zgurskaya *et al*., 2009). In gram-negative bacteria, efflux pumps are comprised of an outer membrane factor (OMF), membrane fusion protein (MFP), and a pump protein. The major antibiotic efflux pump system in *E. coli* is the TolC-AcrAB system.

TolC

Unlike most other OMPs, TolC is an outer membrane protein with the three monomers each contribute one third of the trimeric, 12 stranded, β-barrel protein. In addition to the 12-stranded β-barrel, the protein also contains a 100Å α-helical barrel that protrudes into the periplasmic space (Fig 1). The α-helical barrel constricts at the equatorial domain, below which sits the aperture. In the α-helical barrel, each monomer contributes four full and four pseudo helices (Koronakis, 2003; Koronakis *et al.*, 2000; Koronakis *et al.*, 2004). These full and pseudo helices act in a pairwise fashion, such that a full length helix is connected to a pseudo helix via the two β-sheets on one end and a periplasmic turn at the other. For example, H2 and H4 contribute to one pseudo helix while H3 is paired with it. H3 and H4 are connected by turn 1 and remain static during aperture opening. The other two "helices" consist of H6, H7, and H8, of which H7 and H8 are connected by turn 2 and swing outward during aperture opening. In its closed state, the channel is constricted to a diameter of 3Å (Federici *et al.*, 2004) from an internal diameter of about 35Å (Andersen *et al.*, 2003). This allows TolC to selectively allow the passage of antibiotics through the channel.

The aperture is kept closed by a network of salt and hydrogen bonds consisting of residues Q136, T152, D153, E359, Y362, and R367, with R367 playing the primary role in maintaining a locked aperture (Bavro *et al.*, 2008; Koronakis *et al.*, 2000; Andersen *et al.*, 2002). Alterations of R367 cause a severe antibiotic hypersensitivity phenotype, which is presumably due to antibiotic influx

7
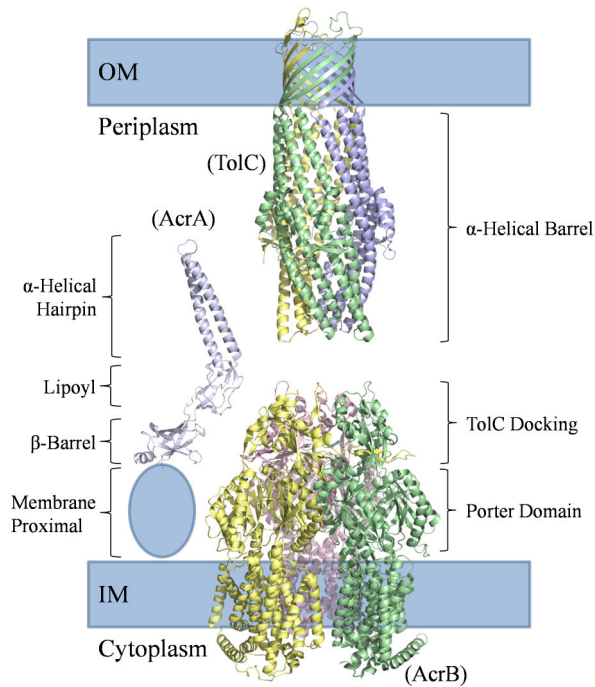
Figure 1. A cartoon schematic of the *E. coli* envelope showing the AcrAB-TolC complex. X-ray crystal structures of TolC (1EK9), AcrA (2F1M), and AcrB (2GIF) are shown. The membrane proximal domain of AcrA has not been crystallized and is shown as an oval protruding from the β-barrel. The periplasmic domains of each of the proteins are indicated next to the protein.

(Andersen *et al*., 2002; Augustus *et al*., 2004). Recently, crystal structures have been solved for two different mutants of R367, each showing the aperture is in a dilated conformation (Bavro *et al*., 2008, Pei *et al*., 2010). These crystal structures of TolC show significant rearrangement of the inner helices (H7/H8), while the outer helices (H3/H4) remain fairly static.

AcrB

AcrB is also a trimeric protein. It utilizes the proton gradient of the inner membrane to derive energy and acts as a proton/drug antiporter. Each monomer contributes 12 transmembrane helices and two large periplasmic loops (Fischer *et al*., 2011; Seeger *et al*., 2006; Takatsuka and Nikaido, 2006; Takatsuka *et al*., 2010; Fig 1). The transmembrane helices contain a proton relay system, which has been clearly defined. Alterations to three specific charged residues, D407, D408, R971, completely abolish proton translocation, thereby stopping antibiotic efflux (Takatsuka and Nikaido, 2006). The large periplasmic loops contain the drug binding pocket and tunnels used for drug capture and release (Bohnert *et al*., 2010; Seeger *et al*., 2006; Husain and Nikaido, 2010). When properly folded, this domain spans 70Å into the periplasm to potentially meet TolC at its lowest point there. This large periplasmic structure is divided into two domains, the TolC docking (D) and periplasmic porter (P), which are further subdivided based on the N-terminal (PN1, PN2, DN) and C-terminal (PC1, PC2, DC) region (Seeger *et al*., 2006; Murakami *et al*., 2006; Yu *et al*., 2003). The exterior surface of AcrB is

used to dock AcrA along a specified grove running along DN, DC, PN2, and PC1 (Symmons, 2009). This cross-linking analysis led to the conclusion that AcrA, AcrB, and TolC interact in a 1:1:1 manner. Interestingly, as AcrB goes through its conformational changes, PC2 is shown to go through signification movement at the surface, whereas the area where AcrA is proposed to lie remains relatively static (Symmons *et al.*, 2009). This indicates that AcrA may not gain conformational energy from AcrB for complex assembly and TolC aperture opening (see below). Recent co-crystals of CusBA, the homologous copper/silver efflux pump in *E. coli*, show CusB, the AcrA homologue, interacts with CusA and CusC, the AcrB and TolC homologues, respectively, in a 2:1:1 manner. If this is the case for AcrAB/TolC, it could be possible for AcrA to derive conformational energy from AcrB to transmit to TolC for aperture opening (Su *et al.*, 2011). Additionally, by the use of Surface Plasmon Resonance (SPR) Tikhonova *et al.* (2009) showed two independent binding affinities for AcrA and TolC, as well as other membrane fusions proteins. This was further validated when they showed similar results between AcrA and AcrB (Tikhonova *et al.*, 2011).

While the exterior of the periplasmic domain acts as a scaffold for AcrA, its interior contains the tunnels and pocket used for drug capture and release (Seeger *et al.*, 2006; Murakami *et al.*, 2006). The drug transport pathway begins with two entrance tunnels, which are positioned facing the periplasmic space and the surface of the outer leaflet of the inner membrane and are used by AcrB to sequester antibiotics (Loose). During its functional rotation, these tunnels will

10

close and a drug binding pocket will open (Tight). This pocket is highly

hydrophobic, containing 6 phenylalanine residues. The final stage of functional

rotation causes the drug binding pocket to be collapsed and a third tunnel to open

toward the TolC docking domain (Seeger *et al*. 2006; Murakami *et al*., 2006).

Once the antibiotic has reached this location, it is then transferred to TolC to be

expelled directly into the extracellular milieu, thus bypassing the periplasmic

space.

AcrA

Unlike TolC and AcrB, the crystal structures of AcrA and its homologue

in *Pseudomonas aeruginosa*, MexA, do not show trimeric assemblies. AcrA

contains four structurally distinct domains; a membrane proximal (MP), β-barrel,

lipoyl, and α-helical (Mikolosko *et al*., 2006; Symmons *et al*., 2009; Vacaro *et al*.,

2006; Fig 1). The membrane proximal domain is the most unstructured domain,

showing multiple confirmations. This region also contains the only native

cysteine residue in AcrA, which becomes lipidated to anchor AcrA to the outer

leaflet of the inner membrane. The β-barrel domain has been proposed to lie at the

interface between the TolC docking and porter domains. It contains six anti-

parallel β-sheets and a single α-helix. The lipoyl domain can be divided into the

N- and C-termini, each of which consists of four β-sheets. The two halves are

separated by the coiled α-helices (Mikolosko *et al*., 2006). This domain sits at the

crown of AcrB in a cleft between the DN and DC domains (Symmons *et al*.,

2009). These three domains have been shown to interact directly with AcrB. Finally, cysteine mediated chemical cross-linking experiments showed that the α-helical domain interacts with TolC in a coiled-coil manner, whereby the coils of AcrA align themselves with TolC (Lobedanz *et al*., 2007). It has been proposed that the coiled-coil alignment of the α-helices of AcrA and TolC are such that the first AcrA α-helix lies in a groove between the TolC α-helices H3, H8, and H7, known as the intraprotemer groove.

When AcrA was crystallized, there appeared to be four different conformations of the protein. These four different isoforms suggest that AcrA is a relatively flexible protein to allow for proper interaction with both AcrB and TolC. If the lipoyl domain is fixed in space, the α-helical domain shows a 15° rotation (Mikolosko *et al*., 2006). Like AcrA, the MexA α-helical domain shows a 35° rotation (Symmons *et al*., 2009; Vaccaro *et al*., 2006). In addition to this 35° rotation for the α-helical domain, the MP and β-barrel domains show a 25° rotation from the lipoyl domain. From the β-barrel domain, the MP domain shows a further 25° rotation. These combined rotations would allow AcrA to transmit conformational energy from AcrB to TolC and also allow AcrA to be completely aligned with both proteins. Initial studies attributed the conformational flexibility of AcrA to AcrA unfolding and elongating to connect to the outer membrane. By the use of electron paramagnetic resonance and site-directed spin labeling, specific residues within the MP domain show a high degree of conformational flexibility independent of pH (Ip *et al*., 2003). Additionally, spin labels added to

the α-helical domain showed a high degree of conformational flexibility at pH 7. However, when the pH was dropped to pH 5, these same residues showed a broadening of the peak. This shows that the helices of AcrA have conformational flexibility, which can become fixed into a specific conformation.

Mechanisms of Tripartite Complex Assembly

Originally, it had been proposed that AcrA interacted with AcrB and TolC in a 1:1:1 ratio, whereby one monomer of AcrA interacted with one monomer of AcrB and TolC (Fernandez-Recio *et al.*, 2004; Misra and Bavro, 2009; Symmons *et al.*, 2009). This interaction had been proposed by chemical cross-linking analysis using cysteine engineered AcrB/AcrA and TolC/AcrA complexes (Lobedanz *et al.*, 2007; Symmons *et al.*, 2009). Through structural analysis, Symmons *et al.* proposed the first model of the trimeric assembly of the complex. Through these studies, it had been proposed that AcrB and TolC directly interacted with one another. This was further supported by direct disulfide bond formation of AcrB and TolC proteins modified with single cysteine substitutions in their hairpin loop and periplasmic turn regions, respectively (Tamura *et al.*, 2005).

In addition to chemical cross-linking experiments which have been done to determine specifically where AcrA and its homologues aligned with AcrB or TolC and their respective homologues, analysis of chimeric complexes has been used to map the potential sites of interaction between members of the complex

(Bai *et al*., 2010; Elkins and Nikaido, 2003; Krishnamoorthy *et al*., 2008; Vediyappan *et al*., 2006; Welch *et al*., 2010). Chimeric complexes typically are not functional; however, gain-of-function point mutations can be (and have been) isolated that make these complexes functional. These mutations have been helpful in determining where the proteins potentially align. When the *P. aeruginosa* TolC homologue, OprM, containing a mutation of its C-terminus was combined with the *Vibrio cholerae* AcrAB homologues, VceAB, the chimeric complex showed a drug hypersensitivity phenotype. Gain-of-function mutations mapped to the VceA α-helical tip region, indicating the α-helical region was important for interaction between the membrane fusion protein (MFP, AcrA) and outer membrane factor (OMF, TolC) (Bai *et al*., 2010). Additional chimeric studies of VceC, the *V. cholerae* TolC homologue, and *E. coli* AcrAB led to drug hypersensitivity, which was suppressed by mutations in VceC within the intraprotomer groove (Vediyappan *et al*., 2006). A similar analysis was performed using the chimeric complex of TolC and MexAB. Gain-of-function mutations found within TolC mapped to the same groove as those isolated within VceC (Bokma *et al*., 2006). Taken together, these gain-of-function mutations help to identify the interacting surfaces of the MFP and OMF.

In an attempt to identify exactly where OMF and MFP interact, reconstituted proteoliposomes of MexA and OprM were mixed and used for cryo-electro tomography. By analyzing the images and constructing tomograms of the MexA-OprM complexes, it was determined that the α-helices of MexA lie along

14

the face of the α-helical barrel near the tip of the aperture (Trépout *et al*., 2010).

While this alignment is slightly offset from the data observed by Symmons *et al*.

(2009), the authors proposed that the MFP and OMF may initially interact via the

lower regions of the aperture and upper regions of the α-helices and then slide

into one another, allowing the proton-antiporter (PAP) and OMF to interact. This

alignment was also constructed using parameters similar to those used by

Symmons *et al*., such that MexA is in an extended form like AcrA. Additionally,

this alignment used data previously published on suppressor mutations mapping

within OprM of a MexA α-helical inactivating mutation.

Mapping of gain-of-function mutations between OMF and MFP chimeras

and intergenic suppressors of interaction defective mutants within native

complexes has been useful in potentially identifying interaction domains of OMF

to MFP. However, gain-of-function mutations between MFP and PAP have not

shown similar results. An analysis of AcrA and MexB gave mutations in AcrA

that are not directly in contact with the PAP, as well as mutations within MexB

that are in varied locations, including a mutation within the transmembrane

helices (Krishnamoorthy *et al*., 2008). The gain-of-function mutations isolated in

this study may be stabilizing complex assembly of the trimeric complex and not

directly between the bipartite complex of MFP and PAP.

These findings from chemical cross-linking, engineered disulfide bond

formation, and gain-of-function suppressor analyses lead to the conclusion that

OMF and PAP directly interact with one another and that the MFP helps to

facilitate this interaction and stabilize it. In this mechanism of interaction, the initial stages of interaction begin between loop 1 of AcrB and turn 1 of TolC (Weeks *et al*., 2010). This initial interaction then facilitates the interaction between loop 2 and turn 2, which in turn destabilizes the salt bridges that keep the TolC aperture locked. At this time AcrB will go through its functional rotation and will stimulate conformational changes in AcrA. These conformational changes will be transmitted from the α-helices to the coiled-coils of TolC. This will cause the full alignment of the AcrA α-helices with the intraprotomer groove, causing full dilation of the aperture. At this point, the drug will have moved from the entrance tunnels, through the drug binding pocket, and finally to the exit tunnels, where it will enter TolC and be extruded to the extracellular space (Fig 36).

In opposition to this proposed mechanism of interaction, data exist that the MFP interacts in a 2:1:1 fashion with the PAP and OMF. The recent co-crystal of the *E. coli* CusBA copper/silver efflux system, homologous to AcrAB, respectively, showed that CusB had 2 monomers per monomer of CusA (Su *et al*., 2011). If this is the case, the MFP would be properly positioned to receive and transmit conformational energy to the OMF and facilitate aperture opening. In addition to these data, the MFP from the macrolide-specific efflux system, MacAB, has been shown to interact as a hexamer (Yum *et al*., 2009, Xu, *et al*., 2010). This hexameric conformation of the MFP causes a loss of interaction between the PAP and the OMF. In this model, the α-helices interact side by side

and form a stem-like structure extruding from the funnel-like conformation of the lipoyl and β-barrel domains. The tip of this stem-like structure has an internal diameter of ~30Å, which is roughly equivalent to the internal diameter of the open aperture of TolC, as well as the internal diameter of the upper half of the TolC α-helical barrel (Yum *et al.*, 2009). In addition to the identification of MacA acting as a trimer of dimers, a covalently linked AcrA dimer was found to functionally replace the native AcrA, indicating AcrA functionally acts as a dimer (Xu *et al.*, 2011). Additionally, when analyzing column elutes from size-exclusion chromatography, the covalently linked AcrA dimer showed a peak at the same position as the *Actinobacillus actinomycetemcomitans* MacA, which has been shown to spontaneously form hexamers and that the hexameric state is functionally relevant.

While analyzing the polymeric state of AcrA and MacA, Xu *et al.* (2010) and Kim *et al.* (2010) have identified three key residues at the extreme tip region of AcrA and MacA. When looking at the hexameric assembly of MacA, these residues form a pocket where it has been proposed that the open TolC aperture turns fit. Xu *et al.* (2011) later cloned the DNA encoding the extreme tip regions of AcrA's α-helices and TolC's turn regions into *E. coli macA* and *A. actinomycetemcomitans macA*, respectively (Kim *et al.*, 2008). These two hybrid proteins were able to interact via size exclusion chromatography and analyzing negatively stained protein samples through electron microscopy. By analyzing these protein samples, a density map was constructed and modeled proteins were

inserted. This showed the TolC aperture turns situated, as proposed at the extreme α-helical tip region of AcrA. This led the authors to the conclusion that the MFP forms a hexameric structure, which sits on the periplasmic crown of the PAP. The opening of the OMF is facilitated entirely by the extreme α-helical tip regions of the MFP. Additionally, this model of interaction places no interaction between PAP and OMF due to the 40 - 50Å length of the α-helical barrel formed by the MFP α-helices.

Through mutational analysis of TolC turn 1, the AcrB hairpin loops 1 and 2, and reversion analysis, there is proposed to be a direct interaction between AcrB and TolC. In these studies, the importance of TolC turn 1 residues in functional complex assembly have been identified. Additionally, a TolC mutant that was completely defective in export functions, but maintained import function was isolated. Furthermore, residues of AcrB's hairpin loop 1 which are important in maintaining antibiotic resistance were identified. By utilizing antibiotic hypersensitive mutants of TolC and AcrB, alterations in all three proteins which primarily restore interaction through stabilizing functional complex assembly and secondarily open the TolC aperture have been isolated. These intra- and intergenetic suppressor alterations, as well as the original defective proteins, give cues to the defects and evidence to the direct interaction between AcrB and TolC.

Mutational and Suppression Analysis

In order to determine the function of a gene or important domains of a protein, mutations are commonly introduced which alter the functionality of the protein. These mutations can cause the protein to simply not be expressed or change protein through physical alteration. Once a protein has been rendered non-functional, the effects within the cell can be monitored to determine the functional role of the protein or a domain within the protein. In order to determine the function of specific residues, three common techniques are put to use: deletions, frameshift, and alanine scanning. These cause mutations within the coding region of the gene to determine the importance of specific amino acids within the structure of a protein. After a protein has been rendered non-functional, reversion analysis is commonly used to determine other domains within the protein which are important and to determine other proteins which may be important in functionality of the original protein. The term intragenic suppressor refers to a secondary mutation within the coding region of the gene of a protein being studied, while maintaining the original mutation within the gene. Intragenic suppressors often will shed light upon the original defect and how the mutation is acting to restore the functionality of the original mutant. On the other hand, intergenic suppressors are mutations within other genes which overcome the defect caused by the mutation of the first. These types of mutations give clues to the network of interactions involved in maintaining a specific phenotype. In addition to identifying genes which interact to restore a phenotype, intergenic

19

suppressors can identify the specific regions of interaction between the two

proteins.

Results 1: Importance of TolC's periplasmic turn 1

Identification of Turn 1 Residues Involved in Functional Complex Assembly

After the structure of AcrB was determined, it was proposed that the hairpin loops of AcrB could directly interact with the α-helix-turn-α-helix structures of TolC (Murakami *et al.,* 2006). Initial evidence for this came when Tamura *et al*. showed that when the hairpin residues of AcrB and the turn residues of TolC were both mutated to cysteines, TolC and AcrB could form spontaneous disulfide bonds (2005). This direct interaction between AcrB and TolC was further supported when Tikhonova *et al*. showed, using Surface Plasmon Resonance, that TolC and AcrB directly bind to one another with as strong of a binding affinity as either AcrA/AcrB or AcrA/TolC (2011). Additionally, these data were confirmed by the first model of interaction proposed through molecular docking using cysteine mediated cross-linking data (Symmons *et al*., 2009). This docked model showed the TolC turns embedded within groves created by the hairpin turns of AcrB.

If the turns of TolC do interact directly with AcrB, it is possible that alteration of either of the two TolC turn residues may disrupt interactions with AcrB and prevent functional complex assembly. However, the second turn residues are shown to lock the aperture in a closed state. Alterations of these residues, primarily R367 and Y362, leads to a leaky phenotype whereby antibiotics are able to pass back through TolC into the periplasmic space (Augustus *et al*., 2004; Bavro *et al*., 2008). Therefore it was decided to investigate

the importance of the turn 1 residues for their function in interacting with AcrB. The turn 1 is situated between the more static helices, H3 and H4, of TolC and consists of the residues $_{147}$GLVA$_{150}$.

To investigate the importance of these turn 1 residues, mutations were introduced into the pTrc9a plasmid containing the *tolC* gene expressed from the IPTG inducible promoter. Without induction using IPTG, wild type TolC is expressed to nearly the same level from the chromosomal copy and complements the chromosomal deletion. The plasmids expressing the turn 1 mutant TolC proteins were transformed into a chromosomal Δ*tolC*::Cm^r strain and examined for their ability to complement the chromosomal deletion. In order to test the importance of these residues two approaches were taken: alanine scanning and localized frameshift mutagenesis (Fig 2A). Three alanine mutants were created, $_{147}$ALVA$_{150}$, $_{147}$GAAA$_{150}$, and $_{147}$AAAA$_{150}$, of which only the $_{147}$AAAA$_{150}$ derivative had a modest antibiotic hypersensitivity phenotype (Fig 2B). Interestingly, both the $_{147}$ALVA$_{150}$ and the $_{147}$AAAA$_{150}$ mutants had similar protein levels, roughly 50% of wild type, indicating that reduced protein levels was not the sole reason for $_{147}$AAAA$_{150}$'s reduced antibiotic resistance. That TolC$_{147GAAA150}$ level is not significantly reduced, indicating that G147 is most likely important in proper folding of TolC. Since L148 and V149 both have hydrophobic side chains, they are not expected to be surface exposed and form contacts with AcrB. Most likely, these hydrophobic residues are important in hydrophobic packing and are turned away from the solvent exposed surface, as

22

A

B

	(Null)	GLVA (WT)	ALVA	GAAA	AAAA
TolC levels:	0.0	1.0	0.43	0.67	0.46
Nov (mm):	19.7	8.8	8.6	9.0	11.4

C

	(Null)	AGSG	GGSG	GLSG	DLVA	GSVA	GLSA
TolC levels:	1.0	0.0	0.50	0.62	0.84	0.58	0.95	0.86
Nov (mm):	8.7	21.9	21.9	12.0	8.7	8.7	9.2	8.7
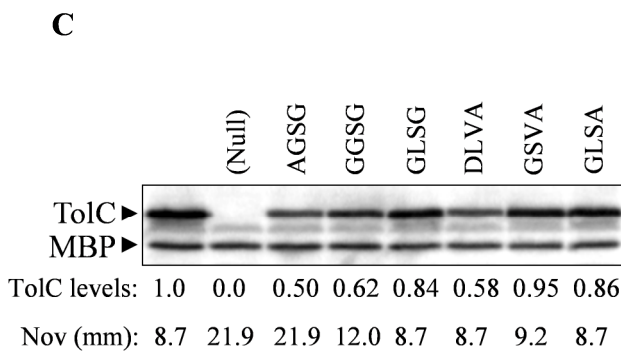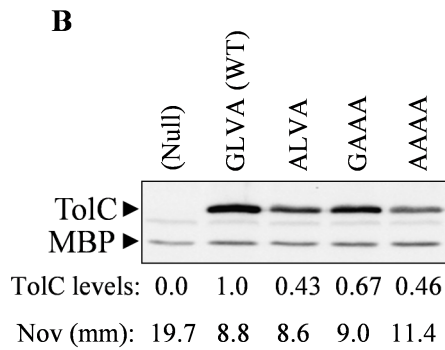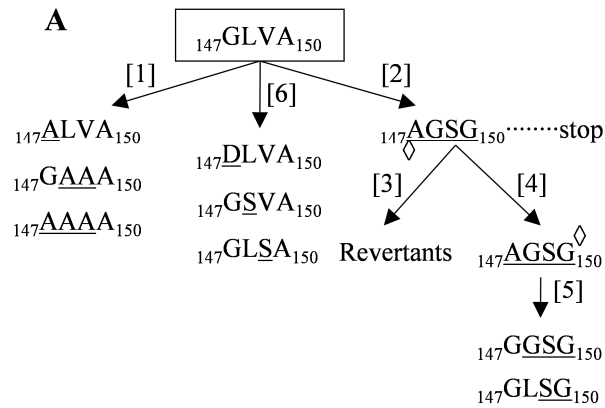
Figure 2. Mutagenesis of TolC turn 1 residues and characterization of various TolC turn 1 mutants.

A. The wild type TolC turn 1 residues $_{147}GLVA_{150}$ were substituted with alanine [1] or subjected to -2 frameshift [2] mutagenesis. The TolC frame was subsequently restored either through reversion analysis [3] or by +2 frameshift site-directed mutagenesis [4]. Open diamonds point to the sites of frameshift mutations. The two residues of the resulting frameshift mutant [4] were further altered by site directed mutagenesis [5]. Individual alterations of the wild type turn 1 residues were made by site-directed mutagenesis [6]. All mutant residues are underlined. Western blots to determine the levels of various TolC turn 1

alanine (B) and framshift-derived (C) mutants (amino acid substitutions in mutants are underlined). Protein extracts from approximately 5 x 10^7 cells grown overnight at 37°C were analysed by SDS-PAGE and electro-transferred to PVDF membranes. Membranes were blotted with primary antibodies against TolC-MBP (maltose binding protein). MBP was used as a gel loading control. Protein levels were quantified using Quantity One software (Bio-Rad). Wild type TolC level was taken as 1 and other values were adjusted relative to wild type TolC. Zones of inhibition around pre-soaked novobiocin disks (30 µg) are shown in millimeters (mm). Average inhibition zones recorded from two independent assays are shown, with zones varying no greater than 10%.

seen in the closed, partially open, and fully opened TolC structures (PDB ID

1EK9, 2WMZ, and 2XMN, respectively; Koronakis *et al.*, 2000; Pei *et al.*, 2011).

Thus substitution of these residues to a less hydrophobic side chain would prevent

the backbone from being exposed for interaction with the hairpin loops of AcrB.

However, this importance could only be revealed when reduced protein levels,

G147A, as well as reduced hydrophobic packing, $_{148}LV_{149} \rightarrow {_{148}}AA_{149}$, were

combined.

The second approach was to induce a frameshift at the beginning of the

turn (Fig 2A). As this frameshift would cause a premature stop codon, TolC

would not be properly synthesized and would cause a drug hypersensitivity

phenotype. This was used to isolate spontaneous revertants that restored the

reading frame and produced a functional TolC protein. Through this analysis the

flexibility of the turn residues and those in the surrounding helices could be

gauged. However, after being exposed to selection with substrate antibiotics, all

revertants restored the original turn sequence. This indicated that all the turn

residues were important for functional efflux function. In addition to looking for

spontaneous antibiotic resistant revertants, the reading frame was restored after

the fourth residue of the turn to create the $_{147}AGSG_{150}$ mutant. This mutant

showed a dramatic drug hypersensitivity phenotype, equivalent to null, again

underscoring the importance of this region in antibiotic efflux (Fig 2C and Table

1).

After creating the $_{14}$AGSG$_{150}$ frameshift mutant, the goal was to identify which residues were most important by individually restoring the residues to restore antibiotic resistance. As had been observed with mutation of G147, restoring individual residues increased in TolC protein levels, which was accompanied by a marked increase in antibiotic resistance. Simultaneous restoration of G147 and L148 lead to complete restoration of protein levels and antibiotic resistance (Fig 2C). These findings indicate that the combination of reduced protein levels (G147) and reduced hydrophobicity (L148) are important in maintaining functional interactions involved in antibiotic efflux (Vakharia *et al*., 2001). Interestingly, when any of the turn residues are individually altered, there is no increase in antibiotic hypersensitivity, indicating that it is the combined action of multiple alterations which causes the increase in antibiotic sensitivity. Additionally, when either L148 or V149 was mutated to serine, the presence of the polar side chain did not cause an increase in sensitivity.

Phenotypic Investigation of the TolC $_{147}$AGSG$_{150}$ Turn 1 Mutation

After observing that the TolC$_{147AGSG150}$ turn 1 mutation was not able to complement the *tolC* deletion with regards to resistance to novobiocin and erythromycin, further investigation of the phenotypes associate with TolC were observed. TolC is used as a receptor for the bacteriophage TLS, as well as a secondary receptor for colicin E1. Without TolC, cells are resistant to both of these toxic agents. The TLS phage uses the external loops of TolC, as well as LPS, to mediate infection of *E. coli* (German *et al*., 2006). Colicins are a group of

26

Table 1. Detailed characterization of the TolC turn 1 $_{147}$AGSG$_{150}$ mutant.

Inhibitors[a]	Sensitivity to Inhibitors		
	TolC$_{WT}$	TolC$^-$	TolC$_Q$[b]
Novobiocin	15.8	1.0	1.0
Erythromycin	61.6	1.9	1.2
CCCP	11.2	1.1	1.0
Vancomycin	(8.4)	(6.6)	(6.6)
HlyA	+	-	-
TLS Phage	1	$>10^{-6}$	1
Colicin E1	1	2^{-12}	1

[a] Numbers for novobiocin, erythromycin, and CCCP represent minimal inhibitory concentration. For vancomycin, zones of inhibition in mm are shown in parenthesis. A 10 µl of solution containing 75 µg of vancomycin was spotted on paper disks of 6.5 mm diameter. Average inhibition zones recorded from two independent assays are shown, with diameter varying no greater than 10%. Plus and minus signs indicate the presence (+) or absence (-) of hemolytic zones on blood agar medium. Sensitivity to TLS phage is measured as efficiency of plaquing. Colicin E1 sensitivity data report inhibition zones after spotting 10 µl of twofold serial dilutions of colicin E1 stock on an agar plate overlayed with bacterial cultures.

[b] TolC$_Q$ denotes TolC turn 1 $_{147}$AGSG$_{150}$ quadruple mutant.

proteins synthesized by certain strains of *E. coli* to kill other *E. coli*. Colicin E1 specifically uses TolC as a secondary receptor for entry into the cell, after initially interacting with the vitamin B1 receptor, BtuB (Masi *et al*., 2007; reviewed in Cascales *et al*., 2007). When bacteria harboring the plasmid encoding the TolC$_{147AGSG150}$ mutant were tested for their sensitivity to TLS phage or colicin E1, the bacteria showed the same sensitivity to TLS phage and colicin E1 as bacteria expressing wild type TolC (Table 1). This sensitivity indicates that the mutant protein is able to properly fold and insert into the outer membrane and that the effects of $_{147}$AGSG$_{150}$ did not propagate up the portion of TolC exposed to the extracellular environment.

In addition to testing the import functions of the mutant TolC protein, it was asked whether the TolC$_{147AGSG150}$ mutant had specifically lost functional interaction with AcrA and AcrB to pump out novobiocin or whether it had additionally lost the ability to functionally interact with other efflux pumps. In order to test this, the $_{147}$AGSG$_{150}$ mutant was tested for its ability to confer resistance to novobiocin, erythromycin, and carbonyl cyanide *m*-chlorophenyl hydrazone (CCCP), as well as to secrete α-haemolysin. Novobiocin and erythromycin are both substrates of AcrAB-TolC, while CCCP is a substrate of the EmrAB-TolC complex. Finally, α-haemolysin is secreted through the HlyDB-TolC complex. When all of these substrates were tested for their ability to be extruded from cells expressing the turn 1 mutant TolC protein, the bacteria showed an inability to pump out the substrate, equivalent to null (Table 1).

28

Additionally, the antibiotic vancomycin was used to determine the status of the TolC aperture. Vancomycin is a large antibiotic, which normally cannot permeate the outer membrane. Only when alterations which force open the TolC aperture or otherwise compromise the outer membrane do cells become sensitive (Vuong *et al*., 2008; Bavro *et al*., 2008). Cells expressing $TolC_{147AGSG150}$ remained resistant to vancomycin indicating that the mutation in TolC turn 1 does not cause the aperture to remain in an open state or the protein does not mis-insert into the outer membrane causing a permeability defect. Thus, $TolC_{147AGSG150}$ is the first mutant of its kind, being completely wild type in its ability to import lethal agents, but unable to export substrates.

Alterations in TolC Turn 1 Prevent Functional Complex Assembly While Maintaining Physical Interaction

In observing the lost ability to remove antibiotics and secrete haemolysin, it was questioned whether the turn 1 $_{147}AGSG_{150}$ mutant TolC protein was now unable to physically interact with efflux complex components. It is possible that disruption of these turn residues prevents the proper physical interaction with the AcrAB proteins, thus preventing assembly of the complex and antibiotic efflux. If this is the case, the mutant TolC protein should not be able to be chemically cross-linked to either AcrA or AcrB. In order to test this, *in vivo* cross-linking was carried out using the amine-specific cross-linker dithiobis (succinimidylpropionate), DSP (Husain *et al*., 2004; Fig 3A). When the mutant

A

| | 1 | 2 | 3 | 4 | 5 | 6 | 7 | 8 |

AcrB ▶

TolC$_{His}$ ▶
AcrA ▶

DSP: + − + − + − + −

α-AcrB$_{His}$ α-AcrA$_{His}$

B

TolC-Q (Q142C)   TolC-Wt (Q142C)

CL: DSP SPDP (none)   DSP SPDP (none)

Cross-
linked
products

AcrA ▶

C
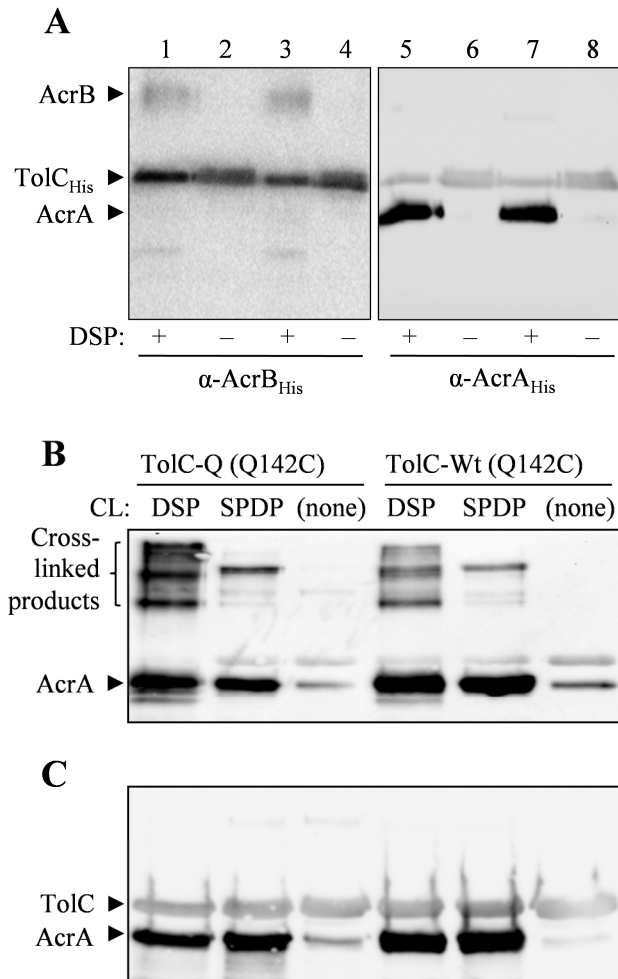
TolC ▶
AcrA ▶

Figure 3. *In vivo* cross-linking analysis to probe TolC-AcrAB interactions and TolC-AcrA interactions.

A. To analyse TolC-AcrAB interactions, freshly grown bacterial cultures were incubated with or without DSP. TolC$_{His}$ was purified through a Ni^{2+} affinity column, and AcrB and AcrA for two identical sets of elutes were probed by Western analysis using AcrB$_{His}$ or AcrA$_{His}$ antibodies. These antibodies also recognize TolC due to the presence of a C-terminal 6XHis tag in TolC. Note that the wild type (lanes 1, 2, 5, and 6) and mutant TolC$_{14AGSG150}$ (lanes 3, 4, 7, and 8) proteins can pull down AcrB and AcrA only in the presence of DSP cross-linker. All protein samples were boiled in sample buffer containing β-mercaptoethanol prior to gel electrophoresis.

B and C. To analyse TolC-AcrA interactions, a Q142C substitution was introduced into both wild type (TolC-WT) and the TolC turn 1 $_{147}$AGSG$_{150}$ mutant (TolC-Q) to facilitate SPDP-mediated cross-linking. Both wild type and mutant TolC proteins contain a 6XHis tag at the C-terminal end of the protein for

30

affinity purification. TolC from cultures incubated with DSP, SPDP, or no cross-linker (CL) was affinity purified through Ni^{2+} affinity columns, AcrA and TolC from two identical sets of elutes were detected through Western blots using $AcrA_{His}$ antibodies, which also recognize $TolC_{His}$. Prior to gel electrophoresis, protein samples were boiled either without (B) or with (C) β-mercaptoethanol.

TolC protein was compared with wild type TolC, we saw no difference in the ability of the mutant or wild type proteins to pull down either AcrA or AcrB in a DSP dependent manner was observed, indicating no gross defect in the ability of the mutant to interact with the other two members of the complex.

As TolC and AcrA share a larger surface area, it is possible that the $_{147}AGSG_{150}$ mutation has disrupted this, causing the drug hypersensitivity phenotype. To determine the status of interaction between TolC and AcrA with more stringency, a more specific cross-linking was carried out utilizing the amine-to-sulfhydryl specific cross-linker succinimidyl 3-(2-pryidylthio) propionate, SPDP. As TolC does not contain any native cysteine residues, a Q142C substitution was introduced into both wild type and the $_{147}AGSG_{150}$ mutant TolC protein. This substitution was previously shown useful in gauging TolC-AcrA interactions (Lobedanz *et al*., 2007). Introduction of a 6 His-tag and the Q142C substitution into either wild type or the $_{147}AGSG_{150}$ mutant did not alter the phenotype of each protein (data not shown). After cross-linking, cell lysates were applied to a Ni-NTA Spin Column, and elutes were probed for the presence of AcrA pulled down with TolC. As seen with DSP, AcrA was effectively pulled down with both TolC proteins in the presence of either cross-linker (Fig 3B and C).

In order to determine the defect in $TolC_{147AGSG150}$ mediated interactions, novobiocin and erythromycin resistant suppressors of the $TolC_{147AGSG150}$ protein were isolated. All of these suppressors mapped to AcrA, leading to the belief that
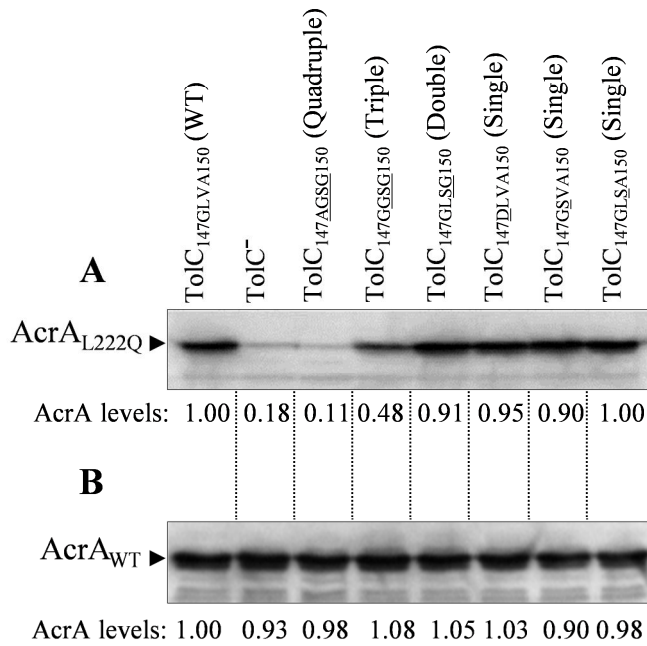
Figure 4. Effect of TolC on $AcrA_{L222Q}$ and wild type AcrA levels. AcrA levels from approximately 5×10^7 cells grown overnight at 37°C were determined by Western blot analysis using antibodies against $AcrA_{His}$. $AcrA_{L222Q}$ (A) and wild type (B) levels from the wild TolC background were taken as 1 and other values were adjusted relative to it.

the mutant TolC was unable to make functional interactions with AcrA.

Alternatively, it is possible that TolC and AcrB are not able to make functional interactions, but the suppressor mutations in AcrA are able to restore these interactions. (Isolation, characterization, and determining the mechanisms of suppressors for AcrA mapping suppressors will be discussed in Chapter 3)

As no apparent defect in interaction could be readily observed through chemical cross-linking a second and perhaps more sensitive means of determining the *in vivo* interactions between AcrAB-TolC complex members was utilized. A labile AcrA mutant, $AcrA_{L222Q}$, has previously been characterized (Gerken and Misra, 2004). The stability of this mutant protein is dependent on the ability to interact with TolC; without TolC, $AcrA_{L222Q}$ is readily degraded by the periplasmic protease DegP (Gerken and Misra, 2004; Weeks *et al.*, 2010). In addition to being dependent on TolC, $AcrA_{L222Q}$ levels are dependent on the presence of AcrB. To test the stability of $AcrA_{L222Q}$, strains where $AcrA_{L222Q}$ was expressed from the native chromosomal locus were transformed with plasmids expressing *tolC* mutants. As expected, in the absence of TolC, $AcrA_{L222Q}$ was readily degraded (Fig 4A). In the presence of TolC turn 1 mutants expressing single or double substitutions, $AcrA_{L222Q}$ was stabilized to the same extent as with wild type TolC. However, in the TolC turn 1 triple ($_{147}GGSG_{150}$) or quadruple ($_{147}AGSG_{150}$) mutant, $AcrA_{L222Q}$ was modestly or significantly degraded, respectively (Fig 4A). Additionally, these mutants showed a moderate to severe drug hypersensitivity phenotype, showing the $AcrA_{L222Q}$ stability test is a more

sensitive means of determining functional interaction than *in vivo* chemical cross-linking data (Fig 3). Note that wild type AcrA is typically a stable protein regardless of whether or not TolC is expressed (Fig 4B).

Loosening of the TolC Aperture Can Suppress the Turn 1 Mutation

As it was shown that the TolC turn 1 $_{147}$AGSG$_{150}$ mutant is defective in functional interaction with AcrA and potentially AcrB, it is believed that the final step of TolC aperture opening has been precluded. If this is the case then it is possible that alterations which open TolC may be able to suppress the turn 1 TolC mutant defects. In order to test this, two different alterations which have been shown to induce aperture opening were introduced into the TolC$_{147AGSG150}$ mutant background. A R367E or R390E mutation was separately introduced into the TolC$_{147AGSG150}$ background. These alterations cause TolC aperture opening either by preventing the salt bridges directly (R367) or by preventing supercoiling of the inner helices (R390) (Andersen *et al.*, 2002; Augustus *et al.*, 2004; Bavro *et al.*, 2008; Fig 5A, B, and C).

When tested for their susceptibility to substrate antibiotics, it was observed that the R367E and R390E mutations cause sensitivity to both novobiocin and vancomycin, as predicted, due to the aperture being unable to close, with R367E expressing a leakier phenotype. The TolC$_{147AGSG150, R367E}$ and TolC$_{147AGSG150, R390E}$ mutants showed a marked reduction in sensitivity to vancomycin compared to their wild type counterparts, as well as being
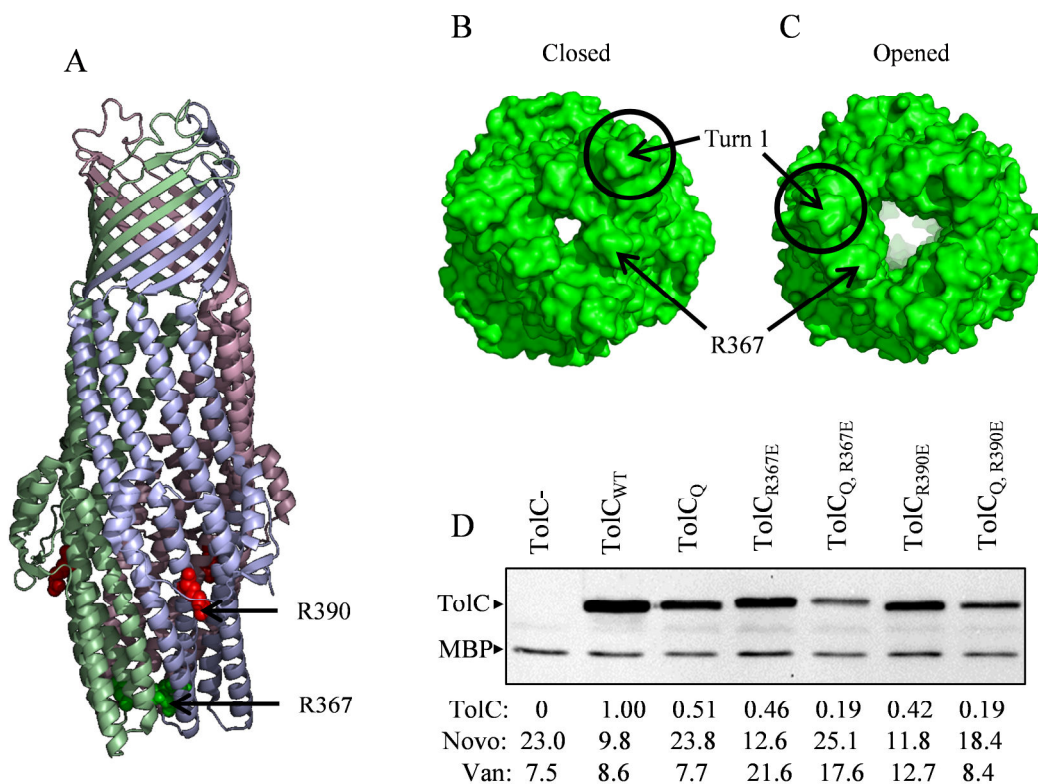
Figure 5. Effects TolC aperture/channel opening on $TolC_{147AGSG150}$.

A. A cartoon of the TolC structure (1EK9) in which the two R367 and R390 have been identified. These residues are involved in maintaining TolC aperture closed. R367 (green) is directly involved in the network of salt bridges at the aperture, whereas R390 (red) is distal to the aperture and is thought to maintain the supercoiling of the inner helices.

B and C. These cartoons show the TolC aperture in its resting, closed state (B, 1EK9) or open state (C, 2XMN). Note turn 1 remains static while turn 2 moves out, opening the channel. R367 is directly involved in the network of salt bridges responsible for maintaining the closed aperture.

D. Effects of mutations R367E and R390E, which increase the aperture/channel opening, on TolC levels and novobiocin and vancomycin sensitivities. The $TolC_Q$ denotes the turn 1 $_{147}AGSG_{150}$ mutant. Proteins were detected by Western blots as described in Fig. 2 legend. Antibiotic sensitivities were described as in Fig. 2 and Tables 1 legends. Average inhibition zone diameters were plotted from two independent experiments, with zones varying no greater than 10%.

accompanied by a significant reduction in protein level, compared to TolC$_{147AGSG150}$ (Fig 5D). Interestingly, the TolC$_{147AGSG150, R367E}$ mutant showed increased sensitivity to the substrate novobiocin, whereas the TolC$_{147AGSG150, R390E}$ mutant showed reduced sensitivity. It is worth noting that the protein levels of both the TolC$_{147AGSG150, R367E}$ and the TolC$_{147AGSG150, R390E}$ mutants showed significantly reduced protein levels. As the protein levels decreased similarly in both mutants, while antibiotic sensitivity decreased in the TolC$_{147AGSG150, R390E}$, but not the TolC$_{147AGSG150, R367E}$ mutant it seems that alterations distal to the aperture loosen the helices in such a way that functional interaction resulting in antibiotic resistance can be partially obtained. Said differently, this seems to indicate that loosening of the TolC aperture by alterations distal to the aperture allows slight changes in the helices, which partially decreases sensitivity to antibiotics.

Alterations within the α-Helices of TolC Suppress the Turn 1 Defect

It was observed that the TolC turn 1 $_{147}$AGSG$_{150}$ mutant did not stabilize the AcrA$_{L222Q}$ protein, nor did the AcrA$_{L222Q}$ mutation suppress the TolC$_{147AGSG150}$ hypersensitivity phenotype. Mutations were sought that could restore antibiotic resistance, and simultaneously stabilize the AcrA$_{L222Q}$ protein. Approximately 5 X 10^8 cells from 8 independent cultures of the TolC$_{147AGSG150}$/AcrA$_{L222Q}$ mutant were plated onto medium containing novobiocin and erythromycin, and incubated at 37°C for 20 hours. Each of the eight independent cultures gave rise to an

37
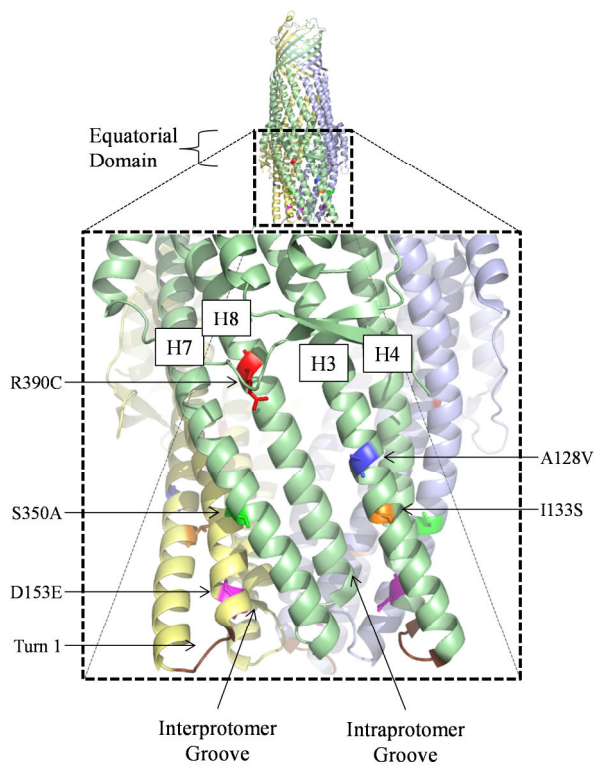
Figure 6. Location of TolC mutations which suppress the TolC$_{147AGSG150}$/AcrA$_{L222Q}$ drug hypersensitivity. A cartoon showing the X-ray structure of TolC (1EK9) shows the TolC mapping suppressors of AcrA$_{L222Q}$/TolC$_{147AGSG150}$. Mutations are depicted using the mature residue numbering. The molecule has been aligned to show the intraprotomer groove, with the adjacent monomers in the background.

average of 15 antibiotic resistant mutants, at a frequency of about 10^{-8}, indicating

the presence of missense mutations. From these antibiotic resistant mutants, 28

revertants were selected based on colony size. To test whether the mutation

mapped in the *tolC* gene, plasmids were extracted and transformed into $\Delta tolC$

acrA (AcrA$_{L222Q}$) and tested for their ability to support growth on medium

supplemented with novobiocin and erythromycin. Transformants from 9 of the 28

spontaneous mutants were able to grow on medium supplemented with

novobiocin and erythromycin. The *tolC* gene was then sequenced for those

transformants. The suppressors contained one of three TolC alterations, D153E,

S350A, and R390C, as well as the original $_{147}$AGSG$_{150}$ substitution. These

mutations were isolated a total of one, one, and seven times, respectively.

Additionally, a second similar selection was performed in which two additional

substitutions were isolated, A128V and I133S. In addition to these 5 missense

alterations in the TolC$_{147AGSG150}$ background, we isolated secondary missense

alterations in *acrA* (AcrA$_{L222Q}$) gene, which will be described in detail in Chapter

3.

　　These five mutations all map to the bottom half of the α-helical barrel of

TolC, below the equatorial domain (Fig 6). Interestingly, R390C has previously

been isolated as an open state alteration, conferring a leaky phenotype. While

R390 does not directly influence gating of the aperture, it is believed to be

important in maintaining the inner coils H7/H8 in their packed position (Augustus

et al., 2004; Bavro *et al.*, 2008). Residue D153 is directly involved in the network

of salt bridges at the aperture; however, alteration of D153 typically has less severe consequences than mutation of R367 which is the main residue involved in gating the aperture (Andersen *et al.*, 2002; Augustus *et al.*, 2004). Residues A128 and I133 lie on helix H3 in the intraprotomer groove, with A128 on the exterior surface and I133 pointed toward H4 close to the interior surface of the channel. The final substitution isolated in this study, S350A, is the only residue to reside in the interprotomer groove. It is located on helix H7, partially exposed to the exterior surface and directly pointed toward H4. Additionally, in the crystal structure of TolC (Andersen, 2002; Eswaran *et al.*, 2003), S350 forms an important hydrogen bond with D162 of the neighboring protomer. An alteration of this residue is thought to cause defects in trimerization and maintaining the supercoiling of the inner helices.

The isolated suppressors showed significant increases in resistance to erythromycin and novobiocin, as expected, as well as increased resistance to CCCP. In some cases, the $TolC_{14AGSG150}$ suppressor alterations exhibit an increased ability to secrete α-haemolysin (Table 2). When tested for their ability to confer resistance to CCCP in an *acrB* null or *emrAB* null background, the suppressors showed a subtle decreased in resistance compared to when both complexes were intact (Table 3). This indicates the TolC mutants have partially restored interaction with both EmrAB and $AcrA_{L222Q}/AcrB$ to remove CCCP. Likewise, the $TolC_{147AGSG150}$ suppressors were tested for their ability to secrete α-haemolysin in the absence or presence of $AcrA_{L222Q}$. $TolC_{147AGSG150, I133S,}$

TolC$_{147AGSG150, S350A}$, and TolC$_{147AGSG150, R390C}$ showed hemolytic zones on blood agar plates whether AcrA$_{L222Q}$ was present or not, however these zones were still comparably smaller than when wild type TolC was expressed. The requirement of both the AcrAB and the EmrAB efflux complexes to remove CCCP and the increased ability to secrete α-haemlysin, regardless of the absence or presence of AcrA$_{L222Q}$, indicates these suppressors are partially restoring interaction with the membrane fusion proteins, which had been lost by the TolC turn 1 $_{147}$AGSG$_{150}$ mutation.

In order to determine how these alterations were able to restore efflux functions of TolC, it was desired to determine whether or not the aperture was being opened. When zones of inhibition were measured for vancomycin, it was seen that the single amino acid substitutions increased sensitivity to vancomycin. This indicates that AcrA$_{L222Q}$ is now acting to open the TolC$_{147AGSG150}$/suppressor proteins.

Suppressor Alterations Stabilize Interactions with the Membrane Fusion Protein

While examining the various phenotypes of the suppressor mutants, the TolC or AcrA levels were analyzed. It is possible that the mutations were acting to restore proper folding of TolC, which would be reflected by increased mutant TolC protein levels. When TolC levels were analyzed, the alterations did not increase protein levels (Fig 7A). Interestingly, when analyzing AcrA levels, only two of the suppressors, S350A and R390C, significantly stabilized AcrA$_{L222Q}$ (Fig

41

Table 2. TolC mapping suppressors restore efflux functions.

Nature of TolC Protein[b]	Sensitivity to Select Inhibitors[a]				
	Novo	Ery	Vanco	CCCP	HlyA
TolC$_{WT}$	9.9	13.5	8.9	(9.7)	+++
TolC$_Q$	21.6	19.9	8.0	(1.1)	-
TolC$_{Q, A128V}$	11.6	16.1	9.8	(3.0)	-
TolC$_{Q, I133S}$	10.0	16.8	9.7	(3.4)	+
TolC$_{Q, D153E}$	10.9	10.5	11.3	(3.0)	-
TolC$_{Q, S350A}$	10.7	10.5	12.5	(3.4)	++
TolC$_{Q, R390C}$	9.5	9.9	8.9	(3.3)	+

[a] Novo is novobiocin, Ery is erythromycin, Vanco is vancomycin, CCCP is carbonyl cyanide *m*-chlorophenyl hydrazone, and HlyA is the α-haemolysin toxin. Numbers for CCCP represent minimal inhibitory concentrations. For novo, ery, and vanco, zones of inhibition in mm are shown in parenthesis. Novo (30 µg) and Ery (15 µg) pre-soaked disks or 10 µl of solution containing 75 µg of vancomycin was spotted on paper disks of 6.5 mm diameter. Average inhibition zones recorded from two independent assays are shown, with diameter varying no greater than 10%.
[b] TolC$_Q$ denotes TolC turn 1 $_{147}$AGSG$_{150}$ quadruple mutant.

Table 3. TolC mapping suppressors restore efflux functions independent of AcrA.

TolC Protein[c]	Haemolysin Secretion[a]		CCCP Minmal Inhibitory Concentration[b]		
	$AcrA_{L222Q}$[d]	$\Delta acrA$	$AcrA_{L222Q}$	$\Delta acrA$	$\Delta emrAB$
TolC-	-	-	ND[e]	ND	ND
$TolC_{WT}$	+++	+++	9.7	8.7	5.5
$TolC_Q$	-	-	1.1	1.0	0.6
$TolC_{Q,\ A128V}$	-	-	3.0	ND	ND
$TolC_{Q,\ I133S}$	+	+	3.4	1.9	2.8
$TolC_{Q,\ D153E}$	-	-	3.0	ND	ND
$TolC_{Q,\ S350A}$	++	++	3.4	ND	ND
$TolC_{Q,\ R390C}$	+	+	3.3	2.1	3.1

[a] Haemolisin secretion was determined using strains containing the pSF4000-*hlyCABD* (Cm^r) plasmid expressing the α-haemolysin toxin and its native ABC transporter.

[b] Numbers for CCCP are minimal inhibitory concentrations.

[c] $TolC_Q$ denotes $TolC_{147AGSG150}$, subsequent suppressor mutations are listed in addition.

[d] $AcrA_{L222Q}$ denotes the native *acrA* sequence contains a point mutation, whereas *acrA* indicates the *acrA* gene has been deleted as described previously (Augustus *et al.*, 2004) non-polar to the *acrB* gene. The *emrAB* locus was deleted using the Waner and Datsenko method (2000) by a Km^r and transduced into a strain containing *acrA* ($AcrA_{L222Q}$).

[e] ND indicates No Data.
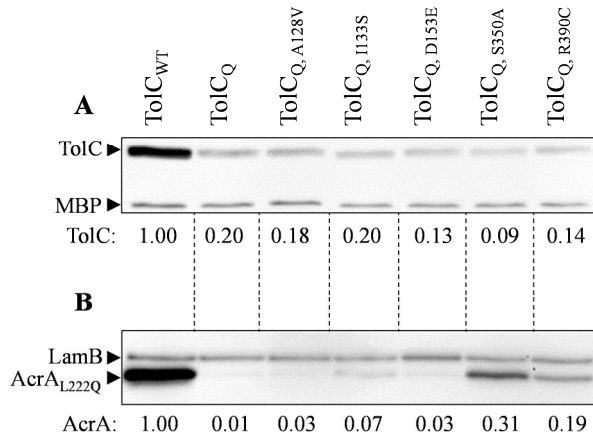
Figure 7. Effects of TolC mutations on TolC and AcrA$_{L222Q}$. Protein extracts from cultures grown at 37°C for 16 h were used to detect TolC and MBP (A) or AcrA and LamB (B). MBP and LamB were used as gel loading controls. Whole cell extracts from approximately 5×10^7 cells were used to determine TolC (A), while membrane extracts from approximately 7.5×10^8 cells were used to determine AcrA levels (B). TolC variants are expressed from a plasmid replicon, whereas AcrA$_{L222Q}$ is expressed from its native chromosomal replicon. TolC and AcrA$_{L222Q}$ levels in the wild type TolC were taken as 1 and TolC variants or AcrA$_{L222Q}$ levels were calculated relative to expression in the wild type TolC.

	TolC$_{WT}$	TolC$_Q$	TolC$_{Q,A128V}$	TolC$_{Q,I133S}$	TolC$_{Q,D153E}$	TolC$_{Q,S350A}$	TolC$_{Q,R390C}$
LamB ►							
AcrA$_{P265R}$ ►							
AcrA levels:	1.00	0.05	0.02	0.05	0.04	0.61	0.42
Nov (mm):	9.2	21.6	14.1	10.5	12.3	11.0	10.2
Ery (mm):	12.8	19.2	17.0	15.2	10.9	10.6	14.7
Vanco (mm):	8.8	7.8	9.1	10.4	11.2	13.1	8.5
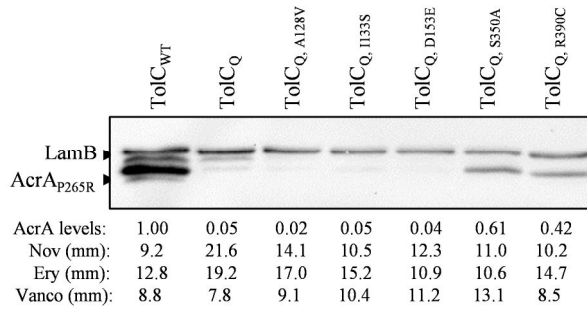
Figure 8. TolC mapping suppressors restore antibiotic efflux with AcrA$_{P265R}$ while stabilizing this labile AcrA variant. Membrane extracts from approximately 7.5×10^8 cells, grown at 37°C for 16 h, were used to determine AcrA$_{P265R}$ levels. Sensitivity to novobiocin (30 µg), erythromycin (15 µg), and vancomycin (75 µg) were determined by measuring zones of inhibition around disks of 6.5 mm diameter. Values are the average from two independent cultures varying no greater than 10% are listed.

7B).

In addition to the $AcrA_{L222Q}$ mutant, a second labile AcrA mutant has been described, $AcrA_{P265R}$. Both of these mutations were identified in a screen to find suppressors of the labile $TolC_{P246R, S350C}$ protein. Like $AcrA_{L222Q}$, the stability of $AcrA_{P265R}$ is dependent on functional interactions with TolC (Gerken and Misra, 2004, Figure 8). When the $TolC_{147AGSG150}$ mutant is introduced into the $AcrA_{P265R}$ background, the AcrA protein is readily degraded. In addition to the decreased protein levels, increased sensitivity to antibiotics was observed. When the TolC turn 1 mapping suppressors were introduced into the $AcrA_{P265R}$ background, all suppressors acted to reduce antibiotic hypersensitivity. As in the $AcrA_{L222Q}$ background, $AcrA_{P265R}$ protein levels increased significantly in two of the mutant backgrounds. $TolC_{14AGSG150, S350A}$ and $TolC_{147AGSG150, R390C}$. It is worth noting that $TolC_{147AGSG150, S350A}$ showed decreased TolC levels in the presence of $AcrA_{L222Q}$, but increased AcrA levels most significantly in both the $AcrA_{L222Q}$ and $AcrA_{P265R}$ backgrounds, and showed most significant improvement in haemolysin secretion. Also the three mutations, $TolC_{147AGSG150, A128V}$, $TolC_{147AGSG150, I133S}$, and $TolC_{147AGSG150, D153E}$ do not appear to stabilize $AcrA_{P265R}$ and only partially stabilize $AcrA_{L222Q}$, but significantly reduce sensitivity to substrates. This seems to indicate that these suppressor alterations are subtly changing the TolC conformation in such a way to reduce antibiotic hypersensitivity, but only two of these mutants, S350A and R390C, drastically stabilize the two labile AcrA mutant proteins.

46
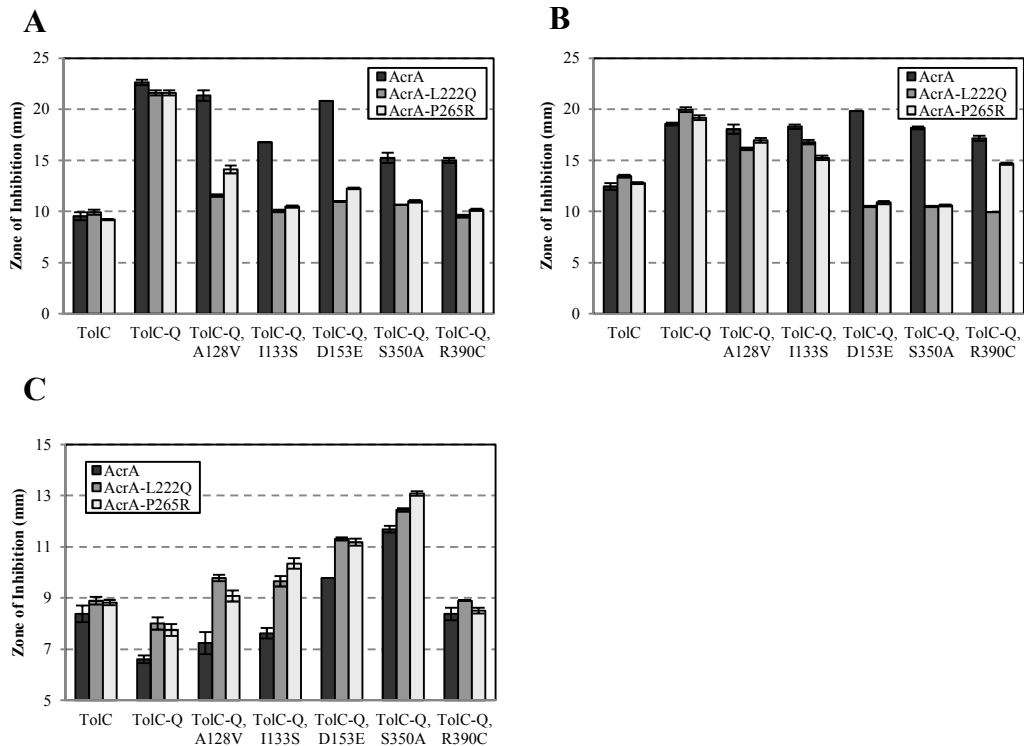
Figure 9. TolC suppressors show specificity towards mutant AcrA alleles. Sensitivity to the substrate inhibitors novobiocin (A) and erythromycin (B) are not decreased when wild type AcrA was combined with the $TolC_{147AGSG150}$ suppressors as with $AcrA_{L222Q}$ or $AcrA_{P265R}$. Vancomycin sensitivity (C) shows the TolC aperture is constitutively dilated in the presence of the D153E and S350A mutant, whereas the other three revertants show minimal increases in sensitivity. Zones of inhibition around pre-soaked novobiocin (30 µg) and erythromycin (15 µg) disks are shown in millimeters (mm). For vancomycin, a 10 µl of solution containing 75 µg of vancomycin was spotted on paper disks of 6.5 mm diameter. Average inhibition zones recorded from two independent assays are shown, with zones varying no greater than 10%.

α-Helical Alterations in TolC$_{147AGSG150}$ Require Constitutively Active AcrA

As these TolC alterations were isolated in the presence of AcrA$_{L222Q}$, it was inquired whether they were able to suppress the TolC$_{147AGSG150}$ defect in the wild type AcrA background. Interestingly, when wild type AcrA was combined with the TolC turn 1 mutant, A128V and D153E did not decrease sensitivity to novobiocin (Fig 9A). The remaining three point mutations, I133S, S350A, and R390C, did partially reduce the turn 1 antibiotic hypersensitivity phenotype, but not to the extent as in the AcrA$_{L222Q}$ or AcrA$_{P265R}$ backgrounds (Fig 9A). These three alterations also partially restored haemolysin secretion indicating their ability to restore interaction with the HlyCABD complex (Table 3). When tested for sensitivity to erythromycin, all the suppressors showed little to no suppression of the hypersensitivity phenotype (Fig 9B). Additionally, sensitivity to vancomycin was determined to see whether the point mutations caused the TolC aperture to open, as was observed when these altered proteins were combined with AcrA$_{L222Q}$. TolC$_{147AGSG150, S350A}$ and TolC$_{147AGSG150, D153E}$ showed sensitivity to vancomycin greater than TolC$_{WT}$/AcrA$_{WT}$ indicating that the aperture of these two mutants is remaining in a partially open state (Fig 9C).

After seeing that the TolC mapping suppressors were able to reduce antibiotic hypersensitivity of the TolC$_{147AGSG150}$ mutant in the presence of AcrA$_{L222Q}$ and AcrA$_{P265R}$ but unable to suppress this phenotype in the presence of wild type AcrA, it was asked whether these suppressors can reduce the antibiotic hypersensitivity phenotype in the presence of constitutively active forms of AcrA.

48

In order to test this, the plasmids containing wild type TolC, the TolC turn 1 mutant, or the TolC$_{147AGSG150}$ suppressors transformed into strains lacking *tolC*, while expressing one of five mutant AcrA proteins from the native chromosomal locus: AcrA$_{\Delta217-218}$, AcrA$_{T30A}$, AcrA$_{N146T}$, AcrA$_{S83G}$, and AcrA$_{T153P}$. These AcrA alterations were isolated among antibiotic resistant revertants of the antibiotic hypersensitive mutants TolC$_{P246R, S350C}$ or TolC$_{147AGSG150}$ (Gerken and Misra, 2004; Weeks *et al.*, 2010; Chapter 3). As these alterations all support functional complex assembly, as seen by stabilization of a labile TolC mutant and reduced antibiotic hypersensitivity in the background in which they were isolated (Gerken and Misra, 2004; Weeks *et al.*, 2010, Chapter 3), it is believed that they cause AcrA to stay in an active state, which wild type only transiently adopts during antibiotic efflux.

The alterations map to the three crystallized domains of AcrA: Δ217-218 and T30A, as well as L222Q and P265R, map to the β-barrel; S83G and N146T map to the α-helical domain; and T153P maps to the lipoyl domain (Fig 10). Wild type TolC confers resistance to antibiotics with AcrA$_{\Delta217-218}$, AcrA$_{T30A}$, AcrA$_{S83G}$, and AcrA$_{T153P}$, like AcrA$_{L222Q}$ and AcrA$_{P246R}$, whereas AcrA$_{N146T}$ only confers partial resistance to antibiotics. As AcrA$_{S83G}$ and AcrA$_{T153P}$ were isolated as suppressors of TolC$_{147AGSG150}$, these alterations caused reduced sensitivity to antibiotics. Of the three additional alterations isolated against TolC$_{P246R, S350C}$, AcrA$_{T30A}$ and AcrA$_{\Delta217-218}$, did not suppress the hypersensitivity caused by

TolC$_{147AGSG150}$, whereas AcrA$_{N146T}$ was able to partially reverse the antibiotic hypersensitivity (Fig 11 and 24).

When the TolC$_{147AGSG150}$ suppressors were tested for their ability to reduce sensitivity to antibiotics in the mutant AcrA backgrounds, there was an overall trend that the TolC$_{147AGSG150}$ mapping suppressors decreased sensitivity to novobiocin more than they did with AcrA$_{WT}$ (Fig 11A). This indicates that TolC$_{147AGSG150}$ suppressors are able to more properly interact with the constitutively active forms of AcrA to reduce the hypersensitivity phenotype. However, when comparing resistance to erythromycin, the TolC mapping suppressors can be divided into two classes, those that marginally increase resistance and those drastically reduce sensitivity (Fig 11B). TolC$_{147AGSG150, A128V}$ and TolC$_{147AGSG150, I133S}$ marginally increase resistance to erythromycin in the presence of the "active" forms of AcrA. Interestingly these two suppressors did not drastically increase levels of AcrA$_{L222Q}$ or AcrA$_{P265R}$ (Fig 7B and 8). The residues A128 and I133 are located on the intraprotomer groove and are not involved in constricting the TolC aperture. Additionally, these two revertants show no increase in sensitivity to vancomycin in the presence of wild type AcrA (Fig 9C), as well as showing an overall trend of subtly increasing vancomycin sensitivity in the altered AcrA backgrounds (Fig 11C).

While TolC$_{147AGSG150, D153E}$ did not significantly increase AcrA levels of the two labile mutant AcrA proteins, D153 is one of the residues directly involved
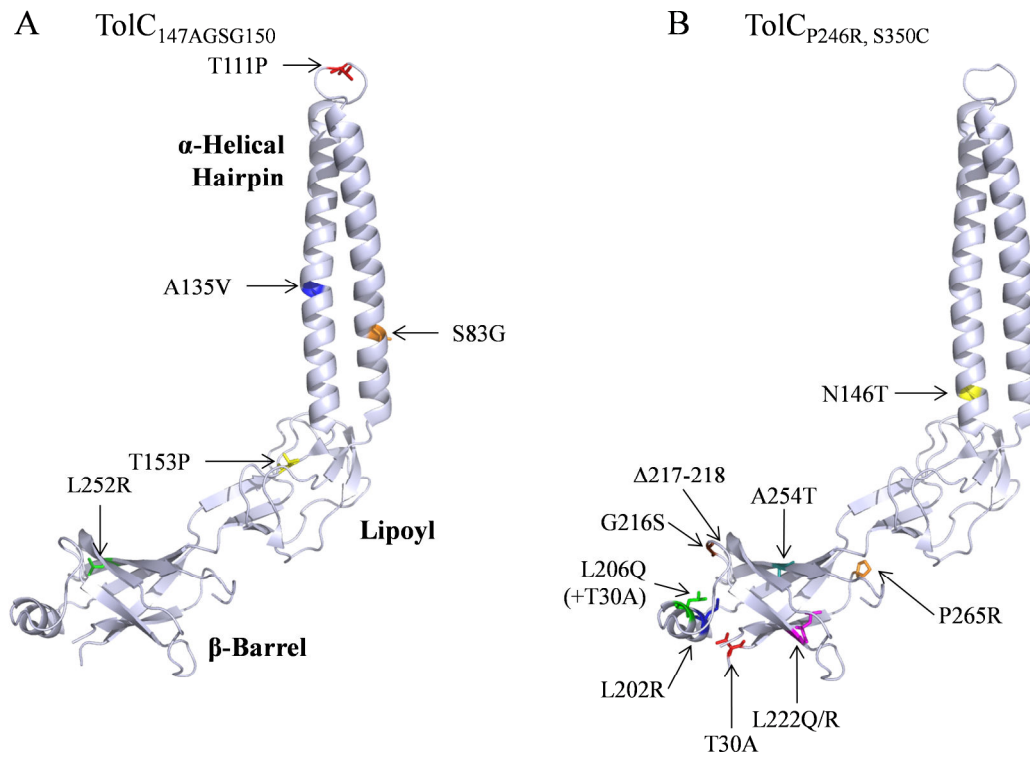
Figure 10. A cartoon showing X-ray structures of AcrA (2F1M). Locations of five AcrA substitutions obtained in this study and those obtained previously (Gerken and Misra, 2004) are shown in A and B, respectively. AcrA residue numbering corresponds to that of the mature protein.
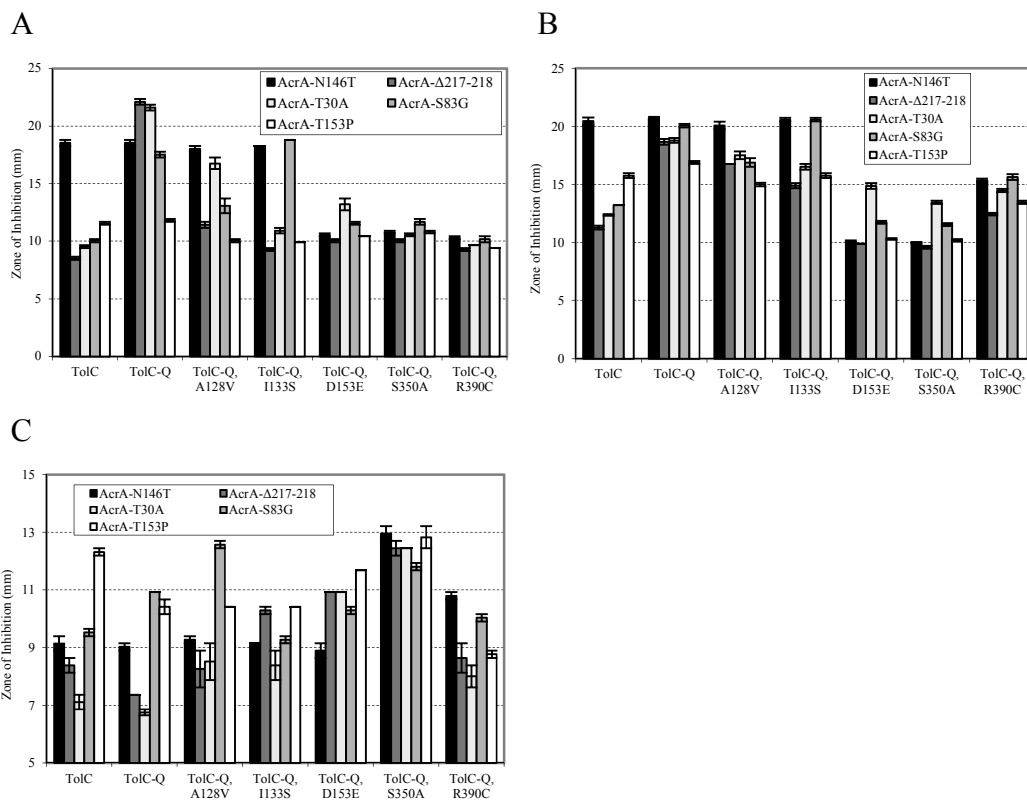
Figure 11. TolC suppressors show specificity towards constitutively active forms of AcrA. Sensitivity to the substrate inhibitors novobiocin (A) and erythromycin (B) are decreased when the point mutations are combined with the $TolC_{147AGSG150}$ mutant and conformationally active forms of AcrA. As seen by increased sensitivity to vancomycin (C), the combination of mutations in AcrA and TolC causes the aperture to open. Zones of inhibition around pre-soaked novobiocin (30 µg) and erythromycin (15 µg) disks are shown in millimeters (mm). For vancomycin, a 10 µl of solution containing 75 µg of vancomycin was spotted on paper disks of 6.5 mm diameter. Average inhibition zones recorded from two independent assays are shown, with zones varying no greater than 10%.

in forming the salt bridges which lock the TolC aperture (Fig 7B and 8).

Additionally, S350 and R390 are distally involved in holding the inner helices in their closed conformation. These three suppressors (D153E, S350A, and R390C) all drastically reduced the hypersensitivity to erythromycin (Fig 11B). Interestingly, when comparing sensitivity to vancomycin (Fig 11C), all of the TolC mapping suppressors tend to increase sensitivity over $TolC_{147AGSG150}/AcrA_{WT}$, showing the TolC aperture is being opened. While R390C is an open state mutant of TolC (Augustus $et\ al.$, 2004), when in combination with $TolC_{147AGSG150}$, this mutation does not increase sensitivity to vancomycin over $TolC_{WT}/AcrA_{WT}$. However $TolC_{147AGSG150,\ R390C}$ does confer sensitivity greater than the parental strain expression $TolC_{147AGSG150}$ alone.

Taken together the data indicates that the novobiocin/erythromycin antibiotic resistant revertants of $TolC_{147AGSG150}/AcrA_{L222Q}$ act primarily to loosen the TolC aperture in such a way that constitutively active forms of AcrA are able to act upon the mutant TolC proteins to reduce antibiotic hypersensitivity of the parental strain. While not all of the $TolC_{147AGSG150}$ suppressors act equally to reduce the antibiotic hypersensitivity of the $TolC_{147AGSG150}$ mutant with each of the AcrA suppressor proteins, the overall trend is such that the altered TolC proteins interact better with these mutant forms of AcrA. Additionally, the $TolC_{147AGSG150}$ suppressors show increased sensitivity to vancomycin indicating the TolC aperture is able to be opened alterations in the AcrA protein.

Results 2: Genetic Evidence for the Importance of AcrB's Periplasmic Hairpin Loops

AcrB's Periplasmic Hairpin Loops Interact Via both Side Chain and Backbone Mediated Interactions

Previously it has been reported that AcrB's periplasmic hairpin loops directly interact with TolC's periplasmic turns via spontaneous disulfide formation of cysteine-derived TolC and AcrB variants (Tamura *et al*., 2005). Additionally, in the proposed tripartite model based on chemical cross-linking experiments, these regions of the two proteins directly intermesh (Symmons *et al*., 2009). These data suggest that D256 and D795 of AcrB's periplasmic hairpin loops 1 and 2, respectively, are important in facilitating interaction with TolC. However, when these residues were mutated, either individually or simultaneously, there was no increase in sensitivity (Fasahath, 2006). In order to determine whether residues of the hairpin loops do in fact play a role in functional complex assembly, two approaches were employed. The two approaches were designed to determine side chain importance and backbone importance. In the first approach all loop 1, loop 2 or both loop residues were simultaneously replaced by alanines. In the second approach, either loop 1 or loop 2 residues were deleted. In loop 1, this affected residues $_{252}$KVNQD$_{256}$. In loop 2, the first two residues are already alanines, which left $_{795}$DGQ$_{797}$ to be substituted with alanines, while a deletion removed residues 793 to 797 (Fig 12).
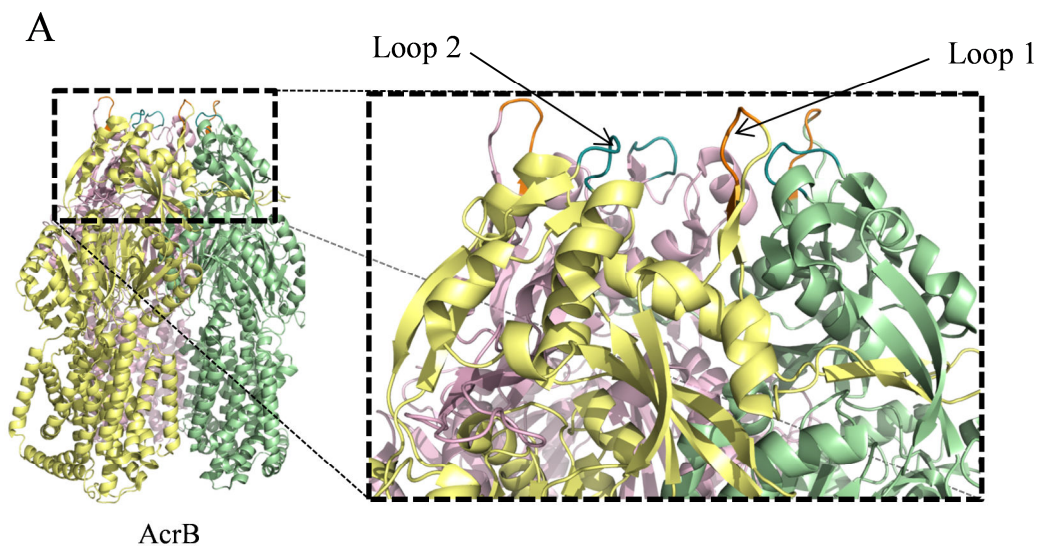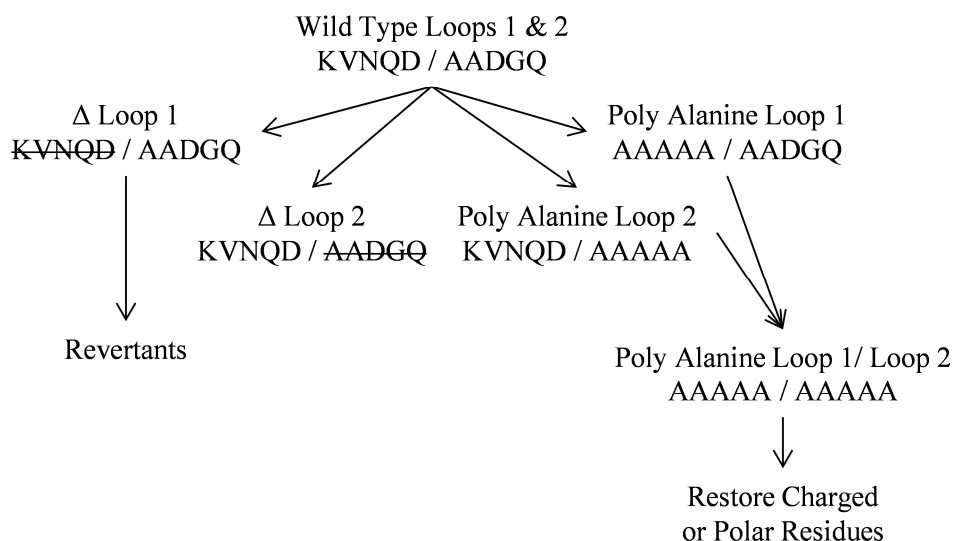
Figure 12. Schematic of AcrB hairpin loop residues and mutational analysis.
A. A cartoon showing the asymmetric AcrB (2GIF) where each of the monomers has been colored corresponding to the Loose (L, yellow), Tight (T, green), and Open (O, pink) conformation. Loop residues are colored and have been pointed out in the loose monomer.
B. In order to determine the importance of the hairpin loops, either deletion analysis or poly alanine mutagenesis was performed. Loop residues are noted for each of the mutations. For the deletion mutants, the residues have been crossed out. Loop residues correspond to residues 252-256 and 793-797 for loop 1 and loop 2, respectively.

In order to determine the ability of the AcrB hairpin loop engineered mutants to form a functional complex AcrA and TolC, drug sensitivity assays were performed and relative growth on medium supplemented with substrate drugs. In an *acrAB* null mutant there is a severe antibiotic hypersensitivity phenotype, however, the presence of wild type copies of these genes complemented the drug sensitivity phenotype (Fig 13A and C). When only one of the two AcrB hairpin loops was substituted with alanines (AcrB$_{PAL1}$ or AcrB$_{PAL2}$) the mutant AcrB proteins were able complement the $\Delta acrAB$ phenotype. However, substitutions of both loop residues with alanines (AcrB$_{PAL1/L2}$) failed to fully complement. Deletion of loop 1 (AcrB$_{\Delta L1}$), but not loop 2 (AcrB$_{\Delta L2}$) failed to complement the hypersensitivity phenotype. Taken together these data show the side chains of both AcrB loops are functionally interchangeable, but that loop 1 residues are more important since deletion of loop 1, but not loop 2 disabled AcrB's activity. Additionally, these data indicate that the side chains of loop 1 and 2 have a conserved function. Thus without the side chains of both loops, the protein partially looses functionality.

Identification of AcrB Hairpin Loop Residues Which Facilitate Functional Interaction

In observing the loss of activity of the AcrB$_{PAL1/L2}$ mutant, it was questioned which side chains were important for AcrB activity. In loop 1 there are 4 charged or polar residues which could be important in potentially interacting

A

B

C

1.	AcrB-	5.	AcrB$_{\Delta L2}$
2.	AcrB+	6.	AcrB$_{PAL2}$
3.	AcrB$_{\Delta L1}$	7.	AcrB$_{PAL1/L2}$
4.	AcrB$_{PAL1}$		
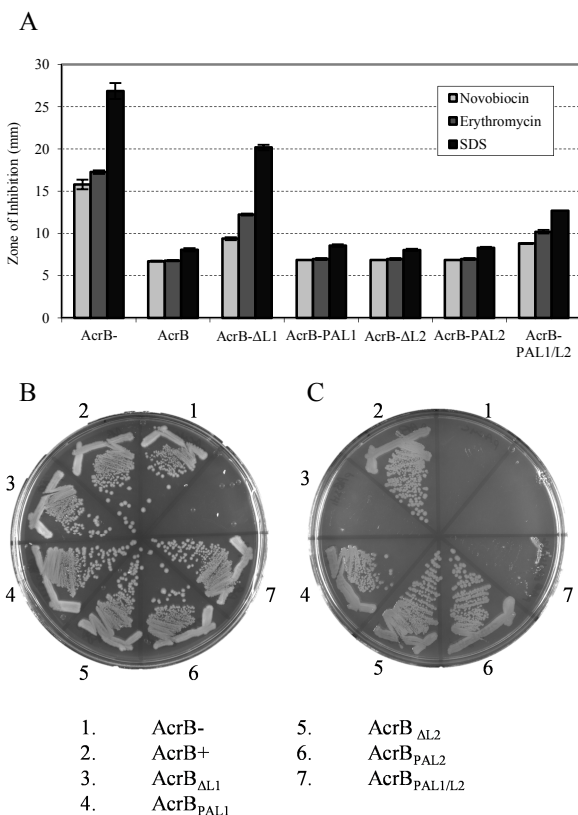
Figure 13. Phenotypic characterization of AcrB loop mutants.
A. Sensitivity to select inhibitors was determined by performing disk assays.
Zones are an average of two independent cultures varying no greater than 10%.
For SDS, 1 mg was spotted onto blank disks. Deletion analysis shows loop 1 is
more important in antibiotic efflux as deletion of loop 1, but not loop 2 causes
increased sensitivity to the three inhibitors. However, both loops are important in
maintaining proper interactions as poly alanine mutagenesis requires mutation of
both loops simultaneously to cause increased sensitivity.
B and C. Relative growth of the AcrB mutant strains on medium without (B) or
with (C) the substrate inhibitors: novobiocin, erythromycin, and SDS. A single
colony was purified on medium with or with substrates and growth was
determined after 16 hr at 37°C. Medium was supplemented with 5 µg ml^{-1}
novobiocin and erythromycin, and 0.1% SDS. Deletion of AcrB loop 1, but not
loop 2 residues leads to a drug hypersensitivity phenotype. Simultaneous
alteration of both loop 1 and loop 2 residues leads to a hypersensitivity phenotype.
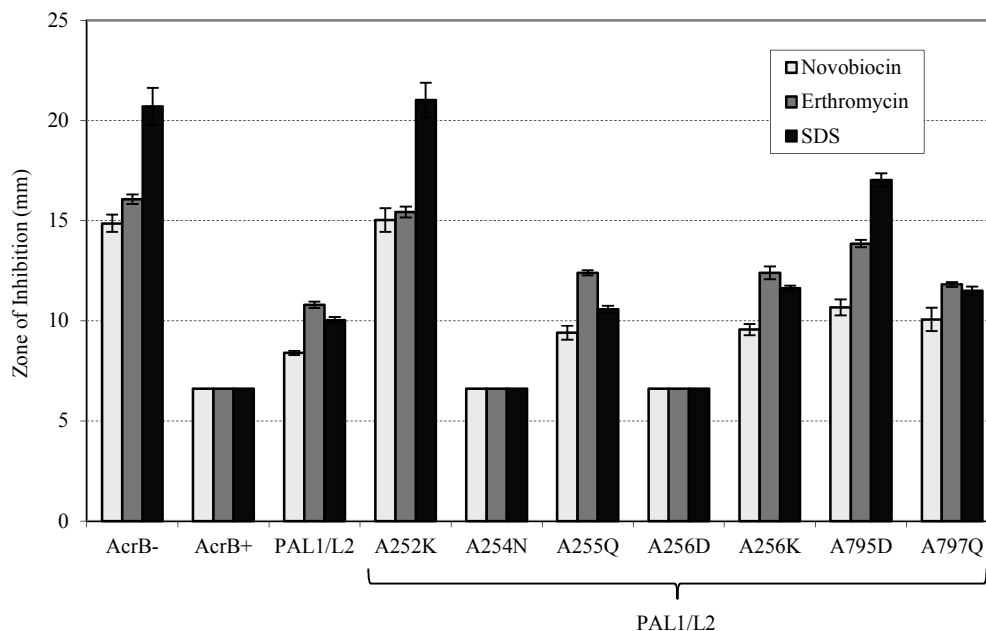
Figure 14. Characterization of single charged/polar side chain restoration mutants. As simultaneous mutation of both loops 1 and loop 2 residues to alanine caused increased sensitivity to substrate inhibitors, restoration of residues important in maintaining proper interaction should reduce antibiotic sensitivity. Restoration of either N254 or D256 leads to reduced sensitivity of the PAL1/L2 AcrB mutant. Sensitivity assays were performed as described in Figure 2 and Table 1.

with TolC, whereas in loop 2 there are 2 charged or polar residues. In order to determine which residues were important, each alanine residue was individually restored to its original side chain. Interestingly, only restoration of N254 or D256 was able to restore antibiotic resistance (Fig 14). In order to test whether it was the presence of a charged residue at position 256 that was important for functionality, a K256 alteration was created. This variant was unable to complement the drug sensitivity phenotype of the AcrB$_{PAL1/L2}$ mutant, indicating that it is specifically the presence of a negatively charged residue at position 256 that is important for AcrB activity.

Together with the disulfide bond formation data by Tamura *et al*, (2005), these results revealed for the first time (a) the significance of loop 1 over loop 2, and (b) exposed the importance of the D256 residue of loop 1 for AcrB activity.

AcrB Loop Alterations Destabilize Functional Interactions with TolC and AcrA

To assess mutant AcrB's ability to interact with TolC, an attempt to repeat the experiments of Tamura *et al*. (2005) was made. In this study spontaneous disulfide bond formation between cysteine derivatives of AcrB and TolC was demonstrated. However, when tested it was found that cysteine derivatives of wild type TolC and AcrB caused a synthetic lethal phenotype. This lethal phenotype could be partially reversed in a DsbA$^-$ background (data not shown). Because of this synthetic lethal phenotype, a further protein analysis could not be carried out.

In order to determine whether loss of physical interaction between mutant

AcrB and TolC caused the increased drug sensitivity, an attempt was made to co-

purify AcrA and TolC with AcrB. If the alterations in the loops caused AcrB to

not to physically interact with AcrA or TolC, AcrA and TolC should not be able

to co-purify with AcrB. To test this, membranes were prepared from cells

expressing a His-tagged and cysteine-less AcrB, as well as AcrB$_{\Delta L1}$ and

AcrB$_{PAL1/L2}$ followed by overnight solubilization in AcrB extraction buffer (5 mM

imidazole, 20 mM Tris-HCl pH 8.0, 500 mM NaCl, 1% DDM). Insoluble

fractions were spun down and the soluble fraction was applied to a nickel

chelating column (GE Healthcare) pre-equilibrated with AcrB extraction buffer

containing 0.03% DDM. The samples were washed in a similar buffer (20 mM

Tris-HCl pH 8.0, 500 mM NaCl, 0.03% DDM, 2 mM PMSF) with increasing

concentrations of imidazole (5 mM, 20 mM, 50 mM, and 100 mM). Finally the

protein was eluted with AcrB Elution Buffer and analyzed on a 7.5% SDS

polyacrylamide gel.

By Coomassie staining, the eluted protein was determined to be of

relatively high purity (data not shown). Additionally, when the samples were

probed for AcrA it co-puirified with AcrB, AcrB$_{\Delta L1}$, and AcrB$_{PAL1/L2}$ at relatively

similar levels (Tikhonova and Zgurskaya, 2004; Fig 15A). This indicates that

even though the complex is not functioning properly to pump out antibiotics,

AcrA and mutant AcrB are able to interact with one another physically.
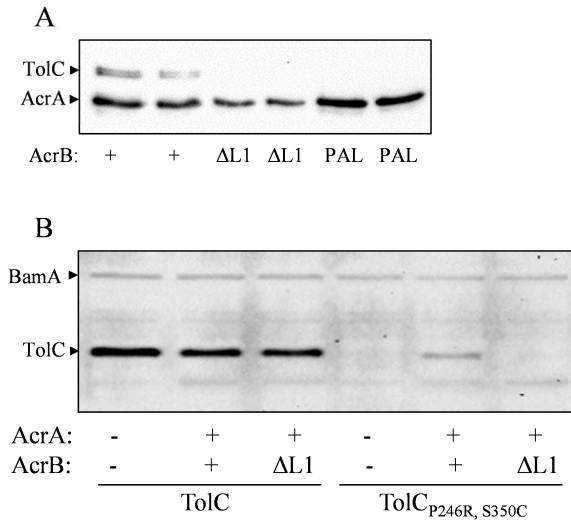
Figure 15. Deletion of AcrB Loop 1 causes defects in interaction with TolC.
A. AcrB proteins was performed as described by Tikhonova *et al*. 2011. Elutes
were probed for TolC and AcrA using α-TolC-MBP and α-AcrA$_{His}$ antibodies.
Mutation of AcrB hairpin loops prevents TolC, but not AcrA, from co-purifying
with AcrB. The AcrB$_{\Delta L1}$ mutant is designated by ΔL1, while PAL indicates the
AcrB$_{PAL1/L2}$ mutant.
B. Stabilization of TolC$_{P26R, S350C}$ was determined by analyzing whole cell extracts
from overnight cultures as described in Figure 2. Wild type TolC is normally
stable and does not depend on functional interaction with AcrA or AcrB. The
labile TolC$_{P246R, S350C}$ mutant is readily degraded in the absence of AcrA and
AcrB, as well as in the AcrB$_{\Delta L1}$ mutant background.

Interestingly, no TolC was able to be co-purified with the AcrB mutants, indicating an aberrant interaction between the mutant AcrB protein and TolC.

A second method to investigate interaction between the mutant AcrB proteins and TolC was employed. For this a labile TolC mutant ($TolC_{P246R, S350C}$), whose stability is dependent on functional complex assembly with AcrA and AcrB was utilized (Gerken and Misra, 2004). As can be seen, when AcrA and AcrB are missing, the TolC protein is readily degraded, however, when AcrA and AcrB are normally expressed from the plasmid vector, the protein is stabilized. When the mutant TolC was combined with $AcrB_{\Delta L1}$, TolC is again readily degraded, indicating that $AcrB_{\Delta L1}$ is unable to properly recruit and stabilize TolC (Fig 15B).

After observing that $AcrB_{\Delta L1}$ is unable to stabilize $TolC_{P246R, S350C}$, it was questioned whether the AcrB mutant is defective in interaction with wild type TolC. To test this, the technique of surface plasmon resonance (SPR) was employed. (This work was carried out in collaboration with the lab of Dr. Helen Zgurskaya.) In short, variants of TolC containing a single cysteine in the exterior loops were used for biotinylation and adherence to a glass chip. These cysteine variants were tested for their ability to complement a *tolC* null strain. Both of these cysteine derivatives of TolC were able to fully complement *tolC* null with regards to both export and import related functions. Sensitivity to novobiocin, erythromycin, and SDS were used to determine that the TolC cysteine variants maintained functional interaction with AcrA and AcrB (Table 4). Additionally,

Table 4. Characterization of TolC cysteine mutants used in Surface Plasmon
Resonance.

| TolC Protein[b] | Sensitivity to Select Inhibitors[a] | | | | |
	Novo	Ery	SDS	TLS	E1
TolC-	19.1	17.4	23.0	10^{-10}	2^{-11}
TolC$_{WT}$	9.2	12.6	6.6	1	1
TolC$_{A269C}$	10.1	12.6	6.6	1	2^{-1}
TolC$_{T272C}$	10.5	13.3	6.6	1	2^{-1}

[a] Numbers for Novo, Ery, and SDS indicate zones of inhibition as described in
Figure 2 and Table 1. Sensitivity to TLS phage and colicin E1 were determined
by spotting either 10- or two-fold serial dilutions onto a lawn of bacteria, fold
differences are listed.
[b] TolC proteins were expressed from the pTrc99a vector in a ΔtolC strain.
Alterations are of the mature protein sequence.

sensitivity to TLS phage and colicin E1 were used to determine whether the TolC variants were properly folding and inserting into the outer membrane. Both of these variants show no defect in their abilities to be used as a receptor for the TLS phage or colicin E1. These data indicate that both of these mutants could be used for immobilization and examination of their ability to bind to AcrB wild type or the loop mutants. After immobilizing the TolC$_{A269C}$ mutant to the glass chip, purified AcrB or mutant AcrB was passed over and allowed to bind and washed with buffer. By observing the association/dissociation rates, it was determined that both the ΔL1 and PAL1/L2 variants showed a reduction in binding affinity compared with wild type AcrB (data not shown). The binding association between the immobilized TolC and free-floating AcrB is comparable to that obtained for immobilized AcrB and free-floating TolC (Tikonova *et al.*, 2011).

Loop Alterations do not Alter Protease Sensitivity despite Reduced Protein Levels

While characterizing the AcrB loop mutants, it was noticed that alterations of loop 2 caused complete loss of visualization of the AcrB protein levels using polyclonal AcrB$_{His}$ antibodies, indicating either reduced protein levels or altered recognition by these antibodies. In order to determine the effects on protein levels, the AcrB loop mutations were moved into pACYC184- *acrA acrB* (6His), which allowed for protein visualization via HisProbe (Sigma). When comparing protein levels, it can be seen that protein levels were significantly reduced in the PAL1/L2 variant, the N254 and D256 derivatives, and AcrB$_{\Delta L1, Q737L}$. Thus it is

A

1   2   3   4   5   6   7

B   C

1. AcrB-   5. AcrB-PAL1/L2
2. AcrB   6. AcrB-A254N
3. AcrB-ΔL1   7. AcrB-A256D
4. AcrB-ΔL1, Q737L
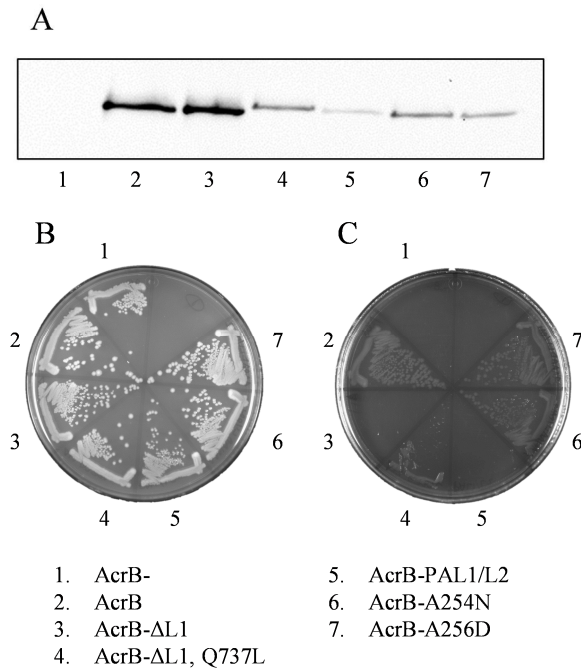
Figure 16. AcrB levels do not correlate with antibiotic resistance.
A. Membranes isolated from approximately 7.5×10^8 cells were heated to 60°C
for 10 min and analyzed on 7.5% acrylamide gels. Samples were probed with
HisProbe-HRP to determine relative amounts of AcrB mutant proteins. While
AcrB$_{ΔL1}$ shows the greatest sensitivity to substrates, it shows no decrease in
HisProbe recognition. AcrB$_{PAL1/L2}$ shows the lowest protein levels, yet has a less
severe phenotype than AcrB$_{ΔL1}$.
B and C. Relative growth of the AcrB mutant strains on medium without (B) or
with (C) the substrate inhibitors: novobiocin, erythromycin, and SDS. A single
colony was purified on medium with or with substrates and growth was
determined after 16 hr at 37°C. Medium was supplemented with 5 μg ml^{-1}
novobiocin and erythromycin, and 0.1% SDS. Deletion of AcrB loop 1 residues
leads to a drug hypersensitivity phenotype which is reversed by the Q737L
intragenic suppressor. Similarly, simultaneous alteration of both AcrB loop
residues to alanine increases sensitivity to substrate drugs, which is reversed by
restoring N254 or D256 in the AcrB$_{PAL1/L2}$ mutant.
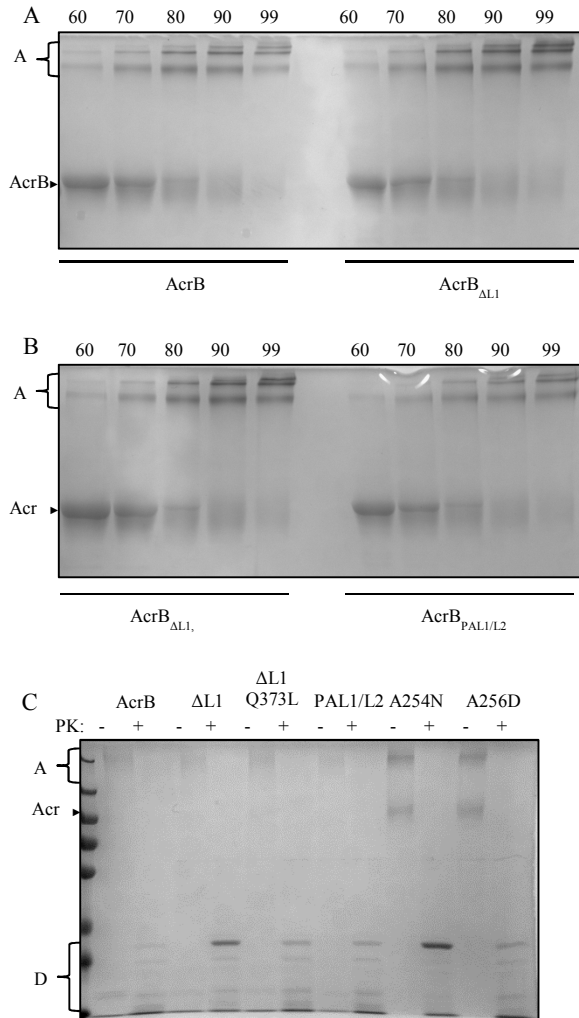
Figure 17. AcrB thermostability and protease sensitivity profiles.

A and B. Thermostability of AcrB wild type and mutants was determined by exposing purified AcrB to varying temperatures (60-99°C) for 10 min. Mutant AcrB proteins do not show an increased propensity to aggregate at elevate temperatures compared to wild type. Approximately 4 µg of purified protein was loaded for each temperature.

C. Approximately 4 µg of purified AcrB protein was treated for 5 min with Proteinase K (PK; 10 µg) at 25°C. Samples were analyzed by SDS-PAGE and proteins were visualized after staining with Coomassie brilliant blue. Mutant AcrB proteins do not cause significant changes in the degradation fragments generated by PK.

possible that the reduced protein levels contribute to the antibiotic

hypersensitivity phenotype observed. It has been shown that increasing expression

of AcrAB leads to increased resistance to the substrate antibiotics. However it can

be seen that the $AcrB_{\Delta L1}$ protein is present at roughly the same level as wild type

AcrB, but confers significantly less resistance, whereas $AcrB_{\Delta L1, Q737L}$ is present at

even lower levels and yet confers resistance similar to wild type. Additionally,

$AcrB_{PAL1/L2}$, $AcrB_{AANAA\ L1/PAL2}$ and $AcrB_{AAAAD\ L1,\ PAL2}$ are present at similar

levels, but $AcrB_{AANAA\ L1/PAL2}$ and $AcrB_{AAAAD\ L1/PAL2}$ confer antibiotic resistance

but $AcrB_{PAL1/L2}$ does not (Fig 16). In order to determine whether the loop

alterations cause AcrB to become unstable and therefore unable to interact with

TolC, the thermostability and protease sensitivity of the purified AcrB mutant

proteins were tested. If the mutants showed different profiles than wild type AcrB,

it would show that these alterations are causing a gross defect in protein structure,

resulting in premature aggregation of the protein or exposing protease sensitive

sites which are typically buried in the protein but are now exposed to due to

altered conformation. To test the thermostability of the AcrB mutants, equivalent

amounts of purified protein were heated to temperatures between 60 and 99°C in

10°C intervals. Samples were then analyzed on 7.5% acrylamide gels and stained

with coomassie brilliant blue. As can be seen, the three mutants ($AcrB_{\Delta L1}$,

$AcrB_{\Delta L1, Q737L}$, and $AcrB_{PAL1/L2}$) show no difference in thermostability compared

to wild type AcrB (Fig 17A and B). Additionally, after incubation with proteinase

K for 5 minutes, wild type and mutant proteins showed the same pattern of

degradation (Fig 17C). This indicates that while the mutant protein levels are decreased *in vivo,* the population that localizes to the membrane has conformations similar to wild type.

Intragenic Suppressor of AcrB ΔLoop 1 Acts by Promoting Functional Complex Assembly

Since the $AcrB_{\Delta L1}$ mutant showed a more drastic phenotype, it was favorable to look for spontaneous antibiotic resistant suppressors. These suppressor mutations could potentially identify other regions of importance involved in complex assembly. The majority of suppressors mapped to AcrA and will be discussed in Chapter 3. However, a single AcrB missense mutation was obtained through selection in the presence of novobiocin, erythromycin, and sodium dodecyl sulfate (SDS). This mutation was then confirmed by site-directed mutagenesis on the pACYC184- *acrA acrB* ($AcrB_{\Delta L1}$) plasmid. Additionally, this alteration was introduced into the pACYC184- *acrA acrB* ($AcrB_{PAL1/L2}$) plasmid.

When the alteration was moved into these plasmids, its ability to suppress both AcrB mutant proteins was tested by growth on plates and disk sensitivity assays (Fig 18B). As seen by both increased growth on plates containing inhibitors (16B) and smaller zones of inhibition (Fig 18B), this intragenic suppressor is able to reduce antibiotic sensitivity of cells expressing $AcrB_{\Delta L1}$ or $AcrB_{PAL1/L2}$ mutant proteins (Fig 18B and C). This indicates that while these two

68
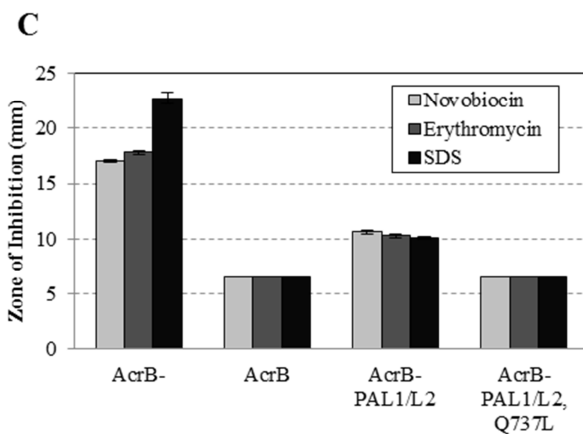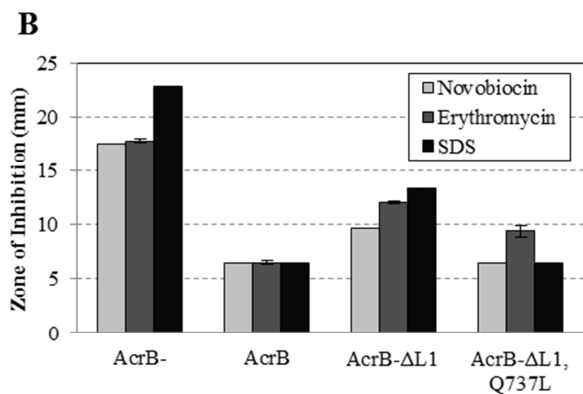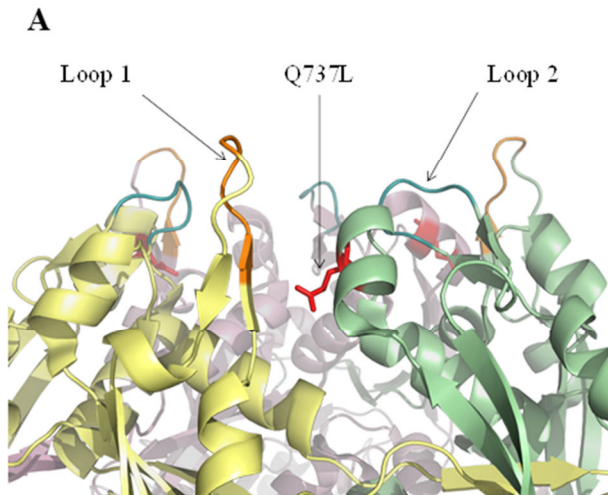
Figure 18. Intragenic suppression of an AcrB loop mutant.

A. A cartoon showing the X-ray structure of AcrB (2GIF). The location of the intragenic suppressor of AcrB Δ Loop 1 is shown in relation to the hairpin loops. Loop 1 and Loop 2 are shown in each of the monomers and pointed out in monomer A and monomer B, respectively.

B and C. Sensitivity to substrate inhibitors. Zones of inhibition around pre-soaked novobiocin (30 µg) and erythromycin (15 µg) disks are shown in millimeters (mm). For SDS, a 10 µl of solution containing 1 mg of SDS was spotted on paper disks of 6.5 mm diameter. Average inhibition zones recorded from three independent assays are shown, with zones varying no greater than 10%.
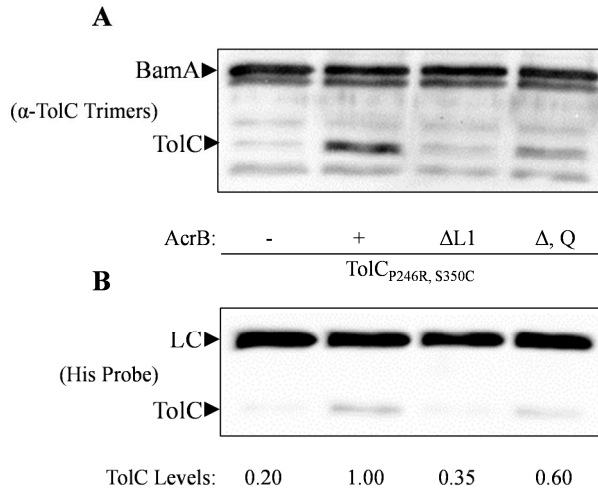
Figure 19. Intragenic suppressor of AcrB$_{\Delta L1}$ acts to stabilize functional complex assembly. Whole cell extracts from approximately 5 x 10^7 cells from overnight cultures were probed for the stabilization of TolC$_{P246R, S350C}$. Relative amounts of TolC were determined using either BamA or the Loading Control (LC). TolC$_{P246R, S350C}$ levels for wild type AcrB were taken as 1 and mutant levels were adjusted accordingly. Protein levels were determined from four independent gels with amounts varying no greater than 10%.

loop alterations show slightly different phenotypes, they both cause a similar defect.

Next it was inquired whether the Q737L substitution caused increased resistance to antibiotics by stabilizing complex assembly. This was tested by examining the *in vivo* stability of a labile $TolC_{P246R, S350C}$ protein that readily degrades in the absence of other complex members. An increase in the $TolC_{P246R, S350C}$ level in the $AcrB_{\Delta L1, Q737L}$ background would indicate stable complex formation. As can be seen in Figure 19, $AcrB_{\Delta L1, Q737L}$ increases $TolC_{P246R, S350C}$ protein levels roughly 2-fold over $AcrB_{\Delta L1}$.

Opening of the TolC Aperture Restores Antibiotic Resistance of the AcrB Loop Mutants

In the proposed mechanism of TolC-AcrAB interaction, it is thought that TolC and AcrB directly interact with one another to facilitate the initial steps of aperture opening. If alterations in the AcrB loops disrupt this interaction, thus preventing TolC aperture opening, it is possible that an alteration in TolC that forces the TolC aperture open could reverse the antibiotic hypersensitivity phenotype of $AcrB_{\Delta L1}$ and $AcrB_{PAL1/L2}$ mutants. To test this, two different TolC alterations were employed. In one case, the aperture closing was directly influenced by a R367E substitution that disrupts critical salt bridges at the aperture (Andersen *et al.*, 2002; Augustus *et al.*, 2004; Bavro *et al.*, 2008). In the second case, the aperture closing was indirectly influenced by a R390E

72

substitution that affects supercoiling of TolC inner helices guarding the aperture (Augustus *et al*., 2004; Bavro *et al*., 2008).

As can be seen by decreased zones of inhibition, forced opening of the TolC aperture can partially reverse the hypersensitivity phenotype observed in the AcrB$_{\Delta L1}$ (Fig 20). Interestingly, when grown on plates containing the same concentration of antibiotics used for selection of spontaneous drug resistant mutants, neither of the two open state TolC substitutions with AcrB$_{\Delta L1}$ were able to grow indicating that while forcing open the TolC aperture decreases sensitivity to substrate antibiotics, permanent opening of the aperture cannot completely complement the hypersensitivity to the same degree as suppressor alterations in AcrB or AcrA (data not shown). Permanent opening the aperture may allow substrates to pass back through the open TolC channel and was ultimately selected against in our genetic selection. While the open state TolC mutants showed limited restoration of growth for AcrB$_{\Delta L1}$ on plates containing substrate inhibitors, these TolC alterations significantly improved growth of AcrB$_{PAL1/L2}$ on selection medium (data not shown).
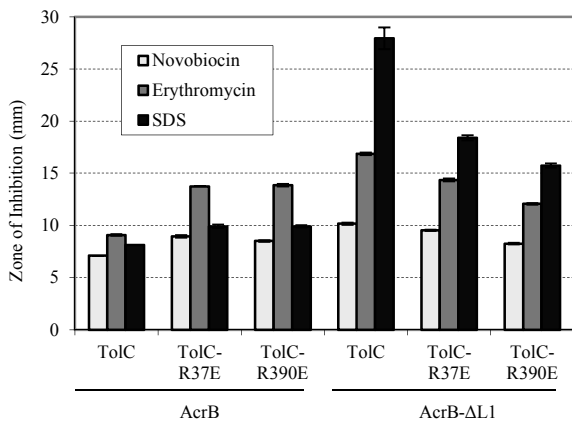
Figure 20. Opening of the TolC aperture suppresses AcrB Δloop 1 mutation. Sensitivity assays were performed as described in Figure 2 and Table 1. While mutations which affect the TolC aperture cause increased sensitivity to substrate inhibitors, these mutations reduce the hypersensitivity phenotype observed in the AcrB$_{\Delta L1}$ mutant. Zones are an average of two independent cultures and vary no greater than 10%.

Results 3: AcrA Suppressors of TolC and AcrB Interaction Defective Mutants

Isolation of Suppressors of the TolC Turn 1 Drug Hypersensitive Mutant

Chemical cross-linking failing to reveal defects in interaction of TolC$_{147AGSG150}$ turn 1 with AcrA and AcrB.Thus, reversion analysis was carried out to look for suppressors that could provide insight into the mutant TolC's defect. The TolC turn 1 $_{147}$AGSG$_{150}$ mutant is unable to stabilize AcrA$_{L222Q}$, indicating that the mutant TolC protein is unable to functionally interact with AcrA or AcrB. If so, it is possible that compensatory alterations in TolC, AcrA, or AcrB would be able to restore functional interaction between the members of the complex and restore efflux activity. In order to obtain antibiotic resistant revertants, two antibiotics, novobiocin and erythromycin, were simultaneously used in selection so as to prevent mutations which affect the cellular targets of these antibiotics. Approximately 5 X 10^8 cells from 24 independent cultures were incubated on selection medium at 37°C for 20 h. Nineteen of the 24 cultures produced a total of 55 antibiotic resistant revertants at a frequency of about 5 x 10^{-8}, indicating the presence of missense mutations. To determine whether the mutations mapped with the plasmid DNA, which expresses the *tolC* gene, plasmids were extracted and transformed into a Δ*tolC* strain and transformants were grown on selection medium. In no cases did the mutation move with the plasmid. P1 transductional mapping using a linked marker, Tn*10*-Tc^r, which co-
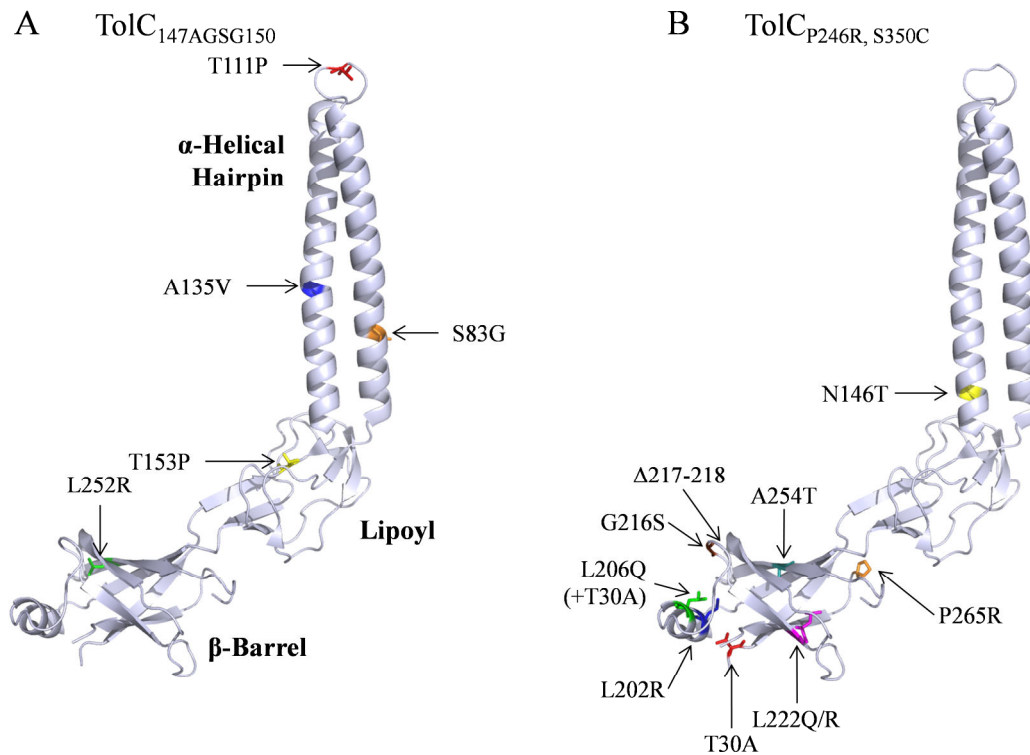
Figure 21. A cartoon showing X-ray structures of AcrA (2F1M). Locations of five AcrA substitutions obtained in this study and those obtained previously (Gerken and Misra, 2004) are shown in A and B, respectively. AcrA residue numbering corresponds to that of the mature protein.

transduces with the *acrAB* loci (40% co-transducible by P1 phage) was carried

out. In all cases the mutation moved with the Tn*10* marker at the expected

frequency, indicating the mutations mapped in or near the *acrAB* genes.

Nucleotide sequence analysis was carried out from PCR-amplified *acrAB*

DNA for 24 of the 55 revertants, representing different phenotypes and multiple

independent cultures. Five different missense mutations were identified in the

acrA gene corresponding to single amino acid substitutions within the mature

AcrA sequence: an A135T alteration was isolated once, while S83G, T111P,

T153P, and L252R were obtained in seven, three, eight, and five isolates,

respectively. These alterations map to three crystallized domains of AcrA: S83G,

T111P, and A135T to the α-helical hairpin, T153P to the lipoyl, and L252R to the

β-barrel domain (Fig 21A). Despite affecting some of the same domains, the five

suppressors isolated in this study affect different AcrA residues than 10

previously isolated AcrA suppressors of an assembly defective TolC (Gerken and

Misra, 2004; Fig 21B).

As expected, the AcrA suppressors decreased the hypersensitivity

phenotype observed in the TolC$_{147AGSG150}$ mutant. The increase in resistance to

CCCP is consistent with this data and that of Colmer *et al*. (1998) that shows

AcrAB can confer resistance to this inhibitor independent of EmrAB (Table 5 and

6). The suppressors, however, do not restore interaction with other efflux pumps

nor have they gained a new ability to secrete substrates which are not recognized

Table 5. Sensitivity of wild type TolC, mutant TolC, and mutant TolC containing AcrA suppressors to various inhibitors.

TolC and AcrA proteins[a]	Sensitivity to inhibitors[b]			
	Novobiocin	Erythromycin	CCCP	HlyA
$TolC_{WT}$ $AcrA_{WT}$	15.80	61.60	11.20	+
$TolC_Q$ $AcrA_{WT}$	1.00	1.82	0.97	-
$TolC_Q$ $AcrA_{S83G}$	2.00	7.15	1.05	-
$TolC_Q$ $AcrA_{T111P}$	3.60	24.60	2.50	-
$TolC_Q$ $AcrA_{A135T}$	3.80	13.50	1.20	-
$TolC_Q$ $AcrA_{T153P}$	7.70	13.70	2.70	-
$TolC_Q$ $AcrA_{L252R}$	14.50	31.10	4.20	-

[a] $TolC_Q$ denotes the turn 1 $TolC_{147AGSG150}$ mutant.

[b] Numbers for novobiocin, erythromycin, and CCCP represent minimal inhibitory concentrations ($\mu g\ ml^{-1}$). Plus and minus indicate the presence (+) or absence (-) of hemolytic zones on blood agar medium. For hemolysin sensitivity tests, strains were transformed with a plasmid containing the entire hemolysin operon.

Table 6. Effects of *acrAB* and *emrAB* mutations on CCCP resistance.

Strain	MIC[a]
Wild type	8-16
Δ*acrAB*	4-8
Δ*emrAB*	4-8
Δ*acrAB*, Δ*emrAB*	2-4
Δ*tolC*	1

[a] Minimal inhibitory concentrations were done by a two-fold dilution method. The inhibitor was mixed with approximately 5 x 10^5 cells/ml. Cultures were incubated at 37°C for 18 h without shaking.

Table 7. Effects of TolC and AcrA levels in the turn 1 $_{147}$AGSG$_{150}$ mutant and wild type TolC backgrounds.

| AcrA protein | TolC$_{147AGSG150}$ mutant | | TolC wild type | |
	TolC levels[a]	AcrA levels	TolC levels	AcrA levels
AcrA$_{WT}$	0.50	1.00	1.00	1.00
AcrA$_{S83G}$	0.48	1.01	1.05	0.93
AcrA$_{T111P}$	0.54	0.64	0.87	0.66
AcrA$_{A135T}$	0.59	1.12	0.97	1.49
AcrA$_{T153P}$	0.49	1.09	0.89	1.40
AcrA$_{L252R}$	0.58	0.94	1.00	1.25

[a] Protein levels are an average of two independent cultures obtained from approximately 5 x 10^7 cells. Wild type TolC and AcrA levels were taken as 1 and the mutant TolC and AcrA protein levels were determined relative to wild type TolC and AcrA, respectively.

by the AcrB pump, as seen by no increased ability to secrete α-haemolysin (Table 5). The suppressor alterations do not increase TolC levels. In only one case were AcrA levels altered: the T111P mutant showed decreased AcrA protein levels regardless of whether it was in the turn1 $_{147}$AGSG$_{150}$ or wild type TolC background (Table 7). Thus, this alteration appears to change AcrA's conformation and stability independent of TolC. Isolation of mutations in *acrA* which suppress the TolC turn 1 $_{147}$AGSG$_{150}$ quadruple mutant, along with the observation that this mutant TolC is not able to stabilize AcrA$_{L222Q}$ or AcrA$_{P265R}$ suggests the mutant TolC causes a defect in interaction with wild type AcrA and that specific alterations in AcrA are able to restore the aberrant interaction between the mutant TolC and AcrB.

AcrA Mapping Suppressors Act to Open the TolC Aperture

Several proposed mechanisms of the interaction between the three members of the complex predict that AcrA plays an active role to transmit conformational energy from AcrB to TolC (Fernández-Recio *et al*., 2004; Murakami *et al*., 2006; Seeger *et al*., 2006; Bavro *et al*., 2008; Misra and Bavro, 2009). This mechanism envisages the large periplasmic domain of AcrB changing at its surfaces when drug/proton bound. These large shifts on AcrB's surface are felt by the membrane proximal (MP), β-barrel, and lipoyl domains of AcrA and transmitted through the α-helical hairpin of AcrA to the aperture of TolC, thereby
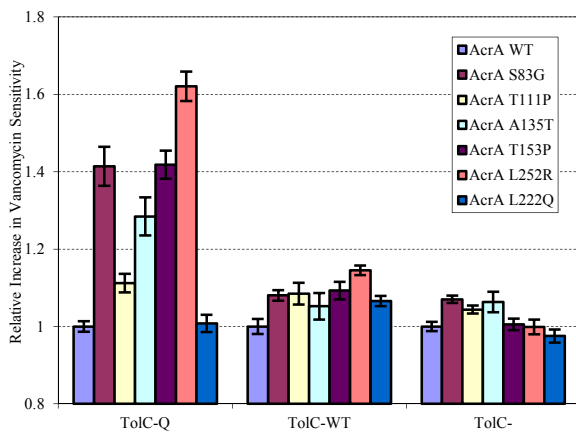
Figure 22. AcrA suppressor alterations induce opening of the mutant TolC aperture. Vancomycin sensitivity, which reflects an open state of the TolC aperture, was tested in wild type and suppressor AcrA strains expressing TolC$_{14AGSG150}$, wild type TolC (TolC-WT), or no TolC (TolC$^-$). A strain expressing AcrA$_{L222Q}$, which does not suppress TolC$_{147AGSG150}$, was included as a control. Zones of inhibition around disks soaked with vancomycin (75 µg) were measured after incubating plates for 16 h at 37°C. Average inhibition zones were recorded from three independent assays are shown as relative increase, where wild type AcrA has been taken as 1. Zones varied no greater than 10%.

forcing the aperture into an open state to allow antibiotics to be extruded from the exit ducts of AcrB into the open channel of TolC. The conformational changes AcrA is thought to undergo would allow for stable interaction between the AcrA hairpin helices and the grooves of the TolC helices. It is possible that the AcrA suppressors identified here are in a constitutively "active" form of AcrA, which wild type AcrA only transiently goes through. If this is so, it is conceivable that these AcrA suppressors would cause TolC to remain in a constitutively open state. In order to test this, vancomycin sensitivity was tested as it has been shown previously to be an effective way to monitor the open or closed state of the TolC aperture/channel *in vivo* (Augustus *et al*., 2004; Bavro *et al*., 2008).

When the TolC turn 1 $_{147}$AGSG$_{150}$ suppressors were tested, four of the five suppressors significantly increased sensitivity to vancomycin. These suppressors specifically increased this sensitivity in the TolC$_{147AGSG150}$ mutant background (Figs 22, 23, and 25). This indicates the mode of suppression for these AcrA suppressors involves constitutively dilating the TolC aperture. The last suppressor, AcrA$_{T111P}$, was able to modestly (11%) increase sensitivity to vancomycin. This mutant also showed decreased AcrA levels, so it is possible that this mutant does not show as high of sensitivity to vancomycin due to the decreased AcrA level.
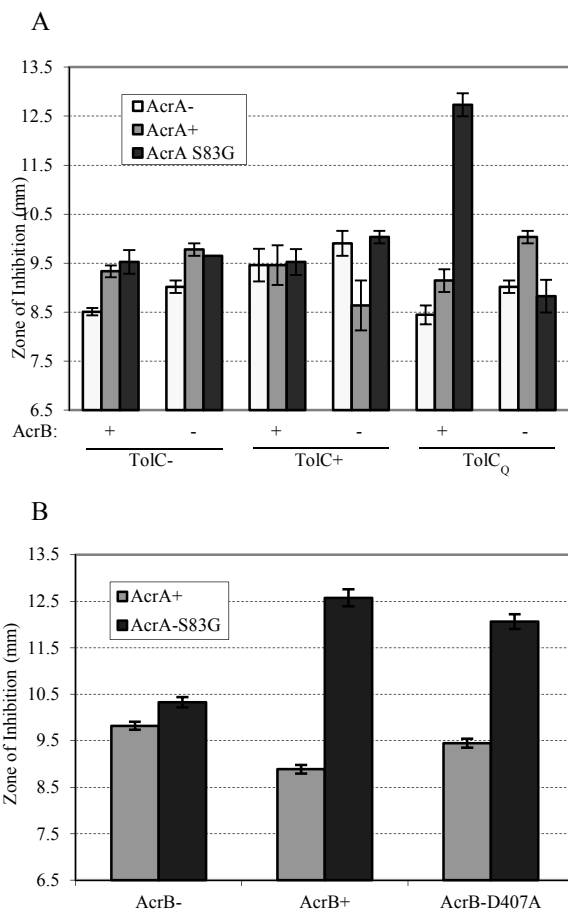
Figure 23. AcrA suppressor mediated opening of TolC is dependent on AcrB as a scaffold.

A. Sensitivity to vancomycin was used to determine whether opening of the TolC turn 1 $_{147}$AGSG$_{150}$ mutant was dependent on the presence of AcrB. Only in the presence of AcrA$_{S83G}$ and AcrB was the TolC$_{147AGSG150}$ (TolC$_Q$) mutant able to be opened, causing sensitivity to vancomycin. As can be seen in the control experiments, the absence of TolC, AcrA, or AcrB cause increased sensitivity.

B. As sensitivity to vancomycin was only observed in the presence of AcrA$_{S83G}$ along with wild type, we tested whether this was attributed to the functionality of AcrB. A D407A mutation was introduced in AcrB which prevents proton translocation and therefore functional rotation. Vancomycin sensitivity caused by AcrA$_{S83G}$ was still observed in the AcrB$_{D407A}$ mutant, indicating AcrA$_{S83G}$ mediated vancomycin sensitivity requires the physical presence of AcrB.

Assays were performed as described in Figure 2 and Table 1. Zones are of two independent cultures and vary no greater than 10%.

84

AcrA Suppressors Require AcrB to Open the TolC Aperture

After observing that the AcrA suppressors act to open the TolC aperture in the presence of the mutant TolC, it was inquired whether the opening of TolC was dependent on AcrB. To test this, the AcrA$_{S83G}$ mutant was introduced into the pACYC184 plasmid containing the *acrA* gene (Weeks *et al.*, 2010). This, along with wild type AcrA, or the empty vector were introduced into a Δ*tolC* Δ*acrA* *acrB*$^+$ or Δ*tolC* Δ*acrAB* strain in which TolC wild type, TolC$_{147AGSG150}$, or pTrc99a empty vector had also been transformed. Vancomycin sensitivity was observed in these strains. Interestingly, increased sensitivity to vancomycin was only observed in the presence of the TolC turn 1 mutant, AcrA$_{S83G}$, and AcrB (Fig 23A). The AcrA suppressor showed sensitivity to vancomycin in the presence of AcrB, which could have been used as a scaffold, a source of energy or both. To determine this, an AcrB$_{D407A}$ alteration was introduced into plasmids expressing wild type AcrA and AcrA$_{S83G}$. In AcrB, D407 is one of the key residues involved in proton translocation and therefore energizing AcrB (Takatsuka and Nikaido, 2006). In addition to the two plasmids expressing either AcrA$_{S83G}$ or wild type AcrA along with AcrB$_{D407A}$, plasmids expressing either wild type or AcrA$_{S83G}$ with or without wild type AcrB were transformed into a Δ*tolC* Δ*acrAB*/pTrc99a-*tolC* (TolC$_{147AGSG150}$) strain. When tested for sensitivity to vancomycin, the AcrA$_{S83G}$ suppressor showed sensitivity in the presence of both wild type and the AcrB$_{D407A}$ mutant backgrounds. From this, it was concluded that the AcrA

suppressors are in a conformation such that AcrB is required only as a scaffold in order to open the TolC aperture (Fig 23B).

Combined Effects of TolC Open State Mutants and AcrA Suppressors

After observing the AcrA suppressors increased sensitivity to vancomycin and the TolC$_{147AGSG150, R390E}$ mutant was able to partially reverse the antibiotic hypersensitivity phenotype of the TolC$_{147AGSG150}$ mutation, it was inquired whether the AcrA suppressors and the TolC open state mutants would act in the same pathway to reduce sensitivity to substrate antibiotics. If the AcrA suppressors and TolC$_{147AGSG150, R390E}$ were both acting to open the TolC aperture, an additive affect might be observed with regards sensitivity to novobiocin and vancomycin. Plasmids expressing the TolC$_{147AGSG150, R367E}$ or TolC$_{147AGSG150, R390E}$ mutants were introduced into a Δ*tolC acrA* strain, where the AcrA proteins expressed were either wild type or a suppressor variant.

All of the AcrA suppressors reduced novobiocin sensitivity in both the TolC$_{147AGSG150, R367E}$ (Fig 24A) and TolC$_{147AGSG150, R390E}$ (Fig 24B) backgrounds while increasing mutant TolC levels between 18 and 200%. This indicates that the AcrA suppressors are acting to stabilize the complex. Interestingly, when the AcrA suppressors were in a TolC$_{147AGSG150}$ background, they showed different increases in vancomycin sensitivity without significantly altering TolC levels (Fig 22 and 25, Table 7), but in the TolC$_{147AGSG150, R367E}$ or TolC$_{147AGSG150, R390E}$ background all the suppressors showed similar sensitivities to vancomycin (Fig

86
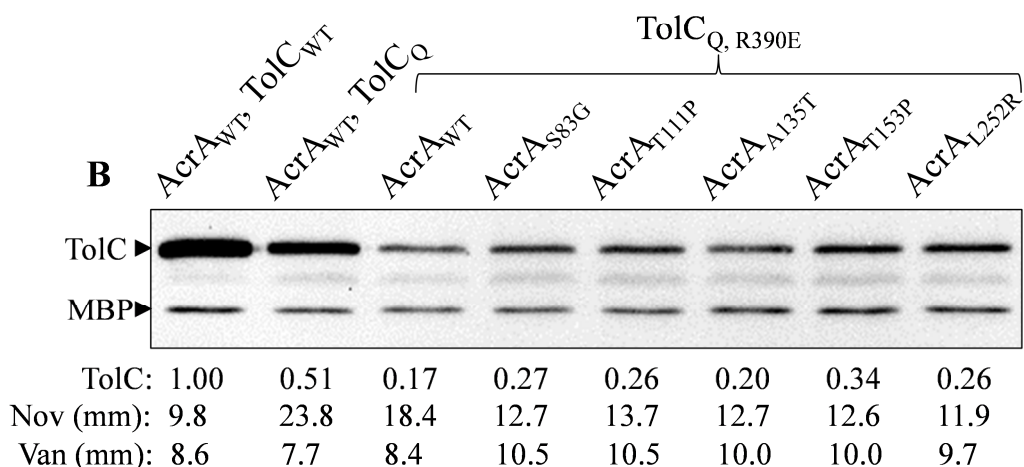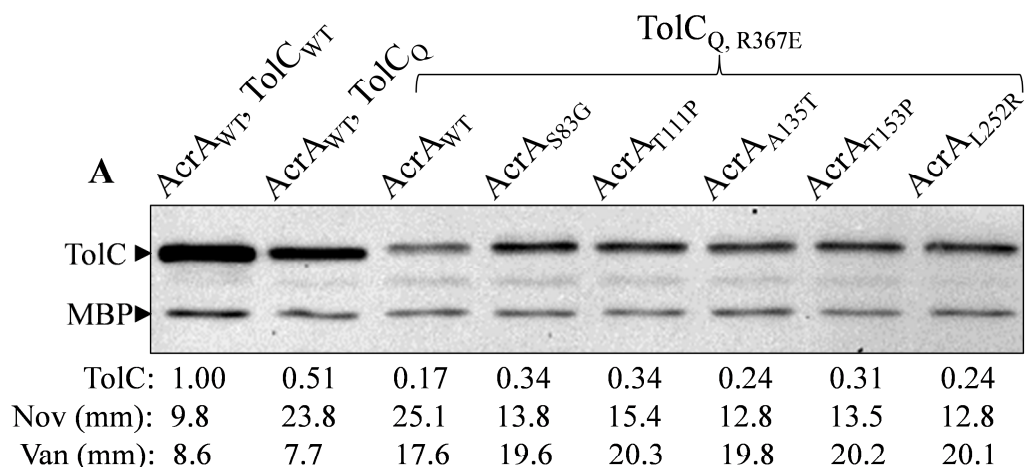
Figure 24. Combined effects of TolC alterations which influence the TolC aperture/channel opening and various AcrA suppressors on $TolC_{147AGSG150}$. Effects of various AcrA suppressors on $TolC_{147AGSG150, R367E}$ (A) and $TolC_{147AGSG150, R390E}$ (B) levels and novobiocin and vancomycin sensitivities. $TolC_Q$ denotes the turn 1 $_{147}AGSG_{150}$ mutant. Proteins were detected by Western blots as described in Fig. 2 legend. Antibiotic sensitivities were described as in Fig. 2 and Tables 1 legends. Average inhibition zone diameters were plotted from two independent experiments, with zones varying no greater than 10%.

24). This seems to show that increased vancomycin sensitivity is a product of increased TolC stability and not due to individual effects of the AcrA suppressors. In other words, there was not an additive effect of the open state TolC alterations and the activity of AcrA suppressors to further open the TolC aperture/channel.

Suppression Specificity

Previously an assembly-defective TolC mutant ($TolC_{P246R, S350C}$) and 10 AcrA mutants which stabilize the defective TolC were described (Gerken and Misra, 2004). These alterations affect different residues within the same domains of AcrA. In order to determine whether these alterations could reverse the defect caused by the $TolC_{147AGSG150}$ turn 1 mutant, the plasmid expressing this mutant was transformed into each of the 10 AcrA mutant backgrounds and sensitivity to both novobiocin and vancomycin was determined. Six of the 10 AcrA suppressors of $TolC_{P246R, S350C}$ were unable to suppress the novobiocin hypersensitivity phenotype, indicating an allelic bias towards $TolC_{P249R, S350C}$ (Fig 25). The remaining four AcrA alterations caused a modest decrease in novobiocin sensitivity, however showed minimal increase in vancomycin sensitivity (less than 8% of wild type AcrA; Fig 24). In contrast, the majority of the AcrA suppressors isolate in this study showed significant (greater than 28%; Figs 22 and 25) increases in vancomycin sensitivity, suggesting the cross suppression of the previous AcrA suppressors is through complex stabilization and not TolC aperture/channel opening.
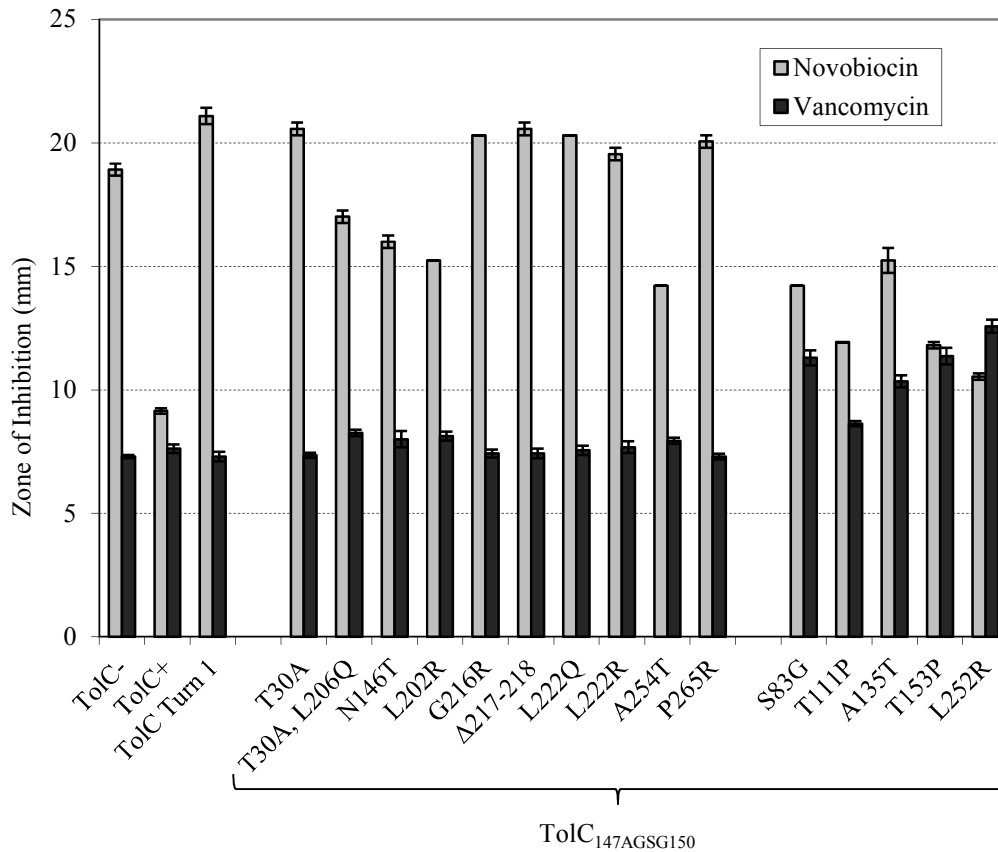
Figure 25. Effects of different AcrA suppressors on efflux function and TolC aperture in a background expressing the TolC turn 1 mutant (TolC$_{147AGSG150}$). These were assessed by the use of novobiocin and vancomycin, respectively. Control strains expressing wild type AcrA expressing no TolC (TolC-), wild type TolC (TolC-WT), or TolC turn 1 mutant (TolC$_{147AGSG150}$) were observed simultaneously. AcrA suppressors of TolC$_{P246R, S350C}$ show allelic specificity against TolC$_{147AGSG150}$ turn 1 mutation and those suppressors that do decrease sensitivity to novobiocin do so without altering the aperture. Conversely, suppressors isolated against TolC$_{147AGSG150}$ increase sensitivity to vancomycin, indicating aperture opening. Zones of inhibition are shown as the average of two independent cultures with zones varying less than 10% and were carried out as described in Figure 2 and Table 1.

	AcrA$_{Wt}$	AcrA$_{Wt}$	AcrA$_{Wt}$	AcrA$_{S83G}$	AcrA$_{T111P}$	AcrA$_{A135T}$	AcrA$_{T153P}$	AcrA$_{L252R}$
TolC levels:	1.00	0.00	0.03	0.15	0.07	0.20	0.05	0.32
Nov (mm):	8.9	20.5	17.8	13.2	14.7	11.9	15.5	11.7
Van (mm):	7.6	7.3	7.3	8.3	8.0	8.0	7.1	8.1
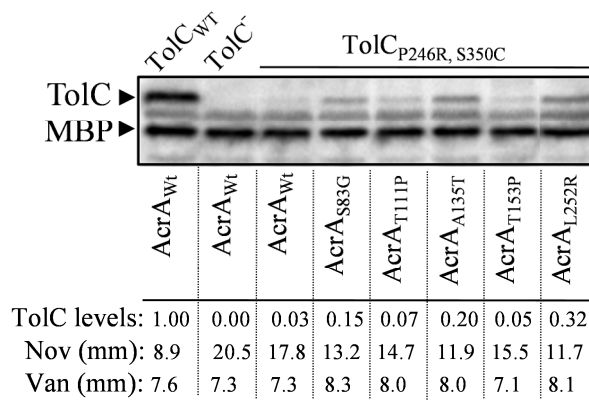
Figure 26. AcrA suppressors of TolC$_{14AGSG150}$ stabilize TolC$_{P246R, S350C}$. By introducing TolC$_{P246R, S350C}$ into the AcrA suppressors of TolC$_{147AGSG150}$ backgrounds, stabilization of TolC$_{P246R, S350C}$ could be measured and sensitivity to inhibitors was measured. These AcrA suppressors are generally able to restore antibiotic resistance lost by the TolC mutant. Additionally, these suppressors increase TolC levels significantly. Relative protein levels were assessed on cell extracts from approximately 5 x 10^7 cells. Wild type TolC levels were determined using MBP as a loading control and mutant TolC levels were adjusted relative to wild type TolC. Zones of inhibition are the average of three independent cultures with zones varying no greater than 10% and were performed as described in Figure 2 and Table 1.

It was subsequently questioned whether the AcrA mutants isolated in this study could stabilize the labile $TolC_{P246R, S350C}$ protein and reverse the antibiotic sensitivity phenotype. All of the AcrA mutations significantly (2 to 10 fold) increased $TolC_{P246R, S350C}$ levels, as well as reduced antibiotic sensitivity, indicating functional complex assembly (Fig 26). As was seen with wild type TolC, the AcrA mutants showed no increase in sensitivity to vancomycin; suggesting that aperture opening as a means of suppression was specific to $TolC_{147AGSG150}$ and that cross suppression is primarily achieved through inducing functional complex assembly.

Secondary Alterations within AcrA Stabilize $AcrA_{L222Q}$

As described in the first chapter, $AcrA_{L222Q}$'s stability is dependent on TolC. Accordingly, the mutant AcrA protein is readily degraded in the $TolC_{147AGSG150}$ mutant background, indicating weak interactions between $AcrA_{L222Q}$ and TolC turn 1 $_{147}AGSG_{150}$. Antibiotic resistance revertants of the $TolC_{147AGSG150}/AcrA_{L222Q}$ mutant were sought, so that $AcrA_{L222Q}$'s stability can be used to determine the suppression mechanism. In nine of the 28 revertants, the suppressor mutations were mapped to the plasmid DNA expressing the *tolC* gene. For the remaining 19 revertants, genetic mapping using a Tn*10* marker linked to the *acrAB* loci (40% co-transducible) was carried out. In nine cases, the suppressor mutation was found to be linked to the Tn*10* marker. DNA corresponding to the *acrAB* region was amplified by PCR from these revertants

A

B

			L222Q	S83G	G110A	G110D	T111A	T111S	A135V	N146Y
AcrA:	1.00	1.00	0.04	0.07	0.24	0.09	0.15	0.13	0.09	0.07
Novo:	9.6	19.3	21.3	11.9	12.2	13.5	11.4	11.8	11.8	13.5
Ery:	10.8	19.3	19.2	12.3	13.5	15.0	12.5	13.7	11.8	13.0
Vanco:	7.8	7.0	7.9	11.4	8.4	8.1	8.8	9.2	10.7	11.3
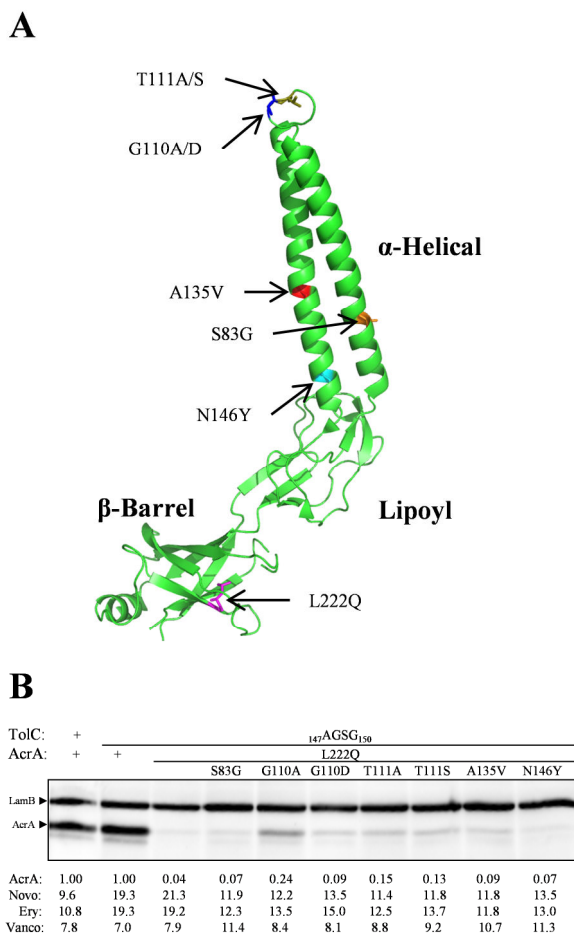
Figure 27. Secondary site substitutions within AcrA restore interaction between the TolC turn 1 $_{147}AGSG_{150}$ mutant and $AcrA_{L222Q}$.

A. A cartoon showing the X-ray structure of AcrA (2F1M). Locations of seven substitutions obtained in a screen of the $TolC_{147AGSG150}$ and $AcrA_{L222Q}$ strain. AcrA numbering corresponds to that of the mature protein.

B. AcrA protein levels were compared from whole cell extracts of approximately 5×10^8 cells from overnight cultures. Wild type AcrA was taken as 1.0 and mutant levels are relative to this. Sensitivity to select inhibitors is listed as zones of inhibition (mm) around 6 mm disks soaked with novobiocin (30 µg), erythromycin (15 µg), or vancomycin (75 µg) and are an average of at least 3 independent cultures with zones varying less than 10% .

and subjected to nucleotide sequencing analysis. In all cases, the DNA contained the original mutation as well as a missense mutation within the *acrA* gene leading to the following single amino acid substitutions in mature AcrA sequence: S83G, G110A, G110D, T111A, T111S, A135V, and N146Y. Interestingly, with the exception of G110, all of these locations have been previously identified in genetic screens and substitutions in these locations have been shown to stabilize functional complex assembly (Fig 27A). S83G was the only identical substitution, while the others were previously isolated at the same amino acid position. It is also interesting to note that when suppressor mutations were previously isolated there was little conservation as to which domain the suppressor alterations mapped to, however, when using the labile AcrA and turn 1 mutant TolC proteins, all the suppressor alterations map to the α-helical hairpin domain, while maintaining the original β-barrel alteration (L222Q).

In order to determine whether these suppressors were acting to stabilize the labile AcrA to restore interaction with the mutant TolC, AcrA levels were examined (Fig 27B). All of the suppressors showed increases in AcrA levels (ranging between 1.75 and 6 fold increase). Not surprisingly, the AcrA mapping suppressors of the labile $AcrA_{L222Q}$ and TolC turn 1 $_{147}AGSG_{150}$ mutant increased resistance to novobiocin and erythromycin (Fig 27B). When comparing the sensitivity to vancomycin, three (S83G, A135V, and N146Y) substitutions increase sensitivity to vancomycin (35 to 45% increase in sensitivity), whereas the remaining four substitutions (G110A, G110D, T111A, T111S) did not

93
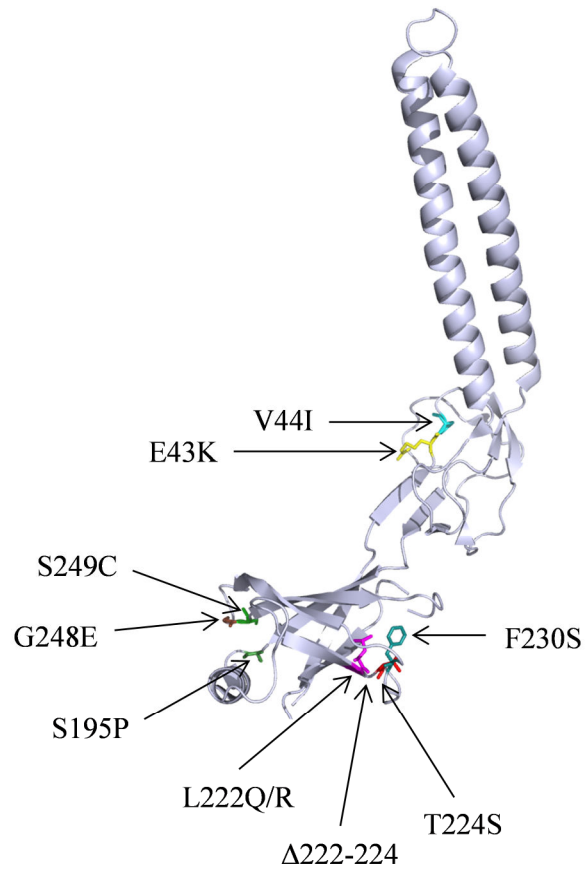
Figure 28. Location of AcrA suppressors of AcrB$_{\Delta L1}$. A cartoon showing the X-ray structure of AcrA (2F1M). Locations of ten substitutions obtained in this study are shown. AcrA numbering corresponds to that of the mature protein.

significantly alter vancomycin sensitivity. It appears that alterations in the extreme tip region of AcrA, while able to restore complex assembly, do not induce constitutive TolC aperture/channel opening, as the remaining suppressors do.

Suppressors that Overcome the Drug Hypersensitive Phenotype of the AcrB ΔLoop 1 Mutant

It was determined that the perplasmic hairpin loop 1 of AcrB is critical for drug efflux. This defect of the $AcrB_{\Delta L1}$ could be due to aberrant AcrB-TolC interactions. Drug resistant revertants of $AcrB_{\Delta L1}$ were sought to identify suppressor mutations that can help better understand the cause of the $AcrB_{\Delta L1}$ defect. To obtain suppressor alterations, approximately 5 X 10^8 cells from 46 independent cultures were plated onto selection medium containing novobiocin, erythromycin and SDS. These three inhibitors were used to prevent mutations in the target genes and assure mutations were primarily isolated within the *acrAB-tolC* genes. Twenty of the 46 independent cultures gave rise to drug resistant revertants at a frequency of about 5 X 10^{-8}. A total of 24 revertants, representingall of the 20 independent cultures and distinct growth phenotypes on selection medium were selected for further analysis. Plasmids containing the *acrAB* loci were extracted and transformed into a fresh Δ*acrAB* background to determine whether the suppressor mutations moved with the plasmid DNA. In 21 of the 24 revertants, the suppression mutation moved with the plasmid DNA.

95
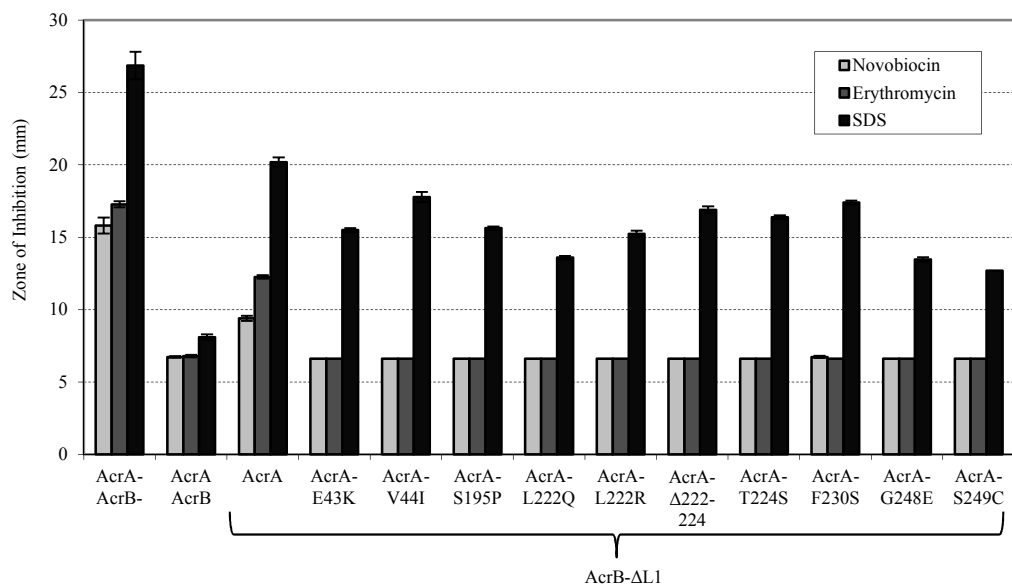
Figure 29. Antibiotic resistance is partially restored by AcrA suppressors. AcrA suppressors of AcrB$_{\Delta L1}$. Selected revertants of the antibiotic hypersensitive AcrB$_{\Delta L1}$ mutant completely restore resistance to novobiocin and erythromycin, while partially restoring resistance to SDS. Sensitivity assays were performed as described in Figure 2 and Table 1. Zones are an average of two independent cultures varying no greater than 10%.

AcrA:	-	+	+	E43K	V44I	S195P	L222Q	L222R	Δ*	T224S	F230S	G248E	S295C
AcrB:	-	+					ΔL1						

LamB ▶

AcrA ▶

| AcrA: | 0.00 | 1.00 | 1.00 | 0.70 | 0.82 | 0.91 | 0.57 | 0.78 | 0.56 | 1.38 | 1.56 | 0.94 | 1.50 |
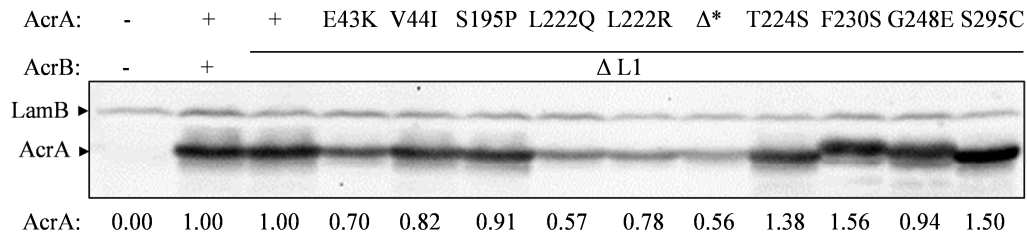
Figure 30. Effect of AcrB$_{\Delta L1}$ suppressors on AcrA protein levels. Most AcrA suppressors show no difference in protein levels or running on 11% acrylamide gels. AcrA$_{E43K}$, AcrA$_{L222Q}$, AcrA$_{L222R}$, and AcrA$_{\Delta222-224}$ show decreased protein levels indicating decreased stability of the mutant protein. AcrA$_{F230S}$ and AcrA$_{G248E}$ show slower migration through 11% acrylamide gels. Whole cell extracts from approximately 5 x 10^7 cells from overnight cultures were probed for AcrA and LamB. LamB was used as a loading control and AcrA wild type levels were taken as 1. Mutant protein levels were adjusted accordingly.

[*] Δ indicates the AcrA$_{\Delta222-224}$ alteration.

Sequence analysis revealed that 19 of the 21 revertants, the *acrA* gene carried a mutation. The residues affected by these mutations of the mature AcrA sequence were E43K, V44I, S195P, L222Q, L222R, Δ222-224, T224S, F230S, G248E, and S249C. These were each isolated 1, 1, 1, 5, 2, 1, 1, 1, 5, and 1 times, respectively. Two of the alterations mapped in the lipoyl domain of AcrA (E43K and V44I), while the remaining substitutions mapped in the β-barrel (Fig 28). The suppressor alterations L222Q and L222R have been isolated in previous studies conducted by our lab and have been shown to stabilize functional complex assembly of the labile TolC$_{P246R, S350C}$, while they themselves destabilize the AcrA protein.

As stated above, AcrA$_{L222Q}$ and AcrA$_{L222R}$ are labile proteins which are readily degraded without TolC and AcrB (Gerken and Misra, 2004; Weeks *et al*. 2010; Figs 4, 7, and 27). Not surprisingly, their levels were found to be markedly reduced in the AcrB$_{ΔL1}$ background (Fig 30). Additionally, AcrA$_{Δ222-224}$ showed a significant reduction in AcrA levels, also not surprising as the other two alterations at L222 showed similar reduction. AcrA$_{E43K}$ was the only other mutant to show decreased protein levels when compared to wild type AcrA. When comparing antibiotic sensitivity of the mutants to the parental AcrB$_{ΔL1}$, all suppressors reduce sensitivity to novobiocin and erythromycin back to wild type levels (Fig 29). The suppressors vary in their abilities to suppress sensitivity to SDS, but all show a significant reduction in sensitivity compared to the parental AcrB$_{ΔL1}$.

98
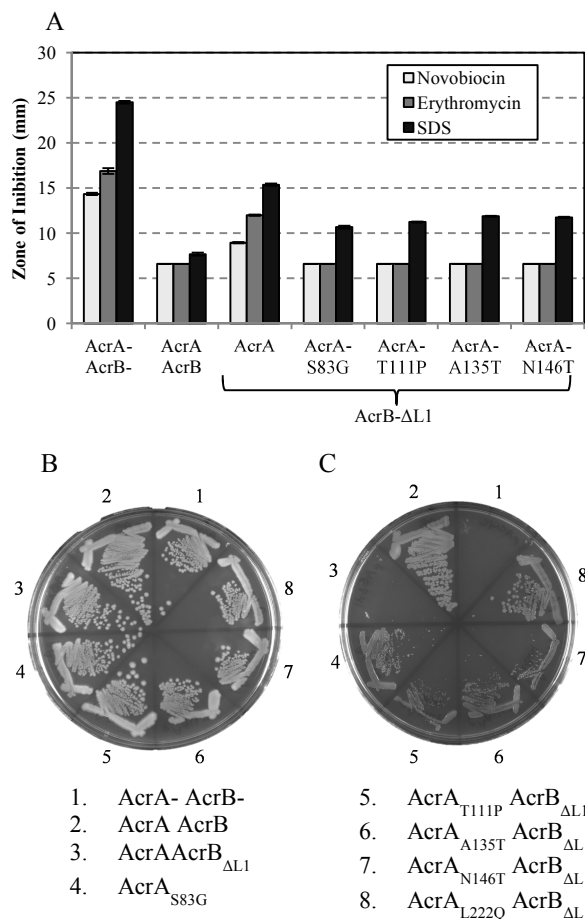
Figure 31. AcrA α-helical mutations suppress AcrB$_{\Delta L1}$.

A. Mutations within the α-helices of AcrA restore resistance to novobiocin and erythromycin while partially restoring resistance to SDS, similar to revertants selected. Sensitivity assays were performed as described in Figure 2 and Table 1. Zones are an average of two independent cultures.

B and C. Relative growth on plates without (B) or with (C) the substrate inhibitors (novobiocin, erythromycin, and SDS) was observed after 16 h. Mutations within the α-helices of AcrA show decreased growth compared to the selected revertant AcrA$_{L222Q}$, but still show significant increase in growth compared to AcrB$_{\Delta L1}$.

99

Forced Mutation of AcrA's α-Helix Suppresses the Drug Hypersensitivity Defect

All the suppressor alterations described above were localized to the β-barrel and lipoyl domains of AcrA, indicating suppression specificity. To test this further, suppressor alterations mapping within the α-helical domain of AcrA, which were isolated through a different selection strategy, were introduced in an AcrB$_{\Delta L1}$ background and drug sensitivity was tested of the resulting strains. More specifically, four alterations which had previously been identified as those that stabilize functional complex assembly were introduced via site-directed mutagenesis into the pACYC184- *acrAB* (AcrB$_{\Delta L1}$) plasmid. The alterations – S83G, T111P, A135T, and N146T – localize to either α-helix 1 (S83G), α-helix 2 (A135T and N146T), or the extreme tip turn between α-helix 1 and α-helix 2 (T111P). Once introduced, the antibiotic hypersensitivity of these mutants were compared to those carrying alterations in the β-barrel domain. Surprisingly, when individual antibiotics were tested, these forced α-helical alterations showed similar zones of inhibition to those carrying the original suppressors altering the β-barrel domain of AcrA, with sensitivity to novobiocin and erythromycin sensitivity returning to a wild type level and slightly elevated zones of inhibition for SDS (Fig 31A). However, when strains carrying these forced α-helical alterations were grown on selection medium simultaneously containing these three inhibitor substrates, they grew significantly weaker than a strain carrying an alteration in the AcrA β-barrel domain (AcrA$_{L222Q}$; Fig 31B). This indicates that while the α-helical alterations in AcrA can reduce sensitivity to antibiotics similar

100

to those revertants carrying β-barrel alterations, the combination of inhibitors used for selection may have biased against selecting the former alterations due to their limited ability to grow in the presence of all three substrates simultaneously.

The ability of AcrA α-helical alterations to suppress the antibiotic sensitivity phenotype of the $AcrB_{PAL1/L2}$ mutant was also tested. It was speculated that this AcrB mutant has a similar defect in its ability to interact with TolC directly, or with TolC and AcrA. If this is the case, the alterations in either the α-helical or β-barrel domains of AcrA should be able to reverse the antibiotic hypersensitivity phenotype of $AcrB_{PAL1/L2}$ as they do for the $AcrB_{ΔL1}$ mutant. $AcrA_{S83G}$, $AcrA_{A135T}$, $AcrA_{L222Q}$, and $AcrA_{G248E}$ were selected for introduction into the $AcrB_{PAL1/L2}$ background. These four alterations map to different areas within the α-helices and β-barrel, additionally, L222Q and G248E were isolated most frequently in the $AcrB_{ΔL1}$ background, potentially indicating a preference of these alterations to suppress the antibiotic hypersensitivity. When comparing growth on selection medium containing all three antibiotics, the four AcrA suppressor alterations showed complete restoration of growth indicating these substitutions were also able to suppress the $AcrB_{PAL1/L2}$ mutant just as well as the $AcrB_{ΔL1}$ mutant (Fig 32A and B). Sensitivity assays showed these AcrA alterations reduce inhibition zones against the inhibitors back to wild type levels (Fig 32C). These results indicate that these two AcrB mutants share a common defect in interaction with other members of the complex, which can be suppressed by the same alterations in AcrA.
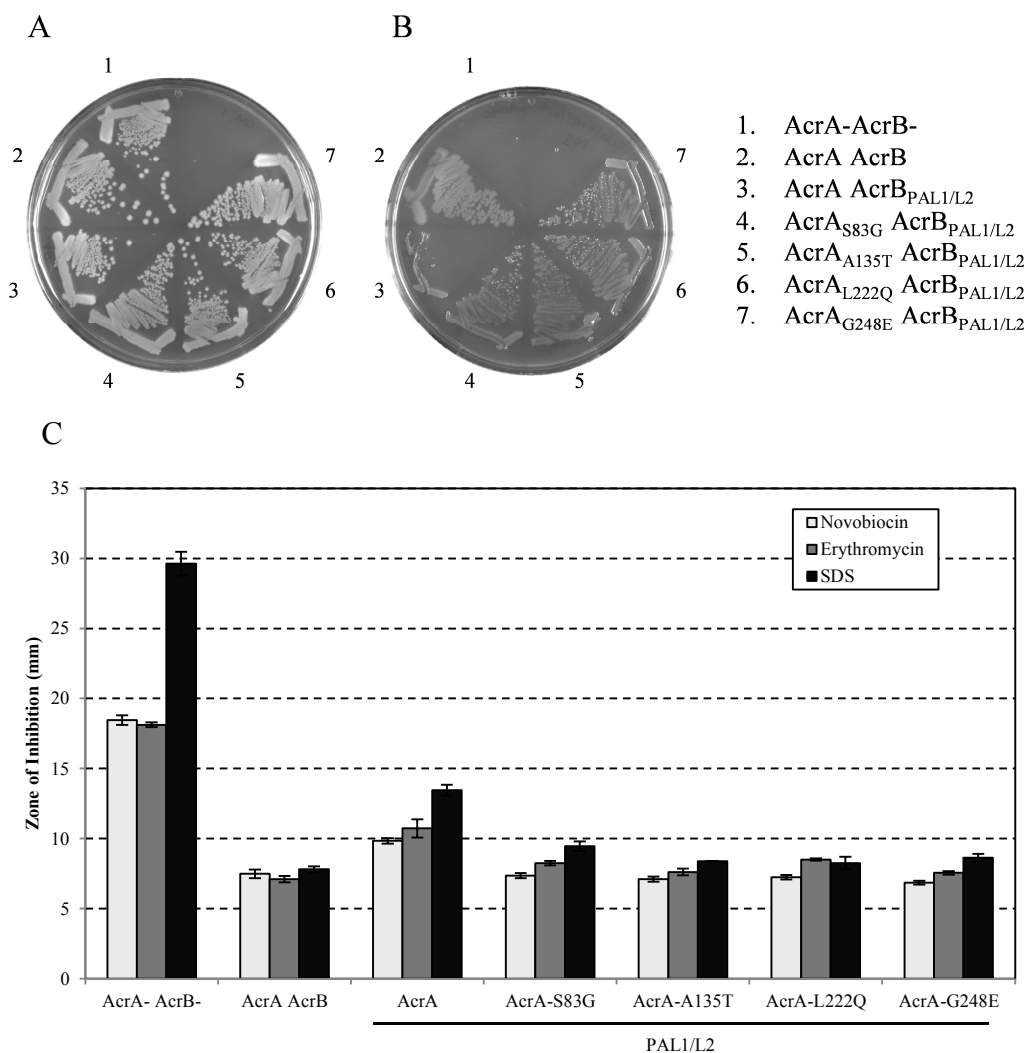
Figure 32. AcrA mutations restore drug efflux of AcrB$_{PAL1/L2}$.

A and B. Relative growth was compared for AcrA mutations with the AcrB$_{PAL1/L2}$ mutant without (A) or with (B) the substrate inhibitors novobiocin, erythromycin, and SDS. Growth was compared after 16 h.

C. Antibiotic resistance was compared for resistance to antibiotics as described in Figure 2 and Table 1.AcrA mutants restore antibiotic resistance comparable to resistance of wild type AcrA and AcrB. Zones are an average of two independent cultures varying less than 10%.

AcrA Mapping Suppressors Act to Stabilize Functional Complex Assembly

The AcrB$_{\Delta L1}$ mutant is unable to stabilize the labile TolC$_{P246R, S350C}$ mutant, indicating a defect in complex assembly. If AcrA suppressor alterations restore complex stability, they may also stabilize the labile TolC protein in the presence of AcrB$_{\Delta L1}$. All but one of the AcrA alterations were able to stabilize TolC$_{P246R, S350C}$ significantly (Fig 33). This led to an increase in TolC$_{P246R, S350C}$ levels from 0.06% to between 47 and 83% of that found in the wild type AcrA/AcrB background, indicating that these suppressors were acting to stabilize the functional complex assembly between AcrB$_{\Delta L1}$, mutant AcrA and TolC. The remaining mutant, AcrA$_{\Delta 222-224}$, was the least stable of the AcrA mutants and it is reasonable to expect that the combination of its intrinsic reduced stability interfered with its ability to stabilize the labile TolC.

Conformational Active AcrA Mutants Cannot be Biochemically Differentiated from Wild Type AcrA

In an attempt to determine whether the mutated forms of AcrA are in a constitutively activated form that may have changed their biochemical properties, protease sensitivity assays were carried out. Three AcrA variants were selected to begin analyzing the differences between wild type and mutant AcrA: E43K, L222Q, and G248E. When comparing steady state levels of AcrA, the E43K and L222Q alterations caused significant decreases in AcrA levels (0.70 and 0.57 of wild type, respectively; Fig 30). G248E does not cause a significant reduction in

A

$TolC_{P246R, S350C, His}$

| AcrA: | - | + | + | E43K | V44I | S195P | L222Q | L222R |
| AcrB: | - | + | | | | ΔL1 | | |

LC ▸

TolC ▸

TolC: 0.02 1.00 0.06 0.73 0.76 0.58 0.80 0.83

B

$TolC_{P246R, S350C, His}$

| AcrA: | - | + | + | Δ | T224S | F230S | G248E | S249C |
| AcrB: | - | + | | | | ΔL1 | | |

LC ▸

TolC ▸

TolC: 0.02 1.00 0.06 0.02 0.73 0.47 0.68 0.65
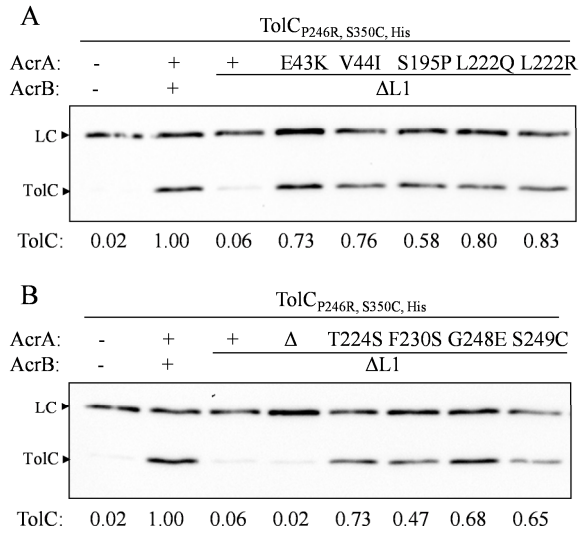
Figure 33. AcrA suppressors of $AcrB_{\Delta L1}$ act to stabilize $TolC_{P246R, S350C}$. Suppressor mutations in AcrA function by stabilizing functional complex assembly as measured by stabilization of the $TolC_{P246R, S350C}$ mutant. All suppressors except $AcrA_{\Delta 222-224}$ increased protein levels between 8 and 14-fold. Whole cell extracts from approximately 5×10^7 cells grown overnight were probed for TolC and a loading control (LC). $TolC_{P246R, S350C}$ levels in wild type AcrA and AcrB were taken as 1 and mutants were adjusted relative to this.

protein levels, 0.94 of wild type, but it does produce a slight shift in mobility when analyzed on 11% acrylamide gels. To determine whether additional differences could be observed between these mutants and wild type AcrA, limited proteolysis using trypsin and proteinase K was conducted (Ge *et al.*, 2009). Cell membranes were prepared from fresh cultures, OD_{600} ~1.0, which were then subjected to 5 minute treatment with trypsin or proteinase K. All three mutants show degradation profiles similar to wild type AcrA after treatment with trypsin (Fig 34). Additionally, $AcrA_{L222Q}$, when treated with proteinase K, showed the same degradation profile as wild type AcrA (Fig 34). Thus, the protease sensitivity assay cannot distinguish between the subtle conformational changes between wild type AcrA and the mutant counterparts. However, the steady state AcrA levels or altered gel mobility, along with the increased ability to stabilize a labile TolC mutant and increased antibiotic efflux, tend to point to an altered state of AcrA.

AcrA Suppressors Specifically Fix Defects in Complex Assembly

The results above showed that alterations in AcrA were able to restore interactions between defective forms of AcrB and TolC. Next it was determined whether the AcrA mutants could restore other defects in AcrB, such as proton translocation or drug-binding. If the AcrA alterations can, it may suggest that AcrA plays roles besides relaying conformational energy from AcrB to TolC. To test this hypothesis, *acrA* alterations $AcrA_{L222Q}$ and $AcrA_{G248E}$ were introduced
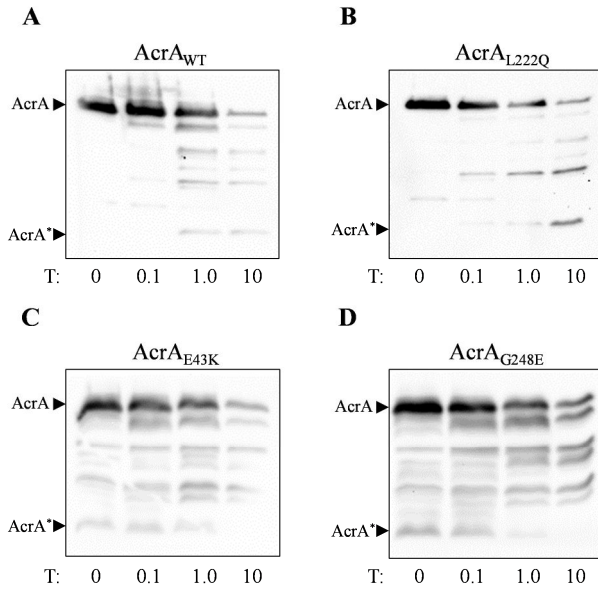
Figure 34. AcrA suppressors show no physical difference between wild type AcrA when exposed to trypsin. Membrane samples were exposed to varying concentrations of trypsin for 5 min. Mutations in AcrA do not alter stability of AcrA by protecting or exposing trypsin cleavage sites within AcrA. Membranes from approximately 7.5 x 10^8 cells were loaded and probed for AcrA. Units of trypsin (T) are in µg µl^{-1}.
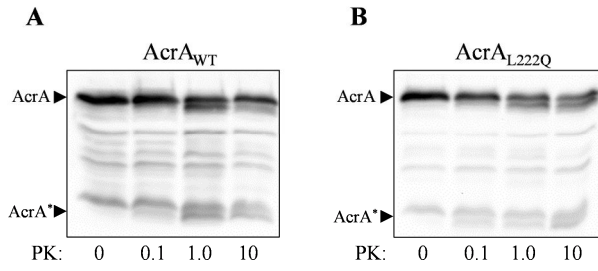
Figure 35. Wild type AcrA and AcrA$_{L222Q}$ show no difference in proteinase K sensitivity. Limited proteolysis using proteinase K (PK) was performed as with trypsin. Both AcrA wild type and AcrA$_{L222Q}$ show similar degradation profiles, indicating PK cleavage sites have not been protected or exposed by the L222Q mutation.

into pACYC184-*acrAB* which expressed AcrB bearing either a D407A or F610A substitution. The D407A alteration disrupts one of the key residues in the proton transport chain within the transmembrane domain of AcrB, thus preventing AcrB from becoming energized and subsequently expelling antibiotics from the cell (Takatsuka and Nikaido, 2006). The F610A alteration is located within the drug-binding cavity of AcrB and prevents substrates from being moved from the entry tunnels to the exit tunnel facing TolC (Bohnert *et al.*, 2010; Husain and Nikaido, 2010). By disrupting either of these, AcrB loses its ability to translocate drugs from the cell and into the extracellular milieu.

Neither alteration in AcrA was able to suppress the AcrB defect in proton translocation, supporting a view that AcrA plays no role in energizing AcrB (Fig 36B). Additionally, neither of these AcrA alteration showed increased ability to stimulate drug-binding in the $AcrB_{F610A}$ mutant (Fig 35A), indicating that unlike the copper efflux pump, CusAB, AcrA does not help facilitate drug-binding of AcrB (Bagai *et al.*, 2007; Bagai *et al.*, 2008). Taken together, these data indicate that alterations within AcrA can restore complex assembly between defective AcrB and TolC proteins, but cannot fix intrinsic defects of AcrB involving proton or drug translocation.
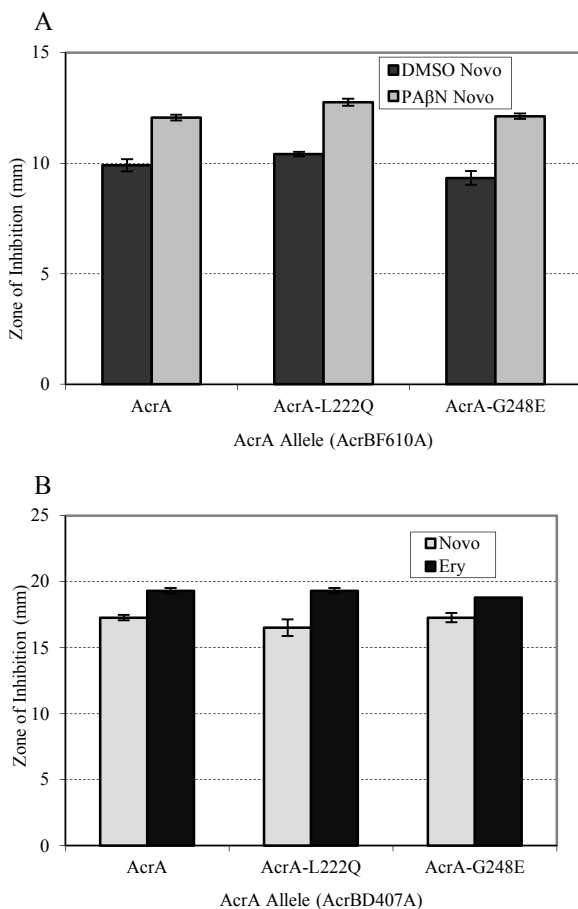
Figure 36. AcrA β-barrel mutations which suppress defects in tripartite complex assembly do not correct AcrB defects in drug-binding or proton translocation. A. AcrA β-barrel mutations were examined for their ability to restore drug efflux for the drug-binding deficient mutant (F610A). Sensitivity to novobiocin was tested without (DMSO) or with (PAβN) the efflux pump inhibitor phenylalanine-arginine-β-naphtylamide. Zones are an average of three independent cultures with zones varying no greater than 10%. As PAβN is soluble in DSMO, 10 μl of DMSO or 25 mg ml^{-1} PAβN in DMSO were spotted onto pre-soaked novobiocin disks (30 μg).

B. Sensitivity to novobiocin and erythromycin were observed in the proton translocation defective AcrB mutant (D407A) with the AcrA β-barrel mutations. Zones of inhibition are and average of three independent cultures with zones varying less than 10%. Sensitivity was determined as described in Figure 2 and Table 1.

109

Discussion:

This work describes the isolation and characterization of TolC and AcrB

mutants of *Escherichia coli* that are defective in proper interactions with other

complex members. The TolC turn 1 $_{147}$AGSG$_{150}$ mutant is the first of its kind,

being completely defective in efflux functions, while maintaining its ability to

properly insert into the membrane and act as a receptor for both TLS phage and

colicin E1. The AcrB hairpin loop mutations (ΔL1 or PAL1/L2) express a similar

defect in their inability to properly interact, likely with TolC, so as to allow proper

alignment with TolC and stimulate opening of its aperture/channel. Functional

defects of TolC and AcrB can be overcome by compensatory alterations in AcrA

that primarily act to facilitate proper complex assembly to allow TolC aperture

opening. Interestingly, compensatory alterations in AcrA did not lead to changes

in the proteins conformations that allowed for interactions only with the protein

against which they were isolated. In other words, suppressor mutations were not

strictly allele specific. Thus, suppressor alterations likely restored broad surface

interactions and not side chain-specific interactions. Alterations within TolC that

cause TolC to exhibit a leaky phenotype, by preventing complete aperture closing,

appear to be able to restore antibiotic efflux function lost when AcrB and TolC

cannot properly interact with one another.

While there are two reported models of interaction, the data presented here

tends to support direct interactions between AcrB and TolC (Tamura *et al.*, 2005,

Bavro *et al.*, 2008; Misra and Bavro, 2009; Symmons *et al.*, 2009; Tikhonova *et*

al., 2011). The similar phenotypes observed between the TolC$_{147AGSG150}$ and

AcrB$_{\Delta L1}$ mutant indicate that the affected regions of the two proteins may directly

interact with one another. In the AcrB-TolC distal model of interaction, it is

possible that the TolC turn 1 mutation disrupts interaction with AcrA, but a

mutation in the AcrB hairpin loops should show little to no phenotype as a direct

interaction between AcrB and TolC should not occur in this model and the AcrB

hairpin loops should have little to no physical interaction with AcrA (Kim *et al*.,

2010; Xu *et al*., 2010; Xu *et al*., 2011). In the AcrB-TolC tip-to-tip model of

interaction, D256 of AcrB has been proposed to mediate interaction directly

between AcrB and TolC (Tamura *et al*., 2005; Symmons *et al*., 2009; Bavro *et al*.,

2008). In the poly alanine AcrB Loop 1 and Loop 2 mutants (AcrB$_{PAL1/L2}$),

restoration of aspartate at position 256 fully restored the protein's function, thus

providing genetic evidence for the importance of D256 in AcrB's function.

Similarly, restoration of N254 in the poly alanine background restored AcrB's

function. Both of these residues are located on the hairpin loop 1 and appear to be

directed toward where the TolC turns have been proposed to sit in the docked

model of TolC-AcrAB (Symmons *et al*., 2009). Additionally, the MexB hairpin

loop 1 shows an incredible identity with AcrB loop 1 and structurally, the aspartic

acid and asparagine residues are oriented in a near identical fashion. Unlike

hairpin loop 1 residues, residues of hairpin loop 2 show little conservation.

Moreover, D795 of AcrB is replaced by K794 of MexB, both of which are

pointing into the periplasm and free to make interactions with TolC or OprM respectively.

The TolC turn 1 residues are primarily hydrophobic and facing away from the periplasm, leaving the peptide backbone free to hydrogen bond with the charged and polar side chains of the AcrB hairpin loops (Koronakis *et al*., 2000; Koronakis *et al*., 2004; Bavro *et al*., 2008; Pei *et al*., 2011). It is interesting to think that in the case of *E. coli*, where TolC is the only channel protein which interacts with multiple drug transporter pumps, a lack of sequence specificity for interaction at the turn would allow interactions of TolC with the multitude of transporters. Previous reports of gain of function mutations that allow VceC, the *Vibrio cholerae* TolC homologue, to function with AcrAB, showed compensatory mutations not within the tip region, but within the intraprotomer groove, allowing VceC to function with AcrAB (Vediyappan *et al*., 2006). Additionally, Nehme and Poole (2007) characterized gain of function mutations in MexA and OprM which act to facilitate functional complex assembly in a defective MexA background. The alterations in OprM localized to the intraprotomer groove and acted to enhance MexA interactions lost by a point mutation in the α-helical tip of MexA. This indicates that the specificity of interaction between outer membrane factor and membrane fusion protein is not at the TolC turn regions, but further up the α-helical barrel of the channel protein.

According to the favored tip-to-tip model shown in figure 37, initial interactions begin between TolC turn 1 backbone and charged/polar residues of

112
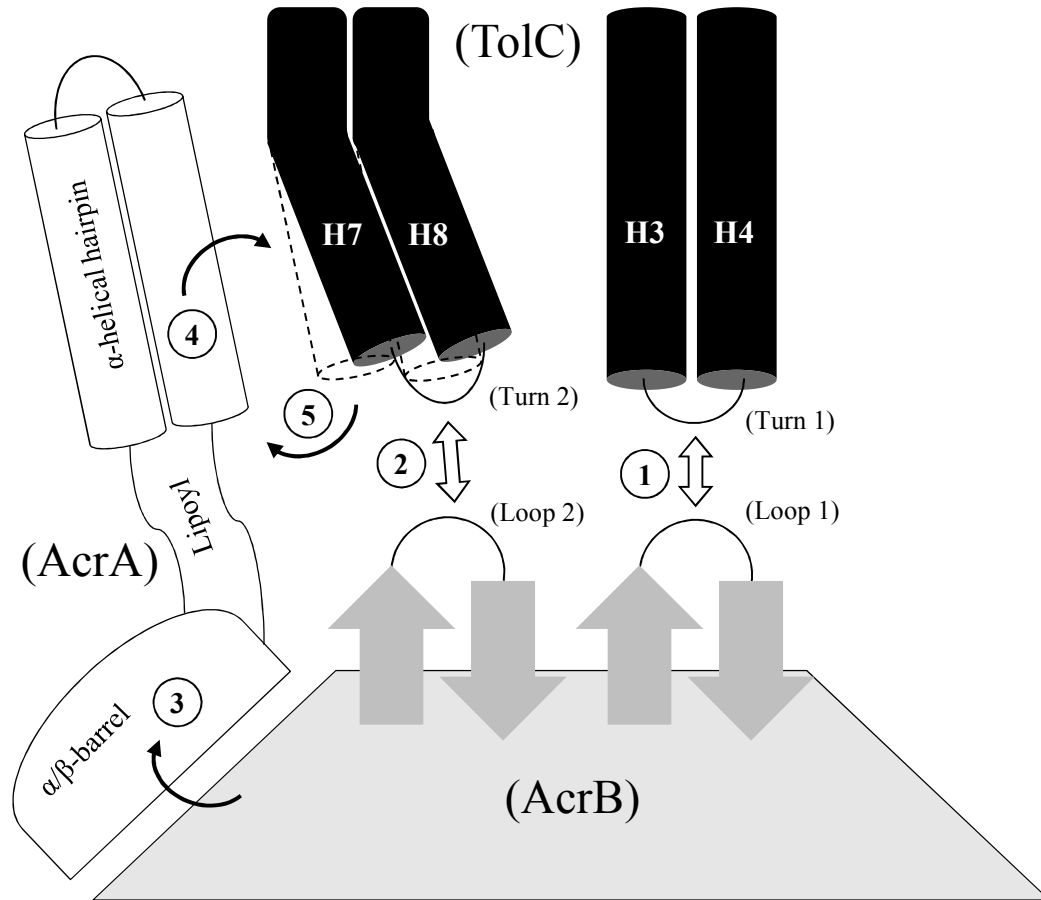
Figure 37. Proposed mechanism of interaction between members of the TolC-AcrAB complex. Initial interaction between TolC loop 1 and AcrB loop 1 cause proper alignment of TolC to AcrB (1). This interaction is stabilized by TolC turn 2 and AcrB loop 2, leading to the disruption of salt bridges holding the TolC aperture in the closed position (2). AcrB, after going through functional rotation, stimulates the β-barrel of AcrA (3) leading to conformational changes transferred through the lipoyl domain allowing alignment of the α-helices with the TolC colied-coils (4). This alignment causes rearrangement of TolC's helices and the iris-like opening of the aperture (5). After TolC has been opened by AcrA through energy derived from AcrB, the drug is released from the AcrB exit ducts directly into the open TolC channel.

AcrB hairpin loop 1. This will lead to proper alignment between TolC and AcrB, allowing for disruption of salt bridges which keep the TolC aperture locked (Fig 37). These initial disruptions would allow for AcrA to align its α-helices in a coiled-coil manner with TolC helices. Conformational activation of AcrA via AcrB would allow a complete alignment of AcrA and TolC helices and full dilation of TolC aperture, allowing antibiotics to be directly transferred from AcrB's exit tunnels into TolC's open channel.

Alterations within the turn regions and hairpin loops of TolC and AcrB, respectively, lead to an antibiotic hypersensitivity phenotype. This is consistent with the proposed mechanism of direct interaction between the two proteins. It was found that single amino acid substitutions within AcrA which overcome the antibiotic hypersensitivity phenotype, do so by stabilizing functional complex assembly in all cases. This leads to the conclusion that AcrA is acting to stabilize the weakened interaction between AcrB and TolC. In the case of the TolC turn 1 $_{147}$AGSG$_{150}$ mutant, AcrA suppressors additionally stimulate TolC aperture opening in an AcrB-dependent manner. This tends to indicate that disruption of the turn 1 residues abolishes proper interactions with AcrB and therefore precludes TolC aperture opening. This then must be fixed through modified alterations within AcrA , which both stabilizes TolC-AcrB intreactions and induces TolC aperture opening. Additionally, a synthetically introduced alteration of R390E is able to partially restore functionality of the turn 1 mutant. This finding supports the notion that disruption of the TolC turn 1 prevents AcrA and

114

AcrB to open the mutant TolC protein. The isolation of alterations in both TolC

and AcrA that increase sensitivity to vancomycin, indicating the TolC aperture

had been opened.

Taken together, the data presented indicate a direct interaction between

AcrB and TolC to expel antibiotics from the cell as indicated in Figure 36. In this

mechanism of interaction, AcrB hairpin loop 1 interacts directly with TolC turn 1

to mediate initial interaction, which allows hairpin loop 2 to interact with turn 2,

of AcrB and TolC respectively. This interaction begins to disrupt the salt bridges

locking TolC's aperture. At this point, AcrB undergoes its conformational

changes upon binding to substrates and transferring them to the exit tunnel as well

as translocating protons across the inner membrane. These changes induce

conformational changes on the external clefts of AcrB which AcrA sits. These

conformational changes in AcrB are then transferred through the AcrA membrane

proximal, β-barrel, and lipoyl domains to the α-helical hairpin domain of AcrA,

which aligns itself with the coiled-coils of TolC, allowing the aperture to become

fully dilated and the substrate to be transferred from AcrB directly through the

TolC channel.

Chemical cross-linking was inefficient at revealing defective interaction

between the mutant TolC turn 1 and AcrB loop mutations, whereas stabilization

of labile AcrA and TolC proteins was able to indicate the mutant proteins are

unable to properly form functional complexes. Additionally, suppressor

alterations within AcrA or the intragenic suppressor $AcrB_{\Delta L1,\ Q737L}$ were able to

stabilize these defective interactions and supported the notion that suppression is primarily mediated by stabilizing the functional complex.

By monitoring vancomycin sensitivity, it was possible to ascertain that a secondary means of restoring functionality of the complex was mediated by opening of the TolC aperture/channel. When analyzing suppressor mutations of $TolC_{147AGSG150}$ which mapped to *acrA*, it was seen that opening of the TolC aperture was specific to $TolC_{147AGSG150}$ and completely dependent on the presence of AcrB. This AcrA-induced TolC aperture opening appears to show that AcrA's conformation has been constitutively fixed into an "activated" state, which wild type AcrA protein transiently adopts during normal drug transport.

Limited protease sensitivity of constitutively activated forms of AcrA showed little to no difference compared to wild type. Altered steady state levels of certain mutants of AcrA, as well as differences in the gel mobility pattern gave some hint that the mutant AcrA proteins have adopted different conformations than wild type AcrA. Additionally, secondary site alterations within $AcrA_{L222Q}$ can stabilize this labile $AcrA_{L222Q}$ protein, indicating the conformation has been altered further to allow the protein to be more stable, but still significantly less so than wild type. It is possible through further biochemical tests or structural determination to know how various alterations within AcrA affect its conformation.

The inability to distinguish by proteolysis between wild type and activated forms of AcrA compares to the inability of cross-linking data to distinguish

116

between defects in functional vs. physical interactions between TolC and AcrB mutants. If one were to solely analyze chemical cross-linking, the inability to distinguish between TolC$_{WT}$ and TolC$_{147AGSG150}$ would suggest no defect in physical interactions with the other members of the complex. However by utilizing a labile AcrA variant (AcrA$_{L222Q}$), it can be seen that as antibiotic resistance is lost by TolC alterations, the labile AcrA protein is readily degraded. This leads to the conclusion that the mutational defect may have impeded functional interaction between mutant TolC and AcrA or AcrB, while physical interactions of the complex shows limited defects. Likewise, alterations in the hairpin loop regions of AcrB do not alter the ability of AcrA to co-purify, yet TolC is no longer able to co-purify with the AcrB mutants. Also, the inability of mutant AcrB proteins to stabilize TolC$_{P246R, S350C}$ gives more solid evidence that these hairpin loop alterations interfere with the proper assembly of the complex. Furthermore, AcrA suppressor mutations are able to restore stability of this mutant TolC.

The proposed docked model of interaction between AcrAB-TolC shows a single monomer of AcrA interacting with both TolC and AcrB. However, the location of AcrA in the model is inconsistent with the idea that AcrB transmits conformational energy through AcrA to TolC. This is most likely not the case because without this energy transfer from AcrB to TolC through AcrA, TolC would remain in a resting closed state. It is assumed that AcrB does in fact transmit this conformational energy through AcrA because the suppressors

117

isolated against the TolC$_{147AGSG150}$ turn 1 mutant cause permanent opening of TolC and therefore AcrA must be maintaining a conformation it only transiently adopts, as stated earlier. If this is the case, then this change in conformation most likely comes from the physical movement within AcrB. During drug binding and proton translocation, the surface of the AcrB porter domain goes through significant structural changes and would most likely be able to transfer the energy needed to AcrA to induce normal TolC aperture opening. If, as in the case of the copper efflux system CusABC, AcrA adopts a trimer of dimers encompassing TolC and AcrB, then AcrA would be situated in the proper location to receive this energy from AcrB to transmit to TolC.

After the tripartite complex model was proposed by Symmons *et al*. (2009), Tikhonova *et al*. (2009) showed two discrete binding affinities of AcrA, as well as other membrane fusion proteins, to TolC. Later they showed AcrA similarly binds AcrB in a 2:1 ratio (Tikhonova *et al*., 2011). The co-crystal structure of CusAB, as well as the functional covalently linked AcrA dimer indicates that the membrane fusion proteins act as in a multimeric state, placing the membrane fusion protein in the appropriate location to receive conformational energy (Su *et al*., 2011).

Tikhonova *et al*. (2011) showed direct binding affinity of TolC to immobilized AcrB with similar binding coefficients as either TolC-AcrA or AcrA-AcrB, other reports suggest interaction only occurs via outer membrane factor and membrane fusion protein. This notion stems from studies of the

MacAB-TolC complex, where the periplasmic domain of MacB is unable to co-purify with TolC, whereas MacA can. These studies also show a physiologically relevant hexameric state of MacA in which the hairpin of MacA intermesh completely in the turns of TolC. Later reports from this lab showed mutations in the tip of the α-helical domain of MacA or AcrA abolished interaction with TolC leading to decreased resistance to substrate inhibitors. Additionally, compensatory alterations in the turn regions of TolC restored interaction between AcrA and TolC as determined by increased antibiotic resistance and ability to be chemically cross-linked to one another.

If AcrB does not directly interact with TolC, how would mutations of the hairpin loops of AcrB cause a defect in functional interaction with TolC, as well as diminished ability of TolC to co-purify with AcrB? According to the AcrB-TolC distal model of interaction, AcrB's hairpin loops should be of little importance in interaction as the membrane proximal, β-barrel, and lipoyl domains of AcrA would directly interact with the surfaces of AcrB, thus leaving the hairpin loops with little to no purpose in interaction. In this research is has been shown that AcrB loop alterations have reduced ability to stabilize the labile TolC$_{P246R, S350C}$ mutant as well as the decreased ability to efflux antibiotics. Based on this, it can be proposed that there must be a direct interaction between TolC and AcrB in order to cause these phenotypes. Additionally, the intragenic AcrB suppressor, Q737L is located directly adjacent to the AcrB loop 1 within a groove where the TolC turn is predicted to sit. This suppressor partially stabilizes the

119

labile TolC protein in the presence of the AcrB loop 1 deletion. This genetic evidence points to a direct interaction between TolC and AcrB. Biophysical evidence came from Tikhonova *et al*. (2011), where they showed AcrB can bind TolC with the same affinity as to AcrA through Surface Plasmon Resonance.

Taken together, the data presented here and the Surface Plasmon Resonance data of Tikhonova *et al*. (2011) support a direct interaction between the periplasmic turns of TolC and loops of AcrB. Alterations in either protein abolish interaction as determined by increased antibiotic sensitivity and labile protein stability. Additionally, single amino acid substitutions within any member of the complex can partially restore antibiotic efflux, primarily through establishing functional complex assembly. In all cases, the final step of TolC aperture opening is disrupted and, therefore, alterations that force open the TolC aperture, either directly or indirectly, can restore antibiotic efflux or establish proper interaction between members of the complex.

Materials and Methods

Strains and Chemicals

  All the strains and plasmids used in this study are listed in Table X. Luria broth (LB) and LB agar (LBA) media were prepared as described by Tom Silhavy *et al.* (1984). When required, ampicillin (50 μg ml^{-1}), chloramphenicol (12.5 μg ml^{-1}), kanamycin (25 μg ml^{-1}), and tetracycline (10 μg ml^{-1}), isopropyl-β-D-thiogalactopryanoside (IPTG; 0.4 mM), L-arabinose (0.2%) was added to bacterial cultures. All other chemicals were of analytical grade.

DNA Manipulations

  The *acrA* gene was cloned into pACYC184 (Chang and Cohen, 1978) and pBAD33 (Guzman *et al.*, 1995) plasmid vectors as described previously (Augustus *et al.*, 2004). Subsequently the *acrB* gene was cloned behind *acrA* on the pACYC184-*acrA* plasmid. The *tolC* gene was cloned into pTrc99a as described previously behind the IPTG inducible promoter (Vakharia *et al.*, 2001, Augustus *et al.*, 2004, Husain *et al.*, 2004). Primers used for cloning, sequencing, and site-directed mutagenesis are listed in Table X. Primers ordered from IDT DNA. Deletion of the chromosomal *tolC, acrA, and acrB* genes were carried out as described previously (Augustus *et al.*, 2004) and was carried out by the method described by Datsenko and Wanner (2000). Gene deletion was confirmed by PCR and DNA sequence anaylsis. Plasmid transformation and P1 transduction were performed according to the standard laboratory procedures.

Site-Directed Mutagenesis was carried out using the QuickChange Lightning Site-Directed Mutagenesis Kit (Stratagene) according to manufacturer's instructions. Sequencing of all chromosomal and plasmid borne mutations were sequenced using primers listed in Table X and sequencing was carried out by the ASU DNA Sequencing Lab.

SDS-PAGE and Western Blot Analysis

Whole cell extracts, membrane fractions, or purified protein were analysed by mini sodium dodecyl sulfate (SDS)-polyacrylamide (7.5% or 11%) gel electrophesis (PAGE). When needed, gels were stained with Coomassie staining (25% (v/v) isolpropanol, 10% (v/v) glacial acetic acid, 2.5 mg ml^{-1} Coomassie brilliant blue) for 15min. The gels were then destained in 5% (v/v) methanol, 7% (v/v) acetic acid. Gels were imaged with Bio-Rad Molecular Imager ChemiDoc XRS System. For Western Blot analysis, samples were run on SDS-PAGE and transferred onto immobilon-P polyvinylidenedifluoride membranes (Milipore). Membranes were blocked overnight in 5% (w/v) non-dairy creamer in TBS. After blocking, membranes were washed and incubated for 1.5 hours in primary antibodies raised against TolC-MBP, AcrB-MBP, AcrA6His, and/or LamB, followed by two 15 minute washes and 1 h incubation in secondary antibodies (goat anti-rabbit horseradish peroxidase [HRP] conjugated IgG). Additionally, 6 histadine tagged proteins were visualized by incubating for 1.5h with HisProbe-HRP (Thermo Scientific). Detection of hybridized proteins was carried out using

immunostar HRP substrate. Protein bands were visualized with the Bio-Rad Molecular Imager ChemiDoc XRS System. When needed, relative protein levels were determined using the Quantity One software, MBP and LamB were used as loading controls to compare the relative amounts of AcrB or TolC (MBP) or AcrA (LamB).

Antibiotic Sensitivity Assays

Sensitivity to antibiotics was analyzed by placing pre-soaked antibiotic disks (Becton Dickinson) on bacterial lawn grown on LBA. In cases where pre-soaked disks were not available, 10μl of the antibiotic was added to a 6mm sterile Whatman disks to contain the following amounts of antibiotic; SDS – 1 mg, vancomycin – 75 μg. Zones of inhibition were measured after 16h of incubation at 37°C. Zones were determined from two independent cultures and in duplicate or in triplicate and values vary by less than 10%.

Minimal Inhibitory Concentrations (MICs) were determined by measuring growth of bacterial cultures on media containing different concentrations of various inhibitors. Approximately 1×10^6 cells, mixed with twofold serial dilutions of inhibitors in microtiter plates, were incubated at 37°C for 18h. OD_{600} was measured by a microtiter plate reader (Molecular Devices VERSA$_{max}$), and values were plotted against inhibitor concentrations. MIC values were extrapolated from linear regressions obtained from OD_{600}/concentration plots. Growth was measured from two independent cultures and in duplicates.

Relative growth in the presence of select inhibitors was done by streaking bacteria onto LBA plates containing specific concentrations of specific substrates of the AcrAB-TolC complex. Plates were grown for 16h at 37°C. Relative colony size of mutants was compared to null and wild type controls. To confirm lack of growth in the presence of a specific substrate combination/concentration was due specifically to the inhibitor, the same colony was simultaneously grown on a plate without substrates.

Membrane Preparation and Protein Isolation

Equivalent amounts of cells from overnight cultures, based on OD_{600}, were pelleted and resuspended in a lysis buffer and membranes were prepared as described by Gerken *et al.* (2010). Membranes were resuspended in 10mM Tris-HCl pH 7.5. Membrane fractions were analyzed by SDS-PAGE followed by either Coomassie Staining or Western Blot.

Overnight cultures were diluted 1:100 and grown to log phase (OD_{600} 0.6 − 0.8) and induced with IPTG (0.4mM) for 4h (TolC) or overnight (AcrB). TolC cultures were lysed as described above and membranes were homogenized in 2X TolC Extraction Buffer (40 mM sodium phosphate pH 7.4, 250 mM NaCl, 40 mM imidazole). Post homogenization, equivalent volumes of 10% Triton was added. Samples were rocked at 4C for 1hr and subsequently centrifuged for 1h at 105,000 X *g*, 4C. The soluble protein was then applied to a pre-equilibrated Ni-nitrilotriacetic acid (NTA) column (HisTrap, GE Healthcare); the column was

equilibrated with TolC Binding Buffer (20 mM sodium phosphate pH 7.4, 125 mM NaCl, 1% Triton X-100, 20 mM imidazole). After applying the solubilized proteins to the column, the column was washed with 6 column volumes of Binding Buffer, followed by 6 column volumes of TolC Wash Buffer 1 (20 mM sodium phosphate pH 7.4, 250 mM NaCl, 50 mM imidazole, 1% Triton X-100) and TolC Wash Buffer 2 (20 mM sodium phosphate pH 7.4, 250 mM NaCl, 50 mM imidazole, 0.03% n-dodecyl-β-D-maltoside). The TolC was then eluted with 13 column volumes of TolC Elution Buffer (20 mM sodium phosphate pH 7.4, 250 mM NaCl, 300 mM imidazole, 0.03% n-dodecyl-β-D-maltoside).

AcrB cultures were spun down and the cell pellet was resuspended in a plasmolysis buffer as described by Morona and Reeves (1981) with the following modifications. For a 500 ml culture, cells were pelleted and resuspended in 4 ml of 20% sucrose in 30mM Tris-HCl pH 7.5, 0.4 ml of 0.1 M PMSF [phenylmethylsufonyl floride] in DMSO, 0.4 ml of 10mg ml^{-1} lysozyme in 0.1 M EDTA pH 8.0, and 20 μl of 10 mg ml^{-1} Dnase I. Cells were incubated on ice for 30 minutes, diluted in 15.2 ml of 3 mM EDTA pH 8.0, and then lysed by French press. Following a low speed spin to remove unlysed cells, cell lysates were centrifuged for 1h at 105,000 X g, 4°C to separate soluble from insoluble (inner and outer membranes). The insoluble fraction was resuspended in an AcrB extraction buffer (5 mM imidazole, 20 mM Tris-HCl pH 8.0, 500 mM NaCl, 1% DDM) and rocked overnight to solubilize the protein from the insoluble fraction. The solution was centrifuged for 1h at 105,000 X g 4°C to separate the soluble

from insoluble fractions. The soluble fraction was then applied to a pre-equilibrated Ni-NTA column. The column was equilibrated and washed with10 column volumes of four buffers (20 mM Tris-HCl pH 8, 500 mM NaCl, 0.03% DDM, 2 mM PMSF) varying only in imidazole concentration; 5 mM, 20 mM, 50 mM, 100 mM. The protein was finally eluted from the column using an extraction buffer (500 mM imidazole, 20 mM Tris-HCl pH 8, 500 mM NaCl, 0.03% DDM, 2 mM PMSF). The protein was dialyzed to remove the Imidazole using dialysis buffer (20 mM Tris-HCl pH 7.5, 500 mM NaCl, 0.03% DDM, 0.1 mM PMSF), which it was then stored in.

Protein concentration was determined using a Coomassie (Bradford) Protein Assay Kit (Pierce) following the manufacturer's instructions. Microtiter plates were read using a microtiter plate reader (Molecular Devices VERSA$_{max}$). Protein quantities were determined using exponential regression from a Bovine Serum Albumin (BSA) standard by the software SoftMax Pro 5.2.

Chemical Cross-Linking

Cross-linking was carried out essentially as described by Vuong *et al*. (2008). Briefly, overnight cultures were diluted 1:100 in LB (40 ml). After an hour, cultures were induced with 0.4 mM IPTG and 0.2% arabinose, and grown for an additional 4 hours. Cells were spun down, washed with 20 mM sodium phosphate pH 7.4, resuspened in 10 ml of 20 mM sodium phosphate pH 7.4, and split into thirds cultures; 12.5 ml cultures were used for each treatment. The

126

cultures were treated with DSP [dithiobis (succinimidylpropionate)] (0.5 mM; Pierce), SPDP [N-succinimidyl 3-(2-pyridyldithio) propionate] (0.2 mM; Pierce), or Dimethyl Sulfoxide (DMSO) for 30min at 37°C on a rotating mixer. The reactions were quenched with 40 mM Tris-HCl pH 7.5/25 mM L-cysteine. Cells were spun down and solubilized in PUTTS Buffer (100 mM NaH_2PO_4, 8 M Urea, 10 mM Tris-HCl pH 7.5, 1% Triton X-100, 0.2% sarkosyl) with 10 mM Imidazole for 1h at room temperature. Cross-linked proteins were purified using Ni-NTA spin columns (Qiagen). Briefly, 600 µl of sample was passed through Ni-NTA columns pre-equilibrated with PUTTS, 10 mM imidazole. The column was washed three times with PUTTS, 100 mM imidazole. Finally, the protein was eluted with 130 µl of PUTTS, 500 mM imidazole. All spins were done at 400 X g or 800 X g. Elutes were mixed with SDS sample buffer, boiled for 5 min, and resolved on an 11% SDS-polyacrylamide gel. Proteins were visualized by Western Blot using α-TolC/MBP or α-AcrA$_{6His}$ primary antibodies followed by goat anti-rabbit HRP conjugated IgG secondary antibodies.

Limited Proteolysis

Limited proteolysis of AcrA was performed as described in Ge *et al.* (2009) with a few modifications. Overnight cultures were diluted 1:100 in LB and grown to OD_{600}. 100 ml samples were taken and membranes were prepared by plasmolysis followed by French press. Samples were resuspended in 100 µl of 10 mM Tris-HCl pH 7.5. 5 µl of membranes were mixed with 43 µl of 10 mM Tris-

HCl pH 7.5, and 2 µl of trypsin (final concentrations of 0, 0.1, 1.0, and 10 µg µl^{-1})

in 10 mM Tris-HCl pH 7.5. The digestion was left for 5min or 60min at 25°C and

stopped with 2 µl of 0.05 M PMSF in isopropyl alcohol (final concentration 2

mM). Samples were mixed with SDS sample buffer, boiled for 5min, and

resolved on an 11% SDS-polyacrylamide gel.

Limited proteolysis of AcrB was performed using purified protein, as

described previously. 4000 ng of protein was mixed with AcrB Storage Buffer

without PMSF (20 mM Tris-HCl pH 7.5, 500 mM NaCl, 0.03% DDM) to a final

volume of 45µl and 5 µl of Proteinase K (final concentrations of 0, 1.0 and 10 µg

µl^{-1}). The reaction was allowed to proceed for 5min at 25°C. 5 µl of PMSF in

isopropyl alcohol or 2.5 µl of PMSF in DMSO were added to stop the reaction.

Sample were mixed in SDS sample buffer, heated to 60°C for 10min, and

resolved by 7.5% SDS-polyacrylamide gels.

Crystal Structures of Mutant Proteins

Molecular models were created of TolC, AcrA, and AcrB using the

program PyMol. The following Protein Data Bank files were used; 1EK9 – TolC

wild type, 2XMN – TolC open state, 2F1M – AcrA, and 2GIF – AcrB. All of the

mutant proteins have been visualized and colored by chain. Point mutations are

shown in stick form. Residue numbers are of the mature protein and missense

mutations are listed.

Table 8. List of Strains.

Strain	Relevant Chromosomal genotype[a]	Plasmid 1[b]	Plasmid 2[b]	Reference
B51-1	MC4100 $\Delta tolC$::Cm^r	pTrc99a- $tolC$ (TolC BspHI Clone)		Augustus et $al.$, 2004
B51-2	MC4100 $\Delta tolC$::Cm^r	pTrc99a-		Augustus et $al.$, 2004
B51-3	MC4100 $\Delta tolC$::Cm^r AcrA$_{L222Q}$ Tn10 @ 10.5	pTrc99a- TolC$_{147AGSG150}$		Weeks et $al.$, 2010
B51-4	MC4100 $\Delta tolC$::Cm^r $\Delta acrA$::Km^r			Augustus et $al.$, 2004
B51-5	MC4100 $\Delta tolC$::Cm^r AcrA$_{L222Q}$ Tn10 @ 10.5	pTrc99a- TolC$_{147AGSG150, A128V}$		This study
B51-6	MC4100 $\Delta tolC$::Cm^r AcrA$_{L222Q}$ Tn10 @ 10.5	pTrc99a- TolC$_{147AGSG150, I133S}$		This study
B51-7	MC4100 $\Delta tolC$::Cm^r AcrA$_{L222Q}$ Tn10 @ 10.5	pTrc99a- TolC$_{147AGSG150, D153E}$		This study
B51-8	MC4100 $\Delta tolC$::Cm^r AcrA$_{L222Q}$ Tn10 @ 10.5	pTrc99a- TolC$_{147AGSG150, S350A}$		This study
B51-9	MC4100 $\Delta tolC$::Cm^r AcrA$_{L222Q}$ Tn10 @ 10.5	pTrc99a- TolC$_{147AGSG150, R390C}$		This study
B51-10	MC4100 $\Delta tolC$::Cm^r AcrA$_{[S83G, L222Q]}$ Tn10 @ 10.5	pTrc99a- TolC$_{147AGSG150}$		This study
B51-11	MC4100 $\Delta tolC$::Cm^r AcrA$_{[G110A, L222Q]}$ Tn10 @ 10.5	pTrc99a- TolC$_{147AGSG150}$		This study
B51-12	MC4100 $\Delta tolC$::Cm^r AcrA$_{[G110D, L222Q]}$ Tn10 @ 10.5	pTrc99a- TolC$_{147AGSG150}$		This study
B51-13	MC4100 $\Delta tolC$::Cm^r AcrA$_{[T111A, L222Q]}$ Tn10 @ 10.5	pTrc99a- TolC$_{147AGSG150}$		This study
B51-14	MC4100 $\Delta tolC$::Cm^r AcrA$_{[T111S, L222Q]}$ Tn10 @ 10.5	pTrc99a- TolC$_{147AGSG150}$		This study
B51-15	MC4100 $\Delta tolC$::Cm^r AcrA$_{[A135V, L222Q]}$ Tn10 @ 10.5	pTrc99a- TolC$_{147AGSG150}$		This study
B51-16	MC4100 $\Delta tolC$::Cm^r AcrA$_{[N146Y, L222Q]}$ Tn10 @ 10.5	pTrc99a- TolC$_{147AGSG150}$		This study
B51-17	MC4100 $\Delta tolC$::Cm^r AcrA$_{[S83G, L222Q]}$ Tn10 @ 10.5			This study
B51-18	MC4100 $\Delta tolC$::Cm^r AcrA$_{[G110A, L222Q]}$ Tn10 @ 10.5			This study
B51-19	MC4100 $\Delta tolC$::Cm^r AcrA$_{[G110D, L222Q]}$ Tn10 @ 10.5			This study
B51-20	MC4100 $\Delta tolC$::Cm^r AcrA$_{[T111A, L222Q]}$ Tn10 @ 10.5			This study
B51-21	MC4100 $\Delta tolC$::Cm^r AcrA$_{[T111S, L222Q]}$ Tn10 @ 10.5			This study
B51-22	MC4100 $\Delta tolC$::Cm^r AcrA$_{[A135V, L222Q]}$ Tn10 @ 10.5			This study
B51-23	MC4100 $\Delta tolC$::Cm^r AcrA$_{[N146Y, L222Q]}$ Tn10 @ 10.5			This study
B51-24	MC4100 $\Delta tolC$::Cm^r	pTrc99a- TolC$_{147AGSG150, A128V}$		This study

B51-25	MC4100 $\Delta tolC$::Cm^r	pTrc99a- TolC	This study
B51-26	MC4100 $\Delta tolC$::Cm^r	147AGSG150, I133S pTrc99a- TolC	This study
B51-27	MC4100 $\Delta tolC$::Cm^r	147AGSG150, D153E pTrc99a- TolC	This study
B51-28	MC4100 $\Delta tolC$::Cm^r	147AGSG150, S350A pTrc99a- TolC	This study
B51-29	MC4100 $\Delta tolC$::Cm^r AcrA$_{[S83G, L222Q]}$ Tn10 @ 10.5	147AGSG150, R390C pTrc99a-	This study
B51-30	MC4100 $\Delta tolC$::Cm^r AcrA$_{[G110A, L222Q]}$ Tn10 @ 10.5	pTrc99a-	This study
B51-31	MC4100 $\Delta tolC$::Cm^r AcrA$_{[G110D, L222Q]}$ Tn10 @ 10.5	pTrc99a-	This study
B51-32	MC4100 $\Delta tolC$::Cm^r AcrA$_{[T111A, L222Q]}$ Tn10 @ 10.5	pTrc99a-	This study
B51-33	MC4100 $\Delta tolC$::Cm^r AcrA$_{[T111S, L222Q]}$ Tn10 @ 10.5	pTrc99a-	This study
B51-34	MC4100 $\Delta tolC$::Cm^r AcrA$_{[A135V, L222Q]}$ Tn10 @ 10.5	pTrc99a-	This study
B51-35	MC4100 $\Delta tolC$::Cm^r AcrA$_{[N146Y, L222Q]}$ Tn10 @ 10.5	pTrc99a-	This study
B51-36	MC4100 $\Delta tolC$::Cm^r AcrA$_{[S83G, L222Q]}$ Tn10 @ 10.5	pTrc99a- TolC (BspHI clone)	This study
B51-37	MC4100 $\Delta tolC$::Cm^r AcrA$_{[G110A, L222Q]}$ Tn10 @ 10.5	pTrc99a- TolC (BspHI clone)	This study
B51-38	MC4100 $\Delta tolC$::Cm^r AcrA$_{[G110D, L222Q]}$ Tn10 @ 10.5	pTrc99a- TolC (BspHI clone)	This study
B51-39	MC4100 $\Delta tolC$::Cm^r AcrA$_{[T111A, L222Q]}$ Tn10 @ 10.5	pTrc99a- TolC (BspHI clone)	This study
B51-40	MC4100 $\Delta tolC$::Cm^r AcrA$_{[T111S, L222Q]}$ Tn10 @ 10.5	pTrc99a- TolC (BspHI clone)	This study
B51-41	MC4100 $\Delta tolC$::Cm^r AcrA$_{[A135V, L222Q]}$ Tn10 @ 10.5	pTrc99a- TolC (BspHI clone)	This study
B51-42	MC4100 $\Delta tolC$::Cm^r AcrA$_{[N146Y, L222Q]}$ Tn10 @ 10.5	pTrc99a- TolC (BspHI clone)	This study
B51-43	MC4100 $\Delta tolC$::Cm^r AcrA$_{[S83G, L222Q]}$ Tn10 @ 10.5	pTrc99a- TolC (NcoI clone)	This study
B51-44	MC4100 $\Delta tolC$::Cm^r AcrA$_{[G110A, L222Q]}$ Tn10 @ 10.5	pTrc99a- TolC (NcoI clone)	This study
B51-45	MC4100 $\Delta tolC$::Cm^r AcrA$_{[G110D, L222Q]}$ Tn10 @ 10.5	pTrc99a- TolC (NcoI clone)	This study
B51-46	MC4100 $\Delta tolC$::Cm^r AcrA$_{[T111A, L222Q]}$ Tn10 @ 10.5	pTrc99a- TolC (NcoI clone)	This study
B51-47	MC4100 $\Delta tolC$::Cm^r AcrA$_{[T111S, L222Q]}$ Tn10 @ 10.5	pTrc99a- TolC (NcoI clone)	This study
B51-48	MC4100 $\Delta tolC$::Cm^r AcrA$_{[A135V, L222Q]}$ Tn10 @ 10.5	pTrc99a- TolC (NcoI clone)	This study
B51-49	MC4100 $\Delta tolC$::Cm^r AcrA$_{[N146Y, L222Q]}$ Tn10 @ 10.5	pTrc99a- TolC	This study
B51-50	MC4100 $\Delta tolC$::Cm^r AcrA$_{[S83G, L222Q]}$ Tn10 @ 10.5	pTrc99a- TolC [P246R, S350C] NCOI	This study

B51-51	MC4100 Δ*tolC*::Cm^r AcrA[G110A, L222Q] Tn10 @ 10.5	pTrc99a- TolC [P246R, S350C] NCOI		This study
B51-52	MC4100 Δ*tolC*::Cm^r AcrA[G110D, L222Q] Tn10 @ 10.5	pTrc99a- TolC [P246R, S350C] NCOI		This study
B51-53	MC4100 Δ*tolC*::Cm^r AcrA[T111A, L222Q] Tn10 @ 10.5	pTrc99a- TolC [P246R, S350C] NCOI		This study
B51-54	MC4100 Δ*tolC*::Cm^r AcrA[T111S, L222Q] Tn10 @ 10.5	pTrc99a- TolC [P246R, S350C] NCOI		This study
B51-55	MC4100 Δ*tolC*::Cm^r AcrA[A135V, L222Q] Tn10 @ 10.5	pTrc99a- TolC [P246R, S350C] NCOI		This study
B51-56	MC4100 Δ*tolC*::Cm^r AcrA[N146Y, L222Q] Tn10 @ 10.5	pTrc99a- TolC [P246R, S350C] NCOI		This study
B51-57	MC4100 Δ*tolC*::Cm^r Δ*acrA*::Km^r	pTrc99a- TolC [147AGSG150, 6 His]		This study
B51-58	MC4100 Δ*tolC*::Cm^r			Augustus *et al*., 2004
B51-59	MC4100 Δ*tolC*::Km^r Δ*acrA*-scar Δ*ara*714	pTrc99a- TolC_6 His	pACYC184-AcrA_L222Q	Weeks *et al*., 2010
B51-60	MC4100 Δ*tolC*::Km^r Δ*acrA*-scar Δ*ara*714	pTrc99a- TolC 147AGSG150, 6 His	pACYC184-AcrA_L222Q	Weeks *et al*., 2010
B51-61	MC4100 Δ*tolC*::Cm^r Δ*acrA*::Km^r	pTrc99a- TolC 147AGSG150, A128V		This study
B51-62	MC4100 Δ*tolC*::Cm^r Δ*acrA*::Km^r	pTrc99a- TolC 147AGSG150, I133S		This study
B51-63	MC4100 Δ*tolC*::Cm^r Δ*acrA*::Km^r	pTrc99a- TolC 147AGSG150, D153E		This study
B51-65	MC4100 Δ*tolC*::Cm^r Δ*acrA*::Km^r	pTrc99a- TolC 147AGSG150, R390C		This study
B51-66	MC4100 Δ*tolC*::Cm^r	pTrc99a- TolC 147AGSG150		Weeks *et al*., 2010
B51-67	MC4100 Δ*tolC*::Cm^r AcrA_L222Q Tn10 @ 10.5			Gerken and Misra, 2004
B51-68	MC4100 Δ*tolC*::Cm^r	pTrc99a- TolC (NcoI clone)		Augustus *et al*., 2004
B51-69	MC4100 Δ*tolC*::Cm^r	pTrc99a- TolC [P246R, S350C] NCOI		Gerken and Misra, 2004
B51-70	MC4100 Δ*tolC*::Cm^r AcrA_L222Q Tn10 @ 10.5	pTrc99a-		Gerken and Misra, 2004
B51-71	MC4100 Δ*tolC*::Cm^r AcrA_L222Q Tn10 @ 10.5	pTrc99a- TolC (*BspH*I clone)		Weeks *et al*., 2010
B51-72	MC4100 Δ*tolC*::Cm^r AcrA_L222Q Tn10 @ 10.5	pTrc99a- TolC (NcoI clone)		Gerken and Misra, 2004
B51-73	MC4100 Δ*tolC*::Cm^r AcrA_L222Q Tn10 @ 10.5	pTrc99a- TolC [P246R, S350C] NCOI		Gerken and Misra, 2004
B51-74	MC4100 Δ*tolC*::Cm^r Δ*acrA*::Km^r			Augustus *et al*., 2004
B51-75	MC4100 Δ*tolC*::Cmr Δ*acrA*::Km^r	pTrc99a-		This Study
B51-76	MC4100 Δ*tolC*::Cm^r Δ*acrA*::Km^r	pTrc99a- TolC (BspHI clone)		This Study
B51-77	MC4100 Δ*tolC*::Cm^r Δ*acrA*::Km^r	pTrc99a- TolC 147AGSG150		This Study

B51-78	MC4100 $\Delta tolC$::Cm^r $\Delta acrA$::Km^r	pTrc99a- TolC (NcoI clone)		This Study
B51-79	MC4100 $\Delta recA$::Km^r	pTrc99a- TolC (BspHI clone)		This Study
B51-80	MC4100 $\Delta recA$::Km^r	pTrc99a-		This Study
B51-81	MC4100 $\Delta recA$::Km^r	pTrc99a- TolC		This Study
B51-82	MC4100 $\Delta recA$::Km^r	pTrc99a- TolC$_{147AGSG150}$		This Study
B51-83	MC4100 $\Delta recA$::Km^r	pTrc99a- TolC$_{147AGSG150,\ A128V}$		This Study
B51-84	MC4100 $\Delta recA$::Km^r	pTrc99a- TolC$_{147AGSG150,\ I133S}$		This Study
B51-86	MC4100 $\Delta recA$::Km^r	pTrc99a- TolC$_{147AGSG150,\ D153E}$		This Study
B51-87	MC4100 $\Delta recA$::Km^r	$_{147AGSG150,\ R390C}$		This Study
B51-88	MC4100			Casaban, 1976
B51-89	MC4100 $\Delta tolC$::Km^r $\Delta acrA$-scar Δara714			This Study
B51-90	MC4100 $\Delta tolC$::Km^r $\Delta acrA$-scar Δara714	pTCR- TolC$_{6\ His}$	pACYC184-AcrA	This Study
B51-91	MC4100 $\Delta tolC$::Km^r $\Delta acrA$-scar Δara714	pTrc99a- TolC$_{[147AGSG150,\ 6\ His]}$	pACYC184-AcrA	This Study
B51-92	MC4100 $\Delta tolC$::Km^r $\Delta acrA$-scar Δara714	pTCR- TolC$_{6\ His}$		This Study
B51-93	MC4100 $\Delta tolC$::Km^r $\Delta acrA$-scar Δara714	pACYC184-AcrA		This Study
B51-94	MC4100 $\Delta tolC$::Km^r $\Delta acrA$-scar Δara714	pACYC184-AcrA$_{L222Q}$		This Study
B51-95	MC4100 $\Delta tolC$::Km^r $\Delta acrA$-scar Δara714	pTrc99a-TolC$_{[A128C,\ 6\ His]}$	pACYC184-AcrA	This Study
B51-96	MC4100 $\Delta tolC$::Km^r $\Delta acrA$-scar Δara714	pTrc99a-TolC$_{[A128C,\ 6\ His]}$	pACYC184-AcrA$_{L222Q}$	This Study
B51-97	MC4100 $\Delta tolC$::Km^r $\Delta acrA$-scar Δara714	pTrc99a- TolC-$_{147AGSG150,\ 6\ His]}$		This Study
B51-98	MC4100 $\Delta tolC$::Km^r $\Delta acrA$-scar Δara714	pTrc99a-TolC$_{[A128C,\ 6\ His]}$		This Study
B51-99	XL1 Blue			Stratagene
B51-100	MC4100 $\Delta tolC$::Km^r $\Delta acrA$-scar Δara714	pTrc99a-TolC$_{[Q142C,\ 6\ His]}$		This Study
B51-101	MC4100 $\Delta tolC$::Km^r $\Delta acrA$-scar Δara714	pTrc99a-TolC$_{[Q142C,\ 6\ His]}$	pACYC184-AcrA	This Study
B51-102	MC4100 $\Delta tolC$::Km^r $\Delta acrA$-scar Δara714	pTrc99a-TolC$_{[Q142C,\ 6\ His]}$	pACYC184-AcrA$_{L222Q}$	This Study
B51-103	MC4100 $\Delta tolC$::Km^r $\Delta acrA$-scar Δara714	pTrc99a- TolC$_{[147AGSG150,\ Q142C,\ 6\ His]}$		This Study
B51-104	MC4100 $\Delta tolC$::Km^r $\Delta acrA$-scar Δara714	pTrc99a- TolC$_{[147AGSG150,\ Q142C,\ 6\ His]}$	pACYC184-AcrA	This Study

B51-105	MC4100 Δ*tolC*::Km^r Δ*acrA*-scar Δ*ara*714	pTrc99a- TolC [147AGSG150, Q142C, 6 His]	pACYC184-AcrA$_{L222Q}$	This Study
B51-106	MC4100 Δ*tolC*::Km^r Δ*acrA*-scar Δ*ara*714	pBAD33-AcrA$_{6\,His}$		This Study
B51-107	MC4100 Δ*tolC*::Km^r Δ*acrA*-scar Δ*ara*714	pBAD33-AcrA$_{[L222Q,\,6\,His]}$		This Study
B51-108	MC4100 Δ*tolC*::Km^r Δ*acrA*-scar Δ*ara*714	pBAD33-AcrA$_{[A79C,\,6\,His]}$		This Study
B51-109	MC4100 Δ*tolC*::Km^r Δ*acrA*-scar Δ*ara*714	pBAD33-AcrA$_{[A79C,\,6\,His]}$	pTrc99a- TolC (BspHI clone)	This Study
B51-110	MC4100 Δ*tolC*::Km^r Δ*acrA*-scar Δ*ara*714	pBAD33-AcrA$_{[A79C,\,6\,His]}$	pTrc99a-TolC$_{147AGSG150}$	This Study
B51-111	MC4100 Δ*tolC*::Km^r Δ*acrA*-scar Δ*ara*714	pBAD33-AcrA$_{[A79C,\,L222Q,\,6\,His]}$		This Study
B51-112	MC4100 Δ*tolC*::Km^r Δ*acrA*-scar Δ*ara*714	pBAD33- AcrA$_{[A79C,\,L222Q,\,6\,His]}$	pTrc99a- TolC (BspHI clone)	This Study
B51-113	MC4100 Δ*tolC*::Km^r Δ*acrA*-scar Δ*ara*714	pBAD33- AcrA$_{[A79C,\,L222Q,\,6\,His]}$	pTrc99a- TolC$_{147AGSG150}$	This Study
B51-114	MC4100 Δ*tolC*::Km^r Δ*acrA*-scar Δ*ara*714	pBAD33-AcrA$_{[S83C,\,6\,His]}$		This Study
B51-115	MC4100 Δ*tolC*::Km^r Δ*acrA*-scar Δ*ara*714	pBAD33-AcrA$_{[S83C,\,6\,His]}$	pTrc99a- TolC (BspHI clone)	This Study
B51-116	MC4100 Δ*tolC*::Km^r Δ*acrA*-scar Δ*ara*714	pBAD33-AcrA$_{[S83C,\,6\,His]}$	pTrc99a- TolC$_{147AGSG150}$	This Study
B51-117	MC4100 Δ*tolC*::Km^r Δ*acrA*-scar Δ*ara*714	pBAD33- AcrA$_{[S83C,\,L222Q,\,6\,His]}$		This Study
B51-118	MC4100 Δ*tolC*::Km^r Δ*acrA*-scar Δ*ara*714	pBAD33-AcrA$_{[S83C,\,L222Q,\,6\,His]}$	pTrc99a- TolC (BspHI clone)	This Study
B51-119	MC4100 Δ*tolC*::Km^r Δ*acrA*-scar Δ*ara*714	pBAD33-AcrA$_{[S83C,\,L222Q,\,6\,His]}$	pTrc99a- TolC$_{147AGSG150}$	This Study
B51-120	MC4100 Δ*tolC*::Km^r Δ*acrA*-scar Δ*ara*714	pTrc99a- TolC $_{[147AGSG150,\,A128C,\,6\,His]}$		This Study
B51-121	MC4100 Δ*tolC*::Km^r Δ*acrA*-scar Δ*ara*714	pTrc99a- TolC $_{[147AGSG150,\,A128C,\,6\,His]}$	pACYC184-AcrA	This Study
B51-122	MC4100 Δ*tolC*::Km^r Δ*acrA*-scar Δ*ara*714	pTrc99a- TolC $_{[147AGSG150,\,A128C,\,6\,His]}$	pACYC184-AcrA$_{L222Q}$	This Study
B51-123	MC4100 Δ*tolC*::Cm^r AcrA$_{[S83G,\,L222Q]}$ Tn10 @ 10.5	pTrc99a- TolC $_{147AGSG150,\,A128V}$		This Study
B51-124	MC4100 Δ*tolC*::Cm^r AcrA$_{[S83G,\,L222Q]}$ Tn10 @ 10.5	pTrc99a- TolC $_{147AGSG150,\,I133S}$		This Study
B51-125	MC4100 Δ*tolC*::Cm^r AcrA$_{[S83G,\,L222Q]}$ Tn10 @ 10.5	pTrc99a- TolC $_{147AGSG150,\,D153E}$		This Study
B51-127	MC4100 Δ*tolC*::Cm^r AcrA$_{[S83G,\,L222Q]}$ Tn10 @ 10.5	pTrc99a- TolC $_{147AGSG150,\,R390C}$		This Study
B51-128	MC4100 Δ*tolC*::Cm^r AcrA$_{[G110A,\,L222Q]}$ Tn10 @ 10.5	pTrc99a- TolC $_{147AGSG150,\,A128V}$		This Study

B51-129	MC4100 $\Delta tolC$::Cm^r AcrA$_{[G110A, L222Q]}$ Tn10 @ 10.5	pTrc99a- TolC 147AGSG150, I133S	This Study
B51-130	MC4100 $\Delta tolC$::Cm^r AcrA$_{[G110A, L222Q]}$ Tn10 @ 10.5	pTrc99a- TolC 147AGSG150, D153E	This Study
B51-132	MC4100 $\Delta tolC$::Cm^r AcrA$_{[G110A, L222Q]}$ Tn10 @ 10.5	pTrc99a- TolC 147AGSG150, R390C	This Study
B51-133	MC4100 $\Delta tolC$::Cm^r AcrA$_{[G110D, L222Q]}$ Tn10 @ 10.5	pTrc99a- TolC 147AGSG150, A128V	This Study
B51-134	MC4100 $\Delta tolC$::Cm^r AcrA$_{[G110D, L222Q]}$ Tn10 @ 10.5	pTrc99a- TolC 147AGSG150, I133S	This Study
B51-135	MC4100 $\Delta tolC$::Cm^r AcrA$_{[G110D, L222Q]}$ Tn10 @ 10.5	pTrc99a- TolC 147AGSG150, D153E	This Study
B51-137	MC4100 $\Delta tolC$::Cm^r AcrA$_{[G110D, L222Q]}$ Tn10 @ 10.5	pTrc99a- TolC 147AGSG150, R390C	This Study
B51-138	MC4100 $\Delta tolC$::Cm^r AcrA$_{[T111A, L222Q]}$ Tn10 @ 10.5	pTrc99a- TolC 147AGSG150, A128V	This Study
B51-139	MC4100 $\Delta tolC$::Cm^r AcrA$_{[T111A, L222Q]}$ Tn10 @ 10.5	pTrc99a- TolC 147AGSG150, I133S	This Study
B51-140	MC4100 $\Delta tolC$::Cm^r AcrA$_{[T111A, L222Q]}$ Tn10 @ 10.5	pTrc99a- TolC 147AGSG150, D153E	This Study
B51-142	MC4100 $\Delta tolC$::Cm^r AcrA$_{[T111A, L222Q]}$ Tn10 @ 10.5	pTrc99a- TolC 147AGSG150, R390C	This Study
B51-143	MC4100 $\Delta tolC$::Cm^r AcrA$_{[T111S, L222Q]}$ Tn10 @ 10.5	pTrc99a- TolC 147AGSG150, A128V	This Study
B51-144	MC4100 $\Delta tolC$::Cm^r AcrA$_{[T111S, L222Q]}$ Tn10 @ 10.5	pTrc99a- TolC 147AGSG150, I133S	This Study
B51-145	MC4100 $\Delta tolC$::Cm^r AcrA$_{[T111S, L222Q]}$ Tn10 @ 10.5	pTrc99a- TolC 147AGSG150, D153E	This Study
B51-147	MC4100 $\Delta tolC$::Cm^r AcrA$_{[T111S, L222Q]}$ Tn10 @ 10.5	pTrc99a- TolC 147AGSG150, R390C	This Study
B51-148	MC4100 $\Delta tolC$::Cm^r AcrA$_{[A135V, L222Q]}$ Tn10 @ 10.5	pTrc99a- TolC 147AGSG150, A128V	This Study
B51-149	MC4100 $\Delta tolC$::Cm^r AcrA$_{[A135V, L222Q]}$ Tn10 @ 10.5	pTrc99a- TolC 147AGSG150, I133S	This Study
B51-150	MC4100 $\Delta tolC$::Cm^r AcrA$_{[A135V, L222Q]}$ Tn10 @ 10.5	pTrc99a- TolC 147AGSG150, D153E	This Study
B51-152	MC4100 $\Delta tolC$::Cm^r AcrA$_{[A135V, L222Q]}$ Tn10 @ 10.5	pTrc99a- TolC 147AGSG150, R390C	This Study
B51-153	MC4100 $\Delta tolC$::Cm^r AcrA$_{[N146Y, L222Q]}$ Tn10 @ 10.5	pTrc99a- TolC 147AGSG150, A128V	This Study
B51-154	MC4100 $\Delta tolC$::Cm^r AcrA$_{[N146Y, L222Q]}$ Tn10 @ 10.5	pTrc99a- TolC 147AGSG150, I133S	This Study
B51-155	MC4100 $\Delta tolC$::Cm^r AcrA$_{[N146Y, L222Q]}$ Tn10 @ 10.5	pTrc99a- TolC 147AGSG150, D153E	This Study
B51-157	MC4100 $\Delta tolC$::Cm^r AcrA$_{[N146Y, L222Q]}$ Tn10 @ 10.5	pTrc99a- TolC 147AGSG150, R390C	This Study
B51-158	MC4100 $\Delta tolC$::Cm^r	pTrc99a- TolC$_6$ His	This Study
B51-159	MC4100 $\Delta tolC$::Cm^r AcrA$_{L222Q}$ Tn10 @ 10.5	pTrc99a - TolC$_6$ His	This Study
B51-160	MC4100 $\Delta tolC$::Cm^r	pTrc99a- TolC [147AGSG150, 6 His]	This Study

B51-161	MC4100 $\Delta tolC$::Cm^r AcrA$_{L222Q}$ Tn10 @ 10.5	pTrc99a- TolC [147AGSG150, 6 His]		This Study
B51-162	MC4100 $\Delta tolC$::Cm^r	pTrc99a- TolC [Q142C, 6 His]		This Study
B51-163	MC4100 $\Delta tolC$::Cm^r AcrA$_{L222Q}$ Tn10 @ 10.5	pTrc99a- TolC$_{[Q142C, 6 His]}$		This Study
B51-164	MC4100 $\Delta tolC$::Cm^r	pTrc99a- TolC$_{[A128C, 6 His]}$		This Study
B51-165	MC4100 $\Delta tolC$::Cm^r AcrA$_{L222Q}$ Tn10 @ 10.5	pTrc99a- TolC$_{[A128C, 6 His]}$		This Study
B51-166	MC4100 $\Delta tolC$::Cm^r	pTrc99a- TolC [147AGSG150, Q142C, 6 His]		This Study
B51-167	MC4100 $\Delta tolC$::Cm^r AcrA$_{L222Q}$ Tn10 @ 10.5	pTrc99a- TolC [147AGSG150, Q142C, 6 His]		This Study
B51-168	MC4100 $\Delta tolC$::Cm^r	pTrc99a- TolC [147AGSG150, A128C, 6 His]		This Study
B51-169	MC4100 $\Delta tolC$::Cm^r AcrA$_{L222Q}$ Tn10 @ 10.5	pTrc99a- TolC [147AGSG150, A128C, 6 His]		This Study
B51-170	MC4100 $\Delta tolC$::Km^r $\Delta acrA$-scar Δara714	pTrc99a- TolC (BspHI clone)		This Study
B51-171	MC4100 $\Delta tolC$::Km^r $\Delta acrA$-scar Δara714	pTrc99a- TolC$_{147AGSG150}$		This Study
B51-172	MC4100 $\Delta tolC$::Km^r $\Delta acrA$-scar Δara714	pBAD33- AcrA$_{6 His}$	pTrc99a- TolC (BspHI clone)	This Study
B51-173	MC4100 $\Delta tolC$::Km^r $\Delta acrA$-scar Δara714	pBAD33- AcrA$_{6 His}$	pTrc99a- TolC$_{147AGSG150}$	This Study
B51-174	MC4100 $\Delta tolC$::Km^r $\Delta acrA$-scar Δara714	pBAD33- AcrA$_{[L222Q, 6 His]}$	pTrc99a- TolC (BspHI clone)	This Study
B51-175	MC4100 $\Delta tolC$::Km^r $\Delta acrA$-scar Δara714	pBAD33- AcrA$_{[L222Q, 6 His]}$	pTrc99a- TolC$_{147AGSG150}$	This Study
B51-176	MC4100 $\Delta tolC$::Cm^r AcrA$_{T30A}$ Tn10 @ 10.5			Gerken and Misra, 2004
B51-177	MC4100 $\Delta tolC$::Cm^r AcrA$_{N146T}$ Tn10 @ 10.5			Gerken and Misra, 2004
B51-178	MC4100 $\Delta tolC$::Cm^r AcrA$_{S83G}$ Tn10 @ 10.5			Weeks *et al*., 2010
B51-179	MC4100 $\Delta tolC$::Cm^r AcrA$_{T153P}$ Tn10 @ 10.5			Weeks *et al*., 2010
B51-180	MC4100 $\Delta tolC$::Cm^r AcrA$_{T30A}$ Tn10 @ 10.5	pTrc99a- TolC (*Bsp*HI clone)		This Study
B51-181	MC4100 $\Delta tolC$::Cm^r AcrA$_{T30A}$ Tn10 @ 10.5	pTrc99a- TolC$_{147AGSG150}$		This Study
B51-182	MC4100 $\Delta tolC$::Cm^r AcrA$_{T30A}$ Tn10 @ 10.5	pTrc99a- TolC 147AGSG150, A128V		This Study
B51-183	MC4100 $\Delta tolC$::Cm^r AcrA$_{T30A}$ Tn10 @ 10.5	pTrc99a- TolC 147AGSG150, I133S		This Study

B51-184	MC4100 $\Delta tolC$::Cm^r AcrA$_{T30A}$ Tn10 @ 10.5	pTrc99a- TolC $_{147AGSG150, D153E}$	This Study
B51-185	MC4100 $\Delta tolC$::Cm^r AcrA$_{T30A}$ Tn10 @ 10.5	pTrc99a- TolC $_{147AGSG150, S350A}$	This Study
B51-186	MC4100 $\Delta tolC$::Cm^r AcrA$_{T30A}$ Tn10 @ 10.5	pTrc99a- TolC $_{147AGSG150, R390C}$	This Study
B51-187	MC4100 $\Delta tolC$::Cm^r AcrA$_{N146T}$ Tn10 @ 10.5	pTrc99a- TolC (*Bsp*HI clone)	This Study
B51-188	MC4100 $\Delta tolC$::Cm^r AcrA$_{N146T}$ Tn10 @ 10.5	pTrc99a- TolC$_{147AGSG150}$	This Study
B51-189	MC4100 $\Delta tolC$::Cm^r AcrA$_{N146T}$ Tn10 @ 10.5	pTrc99a- TolC $_{147AGSG150, A128V}$	This Study
B51-190	MC4100 $\Delta tolC$::Cm^r AcrA$_{N146T}$ Tn10 @ 10.5	pTrc99a- TolC $_{147AGSG150, I133S}$	This Study
B51-191	MC4100 $\Delta tolC$::Cm^r AcrA$_{N146T}$ Tn10 @ 10.5	pTrc99a- TolC $_{147AGSG150, D153E}$	This Study
B51-192	MC4100 $\Delta tolC$::Cm^r AcrA$_{N146T}$ Tn10 @ 10.5	pTrc99a- TolC $_{147AGSG150, S350A}$	This Study
B51-193	MC4100 $\Delta tolC$::Cm^r AcrA$_{N146T}$ Tn10 @ 10.5	pTrc99a- TolC $_{147AGSG150, R390C}$	This Study
B51-194	MC4100 $\Delta tolC$::Cm^r AcrA$_{S83G}$ Tn10 @ 10.5	pTrc99a- TolC (*Bsp*HI clone)	This Study
B51-195	MC4100 $\Delta tolC$::Cm^r AcrA$_{S83G}$ Tn10 @ 10.5	pTrc99a- TolC $_{147AGSG150}$	This Study
B51-196	MC4100 $\Delta tolC$::Cm^r AcrA$_{S83G}$ Tn10 @ 10.5	pTrc99a- TolC $_{147AGSG150, A128V}$	This Study
B51-197	MC4100 $\Delta tolC$::Cm^r AcrA$_{S83G}$ Tn10 @ 10.5	pTrc99a- TolC $_{147AGSG150, I133S}$	This Study
B51-198	MC4100 $\Delta tolC$::Cm^r AcrA$_{S83G}$ Tn10 @ 10.5	pTrc99a- TolC $_{147AGSG150, D153E}$	This Study
B51-199	MC4100 $\Delta tolC$::Cm^r AcrA$_{S83G}$ Tn10 @ 10.5	pTrc99a- TolC $_{147AGSG150, S350A}$	This Study
B51-200	MC4100 $\Delta tolC$::Cm^r AcrA$_{S83G}$ Tn10 @ 10.5	pTrc99a- TolC $_{147AGSG150, R390C}$	This Study
B51-201	MC4100 $\Delta tolC$::Cm^r AcrA$_{T153P}$ Tn10 @ 10.5	pTrc99a- TolC (*Bsp*HI clone)	This Study
B51-202	MC4100 $\Delta tolC$::Cm^r AcrA$_{T153P}$ Tn10 @ 10.5	pTrc99a- TolC $_{147AGSG150}$	This Study
B51-203	MC4100 $\Delta tolC$::Cm^r AcrA$_{T153P}$ Tn10 @ 10.5	pTrc99a- TolC $_{147AGSG150, A128V}$	This Study
B51-204	MC4100 $\Delta tolC$::Cm^r AcrA$_{T153P}$ Tn10 @ 10.5	pTrc99a- TolC $_{147AGSG150, I133S}$	This Study
B51-205	MC4100 $\Delta tolC$::Cm^r AcrA$_{T153P}$ Tn10 @ 10.5	pTrc99a- TolC $_{147AGSG150, D153E}$	This Study
B51-206	MC4100 $\Delta tolC$::Cm^r AcrA$_{T153P}$ Tn10 @ 10.5	pTrc99a- TolC $_{147AGSG150, S350A}$	This Study
B51-207	MC4100 $\Delta tolC$::Cm^r AcrA$_{T153P}$ Tn10 @ 10.5	pTrc99a- TolC $_{147AGSG150, R390C}$	This Study
B51-208	MC4100 $\Delta tolC$::Cm^r AcrA$_{P265R}$ Tn10 @ 10.5		Gerken and Misra, 2004
B51-209	MC4100 $\Delta tolC$::Cm^r AcrA$_{\Delta217-218}$ Tn10 @ 10.5		Gerken and Misra, 2004

B51-210	MC4100 $\Delta tolC$::Cm^r AcrA$_{P265R}$ Tn10 @ 10.5	pTrc99a- TolC (*Bsp*HI clone)		This Study
B51-211	MC4100 $\Delta tolC$::Cm^r AcrA$_{P265R}$ Tn10 @ 10.5	pTrc99a- TolC$_{147AGSG150}$		This Study
B51-212	MC4100 $\Delta tolC$::Cm^r AcrA$_{P265R}$ Tn10 @ 10.5	pTrc99a- TolC $_{147AGSG150, A128V}$		This Study
B51-213	MC4100 $\Delta tolC$::Cm^r AcrA$_{P265R}$ Tn10 @ 10.5	pTrc99a- TolC $_{147AGSG150, I133S}$		This Study
B51-214	MC4100 $\Delta tolC$::Cm^r AcrA$_{P265R}$ Tn10 @ 10.5	pTrc99a- TolC $_{147AGSG150, D153E}$		This Study
B51-215	MC4100 $\Delta tolC$::Cm^r AcrA$_{P265R}$ Tn10 @ 10.5	pTrc99a- TolC $_{147AGSG150, S350A}$		This Study
B51-216	MC4100 $\Delta tolC$::Cm^r AcrA$_{P265R}$ Tn10 @ 10.5	pTrc99a- TolC $_{147AGSG150, R390C}$		This Study
B51-217	MC4100 $\Delta tolC$::Cm^r AcrA$_{\Delta 217-218}$ Tn10 @ 10.5	pTrc99a- TolC (*Bsp*HI clone)		This Study
B51-218	MC4100 $\Delta tolC$::Cm^r AcrA$_{\Delta 217-218}$ Tn10 @ 10.5	pTrc99a- TolC $_{147AGSG150}$		This Study
B51-219	MC4100 $\Delta tolC$::Cm^r AcrA$_{\Delta 217-218}$ Tn10 @ 10.5	pTrc99a- TolC $_{147AGSG150, A128V}$		This Study
B51-220	MC4100 $\Delta tolC$::Cm^r AcrA$_{\Delta 217-218}$ Tn10 @ 10.5	pTrc99a- TolC $_{147AGSG150, I133S}$		This Study
B51-221	MC4100 $\Delta tolC$::Cm^r AcrA$_{\Delta 217-218}$ Tn10 @ 10.5	pTrc99a- TolC $_{147AGSG150, D153E}$		This Study
B51-222	MC4100 $\Delta tolC$::Cm^r AcrA$_{\Delta 217-218}$ Tn10 @ 10.5	pTrc99a- TolC $_{147AGSG150, S350A}$		This Study
B51-223	MC4100 $\Delta tolC$::Cm^r AcrA$_{\Delta 217-218}$ Tn10 @ 10.5	pTrc99a- TolC $_{147AGSG150, R390C}$		This Study
B51-224	MC4100 $\Delta tolC$::Km^r			Augustus *et al*., 2004
B51-225	MC4100	pSF4000-*hlyCABD*		Welch *et al*., 1981
B51-226	MC4100 $\Delta tolC$::Km^r	pTrc99a-		This Study
B51-227	MC4100 $\Delta tolC$::Km^r	pTrc99a- TolC (*Bsp*HI clone)		This Study
B51-228	MC4100 $\Delta tolC$::Km^r	pTrc99a- TolC$_{147AGSG150}$		This Study
B51-229	MC4100 $\Delta tolC$::Km^r	pTrc99a-	pSF4000-*hlyCABD*	This Study
B51-230	MC4100 $\Delta tolC$::Km^r	pTrc99a- TolC (*Bsp*HI clone)	pSF4000-*hlyCABD*	This Study
B51-231	MC4100 $\Delta tolC$::Km^r	pTrc99a- TolC $_{147AGSG150}$	pSF4000-*hlyCABD*	This Study
B51-232	MC4100 $\Delta tolC$::Cm^r AcrA$_{S83G}$ Tn10 @ 10.5	pTrc99a- TolC $_{147AGSG150}$		This Study
B51-233	MC4100 $\Delta tolC$::Cm^r AcrA$_{T111P}$ Tn10 @ 10.5	pTrc99a- TolC $_{147AGSG150}$		This Study
B51-234	MC4100 $\Delta tolC$::Cm^r AcrA$_{A135T}$ Tn10 @ 10.5	pTrc99a- TolC $_{147AGSG150}$		This Study
B51-235	MC4100 $\Delta tolC$::Cm^r AcrA$_{T153P}$ Tn10 @ 10.5	pTrc99a- TolC $_{147AGSG150}$		This Study

B51-236	MC4100 Δ*tolC*::Cm^r AcrA$_{L252R}$ Tn10 @ 10.5	pTrc99a- TolC 147AGSG150		This Study
B51-237	MC4100 Δ*ara*714			Werner and Misra, 2005
B51-238	MC4100 Δ*tolC*-scar Δ*ara*714			Augustus *et al*., 2004
B51-239	MC4100 Δ*tolC*-scar Δ*acrAB*::Km^r Δ*ara*714			Augustus *et al*., 2004
B51-240	MC4100 Δ*acrAB*::Km^r Δ*ara*714			Augustus *et al*., 2004
B51-241	MC4100 Δ*tolC*::Cm^r	pTrc99a- TolC R367E BSPHI		This Study
B51-242	MC4100 Δ*tolC*::Cm^r AcrA$_{L222Q}$ Tn10 @ 10.5	pTrc99a- TolC R367E BSPHI		This Study
B51-243	MC4100 Δ*tolC*::Cm^r	pTrc99a- TolC 147AGSG150, R367E		This Study
B51-244	MC4100 Δ*tolC*::Cm^r AcrA$_{L222Q}$ Tn10 @ 10.5	pTrc99a-TolC 147AGSG150, R367E		This Study
B51-245	MC4100 Δ*tolC*::Cm^r	pTrc99a- TolC R390E-BSPHI		This Study
B51-246	MC4100 Δ*tolC*::Cm^r AcrA$_{L222Q}$ Tn10 @ 10.5	pTrc99a- TolC R390E-BSPHI		This Study
B51-247	MC4100 Δ*tolC*::Cm^r	pTrc99a- TolC 147AGSG150, R390E		This Study
B51-248	MC4100 Δ*tolC*::Cm^r AcrA$_{L222Q}$ Tn10 @ 10.5	pTrc99a- TolC 147AGSG150, R390E		This Study
B51-249	MC4100 Δ*tolC*::Cm^r	pTrc99a- TolC [R367E, R390E]-BSPHI		This Study
B51-250	MC4100 Δ*tolC*::Cm^r AcrA$_{L222Q}$ Tn10 @ 10.5	pTrc99a- TolC [R367E, R390E]-BSPHI		This Study
B51-251	MC4100 ΔtolC::Cm^r	pTrc99a- TolC 147AGSG150, R367E, R390E		This Study
B51-252	MC4100 Δ*tolC*::Cm^r AcrA$_{L222Q}$ Tn10 @ 10.5	pTrc99a- TolC 147AGSG150, R367E, R390E		This Study
B51-253	MC4100 Δ*ara*714 Δ*tolC*-scar AcrA$_{L222Q}$ Tn10 @ 10.5			This Study
B51-254	MC4100 Δ*ara*714 Δ*tolC*-scar AcrA$_{L222Q}$ Tn10 @ 10.5	pSF4000-*hlyCABD*		This Study
B51-255	MC4100 Δ*ara*714 Δ*tolC*-scar AcrA$_{L222Q}$ Tn10 @ 10.5	pSF4000-*hlyCABD*	pTrc99a-	This Study
B51-256	MC4100 Δ*ara*714 Δ*tolC*-scar AcrA$_{L222Q}$ Tn10 @ 10.5	pSF4000-*hlyCABD*	pTrc99a- TolC (*Bsp*HI clone)	This Study
B51-257	MC4100 Δ*ara*714 Δ*tolC*-scar AcrA$_{L222Q}$ Tn10 @ 10.5	pSF4000-*hlyCABD*	pTrc99a-TolC$_{147AGSG150}$	This Study
B51-258	MC4100 Δ*ara*714 Δ*tolC*-scar AcrA$_{L222Q}$ Tn10 @ 10.5	pSF4000-*hlyCABD*	pTrc99a- TolC 147AGSG150, A128V	This Study

B51-259	MC4100 Δara714 ΔtolC-scar AcrA$_{L222Q}$ Tn10 @ 10.5	pSF4000-hlyCABD	pTrc99a- TolC 147AGSG150, I133S	This Study
B51-260	MC4100 Δara714 ΔtolC-scar AcrA$_{L222Q}$ Tn10 @ 10.5	pSF4000-hlyCABD	pTrc99a- TolC 147AGSG150, D153E	This Study
B51-261	MC4100 Δara714 ΔtolC-scar AcrA$_{L222Q}$ Tn10 @ 10.5	pSF4000-hlyCABD	pTrc99a- TolC 147AGSG150, S350A	This Study
B51-262	MC4100 Δara714 ΔtolC-scar AcrA$_{L222Q}$ Tn10 @ 10.5	pSF4000-hlyCABD	pTrc99a- TolC 147AGSG150, R390C	This Study
B51-263	BW25113	pKD3- Cm^r gene		Datsenko and Wanner, 2000
B51-264	BW25113	pKD4- Km^r gene		Datsenko and Wanner, 2000
B51-265	BW25113	pKD46- λ rec genes		Datsenko and Wanner, 2000
B51-266	W4573 (F$^-$ lac ara mal xyl mtl gal rpsL) ΔemrB::Km^r			Thanassi *et al.*, 1997
B51-267	MC 4100 ΔemrAB::Cm^r			This study
B51-268	MC 4100 ΔemrAB::Km^r			This study
B51-269	MC4100 ΔtolC::Km^r AcrA$_{L222Q}$ Tn10 @ 10.5	pSF4000-hlyCABD	pTrc99a-	This study
B51-270	MC4100 ΔtolC::Km^r AcrA$_{L222Q}$ Tn10 @ 10.5	pSF4000-hlyCABD	pTrc99a- TolC (*Bsp*HI clone)	This study
B51-271	MC4100 ΔtolC::Km^r AcrA$_{L222Q}$ Tn10 @ 10.5	pSF4000-hlyCABD	pTrc99a- TolC 147AGSG150	This study
B51-272	MC4100 ΔtolC::Km^r AcrA$_{S83G}$ Tn10 @ 10.5	pSF4000-hlyCABD	pTrc99a- TolC 147AGSG150	This study
B51-273	MC4100 ΔtolC::Km^r AcrA$_{T111P}$ Tn10 @ 10.5	pSF4000-hlyCABD	pTrc99a- TolC 147AGSG150	This study
B51-274	MC4100 ΔtolC::Km^r AcrA$_{A135T}$ Tn10 @ 10.5	pSF4000-hlyCABD	pTrc99a- TolC 147AGSG150	This study
B51-275	MC4100 ΔtolC::Km^r AcrA$_{T153P}$ Tn10 @ 10.5	pSF4000-hlyCABD	pTrc99a- TolC 147AGSG150	This study
B51-276	MC4100 ΔtolC::Km^r AcrA$_{L252R}$ Tn10 @ 10.5	pSF4000-hlyCABD	pTrc99a- TolC 147AGSG150	This study
B51-277	MC4100 ΔtolC::Km^r AcrA$_{L222Q}$ Tn10 @ 10.5	pSF4000-hlyCABD	pTrc99a- TolC 147AGSG150, A128V	This study
B51-278	MC4100 ΔtolC::Km^r AcrA$_{L222Q}$ Tn10 @ 10.5	pSF4000-hlyCABD	pTrc99a- TolC 147AGSG150, I133S	This study
B51-279	MC4100 ΔtolC::Km^r AcrA$_{L222Q}$ Tn10 @ 10.5	pSF4000-hlyCABD	pTrc99a- TolC 147AGSG150, D153E	This study
B51-280	MC4100 ΔtolC::Km^r AcrA$_{L222Q}$ Tn10 @ 10.5	pSF4000-hlyCABD	pTrc99a- TolC 147AGSG150, S350A	This study
B51-281	MC4100 ΔtolC::Km^r AcrA$_{L222Q}$ Tn10 @ 10.5	pSF4000-hlyCABD	pTrc99a- TolC 147AGSG150, R390C	This study
B51-282	MC4100 ΔtolC::Km^r ΔacrAB-scar	pTrc99a-TolC$_{147AGSG150}$		This study
B51-283	MC4100 ΔtolC::Km^r ΔacrAB-scar	pTrc99a- TolC (*Bsp*HI clone)	pACYC184-AcrA	This study
B51-284	MC4100 ΔtolC::Km^r ΔacrAB-scar	pTrc99a-TolC$_{147AGSG150}$	pACYC184-AcrA	This study

B51-285	MC4100 Δ*tolC*::Km^r Δ*acrAB*-scar	pTrc99a-TolC$_{147AGSG150}$	pACYC184-	This study
B51-286	MC4100 Δ*tolC*::Km^r Δ*acrAB*-scar	pTrc99a-TolC$_{147AGSG150}$	pACYC184-AcrA$_{T111P}$	This study
B51-287	MC4100 Δ*tolC*::Km^r Δ*acrAB*-scar	pTrc99a- TolC$_{147AGSG150}$	pACYC184-AcrA$_{A135T}$	This study
B51-288	MC4100 Δ*tolC*::Cm^r AcrA$_{L222Q}$ Δ*acrB*::Km^r Tn10 @ 10.5			This study
B51-289	MC4100 Δ*tolC*::Cm^r AcrA$_{L222Q}$ Δ*acrB*::Km^r Tn10 @ 10.5	pTrc99a- TolC (*Bsp*HI clone)		This study
B51-290	MC4100 Δ*tolC*::Cm^r AcrA$_{L222Q}$ Δ*acrB*::Km^r Tn10 @ 10.5	pTrc99a- TolC $_{147AGSG150}$		This study
B51-291	MC4100 Δ*tolC*::Cm^r AcrA$_{L222Q}$ Δ*acrB*::Km^r Tn10 @ 10.5	pTrc99a- TolC $_{147AGSG150, I133S}$		This study
B51-292	MC4100 Δ*tolC*::Cm^r AcrA$_{L222Q}$ Δ*acrB*::Km^r Tn10 @ 10.5	pTrc99a- TolC $_{147AGSG150, R390C}$		This study
B51-293	MC 4100 Δ*ara*714 Δ*emrAB*::Cm^r			This study
B51-294	MC 4100 Δ*ara*714 Δ*emrAB*::Km^r			This study
B51-295	MC4100 Δ*ara*714 Δ*acrAB*::Km^r Δ*emrAB*::Cm^r			This study
B51-296	MC4100 Δ*tolC*::Km^r AcrA$_{L222Q}$ Tn10 @ 10.5	pTrc99a-		This study
B51-297	MC4100 Δ*tolC*::Km^r AcrA$_{L222Q}$ Tn10 @ 10.5	pTrc99a- TolC (*Bsp*HI clone)		This study
B51-298	MC4100 Δ*tolC*::Km^r AcrA$_{L222Q}$ Tn10 @ 10.5	pTrc99a- TolC $_{147AGSG150}$		This study
B51-299	MC4100 Δ*tolC*::Km^r AcrA$_{L222Q}$ Tn10 @ 10.5	pTrc99a- TolC $_{147AGSG150, A128V}$		This study
B51-300	MC4100 Δ*tolC*::Km^r AcrA$_{L222Q}$ Tn10 @ 10.5	pTrc99a- TolC $_{147AGSG150, I133S}$		This study
B51-301	MC4100 Δ*tolC*::Km^r AcrA$_{L222Q}$ Tn10 @ 10.5	pTrc99a- TolC $_{147AGSG150, D153E}$		This study
B51-302	MC4100 Δ*tolC*::Km^r AcrA$_{L222Q}$ Tn10 @ 10.5	pTrc99a- TolC $_{147AGSG150, S350A}$		This study
B51-303	MC4100 Δ*tolC*::Km^r AcrA$_{L222Q}$ Tn10 @ 10.5	pTrc99a- TolC $_{147AGSG150, R390C}$		This study
B51-304	MC4100 Δ*tolC*::Cm^r AcrA$_{L222Q}$ Δ*emrAB*::Km^r Tn10 @ 10.5			This study
B51-305	MC4100 Δ*tolC*::Cm^r AcrA$_{L222Q}$ Δ*emrAB*::Km^r Tn10 @ 10.5	pTrc99a-		This study

B51-306	MC4100 $\Delta tolC$::Cm^r AcrA$_{L222Q}$ $\Delta emrAB$::Km^r Tn10 @ 10.5	pTrc99a- TolC (*Bsp*HI clone)		This study
B51-307	MC4100 $\Delta tolC$::Cm^r AcrA$_{L222Q}$ $\Delta emrAB$::Km^r Tn10 @ 10.5	pTrc99a- TolC$_{147AGSG150}$		This study
B51-308	MC4100 $\Delta tolC$::Cm^r AcrA$_{L222Q}$ $\Delta emrAB$::Km^r Tn10 @ 10.5	pTrc99a- TolC $_{147AGSG150, I133S}$		This study
B51-309	MC4100 $\Delta tolC$::Cm^r AcrA$_{L222Q}$ $\Delta emrAB$::Km^r Tn10 @ 10.5	pTrc99a- TolC $_{147AGSG150, R390C}$		This study
B51-310	MC4100 $\Delta tolC$::Cm^r $\Delta emrAB$::Km^r			This study
B51-311	MC4100 $\Delta tolC$::Cm^r $\Delta emrAB$::Km^r	pTrc99a-		This study
B51-312	MC4100 $\Delta tolC$::Cm^r $\Delta emrAB$::Km^r	pTrc99a- TolC (*Bsp*HI clone)		This study
B51-313	MC4100 $\Delta tolC$::Cm^r $\Delta emrAB$::Km^r	pTrc99a- TolC $_{147AGSG150}$		This study
B51-314	MC4100 $\Delta tolC$::Cm^r AcrA$_{T111P}$ Tn10 @ 10.5			This study
B51-315	MC4100 $\Delta tolC$::Cm^r AcrA$_{T111P}$ $\Delta emrAB$::Km^r Tn10 @ 10.5			This study
B51-316	MC4100 $\Delta tolC$::Cm^r AcrA$_{T111P}$ $\Delta emrAB$::Km^r Tn10 @ 10.5	pTrc99a- TolC $_{147AGSG150}$		This study
B51-317	MC4100 $\Delta tolC$::Cm^r AcrA$_{L252R}$ Tn10 @ 10.5			This study
B51-318	MC4100 $\Delta tolC$::Cm^r AcrA$_{L252R}$ $\Delta emrAB$::Km^r Tn10 @ 10.5			This study
B51-319	MC4100 $\Delta tolC$::Cm^r AcrA$_{L252R}$ $\Delta emrAB$::Km^r Tn10 @ 10.5	pTrc99a- TolC $_{147AGSG150}$		This study
B51-320	MC4100 $\Delta tolC$-scar $\Delta acrAB$::Km^r Δara714	pACYC184-AcrAB		This study
B51-321	MC4100 $\Delta tolC$-scar $\Delta acrAB$::Km^r Δara714	pTrc99a- TolC$_{[Q142C, 6 His]}$		This study
B51-322	MC4100 $\Delta tolC$-scar $\Delta acrAB$::Km^r Δara714	pTrc99a- TolC$_{[Q142C, 6 His]}$	pACYC184-AcrAB	This study
B51-323	MC4100 $\Delta tolC$-scar $\Delta acrAB$::Km^r Δara714	pTrc99a-TolC $_{147AGSG150, Q142C, 6 His}$		This study
B51-324	MC4100 $\Delta tolC$-scar $\Delta acrAB$::Km^r Δara714	pTrc99a- TolC $_{147AGSG150, Q142C, 6His}$	pACYC184-AcrAB	This study
B51-325	MC4100 $\Delta tolC$-scar $\Delta acrAB$::Km^r ΔaraTn10	pTrc99a- TolC$_{6 His}$	pACYC184-AcrAB	This study
B51-326	MC4100 $\Delta tolC$-scar $\Delta acrAB$::Km^r Δara::Tn10	pTrc99a- TolC $_{147AGSG150, 6 His}$	pACYC184-AcrAB	This study
B51-327	MC4100 $\Delta emrB$::Km^r			This study

B51-328	MC4100 Δ*ara*714 Δ*emrB*::Km^r			This study
B51-329	MC4100 Δ*tolC*::Km^r AcrA$_{L222Q}$ Tn10 @ 10.5			This study
B51-330	MC4100 Δ*tolC*::Km^r AcrA$_{L222Q}$ Tn10 @ 10.5	pSF4000-*hlyCABD*		This study
B51-331	MC4100 Δ*tolC*::Km^r Δ*acrAB*-scar	pTrc99a- TolC (BspHI clone)	pACYC184-	This study
B51-332	MC4100 Δ*tolC*::Km^r Δ*acrA*-scar	pTrc99a- TolC (BspHI clone)	pACYC184-AcrA	This study
B51-333	MC4100 Δ*ara*714 Δ*tolC*-scar AcrA$_{L222Q}$ Tn10 @ 10.5	pTrc99a-		This study
B51-334	MC4100 Δ*ara*714 Δ*tolC*-scar AcrA$_{L222Q}$ Tn10 @ 10.5	pTrc99a- TolC (BspHI clone)		This study
B51-335	MC4100 Δ*ara*714 Δ*tolC*-scar AcrA$_{L222Q}$ Tn10 @ 10.5	pTrc99a- TolC $_{147AGSG150}$		This study
B51-336	MC4100 Δ*ara*714 Δ*tolC*-scar AcrA$_{L222Q}$ Tn10 @ 10.5	pTrc99a- TolC $_{147AGSG150, A128V}$		This study
B51-337	MC4100 Δ*ara*714 Δ*tolC*-scar AcrA$_{L222Q}$ Tn10 @ 10.5	pTrc99a- TolC $_{147AGSG150, I133S}$		This study
B51-338	MC4100 Δ*ara*714 Δ*tolC*-scar AcrA$_{L222Q}$ Tn10 @ 10.5	pTrc99a- TolC $_{147AGSG150, D153E}$		This study
B51-339	MC4100 Δ*ara*714 Δ*tolC*-scar AcrA$_{L222Q}$ Tn10 @ 10.5	pTrc99a- TolC $_{147AGSG150, L169V}$		This study
B51-340	MC4100 Δ*ara*714 Δ*tolC*-scar AcrA$_{L222Q}$ Tn10 @ 10.5	pTrc99a- TolC $_{147AGSG150, R390C}$		This study
B51-341	JM109			This study
B51-342	MC4100 Δ*acrAB*-scar Δ*ara*714	pACYC184-AcrAB$_{H1}$ $_{(252ESESGWF258)}$		Husain, 2006
B51-343	MC4100 Δ*acrAB*-scar Δ*ara*714	pACYC184-AcrAB$_{[H1, R259A]}$		This study
B51-344	MC4100 Δ*acrAB*-scar Δ*ara*714	pACYC184-AcrAB$_{FFS}$ $_{(252ESESGWFPR260)}$		Husain, 2006
B51-345	MC4100 Δ*acrAB*-scar Δ*ara*714	pACYC184-AcrAB$_{[FFS, E254A]}$		This study
B51-346	MC4100 Δ*tolC*::Cm^r	pTrc99a-TolC$_{[K383D, 6 His]}$		Bavro *et al.*, 2008
B51-347	MC4100 Δ*tolC*::Cm^r	pTrc99a-TolC$_{[R390E, 6 His]}$		Bavro *et al.*, 2008
B51-348	MC4100 Δ*acrAB*::Km^r Δ*ara*714	pACYC184-AcrAB		This study
B51-349	MC4100 Δ*acrAB*::Km^r Δ*ara*714	pACYC184-AcrA$_{E118R}$ AcrB		Bavro *et al.*, 2008
B51-350	MC4100 Δ*acrAB*::Km^r Δ*ara*714	pACYC184-AcrA$_{D125K}$ AcrB		Bavro *et al.*, 2008
B51-351	MC4100 Δ*tolC*-scar Δ*acrAB*::Km^r Δ*ara*714	pACYC184-AcrAB		This study
B51-352	MC4100 Δ*tolC*-scar Δ*acrAB*::Km^r Δ*ara*714	pTrc99a-		This study

B51-353	MC4100 $\Delta tolC$-scar $\Delta acrAB$::Km^r Δara714	pTrc99a- TolC$_{6\,His}$		This study
B51-354	MC4100 $\Delta tolC$-scar $\Delta acrAB$::Km^r Δara714	pTrc99a-TolC$_{[K383D,\,6\,His]}$		Bavro *et al.*, 2008
B51-355	MC4100 $\Delta tolC$-scar $\Delta acrAB$::Km^r Δara714	pTrc99a-TolC$_{[R390E,\,6\,His]}$		Bavro *et al.*, 2008
B51-356	MC4100 $\Delta tolC$-scar $\Delta acrAB$::Km^r Δara714	pTrc99a-	pACYC184-	This study
B51-357	MC4100 $\Delta tolC$-scar $\Delta acrAB$::Km^r Δara714	pTrc99a- TolC$_{6\,His}$	pACYC184-AcrAB	This study
B51-358	MC4100 $\Delta tolC$-scar $\Delta acrAB$::Km^r Δara714	pTrc99a- TolC$_{6\,His}$	pACYC184-AcrA$_{D125K}$ AcrB	Bavro *et al.*, 2008
B51-359	MC4100 $\Delta tolC$-scar $\Delta acrAB$::Km^r Δara714	pTrc99a-TolC$_{[K383D,\,6\,His]}$	pACYC184-AcrA$_{D125K}$ AcrB	Bavro *et al.*, 2008
B51-360	MC4100 $\Delta tolC$-scar $\Delta acrAB$::Km^r Δara714	pTrc99a-TolC$_{[K383D,\,6\,His]}$	pACYC184-AcrAB	Bavro *et al.*, 2008
B51-361	MC4100 $\Delta tolC$-scar $\Delta acrAB$::Km^r Δara714	pTrc99a- TolC$_{6\,His}$	pACYC184-AcrA$_{E118R}$ AcrB	This study
B51-362	MC4100 $\Delta tolC$-scar $\Delta acrAB$::Km^r Δara714	pTrc99a-TolC$_{[R390E,\,6\,His]}$	pACYC184-AcrA$_{E118R}$ AcrB	This study
B51-363	MC4100 $\Delta tolC$-scar $\Delta acrAB$::Km^r Δara714	pTrc99a-TolC$_{[R390E,\,6\,His]}$	pACYC184-AcrAB	Bavro *et al.*, 2008
B51-364	MC4100 $\Delta acrAB$-scar Δara714			Augustus *et al.*, 2004
B51-365	MC4100 $\Delta tolC$-scar $\Delta acrAB$::Km^r Δara714	pTrc99a- TolC$_{6\,His}$	pACYC184-	This study
B51-366	MC4100 $\Delta tolC$-scar $\Delta acrAB$::Km^r Δara714	pTrc99a-TolC$_{[K383D,\,6\,His]}$	pACYC184-	This study
B51-367	MC4100 $\Delta tolC$-scar $\Delta acrAB$::Km^r Δara714	pTrc99a-TolC$_{[R390E,\,6\,His]}$	pACYC184-	This study
B51-368	MC4100 $\Delta tolC$::Km^r $\Delta acrA$-scar Δara714	pTrc99a-		This study
B51-369	MC4100 $\Delta tolC$::Km^r $\Delta acrA$-scar Δara714	pTrc99a- TolC$_{6\,His}$		This study
B51-370	MC4100 $\Delta tolC$::Km^r $\Delta acrA$-scar Δara714	pTrc99a-TolC$_{[K383D,\,6\,His]}$		This study
B51-371	MC4100 $\Delta tolC$::Km^r $\Delta acrA$-scar Δara714	pTrc99a-TolC$_{[R390E,\,6\,His]}$		This study
B51-372	MC4100 $\Delta tolC$::Km^r $\Delta acrA$-scar Δara714	pACYC184-		This study
B51-373	MC4100 $\Delta tolC$::Km^r $\Delta acrA$-scar Δara714	pACYC184-AcrA		This study
B51-374	MC4100 $\Delta tolC$::Km^r $\Delta acrA$-scar Δara714	pACYC184-AcrA$_{D125K}$		This study
B51-375	MC4100 $\Delta tolC$::Km^r $\Delta acrA$-scar Δara714	pACYC184-AcrA$_{E118R}$		This study
B51-376	MC4100 $\Delta tolC$::Km^r $\Delta acrA$-scar Δara714	pTrc99a-	pACYC184-	This study

B51-377	MC4100 Δ*tolC*::Km^r Δ*acrA*-scar Δ*ara*714	pTrc99a- TolC$_{6}$ $_{His}$	pACYC184-AcrA	This study
B51-378	MC4100 Δ*tolC*::Km^r Δ*acrA*-scar Δ*ara*714	pTrc99a- TolC$_{6}$ $_{His}$	pACYC184-AcrA$_{D125K}$	This study
B51-379	MC4100 Δ*tolC*::Km^r Δ*acrA*-scar Δ*ara*714	pTrc99a- TolC$_{6}$ $_{His}$	pACYC184-AcrA$_{E118R}$	This study
B51-380	MC4100 Δ*tolC*::Km^r Δ*acrA*-scar Δ*ara*714	pTrc99a-TolC$_{[K383D, 6 His]}$	pACYC184-AcrA	This study
B51-381	MC4100 Δ*tolC*::Km^r Δ*acrA*-scar Δ*ara*714	pTrc99a-TolC$_{[K383D, 6 His]}$	pACYC184-AcrA$_{D125K}$	This study
B51-382	MC4100 Δ*tolC*::Km^r Δ*acrA*-scar Δ*ara*714	pTrc99a-TolC$_{[R390E, 6 His]}$	pACYC184-AcrA	This study
B51-383	MC4100 Δ*tolC*::Km^r Δ*acrA*-scar Δ*ara*714	pTrc99a-TolC$_{[R390E, 6 His]}$	pACYC184-AcrA$_{E118R}$	This study
B51-384	MC4100 Δ*tolC*::Km^r Δ*acrA*-scar Δ*ara*714	pACYC184-AcrA	pTrc99a-	This study
B51-385	MC4100 Δ*tolC*::Km^r Δ*acrA*-scar Δ*ara*714	pACYC184-AcrA$_{D125K}$	pTrc99a-	This study
B51-386	MC4100 Δ*tolC*::Km^r Δ*acrA*-scar Δ*ara*714	pACYC184-AcrA$_{E118R}$	pTrc99a-	This study
B51-387	MC4100 Δ*acrAB*-scar Δ*ara*714	pACYC184-		This study
B51-388	MC4100 Δ*tolC*::Cm^r Δ*degP*::Km^r	pTrc99a-		This study
B51-389	MC4100 Δ*tolC*::Cm^r Δ*degP*::Km^r	pTrc99a- TolC$_{6}$ $_{His}$		This study
B51-390	MC4100 Δ*tolC*::Cm^r Δ*degP*::Km^r	pTrc99a-TolC$_{[K383D, 6 His]}$		This study
B51-391	MC4100 Δ*tolC*::Cm^r Δ*degP*::Km^r	pTrc99a-TolC$_{[R390E, 6 His]}$		This study
B51-392	MC4100 Δ*tolC*::Cm^r	pTrc99a-TolC$_{[ΔL1, 6 His]}$		This study
B51-393	MC4100 Δ*tolC*::Cm^r	pTrc99a-TolC$_{[ΔL2, 6 His]}$		This study
B51-394	MC4100 Δ*tolC*::Cm^r	pTrc99a-TolC$_{[ΔL1, ΔL2, 6 His]}$		This study
B51-400	MC4100 Δ*tolC*::Cm^r Δ*degP*::Km^r			This study
B51-411	MC4100 Δ*tolC*::Cm^r	pTrc99a-TolC$_{[D121R, 6 His]}$		This study
B51-412	MC4100 Δ*tolC*::Cm^r Δ*degP*::Km^r	pTrc99a-TolC$_{[D121R, 6 His]}$		This study
B51-413	MC4100 Δ*tolC*::Cm^r	pTrc99a-TolC$_{[R390D, 6 His]}$		This study
B51-414	MC4100 Δ*tolC*::Cm^r Δ*degP*::Km^r	pTrc99a-TolC$_{[R390D, 6 His]}$		This study
B51-415	MC4100 Δ*tolC*::Cm^r	pTrc99a-TolC$_{[D121R, R390D, 6 His]}$		This study
B51-416	MC4100 Δ*tolC*::Cm^r Δ*degP*::Km^r	pTrc99a-TolC$_{[D121R, R390D, 6 His]}$		This study

B51-417	MC4100 $\Delta tolC$::Cm^r	pTrc99a-TolC$_{[R367E, 6 His]}$	This study
B51-418	MC4100 $\Delta tolC$::Cm^r $\Delta degP$::Km^r	pTrc99a-TolC$_{[R367E, 6 His]}$	This study
B51-419	MC4100 $\Delta tolC$::Cm^r	pTrc99a-TolC$_{[R367E, R390E, 6 His]}$	This study
B51-420	MC4100 $\Delta tolC$::Cm^r $\Delta degP$::Km^r	pTrc99a-TolC$_{[R367E, R390E, 6 His]}$	This study
B51-421	MC4100 $\Delta tolC$::Cm^r	pTrc99a-TolC$_{[\Delta L1, R367E, 6 His]}$	This study
B51-422	MC4100 $\Delta tolC$::Cm^r $\Delta degP$::Km^r	pTrc99a-TolC$_{[\Delta L1, R367E, 6 His]}$	This study
B51-423	MC4100 $\Delta tolC$::Cm^r	pTrc99a-TolC$_{[\Delta L1, R390E, 6 His]}$	This study
B51-424	MC4100 $\Delta tolC$::Cm^r $\Delta degP$::Km^r	pTrc99a-TolC$_{[\Delta L1, R390E, 6 His]}$	This study
B51-425	MC4100 $\Delta tolC$::Cm^r	pTrc99a-TolC$_{[\Delta L1, R367E, R390E, 6 His]}$	This study
B51-426	MC4100 $\Delta tolC$::Cm^r $\Delta degP$::Km^r	pTrc99a-TolC$_{[\Delta L1, R367E, R390E, 6 His]}$	This study
B51-427	MC4100 $\Delta tolC$::Cm^r	pTrc99a-TolC$_{[\Delta L2, R367E, 6 His]}$	This study
B51-428	MC4100 $\Delta tolC$::Cm^r $\Delta degP$::Km^r	pTrc99a-TolC$_{[\Delta L2, R367E, 6 His]}$	This study
B51-429	MC4100 $\Delta tolC$::Cm^r	pTrc99a-TolC$_{[\Delta L2, R390E, 6 His]}$	This study
B51-430	MC4100 $\Delta tolC$::Cm^r $\Delta degP$::Km^r	pTrc99a-TolC$_{[\Delta L2, R390E, 6 His]}$	This study
B51-431	MC4100 $\Delta tolC$::Cm^r	pTrc99a-TolC$_{[\Delta L2, R367E, R390E, 6 His]}$	This study
B51-432	MC4100 $\Delta tolC$::Cm^r $\Delta degP$::Km^r	pTrc99a-TolC$_{[\Delta L2, R367E, R390E, 6 His]}$	This study
B51-433	MC4100 $\Delta tolC$::Cm^r	pTrc99a-TolC$_{[\Delta L1, L2, R367E, 6 His]}$	This study
B51-434	MC4100 $\Delta tolC$::Cm^r $\Delta degP$::Km^r	pTrc99a-TolC$_{[\Delta L1, L2, R367E, 6 His]}$	This study

B51-435	MC4100 $\Delta tolC$::Cm^r	pTrc99a-TolC$_{[\Delta L1, L2, R390E, 6His]}$		This study
B51-436	MC4100 $\Delta tolC$::Cm^r $\Delta degP$::Km^r	pTrc99a-TolC$_{[\Delta L1, L2, R390E, 6His]}$		This study
B51-437	MC4100 $\Delta tolC$::Cm^r	pTrc99a-TolC$_{[\Delta L1, L2, R367E, R390E, 6His]}$		This study
B51-438	MC4100 $\Delta tolC$::Cm^r $\Delta degP$::Km^r	pTrc99a-TolC$_{[\Delta L1, L2, R367E, R390E, 6His]}$		This study
B51-439	MC4100 $\Delta tolC$::Cm^r	pTrc99a-TolC$_{[K383D, 6His]}$		This study
B51-440	MC4100 $\Delta tolC$::Km^r $\Delta acrA$-scar Δara714	pTrc99a-TolC$_{[K383D, 6His]}$	pACYC184-AcrA	This study
B51-441	JM109	pBAD33-		This study
B51-442	MC4100 $\Delta acrA$-scar Δara714			This study
B51-443	MC4100 $\Delta acrB$-scar Δara714			Husain, 2006
B51-444	MC4100 $\Delta acrA$-scar Δara714	pBAD33-AcrA$_{6His}$		This study
B51-445	MC4100 $\Delta acrA$-scar Δara714	pBAD33-AcrA$_{6His}$		This study
B51-446	MC4100 $\Delta acrA$-scar Δara714	pBAD33-AcrA$_{6His}$		This study
B51-507	MC4100 $\Delta tolC$::Cm^r Tn10 @ 10.5			This study
B51-508	MC4100 $\Delta tolC$::Cm^r $\Delta acrA$::Km^r			This study
B51-518	K53	pColicin E1		
B51-519	CA42	pColicin E2		
B51-543	JM109	pACYC184-AcrAB		This study
B51-544	JM109	pACYC184-AcrAB$_{[H1, R259A]}$		This study
B51-545	JM109	pACYC184-AcrAB	(SDM Correct)	This study
B51-546	JM109	pACYC184-AcrAB	(SDM Correct)	This study
B51-547	MC4100 $\Delta acrAB$-scar Δara714	pACYC184-AcrAB	(SDM Correct)	This study
B51-548	MC4100 $\Delta acrAB$-scar Δara714	pACYC184-AcrAB	(SDM Correct)	This study
B51-550	MC4100 $\Delta acrAB$-scar Δara714	pACYC184-AcrAB$_{\Delta L1}$		This study
B51-551	MC4100 $\Delta acrAB$-scar Δara714	pACYC184-AcrAB$_{PAL1}$		This study
B51-562	MC4100 $\Delta tolC$-scar $\Delta acrAB$::Km^r Δara714	pACYC184-		This study
B51-563	MC4100 $\Delta tolC$-scar $\Delta acrAB$::Km^r Δara714	pACYC184-AcrAB		This study

B51-564	MC4100 $\Delta tolC$-scar $\Delta acrAB$::Km^r Δara714	pACYC184-AcrAB$_{\Delta L1}$		This study
B51-565	MC4100 $\Delta tolC$-scar $\Delta acrAB$::Km^r Δara714	pTrc99a-		This study
B51-566	MC4100 $\Delta tolC$-scar $\Delta acrAB$::Km^r Δara714	pTrc99a- TolC$_{6\ His}$		This study
B51-567	MC4100 $\Delta tolC$-scar $\Delta acrAB$::Km^r Δara714	pTrc99a-TolC$_{[R367E,\ 6\ His]}$		This study
B51-568	MC4100 $\Delta tolC$-scar $\Delta acrAB$::Km^r Δara714	pTrc99a-TolC$_{[R390E,\ 6\ His]}$		This study
B51-569	MC4100 $\Delta tolC$-scar $\Delta acrAB$::Km^r Δara714	pACYC184-	pTrc99a-	This study
B51-570	MC4100 $\Delta tolC$-scar $\Delta acrAB$::Km^r Δara714	pACYC184-AcrAB	pTrc99a-TolC$_{6\ His}$	This study
B51-571	MC4100 $\Delta tolC$-scar $\Delta acrAB$::Km^r Δara714	pACYC184-AcrAB$_{\Delta L1}$	pTrc99a-TolC$_{6\ His}$	This study
B51-572	MC4100 $\Delta tolC$-scar $\Delta acrAB$::Km^r Δara714	pACYC184-AcrAB$_{\Delta L1}$	pTrc99a- TolC$_{[R367E,\ 6\ His]}$	This study
B51-573	MC4100 $\Delta tolC$-scar $\Delta acrAB$::Km^r Δara714	pACYC184-AcrAB$_{\Delta L1}$	pTrc99a- TolC$_{[R390E,\ 6\ His]}$	This study
B51-574	MC4100 $\Delta tolC$-scar $\Delta acrAB$::Km^r Δara714	pTrc99a-	pACYC184-	This study
B51-575	MC4100 $\Delta tolC$-scar $\Delta acrAB$::Km^r Δara714	pTrc99a- TolC$_{6\ His}$	pACYC184-AcrAB	This study
B51-576	MC4100 $\Delta tolC$-scar $\Delta acrAB$::Km^r Δara714	pTrc99a- TolC$_{6\ His}$	pACYC184-AcrAB$_{\Delta L1}$	This study
B51-577	MC4100 $\Delta tolC$-scar $\Delta acrAB$::Km^r Δara714	pTrc99a-TolC$_{[R367E,\ 6\ His]}$	pACYC184-AcrAB$_{\Delta L1}$	This study
B51-578	MC4100 $\Delta tolC$-scar $\Delta acrAB$::Km^r Δara714	pTrc99a-TolC$_{[R390E,\ 6\ His]}$	pACYC184-AcrAB$_{\Delta L1}$	This study
B51-579	MC4100 $\Delta tolC$-scar 1			This study
B51-580	MC4100 $\Delta tolC$-scar 2			This study
B51-591	MC4100 $\Delta acrAB$-scar	pACYC184-AcrAB$_{D256A,\ D795A}$		This study
B51-592	MC4100 $\Delta tolC$-scar $\Delta acrAB$::Km^r Δara714	pACYC184-AcrAB	pTrc99a-	This study
B51-593	MC4100 $\Delta tolC$-scar $\Delta acrAB$::Km^r Δara714	pACYC184-AcrAB	pTrc99a-TolC$_{[R367E,\ 6\ His]}$	This study
B51-594	MC4100 $\Delta tolC$-scar $\Delta acrAB$::Km^r Δara714	pACYC184-AcrAB	pTrc99a-TolC$_{[R390E,\ 6\ His]}$	This study
B51-607	$acrF$::Tn10			
B51-608	MC4100 Δara714 $acrF$::Tn10			This study
B51-609	MC4100 Δara714 $acrF$::Tn10			This study
B51-610	MC4100 $\Delta tolC$-scar Δara714 $acrF$::Tn10			This study
B51-611	MC4100 $\Delta tolC$-scar Δara714 $acrF$::Tn10			This study

B51-612	MC4100 $\Delta acrAB$::Km^r Δara714 $acrF$::Tn10			This study
B51-613	MC4100 $\Delta acrAB$::Km^r Δara714 $acrF$::Tn10			This study
B51-614	MC 4100 Δara714 $\Delta emrAB$::Cm^r $acrF$::Tn10			This study
B51-615	MC 4100 Δara714 $\Delta emrAB$::Cm^r $acrF$::Tn10			This study
B51-616	MC4100 Δara714 $\Delta acrAB$::Km^r $\Delta emrAB$::Cm^r $acrF$::Tn10			This study
B51-617	MC4100 Δara714 $\Delta acrAB$::Km^r $\Delta emrAB$::Cm^r $acrF$::Tn10			This study
B51-737	MC4100 $\Delta acrAB$-scar Δara714	pACYC184-AcrAB$_{\Delta L1}$		This study
B51-738	MC4100 $\Delta acrAB$-scar Δara714	pACYC184-AcrAB$_{\Delta L1}$		This study
B51-739	MC4100 $\Delta acrAB$-scar Δara714	pACYC184-AcrA$_{73DP74\rightarrow ET}$ AcrB$_{\Delta L1}$		This study
B51-740	MC4100 $\Delta acrAB$-scar Δara714	pACYC184-AcrA$_{E237V}$ AcrB$_{\Delta L1}$		This study
B51-741	MC4100 $\Delta acrAB$-scar Δara714	pACYC184-AcrAB$_{\Delta L1}$		This study
B51-742	MC4100 $\Delta acrAB$-scar Δara714	pACYC184-AcrAB$_{\Delta L1}$		This study
B51-743	MC4100 $\Delta tolC$-scar $\Delta acrAB$::Km^r Δara714	pACYC184-AcrAB$_{\Delta L1}$		This study
B51-744	MC4100 $\Delta tolC$-scar $\Delta acrAB$::Km^r Δara714	pACYC184-	pTrc99a-TolC$_{6\,His}$	This study
B51-745	MC4100 $\Delta tolC$-scar $\Delta acrAB$::Km^r Δara714	pACYC184-	pTrc99a-TolC$_{[R367E,\,6\,His]}$	This study
B51-746	MC4100 $\Delta tolC$-scar $\Delta acrAB$::Km^r Δara714	pACYC184-	pTrc99a-TolC$_{[R390E,\,6\,His]}$	This study
B51-747	JM109	pBAD24-		This study
B51-748	MC4100 $\Delta acrAB$-scar Δara714	pACYC184-AcrAB$_{\Delta L2}$		This study
B51-750	MC4100 $\Delta acrAB$-scar Δara714	pACYC184-AcrAB$_{PAL2}$		This study
B51-752	MC4100 $\Delta acrAB$-scar Δara714	pACYC184-AcrAB$_{PAL1/L2}$		This study
B51-754	MC4100 $\Delta acrAB$-scar Δara714	pACYC184-AcrAB$_{PAL1/L2}$		This study
B51-756	JM109	pACYC184-		This study
B51-757	JM109	pACYC184-AcrAB$_{\Delta L1}$		This study
B51-758	JM109	pACYC184-AcrAB$_{PAL1}$		This study

B51-759	JM109	pACYC184-AcrAB$_{\Delta L2}$	This study
B51-760	JM109	pACYC184-AcrAB$_{PAL2}$	This study
B51-761	JM109	pACYC184-AcrAB$_{PAL1/L2}$	This study
B51-762	JM109	pACYC184-AcrAB$_{PAL1/L2}$	This study
B51-765	MC4100 $\Delta acrAB$-scar Δara714	pACYC184-AcrA$_{T224S}$ AcrB$_{\Delta L1}$	This study
B51-766	MC4100 $\Delta acrAB$-scar Δara714	pACYC184-AcrA$_{L222Q}$ AcrB$_{\Delta L1}$	This study
B51-767	MC4100 $\Delta acrAB$-scar Δara714	pACYC184-AcrA$_{G248E}$ AcrB$_{\Delta L1}$	This study
B51-768	MC4100 $\Delta acrAB$-scar Δara714	pACYC184-AcrA$_{L222R}$ AcrB$_{\Delta L1}$	This study
B51-769	MC4100 $\Delta acrAB$-scar Δara714	pACYC184-AcrA$_{\Delta 222-224}$ AcrB$_{\Delta L1}$	This study
B51-770	MC4100 $\Delta acrAB$-scar Δara714	pACYC184-AcrA$_{F230S}$ AcrB$_{\Delta L1}$	This study
B51-771	MC4100 $\Delta acrAB$-scar Δara714	pACYC184-AcrA$_{F230S}$ AcrB$_{\Delta L1}$	This study
B51-772	MC4100 $\Delta acrAB$-scar Δara714	pACYC184-AcrA$_{F230S}$ AcrB$_{\Delta L1}$	This study
B51-773	MC4100 $\Delta acrAB$-scar Δara714	pACYC184-AcrA$_{F230S}$ AcrB$_{\Delta L1}$	This study
B51-774	MC4100 $\Delta acrAB$-scar Δara714	pACYC184-AcrA$_{G248E}$ AcrB$_{\Delta L1}$	This study
B51-775	MC4100 $\Delta acrAB$-scar Δara714	pACYC184-AcrA$_{E43K}$ AcrB$_{\Delta L1}$	This study
B51-776	MC4100 $\Delta acrAB$-scar Δara714	pACYC184-AcrA$_{V44I}$ AcrB$_{\Delta L1}$	This study
B51-777	MC4100 $\Delta acrAB$-scar Δara714	pACYC184-AcrA$_{S195P}$ AcrB$_{\Delta L1}$	This study
B51-778	MC4100 $\Delta acrAB$-scar Δara714	pACYC184-AcrA$_{S249C}$ AcrB$_{\Delta L1}$	This study

B51-779	MC4100 $\Delta acrAB$-scar Δara714	pACYC184-AcrA$_{S83G}$ AcrB$_{\Delta L1}$	This study
B51-780	MC4100 $\Delta acrAB$-scar Δara714	pACYC184-AcrA$_{T111P}$ AcrB$_{\Delta L1}$	This study
B51-781	MC4100 $\Delta acrAB$-scar Δara714	pACYC184-AcrA$_{A135T}$ AcrB$_{\Delta L1}$	This study
B51-782	MC4100 $\Delta acrAB$-scar Δara714	pACYC184-AcrA$_{N146T}$ AcrB$_{\Delta L1}$	This study
B51-783	MC4100 $\Delta acrAB$-scar Δara714	pACYC184-AcrAB$_{His}$	This study
B51-784	MC4100 $\Delta acrAB$-scar Δara714	pACYC184-AcrAB$_{His}$	This study
B51-785	MC4100 $\Delta acrAB$-scar Δara714	pACYC184-AcrAB$_{PAL1/L2}$	This study
B51-786	MC4100 $\Delta acrAB$-scar Δara714	pACYC184-AcrAB$_{PAL1/L2}$	This study
B51-787	MC4100 $\Delta recA$::Km$_r$	pACYC184-	This study
B51-788	MC4100 $\Delta recA$::Km^r	pACYC184-	This study
B51-789	MC4100 $\Delta recA$::Km$_r$	pACYC184-AcrAB (old)	This study
B51-790	MC4100 $\Delta recA$::Km^r	pACYC184-AcrAB (old)	This study
B51-791	MC4100 $\Delta recA$::Km$_r$	pACYC184-AcrAB$_{H1}$ (252ESESGWF258)	This study
B51-792	MC4100 $\Delta recA$::Km^r	pACYC184-AcrAB$_{H1}$ (252ESESGWF258)	This study
B51-793	MC4100 $\Delta recA$::Km$_r$	pACYC184-AcrAB (new)	This study
B51-794	MC4100 $\Delta recA$::Km^r	pACYC184-AcrAB (new)	This study
B51-795	MC4100 $\Delta recA$::Km$_r$	pACYC184-AcrAB$_{\Delta L1}$	This study
B51-796	MC4100 $\Delta recA$::Km^r	pACYC184-AcrAB$_{\Delta L1}$	This study
B51-797	MC4100 $\Delta tolC$::Cm^r	pTrc99a-TolC$_{147GAAA150}$	This study
B51-798	MC4100 $\Delta tolC$::Cm^r	pTrc99a-TolC$_{147AAAA150}$	This study
B51-799	MC4100 $\Delta tolC$::Cm^r AcrA$_{L222Q}$ Tn10 @ 10.5	pTrc99a-TolC$_{147GAAA150}$	This study
B51-800	MC4100 $\Delta tolC$::Cm^r AcrA$_{L222Q}$ Tn10 @ 10.5	pTrc99a-TolC$_{147AAAA150}$	This study
B51-817	MC4100 $\Delta acrAB$-scar Δara714	pACYC184-AcrAB$_{KAAAAL1/PAL2}$	This study

B51-818	MC4100 $\Delta acrAB$-scar Δara714	pACYC184-AcrAB$_{\text{AANAAL1/P}}$		This study
B51-819	MC4100 $\Delta acrAB$-scar Δara714	pACYC184-AcrAB$_{\text{AAAQAL1/P}}^{\text{AL2}}$		This study
B51-820	MC4100 $\Delta acrAB$-scar Δara714	pACYC184-AcrAB$_{\text{AAAADL1/P}}^{\text{AL2}}$		This study
B51-821	MC4100 $\Delta acrAB$-scar Δara714	pACYC184-AcrAB$_{\text{AAAAKL1/P}}^{\text{AL2}}$		This study
B51-822	MC4100 $\Delta acrAB$-scar Δara714	pACYC184-AcrAB$_{\text{PAL1/AADA}}^{\text{AL2}}$		This study
B51-823	MC4100 $\Delta acrAB$-scar Δara714	pACYC184-AcrAB$_{\text{PAL1/AAAA}}^{\text{QL2}}$		This study
B51-824	MC4100 $\Delta acrAB$-scar Δara714	pACYC184-AcrAB$_{\text{D256A}}$		This study
B51-825	MC4100 $\Delta acrAB$-scar Δara714	pACYC184-AcrAB$_{\text{D795A}}$		This study
B51-826	MC4100 $\Delta acrAB$-scar Δara714	pACYC184-AcrAB$_{\text{D256A, D795A}}$		This study
B51-827	MC4100 $\Delta tolC$::Cm$^{\text{r}}$	pTrc99a-TolC$_{\text{G147A}}$	1	This study
B51-828	MC4100 $\Delta tolC$::Cm$^{\text{r}}$	pTrc99a-TolC$_{\text{G147A}}$	2	This study
B51-829	MC4100 $\Delta acrAB$-scar Δara714	pACYC184-AcrA$_{\text{S83G}}$ AcrB$_{\text{PAL1/L2}}$		This study
B51-830	MC4100 $\Delta acrAB$-scar Δara714	pACYC184-AcrA$_{\text{A135T}}$ AcrB$_{\text{PAL1/L2}}$		This study
B51-831	MC4100 $\Delta acrAB$-scar Δara714	pACYC184-AcrA$_{\text{L222Q}}$ AcrB$_{\text{PAL1/L2}}$		This study
B51-832	MC4100 $\Delta acrAB$-scar Δara714	pACYC184-AcrA$_{\text{G248E}}$ AcrB$_{\text{PAL1/L2}}$		This study
B51-833	MC4100 $\Delta acrAB$-scar Δara714	pACYC184-AcrAB$_{\text{R971A}}$		This study
B51-834	MC4100 $\Delta acrAB$-scar Δara714	pACYC184-AcrA$_{\text{L222Q}}$ AcrB$_{\text{R971A}}$		This study
B51-835	MC4100 $\Delta acrAB$-scar Δara714	pACYC184-AcrA$_{\text{G248E}}$ AcrB$_{\text{R971A}}$		This study
B51-836	MC4100 $\Delta acrAB$-scar Δara714	pACYC184-AcrAB$_{\text{D407A}}$		This study

B51-837	MC4100 Δ*acrAB*-scar Δ*ara*714	pACYC184-AcrA$_{L222Q}$ AcrB$_{D407A}$	This study
B51-838	MC4100 Δ*acrAB*-scar Δ*ara*714	pACYC184-AcrA$_{G248E}$ AcrB$_{D407A}$	This study
B51-839	MC4100 Δ*acrAB*-scar Δ*ara*714	pACYC184-AcrAB$_{F136A}$	This study
B51-840	MC4100 Δ*acrAB*-scar Δ*ara*714	pACYC184-AcrAB$_{F610A}$	This study
B51-841	MC4100 Δ*acrAB*-scar Δ*ara*714	pACYC184-AcrAB$_{F615A}$	This study
B51-842	MC4100 Δ*acrAB*-scar Δ*ara*714	pACYC184-AcrAB$_{His}$	This study
B51-843	MC4100 Δ*acrAB*-scar Δ*ara*714	pACYC184-AcrAB$_{ΔL1, His}$	This study
B51-844	MC4100 Δ*tolC*-scar Δ*acrAB*::Km^r Δ*ara*714	pACYC184-	This study
B51-845	MC4100 Δ*tolC*-scar Δ*acrAB*::Km^r Δ*ara*714	pACYC184-AcrAB	This study
B51-846	MC4100 Δ*tolC*-scar Δ*acrAB*::Km^r Δ*ara*714	pACYC184-AcrAB$_{PAL1/L2}$	This study
B51-847	MC4100 Δ*tolC*-scar Δ*acrAB*::Km^r Δ*ara*714	pACYC184-AcrAB$_{ΔL1}$	This study
B51-848	MC4100 Δ*tolC*-scar Δ*acrAB*::Km^r Δ*ara*714	pACYC184-AcrA$_{L222Q}$ AcrB$_{ΔL1}$	This study
B51-849	MC4100 Δ*tolC*-scar Δ*acrAB*::Km^r Δ*ara*714	pACYC184-AcrA$_{G248E}$ AcrB$_{ΔL1}$	This study
B51-850	MC4100 Δ*acrAB*-scar Δ*ara*714	pACYC184-AcrA$_{L222Q}$ AcrB	This study
B51-851	MC4100 Δ*acrAB*-scar Δ*ara*714	pACYC184-AcrA$_{G248E}$ AcrB	This study
B51-852	MC4100 Δ*acrAB*-scar Δ*ara*714	pACYC184-AcrA$_{L222Q}$ AcrB$_{F136A}$	This study
B51-853	MC4100 Δ*acrAB*-scar Δ*ara*714	pACYC184-AcrA$_{G248E}$ AcrB$_{F136A}$	This study
B51-854	MC4100 Δ*acrAB*-scar Δ*ara*714	pACYC184-AcrA$_{L222Q}$ AcrB$_{F610A}$	This study
B51-855	MC4100 Δ*acrAB*-scar Δ*ara*714	pACYC184-AcrA$_{G248E}$ AcrB$_{F610A}$	This study
B51-856	MC4100 Δ*acrAB*-scar Δ*ara*714	pACYC184-AcrA$_{L222Q}$ AcrB$_{F615A}$	This study
B51-857	MC4100 Δ*acrAB*-scar Δ*ara*714	pACYC184-AcrA$_{G248E}$ AcrB$_{F615A}$	This study

B51-858	MC4100 $\Delta tolC$-scar $\Delta acrAB$::Km^r Δara714	pTrc99a-	pACYC184-AcrAB$_{PAL1/L2}$		This study
B51-859	MC4100 $\Delta tolC$-scar $\Delta acrAB$::Km^r Δara714	pTrc99a- TolC$_{6\ His}$	pACYC184-AcrAB$_{PAL1/L2}$		This study
B51-860	MC4100 $\Delta tolC$-scar $\Delta acrAB$::Km^r Δara714	pTrc99a-TolC$_{[R367E, 6\ His]}$	pACYC184-AcrAB$_{PAL1/L2}$		This study
B51-861	MC4100 $\Delta tolC$-scar $\Delta acrAB$::Km^r Δara714	pTrc99a-TolC$_{[R390E, 6\ His]}$	pACYC184-AcrAB$_{PAL1/L2}$		This study
B51-862	MC4100 $\Delta acrAB$-scar Δara714	pACYC184-AcrAB$_{His\ (Cys\ less)}$			This study
B51-863	MC4100 $\Delta acrAB$-scar Δara714	pACYC184-AcrAB$_{\Delta L1, His\ (Cys\ less)}$	1		This study
B51-864	MC4100 $\Delta acrAB$-scar Δara714	pACYC184-AcrAB$_{\Delta L1, His\ (Cys\ less)}$	2		This study
B51-865	MC4100 $\Delta acrAB$-scar Δara714	pACYC184-AcrAB$_{PAL1, His\ (Cys\ less)}$			This study
B51-866	MC4100 $\Delta acrAB$-scar Δara714	pACYC184-AcrAB$_{PAL1/L2, His\ (Cys\ less)}$			This study
B51-867	MC4100 $\Delta acrAB$-scar Δara714	pACYC184-AcrA$_{K58C}$ AcrB$_{His\ (Cys\ less)}$			This study
B51-868	MC4100 $\Delta acrAB$-scar Δara714	pACYC184-AcrA$_{S196C}$ AcrB$_{His\ (Cys\ less)}$			This study
B51-869	MC4100 $\Delta acrAB$-scar Δara714	pACYC184-AcrAB$_{\Delta L1, His\ (Cys\ less)}$			This study
B51-870	MC4100 $\Delta acrAB$-scar Δara714	pACYC184-AcrA$_{K58C}$ AcrB$_{\Delta L1, His\ (Cys\ less)}$			This study
B51-871	MC4100 $\Delta acrAB$-scar Δara714	pACYC184-AcrA$_{S196C}$ AcrB$_{\Delta L1, His\ (Cys\ less)}$			This study
B51-872	MC4100 AcrA$_{L222Q}$ $\Delta acrB$::Km^r Tn10 @ 10.5 Δara714		1		This study
B51-873	MC4100 AcrA$_{L222Q}$ $\Delta acrB$::Km^r Tn10 @ 10.5 Δara714		2		This study
B51-874	MC4100 $\Delta tolC$::Cm^r	pTrc99a-TolC$_{G147C}$			This study
B51-875	MC4100 $\Delta tolC$::Cm^r	pTrc99a-TolC$_{G365C}$			This study
B51-876	MC4100 $\Delta acrB$::Km^r Δara714	pACYC184-			This study
B51-877	MC4100 $\Delta acrB$::Km^r Δara714	pACYC184-AcrB			This study

153

B51-878	MC4100 Δ*acrB*::Km^r Δ*ara*714	pACYC184-AcrB$_{ΔL1}$		This study
B51-879	MC4100 Δ*acrB*::Km^r Δ*ara*714	pACYC184-		This study
B51-880	MC4100 Δ*acrB*::Km^r Δ*ara*714	pACYC184-AcrB		This study
B51-881	MC4100 Δ*acrB*::Km^r Δ*ara*714	pACYC184-AcrB$_{ΔL1}$		This study
B51-882	MC4100 Δ*acrAB*-scar Δ*ara*714	pACYC184-AcrAB$_{Q255C, His (Cys less)}$		This study
B51-883	MC4100 Δ*acrAB*-scar Δ*ara*714	pACYC184-AcrAB$_{D795C, His (Cys less)}$		This study
B51-884	MC4100 Δ*acrAB*-scar Δ*ara*714	pACYC184-AcrAB$_{PAL1/L2, A255C, His (Cys less)}$		This study
B51-885	MC4100 Δ*acrAB*-scar Δ*ara*714	pACYC184-AcrAB$_{PAL1/L2, A795C, His (Cys less)}$		This study
B51-886	MC4100 Δ*tolC*-scar Δ*acrAB*::Km^r Δ*ara*714	pACYC184-	pTrc99a-	This study
B51-887	MC4100 Δ*tolC*-scar Δ*acrAB*::Km^r Δ*ara*714	pACYC184-	pTrc99a- TolC (NcoI clone)	This study
B51-888	MC4100 Δ*tolC*-scar Δ*acrAB*::Km^r Δ*ara*714	pACYC184-	pTrc99a-TolC$_{[P246R, S350C] NCOI}$	This study
B51-889	MC4100 Δ*tolC*-scar Δ*acrAB*::Km^r Δ*ara*714	pACYC184-AcrB	pTrc99a-	This study
B51-890	MC4100 Δ*tolC*-scar Δ*acrAB*::Km^r Δ*ara*714	pACYC184-AcrB	pTrc99a- TolC (NcoI clone)	This study
B51-891	MC4100 Δ*tolC*-scar Δ*acrAB*::Km^r Δ*ara*714	pACYC184-AcrB	pTrc99a-TolC$_{[P246R, S350C] NCOI}$	This study
B51-892	MC4100 Δ*tolC*-scar Δ*acrAB*::Km^r Δ*ara*714	pACYC184-AcrB$_{ΔL1}$	pTrc99a-	This study
B51-893	MC4100 Δ*tolC*-scar Δ*acrAB*::Km^r Δ*ara*714	pACYC184-AcrB$_{ΔL1}$	pTrc99a- TolC (NcoI clone)	This study
B51-894	MC4100 Δ*tolC*-scar Δ*acrAB*::Km^r Δ*ara*714	pACYC184-AcrB$_{ΔL1}$	pTrc99a-TolC$_{[P246R, S350C] NCOI}$	This study
B51-895	MC4100 Δ*tolC*-scar Δ*acrAB*::Km^r Δ*ara*714	pACYC184-AcrAB$_{His}$		This study
B51-896	MC4100 Δ*tolC*-scar Δ*acrAB*::Km^r Δ*ara*714	pACYC184-AcrAB$_{ΔL1, His}$		This study
B51-897	MC4100 Δ*tolC*-scar Δ*acrA*::Km^r Δ*ara*714			This study
B51-898	MC4100 Δ*tolC*-scar Δ*acrA*::Km^r Δ*ara*714			This study
B51-899	MC4100 Δ*tolC*-scar Δ*acrA*::Km^r Δ*ara*714	pACYC184-		This study

B51-900	MC4100 $\Delta tolC$-scar $\Delta acrA$::Km^r Δara714	pACYC184-AcrA	Corrected by SDM (JW) - AcrAN244D	This study
B51-901	MC4100 $\Delta tolC$-scar $\Delta acrA$::Km^r Δara714	pACYC184-AcrA$_{S83G}$	Corrected by SDM (JW) - AcrAN244D	This study
B51-902	MC4100 $\Delta tolC$-scar $\Delta acrAB$::Km^r Δara714	pACYC184-AcrA	Corrected by SDM (JW) - AcrAN244D	This study
B51-903	MC4100 $\Delta tolC$-scar $\Delta acrAB$::Km^r Δara714	pACYC184-AcrA$_{S83G}$	Corrected by SDM (JW) - AcrAN244D	This study
B51-904	MC4100 $\Delta tolC$-scar $\Delta acrA$::Km^r Δara714	pACYC184-	pTrc99a-	This study
B51-905	MC4100 $\Delta tolC$-scar $\Delta acrA$::Km^r Δara714	pACYC184-	pTrc99a-TolC (*Bsp*HI clone)	This study
B51-906	MC4100 $\Delta tolC$-scar $\Delta acrA$::Km^r Δara714	pACYC184-	pTrc99a-TolC$_{147AGSG150}$	This study
B51-907	MC4100 $\Delta tolC$-scar $\Delta acrA$::Km^r Δara714	pACYC184-AcrA	pTrc99a-	This study
B51-908	MC4100 $\Delta tolC$-scar $\Delta acrA$::Km^r Δara714	pACYC184-AcrA	pTrc99a-TolC (*Bsp*HI clone)	This study
B51-909	MC4100 $\Delta tolC$-scar $\Delta acrA$::Km^r Δara714	pACYC184-AcrA	pTrc99a-TolC$_{147AGSG150}$	This study
B51-910	MC4100 $\Delta tolC$-scar $\Delta acrA$::Km^r Δara714	pACYC184-AcrA$_{S83G}$	pTrc99a-	This study
B51-911	MC4100 $\Delta tolC$-scar $\Delta acrA$::Km^r Δara714	pACYC184-AcrA$_{S83G}$	pTrc99a-TolC (*Bsp*HI clone)	This study
B51-912	MC4100 $\Delta tolC$-scar $\Delta acrA$::Km^r Δara714	pACYC184-AcrA$_{S83G}$	pTrc99a-TolC$_{147AGSG150}$	This study
B51-913	MC4100 $\Delta tolC$-scar $\Delta acrAB$::Km^r Δara714	pACYC184-	pTrc99a-	This study
B51-914	MC4100 $\Delta tolC$-scar $\Delta acrAB$::Km^r Δara714	pACYC184-	pTrc99a-TolC (*Bsp*HI clone)	This study
B51-915	MC4100 $\Delta tolC$-scar $\Delta acrAB$::Km^r Δara714	pACYC184-	pTrc99a-TolC$_{147AGSG150}$	This study
B51-916	MC4100 $\Delta tolC$-scar $\Delta acrAB$::Km^r Δara714	pACYC184-AcrA	pTrc99a-	This study
B51-917	MC4100 $\Delta tolC$-scar $\Delta acrAB$::Km^r Δara714	pACYC184-AcrA	pTrc99a-TolC (*Bsp*HI clone)	This study
B51-918	MC4100 $\Delta tolC$-scar $\Delta acrAB$::Km^r Δara714	pACYC184-AcrA	pTrc99a-TolC$_{147AGSG150}$	This study
B51-919	MC4100 $\Delta tolC$-scar $\Delta acrAB$::Km^r Δara714	pACYC184-AcrA$_{S83G}$	pTrc99a-	This study
B51-920	MC4100 $\Delta tolC$-scar $\Delta acrAB$::Km^r Δara714	pACYC184-AcrA$_{S83G}$	pTrc99a-TolC (*Bsp*HI clone)	This study

155

B51-921	MC4100 ΔtolC-scar ΔacrA*B*::Kmr Δara714	pACYC184-AcrA$_{S83G}$	pTrc99a-TolC$_{147AGSG150}$	This study
B51-922	MC4100 Δ*tolC*-scar Δ*acrA*::Km^r Δ*ara*714	pACYC184-	pTrc99a-	This study
B51-923	MC4100 Δ*tolC*-scar Δ*acrA*::Km^r Δ*ara*714	pACYC184-	pTrc99a-TolC (*Bsp*HI clone)	This study
B51-924	MC4100 Δ*tolC*-scar Δ*acrA*::Km^r Δ*ara*714	pACYC184-	pTrc99a-TolC$_{147AGSG150}$	This study
B51-925	MC4100 Δ*tolC*-scar Δ*acrA*::Km^r Δ*ara*714	pACYC184-AcrA	pTrc99a-	This study
B51-926	MC4100 Δ*tolC*-scar Δ*acrA*::Km^r Δ*ara*714	pACYC184-AcrA	pTrc99a-TolC (*Bsp*HI clone)	This study
B51-927	MC4100 Δ*tolC*-scar Δ*acrA*::Km^r Δ*ara*714	pACYC184-AcrA	pTrc99a-TolC$_{147AGSG150}$	This study
B51-928	MC4100 Δ*tolC*-scar Δ*acrA*::Km^r Δ*ara*714	pACYC184-AcrA$_{S83G}$	pTrc99a-	This study
B51-929	MC4100 Δ*tolC*-scar Δ*acrA*::Km^r Δ*ara*714	pACYC184-AcrA$_{S83G}$	pTrc99a-TolC (*Bsp*HI clone)	This study
B51-930	MC4100 Δ*tolC*-scar Δ*acrA*::Km^r Δ*ara*714	pACYC184-AcrA$_{S83G}$	pTrc99a-TolC$_{147AGSG150}$	This study
B51-931	MC4100 Δ*tolC*-scar Δ*acrA*::Km^r Δ*ara*714	pACYC184-		This study
B51-932	MC4100 Δ*tolC*-scar Δ*acrA*::Km^r Δ*ara*714	pACYC184-AcrA	Corrected by SDM (JW) - AcrAN244D	This study
B51-933	MC4100 Δ*tolC*-scar Δ*acrA*::Km^r Δ*ara*714	pACYC184-AcrA$_{S83G}$	Corrected by SDM (JW) - AcrAN244D	This study
B51-934	MC4100 Δ*tolC*-scar Δ*acrAB*::Km^r Δ*ara*714	pTrc99a-TolC$_{[Q142C, 6 His]}$	pACYC184-AcrAB	This study
B51-935	MC4100 Δ*tolC*-scar Δ*acrAB*::Km^r Δ*ara*714	pTrc99a-TolC$_{[Q142C, 6 His]}$	pACYC184-AcrA	This study
B51-936	MC4100 Δ*tolC*-scar Δ*acrAB*::Km^r Δ*ara*714	pTrc99a-TolC$_{[Q142C, 6 His]}$	pACYC184-AcrB	This study
B51-937	MC4100 Δ*tolC*-scar Δ*acrAB*::Km^r Δ*ara*714	pTrc99a- TolC-147AGSG150$_{, Q142C, 6 His]}$	pACYC184-AcrAB	This study
B51-938	MC4100 Δ*tolC*-scar Δ*acrAB*::Km^r Δ*ara*714	pTrc99a- TolC-147AGSG150$_{, Q142C, 6 His]}$	pACYC184-AcrA	This study
B51-939	MC4100 Δ*tolC*-scar Δ*acrAB*::Km^r Δ*ara*714	pTrc99a- TolC-147AGSG150$_{, Q142C, 6 His]}$	pACYC184-AcrB	This study
B51-940	MC4100 Δ*tolC*-scar Δ*acrAB*::Km^r Δ*ara*714	pACYC184-AcrAB$_{PAL1/L2, A255C, His (Cys less)}$	2	This study
B51-941	MC4100 Δ*tolC*-scar Δ*acrAB*::Km^r Δ*ara*714	pACYC184-AcrAB$_{His (Cys less)}$	pTrc99a-TolC	This study

B51-942	MC4100 Δ*tolC*-scar Δ*acrAB*::Km^r Δ*ara*714	pACYC184-AcrAB$_{PAL1/L2, His}$ (Cys less)	pTrc99a-TolC	This study
B51-943	MC4100 Δ*tolC*-scar Δ*acrAB*::Km^r Δ*ara*714	pACYC184-AcrAB$_{Q255C, His}$ (Cys less)	pTrc99a-TolC	This study
B51-944	MC4100 Δ*tolC*-scar Δ*acrAB*::Km^r Δ*ara*714	pACYC184-AcrAB$_{Q255C, His}$ (Cys less)	pTrc99a-TolC	This study
B51-945	MC4100 Δ*tolC*-scar Δ*acrAB*::Km^r Δ*ara*714	pACYC184-AcrAB$_{Q255C, His}$ (Cys less)	pTrc99a-TolC$_{G147C}$	This study
B51-946	MC4100 Δ*tolC*-scar Δ*acrAB*::Km^r Δ*ara*714	pACYC184-AcrAB$_{Q255C, His}$ (Cys less)	pTrc99a-TolC$_{G147C}$	This study
B51-947	MC4100 Δ*tolC*-scar Δ*acrAB*::Km^r Δ*ara*714	pACYC184-AcrAB$_{PAL1/L2, A255C, His}$ (Cys less)	pTrc99a-TolC	This study
B51-948	MC4100 Δ*tolC*-scar Δ*acrAB*::Km^r Δ*ara*714	pACYC184-AcrAB$_{PAL1/L2, A255C, His}$ (Cys less)	pTrc99a-TolC	This study
B51-949	MC4100 Δ*tolC*-scar Δ*acrAB*::Km^r Δ*ara*714	pACYC184-AcrAB$_{PAL1/L2, A255C, His}$ (Cys less)	pTrc99a-TolC$_{G147C}$	This study
B51-950	MC4100 Δ*tolC*-scar Δ*acrAB*::Km^r Δ*ara*714	pACYC184-AcrAB$_{PAL1/L2, A255C, His}$ (Cys less)	pTrc99a-TolC$_{G147C}$	This study
B51-951	MC4100 Δ*tolC*-scar Δ*acrAB*::Km^r Δ*ara*714	pACYC184-AcrAB$_{D795C, His}$ (Cys less)	pTrc99a-TolC	This study
B51-952	MC4100 Δ*tolC*-scar Δ*acrAB*::Km^r Δ*ara*714	pACYC184-AcrAB$_{D795C, His}$ (Cys less)	pTrc99a-TolC	This study
B51-953	MC4100 Δ*tolC*-scar Δ*acrAB*::Km^r Δ*ara*714	pACYC184-AcrAB$_{D795C, His}$ (Cys less)	pTrc99a-TolC$_{G365C}$	This study
B51-954	MC4100 Δ*tolC*-scar Δ*acrAB*::Km^r Δ*ara*714	pACYC184-AcrAB$_{D795C, His}$ (Cys less)	pTrc99a-TolC$_{G365C}$	This study
B51-955	MC4100 Δ*tolC*-scar Δ*acrAB*::Km^r Δ*ara*714	pACYC184-AcrAB$_{PAL1/L2, A795C, His}$ (Cys less)	pTrc99a-TolC	This study
B51-956	MC4100 Δ*tolC*-scar Δ*acrAB*::Km^r Δ*ara*714	pACYC184-AcrAB$_{PAL1/L2, A795C, His}$ (Cys less)	pTrc99a-TolC	This study
B51-957	MC4100 Δ*tolC*-scar Δ*acrAB*::Km^r Δ*ara*714	pACYC184-AcrAB$_{PAL1/L2, A795C, His}$ (Cys less)	pTrc99a-TolC$_{G365C}$	This study
B51-958	MC4100 Δ*tolC*-scar Δ*acrAB*::Km^r Δ*ara*714	pACYC184-AcrAB$_{PAL1/L2, A795C, His}$ (Cys less)	pTrc99a-TolC$_{G365C}$	This study

B51-959	MC4100 Δ*tolC*-scar Δ*acrAB*::Km^r Δ*ara*714	pACYC184-AcrA$_{E43K}$ AcrB$_{ΔL1}$	pTrc99a-TolC$_{[P246R, S350C]}$ NCOI	This study
B51-960	MC4100 Δ*tolC*-scar Δ*acrAB*::Km^r Δ*ara*714	pACYC184-AcrA$_{V44I}$ AcrB$_{ΔL1}$	pTrc99a-TolC$_{[P246R, S350C]}$ NCOI	This study
B51-961	MC4100 Δ*tolC*-scar Δ*acrAB*::Km^r Δ*ara*714	pACYC184-AcrA$_{S195P}$ AcrB$_{ΔL1}$	pTrc99a-TolC$_{[P246R, S350C]}$ NCOI	This study
B51-962	MC4100 Δ*tolC*-scar Δ*acrAB*::Km^r Δ*ara*714	pACYC184-AcrA$_{L222Q}$ AcrB$_{ΔL1}$	pTrc99a-TolC$_{[P246R, S350C]}$ NCOI	This study
B51-963	MC4100 Δ*tolC*-scar Δ*acrAB*::Km^r Δ*ara*714	pACYC184-AcrA$_{L222R}$ AcrB$_{ΔL1}$	pTrc99a-TolC$_{[P246R, S350C]}$ NCOI	This study
B51-964	MC4100 Δ*tolC*-scar Δ*acrAB*::Km^r Δ*ara*714	pACYC184-AcrA$_{Δ222-224}$ AcrB$_{ΔL1}$	pTrc99a-TolC$_{[P246R, S350C]}$ NCOI	This study
B51-965	MC4100 Δ*tolC*-scar Δ*acrAB*::Km^r Δ*ara*714	pACYC184-AcrA$_{T224S}$ AcrB$_{ΔL1}$	pTrc99a-TolC$_{[P246R, S350C]}$ NCOI	This study
B51-966	MC4100 Δ*tolC*-scar Δ*acrAB*::Km^r Δ*ara*714	pACYC184-AcrA$_{F230S}$ AcrB$_{ΔL1}$	pTrc99a-TolC$_{[P246R, S350C]}$ NCOI	This study
B51-967	MC4100 Δ*tolC*-scar Δ*acrAB*::Km^r Δ*ara*714	pACYC184-AcrA$_{G248E}$ AcrB$_{ΔL1}$	pTrc99a-TolC$_{[P246R, S350C]}$ NCOI	This study
B51-968	MC4100 Δ*tolC*-scar Δ*acrAB*::Km^r Δ*ara*714	pACYC184-AcrA$_{S249C}$ AcrB$_{ΔL1}$	pTrc99a-TolC$_{[P246R, S350C]}$ NCOI	This study
B51-969	MC4100 Δ*tolC*-scar Δ*acrAB*::Km^r Δ*ara*714	pACYC184-AcrA$_{S83G}$	pTrc99a-TolC$_{147AGSG150}$	This study
B51-970	MC4100 Δ*tolC*-scar Δ*acrAB*::Km^r Δ*ara*714	pACYC184-AcrA$_{S83G}$	pTrc99a-TolC$_{147AGSG150}$	This study
B51-971	MC4100 Δ*tolC*-scar Δ*acrAB*::Km^r Δ*ara*714	pACYC184-AcrA$_{S83G}$ AcrB	pTrc99a-TolC$_{147AGSG150}$	This study
B51-972	MC4100 Δ*tolC*-scar Δ*acrAB*::Km^r Δ*ara*714	pACYC184-AcrA$_{S83G}$ AcrB	pTrc99a-TolC$_{147AGSG150}$	This study
B51-973	MC4100 Δ*tolC*-scar Δ*acrAB*::Km^r Δ*ara*714	pACYC184-AcrA$_{S83G}$ AcrB$_{D407A}$	pTrc99a-TolC$_{147AGSG150}$	This study
B51-974	MC4100 Δ*tolC*-scar Δ*acrAB*::Km^r Δ*ara*714	pACYC184-AcrA$_{S83G}$ AcrB$_{D407A}$	pTrc99a-TolC$_{147AGSG150}$	This study
B51-975	MC4100 Δ*tolC*-scar Δ*acrAB*::Km^r Δ*ara*714	pACYC184-AcrAB$_{His}$	pTrc99a-TolC	This study
B51-976	MC4100 Δ*tolC*-scar Δ*acrAB*::Km^r Δ*ara*714	pACYC184-AcrAB$_{ΔL1, His}$	pTrc99a-TolC	This study
B51-979	MC4100 Δ*tolC*-scar Δ*acrAB*::Km^r Δ*ara*714	pACYC184-AcrAB	pTrc99a-TolC$_{147AGSG150}$	This study
B51-980	MC4100 Δ*tolC*-scar Δ*acrAB*::Km^r Δ*ara*714	pACYC184-AcrAB	pTrc99a-TolC$_{147AGSG150}$	This study

B51-981	MC4100 $\Delta tolC$-scar $\Delta acrAB$::Km^r Δara714	pACYC184-AcrAB$_{D407A}$	pTrc99a-TolC$_{147AGSG150}$	This study
B51-982	MC4100 $\Delta tolC$-scar $\Delta acrAB$::Km^r Δara714	pACYC184-AcrAB$_{D407A}$	pTrc99a-TolC$_{147AGSG150}$	This study
B51-983	MC4100 $\Delta tolC$-scar $\Delta acrAB$::Km^r Δara714	pACYC184-AcrA$_{L252R}$	pTrc99a-TolC$_{147AGSG150}$	This study
B51-984	MC4100 $\Delta tolC$-scar $\Delta acrAB$::Km^r Δara714	pACYC184-AcrA$_{L252R}$	pTrc99a-TolC$_{147AGSG150}$	This study
B51-985	MC4100 $\Delta tolC$-scar $\Delta acrAB$::Km^r Δara714	pACYC184-AcrA$_{L252R}$ AcrB	pTrc99a-TolC$_{147AGSG150}$	This study
B51-986	MC4100 $\Delta tolC$-scar $\Delta acrAB$::Km^r Δara714	pACYC184-AcrA$_{L252R}$ AcrB	pTrc99a-TolC$_{147AGSG150}$	This study
B51-987	MC4100 $\Delta tolC$-scar $\Delta acrAB$::Km^r Δara714	pACYC184-AcrA$_{L252R}$ AcrB$_{D407A}$	pTrc99a-TolC$_{147AGSG150}$	This study
B51-988	MC4100 $\Delta tolC$-scar $\Delta acrAB$::Km^r Δara714	pACYC184-AcrA$_{L252R}$ AcrB$_{D407A}$	pTrc99a-TolC$_{147AGSG150}$	This study
B51-989	MC4100 $\Delta tolC$::Cm^r AcrA$_{S83G}$ Tn10 @ 10.5	pTrc99a- TolC$_{147AGSG150, R367E}$		This study
B51-990	MC4100 $\Delta tolC$::Cm^r AcrA$_{S83G}$ Tn10 @ 10.5	pTrc99a- TolC$_{147AGSG150, R390E}$		This study
B51-991	MC4100 $\Delta tolC$::Cm^r AcrA$_{T111P}$ Tn10 @ 10.5	pTrc99a- TolC$_{147AGSG150, R367E}$		This study
B51-992	MC4100 $\Delta tolC$::Cm^r AcrA$_{T111P}$ Tn10 @ 10.5	pTrc99a- TolC$_{147AGSG150, R390E}$		This study
B51-993	MC4100 $\Delta tolC$::Cm^r AcrA$_{A135T}$ Tn10 @ 10.5	pTrc99a- TolC$_{147AGSG150, R367E}$		This study
B51-994	MC4100 $\Delta tolC$::Cm^r AcrA$_{A135T}$ Tn10 @ 10.5	pTrc99a- TolC$_{147AGSG150, R390E}$		This study
B51-995	MC4100 $\Delta tolC$::Cm^r AcrA$_{T153P}$ Tn10 @ 10.5	pTrc99a- TolC$_{147AGSG150, R367E}$		This study
B51-996	MC4100 $\Delta tolC$::Cm^r AcrA$_{T153P}$ Tn10 @ 10.5	pTrc99a- TolC$_{147AGSG150, R390E}$		This study
B51-997	MC4100 $\Delta tolC$::Cm^r AcrA$_{L252R}$ Tn10 @ 10.5	pTrc99a- TolC$_{147AGSG150, R367E}$		This study
B51-998	MC4100 $\Delta tolC$::Cm^r AcrA$_{L252R}$ Tn10 @ 10.5	pTrc99a- TolC$_{147AGSG150, R390E}$		This study
B51-999	BL21			Novogen
B51-1000	BL21 (DE3)			Novogen
B51-1001	BL21 (DE3)	pLys		Novogen
B51-1002	MC4100 $\Delta tolC$-scar $\Delta acrAB$::Km^r Δara714	pACYC184-	pTrc99a-TolC$_{[P246R, S350C, 6 His] BspHI}$	This study
B51-1003	MC4100 $\Delta tolC$-scar $\Delta acrAB$::Km^r Δara714	pACYC184-AcrAB	pTrc99a-TolC$_{[P246R, S350C, 6 His] BspHI}$	This study
B51-1004	MC4100 $\Delta tolC$-scar $\Delta acrAB$::Km^r Δara714	pACYC184-AcrAB$_{\Delta L1}$	pTrc99a-TolC$_{[P246R, S350C, 6 His] BspHI}$	This study

B51-1005	MC4100 Δ*tolC*-scar Δ*acrAB*::Km^r Δ*ara*714	pACYC184-AcrA$_{E43K}$ AcrB$_{ΔL1}$	pTrc99a-TolC$_{[P246R,}$ $_{S350C, 6 His] BspHI}$	This study
B51-1006	MC4100 Δ*tolC*-scar Δ*acrAB*::Km^r Δ*ara*714	pACYC184-AcrA$_{V44I}$ AcrB$_{ΔL1}$	pTrc99a-TolC$_{[P246R,}$ $_{S350C, 6 His] BspHI}$	This study
B51-1007	MC4100 Δ*tolC*-scar Δ*acrAB*::Km^r Δ*ara*714	pACYC184-AcrA$_{S195P}$ AcrB$_{ΔL1}$	pTrc99a-TolC$_{[P246R,}$ $_{S350C, 6 His] BspHI}$	This study
B51-1008	MC4100 Δ*tolC*-scar Δ*acrAB*::Km^r Δ*ara*714	pACYC184-AcrA$_{L222Q}$ AcrB$_{ΔL1}$	pTrc99a-TolC$_{[P246R,}$ $_{S350C, 6 His] BspHI}$	This study
B51-1009	MC4100 Δ*tolC*-scar Δ*acrAB*::Km^r Δ*ara*714	pACYC184-AcrA$_{L222R}$ AcrB$_{ΔL1}$	pTrc99a-TolC$_{[P246R,}$ $_{S350C, 6 His] BspHI}$	This study
B51-1010	MC4100 Δ*tolC*-scar Δ*acrAB*::Km^r Δ*ara*714	pACYC184-AcrA$_{Δ222-224}$ AcrB$_{ΔL1}$	pTrc99a-TolC$_{[P246R,}$ $_{S350C, 6 His] BspHI}$	This study
B51-1011	MC4100 Δ*tolC*-scar Δ*acrAB*::Km^r Δ*ara*714	pACYC184-AcrA$_{T224S}$ AcrB$_{ΔL1}$	pTrc99a-TolC$_{[P246R,}$ $_{S350C, 6 His] BspHI}$	This study
B51-1012	MC4100 Δ*tolC*-scar Δ*acrAB*::Km^r Δ*ara*714	pACYC184-AcrA$_{F230S}$ AcrB$_{ΔL1}$	pTrc99a-TolC$_{[P246R,}$ $_{S350C, 6 His] BspHI}$	This study
B51-1013	MC4100 Δ*tolC*-scar Δ*acrAB*::Km^r Δ*ara*714	pACYC184-AcrA$_{G248E}$ AcrB$_{ΔL1}$	pTrc99a-TolC$_{[P246R,}$ $_{S350C, 6 His] BspHI}$	This study
B51-1014	MC4100 Δ*tolC*-scar Δ*acrAB*::Km^r Δ*ara*714	pACYC184-AcrA$_{S249C}$ AcrB$_{ΔL1}$	pTrc99a-TolC$_{[P246R,}$ $_{S350C, 6 His] BspHI}$	This study
B51-1015	JM109	pET24a(+) -		This study
B51-1016	JM109	pET24a(+) - AcrB$_{[G288C, F615A, His]}$		This study
B51-1017	JM109	pET24a(+) - AcrB$_{[G288C, F615A, His]}$		This study
B51-1018	JM109	pET24a(+) - AcrB$_{[G288C, F615A, His]}$		This study
B51-1019	MC4100 Δ*tolC*-scar Δ*acrAB*::Km^r Δ*ara*714	pACYC184-AcrAB$_{Q255C, His}$ $_{(Cys less)}$	pTrc99a-TolC$_{G365C}$	This study
B51-1020	MC4100 Δ*tolC*-scar Δ*acrAB*::Km^r Δ*ara*714	pACYC184-AcrAB$_{PAL1/L2,}$ $_{A255C, His (Cys less)}$	pTrc99a-TolC$_{G365C}$	This study

B51-1021	MC4100 Δ*tolC*-scar Δ*acrAB*::Km^r Δ*ara*714	pACYC184-AcrAB$_{PAL1/L2, A255C, His (Cys less)}$	pTrc99a-TolC$_{G365C}$	This study
B51-1022	MC4100 Δ*tolC*-scar Δ*acrAB*::Km^r Δ*ara*714	pACYC184-AcrAB$_{D795C, His (Cys less)}$	pTrc99a-TolC$_{G147C}$	This study
B51-1023	MC4100 Δ*tolC*-scar Δ*acrAB*::Km^r Δ*ara*714	pACYC184-AcrAB$_{PAL1/L2, A795C, His (Cys less)}$	pTrc99a-TolC$_{G147C}$	This study
B51-1033	MC4100 Δ*acrAB*-scar Δ*ara*714 Δ*tolC*::Tn10			This study
B51-1034	MC4100 Δ*acrAB*-scar Δ*ara*714 Δ*tolC*::Tn10			This study
B51-1035	MC4100 Δ*acrAB*-scar Δ*ara*714 Δ*tolC*::Tn10 Δ*dsbA*::Km^r			This study
B51-1036	MC4100 Δ*acrAB*-scar Δ*ara*714 Δ*tolC*::Tn10 Δ*dsbA*::Km^r			This study
B51-1037	MC4100 Δ*ara*714 714 *rfa*2057			This study
B51-1038	MC4100 Δ*acrAB*-scar Δ*ara*714 Δ*tolC*::Tn10	pTrc99a- TolC		This study
B51-1039	MC4100 Δ*acrAB*-scar Δ*ara*714 Δ*tolC*::Tn10 Δ*dsbA*::Km^r	pTrc99a- TolC		This study
B51-1040	MC4100 Δ*acrAB*-scar Δ*ara*714 Δ*tolC*::Tn10	pTrc99a-TolC$_{G147C}$		This study
B51-1041	MC4100 Δ*acrAB*-scar Δ*ara*714 Δ*tolC*::Tn10 Δ*dsbA*::Km^r	pTrc99a-TolC$_{G147C}$		This study
B51-1042	MC4100 Δ*acrAB*-scar Δ*ara*714 Δ*tolC*::Tn10	pTrc99a-TolC$_{G365C}$		This study
B51-1043	MC4100 Δ*acrAB*-scar Δ*ara*714 Δ*tolC*::Tn10 Δ*dsbA*::Km^r	pTrc99a-TolC$_{G365C}$		This study
B51-1044	MC4100 Δ*acrAB*-scar Δ*ara*714 Δ*tolC*::Tn10	pTrc99a- TolC	pACYC184-AcrAB$_{His (Cys less)}$	This study
B51-1045	MC4100 Δ*acrAB*-scar Δ*ara*714 Δ*tolC*::Tn10	pTrc99a- TolC	pACYC184-AcrAB$_{His (Cys less)}$	This study
B51-1046	MC4100 Δ*acrAB*-scar Δ*ara*714 Δ*tolC*::Tn10 Δ*dsbA*::Km^r	pTrc99a- TolC	pACYC184-AcrAB$_{His (Cys less)}$	This study
B51-1047	MC4100 Δ*acrAB*-scar Δ*ara*714 Δ*tolC*::Tn10	pTrc99a- TolC	pACYC184-AcrAB$_{Q255C, His (Cys less)}$	This study
B51-1048	MC4100 Δ*acrAB*-scar Δ*ara*714 Δ*tolC*::Tn10	pTrc99a- TolC	pACYC184-AcrAB$_{Q255C, His (Cys less)}$	This study

B51-1049	MC4100 Δ*acrAB*-scar Δ*ara*714 Δ*tolC*::Tn10 Δ*dsbA*::Km^r	pTrc99a- TolC	pACYC184-AcrAB$_{Q255C, His}$ (Cys less)	This study
B51-1050	MC4100 Δ*acrAB*-scar Δ*ara*714 Δ*tolC*::Tn10	pTrc99a- TolC	pACYC184-AcrAB$_{D795C, His}$ (Cys less)	This study
B51-1051	MC4100 Δ*acrAB*-scar Δ*ara*714 Δ*tolC*::Tn10	pTrc99a- TolC	pACYC184-AcrAB$_{D795C, His}$ (Cys less)	This study
B51-1052	MC4100 Δ*acrAB*-scar Δ*ara*714 Δ*tolC*::Tn10 Δ*dsbA*::Km^r	pTrc99a- TolC	pACYC184-AcrAB$_{D795C, His}$ (Cys less)	This study
B51-1053	MC4100 Δ*acrAB*-scar Δ*ara*714 Δ*tolC*::Tn10	pTrc99a-TolC$_{G147C}$	pACYC184-AcrAB$_{His (Cys less)}$	This study
B51-1054	MC4100 Δ*acrAB*-scar Δ*ara*714 Δ*tolC*::Tn10	pTrc99a-TolC$_{G147C}$	pACYC184-AcrAB$_{His (Cys less)}$	This study
B51-1055	MC4100 Δ*acrAB*-scar Δ*ara*714 Δ*tolC*::Tn10 Δ*dsbA*::Km^r	pTrc99a-TolC$_{G147C}$	pACYC184-AcrAB$_{His (Cys less)}$	This study
B51-1056	MC4100 Δ*acrAB*-scar Δ*ara*714 Δ*tolC*::Tn10	pTrc99a-TolC$_{G147C}$	pACYC184-AcrAB$_{Q255C, His}$ (Cys less)	This study
B51-1057	MC4100 Δ*acrAB*-scar Δ*ara*714 Δ*tolC*::Tn10	pTrc99a-TolC$_{G147C}$	pACYC184-AcrAB$_{Q255C, His}$ (Cys less)	This study
B51-1058	MC4100 Δ*acrAB*-scar Δ*ara*714 Δ*tolC*::Tn10 Δ*dsbA*::Km^r	pTrc99a-TolC$_{G147C}$	pACYC184-AcrAB$_{Q255C, His}$ (Cys less)	This study
B51-1059	MC4100 Δ*acrAB*-scar Δ*ara*714 Δ*tolC*::Tn10	pTrc99a-TolC$_{G365C}$	pACYC184-AcrAB$_{His (Cys less)}$	This study
B51-1060	MC4100 Δ*acrAB*-scar Δ*ara*714 Δ*tolC*::Tn10	pTrc99a-TolC$_{G365C}$	pACYC184-AcrAB$_{His (Cys less)}$	This study
B51-1061	MC4100 Δ*acrAB*-scar Δ*ara*714 Δ*tolC*::Tn10 Δ*dsbA*::Km^r	pTrc99a-TolC$_{G365C}$	pACYC184-AcrAB$_{His (Cys less)}$	This study
B51-1062	MC4100 Δ*acrAB*-scar Δ*ara*714 Δ*tolC*::Tn10	pTrc99a-TolC$_{G365C}$	pACYC184-AcrAB$_{D795C, His}$ (Cys less)	This study
B51-1063	MC4100 Δ*acrAB*-scar Δ*ara*714 Δ*tolC*::Tn10	pTrc99a-TolC$_{G365C}$	pACYC184-AcrAB$_{D795C, His}$ (Cys less)	This study
B51-1064	MC4100 Δ*acrAB*-scar Δ*ara*714 Δ*tolC*::Tn10 Δ*dsbA*::Km^r	pTrc99a-TolC$_{G365C}$	pACYC184-AcrAB$_{D795C, His}$ (Cys less)	This study
B51-1065	MC4100 *tolC*::Tn10			Morano and Reeves, 1981
B51-1066	MC4100 Δ*tolC*::Km^r			Augustus *et al.*, 2004

B51-1070	MC4100 Δ*tolC*-scar Δ*acrAB*::Km^r Δ*ara*714	pACYC184-AcrAB$_{His}$	pTrc99a-TolC	This study
B51-1071	MC4100 Δ*tolC*-scar Δ*acrAB*::Km^r Δ*ara*714	pACYC184-AcrAB$_{His}$	pTrc99a-TolC	This study
B51-1072	MC4100 Δ*tolC*-scar Δ*acrAB*::Km^r Δ*ara*714	pACYC184-AcrAB$_{His}$	pTrc99a-TolC$_{G365C}$	This study
B51-1073	MC4100 Δ*tolC*-scar Δ*acrAB*::Km^r Δ*ara*714	pACYC184-AcrAB$_{His}$	pTrc99a-TolC$_{G365C}$	This study
B51-1074	MC4100 Δ*tolC*-scar Δ*acrAB*::Km^r Δ*ara*714	pACYC184-AcrAB$_{His\ (Cys\ less)}$	pTrc99a-TolC	This study
B51-1075	MC4100 Δ*tolC*-scar Δ*acrAB*::Km^r Δ*ara*714	pACYC184-AcrAB$_{His\ (Cys\ less)}$	pTrc99a-TolC	This study
B51-1076	MC4100 Δ*tolC*-scar Δ*acrAB*::Km^r Δ*ara*714	pACYC184-AcrAB$_{His\ (Cys\ less)}$	pTrc99a-TolC$_{G365C}$	This study
B51-1077	MC4100 Δ*tolC*-scar Δ*acrAB*::Km^r Δ*ara*714	pACYC184-AcrAB$_{His\ (Cys\ less)}$	pTrc99a-TolC$_{G365C}$	This study
B51-1078	MC4100 Δ*tolC*-scar Δ*acrAB*::Km^r Δ*ara*714	pACYC184-AcrAB$_{D795C,\ His\ (Cys\ less)}$	pTrc99a-TolC	This study
B51-1079	MC4100 Δ*tolC*-scar Δ*acrAB*::Km^r Δ*ara*714	pACYC184-AcrAB$_{D795C,\ His\ (Cys\ less)}$	pTrc99a-TolC	This study
B51-1080	MC4100 Δ*tolC*-scar Δ*acrAB*::Km^r Δ*ara*714	pACYC184-AcrAB$_{D795C,\ His\ (Cys\ less)}$	pTrc99a-TolC$_{G365C}$	This study
B51-1081	MC4100 Δ*tolC*-scar Δ*acrAB*::Km^r Δ*ara*714	pACYC184-AcrAB$_{D795C,\ His\ (Cys\ less)}$	pTrc99a-TolC$_{G365C}$	This study
B51-1082	MC4100 Δ*tolC*-scar Δ*acrAB*::Km^r Δ*ara*714	pACYC184-AcrAB$_{His}$	pTrc99a-TolC$_{G147C}$	This study
B51-1083	MC4100 Δ*tolC*-scar Δ*acrAB*::Km^r Δ*ara*714	pACYC184-AcrAB$_{His}$	pTrc99a-TolC$_{G147C}$	This study
B51-1084	MC4100 Δ*tolC*-scar Δ*acrAB*::Km^r Δ*ara*714	pACYC184-AcrAB$_{His\ (Cys\ less)}$	pTrc99a-TolC$_{G147C}$	This study
B51-1085	MC4100 Δ*tolC*-scar Δ*acrAB*::Km^r Δ*ara*714	pACYC184-AcrAB$_{His\ (Cys\ less)}$	pTrc99a-TolC$_{G147C}$	This study
B51-1086	MC4100 Δ*tolC*-scar Δ*acrAB*::Km^r Δ*ara*714	pACYC184-AcrAB$_{Q255C,\ His\ (Cys\ less)}$	pTrc99a-TolC	This study
B51-1087	MC4100 Δ*tolC*-scar Δ*acrAB*::Km^r Δ*ara*714	pACYC184-AcrAB$_{Q255C,\ His\ (Cys\ less)}$	pTrc99a-TolC	This study
B51-1088	MC4100 Δ*tolC*-scar Δ*acrAB*::Km^r Δ*ara*714	pACYC184-AcrAB$_{Q255C,\ His\ (Cys\ less)}$	pTrc99a-TolC$_{G147C}$	This study
B51-1089	MC4100 Δ*tolC*-scar Δ*acrAB*::Km^r Δ*ara*714	pACYC184-AcrAB$_{Q255C,\ His\ (Cys\ less)}$	pTrc99a-TolC$_{G147C}$	This study
B51-1090	MC4100 Δ*tolC*-scar Δ*acrAB*::Km^r Δ*ara*714	pACYC184-AcrAB$_{PAL1/L2,\ His\ (Cys\ less)}$	pTrc99a-TolC	This study

B51-1091	MC4100 Δ*tolC*-scar Δ*acrAB*::Km^r Δ*ara*714	pACYC184-AcrAB$_{PAL1/L2, His}$ (Cys less)	pTrc99a-TolC	This study
B51-1092	MC4100 Δ*tolC*-scar Δ*acrAB*::Km^r Δ*ara*714	pACYC184-AcrAB$_{PAL1/L2, His}$ (Cys less)	pTrc99a-TolC$_{G147C}$	This study
B51-1093	MC4100 Δ*tolC*-scar Δ*acrAB*::Km^r Δ*ara*714	pACYC184-AcrAB$_{PAL1/L2, His}$ (Cys less)	pTrc99a-TolC$_{G147C}$	This study
B51-1094	MC4100 Δ*tolC*-scar Δ*acrAB*::Km^r Δ*ara*714	pACYC184-AcrAB$_{PAL1/L2, His}$ (Cys less)	pTrc99a-TolC$_{G365C}$	This study
B51-1095	MC4100 Δ*tolC*-scar Δ*acrAB*::Km^r Δ*ara*714	pACYC184-AcrAB$_{PAL1/L2, His}$ (Cys less)	pTrc99a-TolC$_{G365C}$	This study
B51-1096	MC4100 Δ*tolC*-scar Δ*acrAB*::Km^r Δ*ara*714	pACYC184-AcrAB$_{PAL1/L2,}$ A255C, His (Cys less)	pTrc99a-TolC	This study
B51-1097	MC4100 Δ*tolC*-scar Δ*acrAB*::Km^r Δ*ara*714	pACYC184-AcrAB$_{PAL1/L2,}$ A255C, His (Cys less)	pTrc99a-TolC	This study
B51-1098	MC4100 Δ*tolC*-scar Δ*acrAB*::Km^r Δ*ara*714	pACYC184-AcrAB$_{PAL1/L2,}$ A255C, His (Cys less)	pTrc99a-TolC$_{G147C}$	This study
B51-1099	MC4100 Δ*tolC*-scar Δ*acrAB*::Km^r Δ*ara*714	pACYC184-AcrAB$_{PAL1/L2,}$ A255C, His (Cys less)	pTrc99a-TolC$_{G147C}$	This study
B51-1100	MC4100 Δ*tolC*-scar Δ*acrAB*::Km^r Δ*ara*714	pACYC184-AcrAB$_{PAL1/L2,}$ A795C, His (Cys less)	pTrc99a-TolC	This study
B51-1101	MC4100 Δ*tolC*-scar Δ*acrAB*::Km^r Δ*ara*714	pACYC184-AcrAB$_{PAL1/L2,}$ A795C, His (Cys less)	pTrc99a-TolC	This study
B51-1102	MC4100 Δ*tolC*-scar Δ*acrAB*::Km^r Δ*ara*714	pACYC184-AcrAB$_{PAL1/L2,}$ A795C, His (Cys less)	pTrc99a-TolC$_{G365C}$	This study
B51-1103	MC4100 Δ*tolC*-scar Δ*acrAB*::Km^r Δ*ara*714	pACYC184-AcrAB$_{PAL1/L2,}$ A795C, His (Cys less)	pTrc99a-TolC$_{G365C}$	This study
B51-1155	BL21(DE3)	pET24d-AcrA$_{45-312}$	1.2	This study
B51-1156	BL21(DE3)	pET24d-AcrA$_{45-312}$	2.1	This study
B51-1157	BL21(DE3)	pLysS	pET24d-AcrA$_{45-312}$	This study
B51-1158	BL21(DE3)	pLysS	pET24d-AcrA$_{45-312}$	This study
B51-1159	MC4100 Δ*tolC*::Cm^r AcrA$_{L222Q}$ Tn10 @ 10.5	pTrc99a- TolC-147AGSG150, S350A		This study
B51-1160	MC4100 Δ*tolC*::Cm^r AcrA$_{L222Q}$ Tn10 @ 10.5	pTrc99a- TolC-147AGSG150, S350A		This study

B51-1161	BL21 (DE3)	pET24d-AcrA$_{His}$ (full length)		This study
B51-1162	JM109	pET24d-AcrA$_{His}$ (full length)		This study
B51-1163	JM109	pBAD18- Kmr		This study
B51-1164	MC4100 $\Delta acrAB$::Km^r Δara714	pACYC184-AcrAB		This study
B51-1165	MC4100 $\Delta acrAB$::Km^r Δara714	pACYC184-AcrA		This study
B51-1166	MC4100 $\Delta tolC$-scar $\Delta acrAB$::Km^r Δara714	pACYC184-AcrA		This study
B51-1167	MC4100 $\Delta acrAB$-scar Δara714 $\Delta degP$::Km^r	pACYC184-	pTrc99a-	This study
B51-1168	MC4100 $\Delta acrAB$-scar Δara714 $\Delta degP$::Km^r	pACYC184-	pTrc99a- TolC	This study
B51-1169	MC4100 $\Delta tolC$-scar $\Delta acrAB$::Km^r Δara714	pACYC184-	pTrc99a-TolC$_{R367E}$	This study
B51-1170	MC4100 $\Delta tolC$-scar $\Delta acrAB$::Km^r Δara714	pACYC184-	pTrc99a-TolC$_{R390E}$	This study
B51-1171	MC4100 $\Delta tolC$-scar $\Delta acrAB$::Km^r Δara714	pACYC184-AcrAB	pTrc99a-	This study
B51-1172	MC4100 $\Delta tolC$-scar $\Delta acrAB$::Km^r Δara714	pACYC184-AcrAB	pTrc99a- TolC	This study
B51-1173	MC4100 $\Delta tolC$-scar $\Delta acrAB$::Km^r Δara714	pACYC184-AcrAB	pTrc99a-TolC$_{R367E}$	This study
B51-1174	MC4100 $\Delta tolC$-scar $\Delta acrAB$::Km^r Δara714	pACYC184-AcrAB	pTrc99a-TolC$_{R390E}$	This study
B51-1175	MC4100 $\Delta tolC$-scar $\Delta acrAB$::Km^r Δara714	pACYC184-AcrA$_{R104D}$ B	pTrc99a-	This study
B51-1176	MC4100 $\Delta tolC$-scar $\Delta acrAB$::Km^r Δara714	pACYC184-AcrA$_{R104D}$ B	pTrc99a- TolC	This study
B51-1177	MC4100 $\Delta tolC$-scar $\Delta acrAB$::Km^r Δara714	pACYC184-AcrA$_{R104D}$ B	pTrc99a-TolC$_{R367E}$	This study
B51-1178	MC4100 $\Delta tolC$-scar $\Delta acrAB$::Km^r Δara714	pACYC184-AcrA$_{R104D}$ B	pTrc99a-TolC$_{R390E}$	This study
B51-1179	MC4100 $\Delta tolC$-scar $\Delta acrAB$::Km^r Δara714	pACYC184-AcrA$_{L108D}$ B	pTrc99a-	This study
B51-1180	MC4100 $\Delta tolC$-scar $\Delta acrAB$::Km^r Δara714	pACYC184-AcrA$_{L108D}$ B	pTrc99a- TolC	This study
B51-1181	MC4100 $\Delta tolC$-scar $\Delta acrAB$::Km^r Δara714	pACYC184-AcrA$_{L108D}$ B	pTrc99a-TolC$_{R367E}$	This study
B51-1182	MC4100 $\Delta tolC$-scar $\Delta acrAB$::Km^r Δara714	pACYC184-AcrA$_{L108D}$ B	pTrc99a-TolC$_{R390E}$	This study
B51-1183	MC4100 $\Delta tolC$-scar $\Delta acrAB$::Km^r Δara714	pACYC184-AcrA$_{S115D}$ B	pTrc99a-	This study
B51-1184	MC4100 $\Delta tolC$-scar $\Delta acrAB$::Km^r Δara714	pACYC184-AcrA$_{S115D}$ B	pTrc99a- TolC	This study
B51-1185	MC4100 $\Delta tolC$-scar $\Delta acrAB$::Km^r Δara714	pACYC184-AcrA$_{S115D}$ B	pTrc99a-TolC$_{R367E}$	This study

B51-1186	MC4100 $\Delta tolC$-scar $\Delta acrAB$::Km^r Δara714	pACYC184-AcrA$_{S115D}$ B	pTrc99a-TolC$_{R390E}$	This study
B51-1187	MC4100 $\Delta acrAB$-scar Δara714	pACYC184-AcrA$_{R104D}$ B		This study
B51-1188	MC4100 $\Delta acrAB$-scar Δara714	pACYC184-AcrA$_{S115D}$ B		This study
B51-1189	MC4100 $\Delta tolC$::Cm^r	pTrc99a-TolC$_{A269C,\,6His}$		This study
B51-1190	MC4100 $\Delta tolC$::Cm^r	pTrc99a-TolC$_{T272C,\,6His}$		This study
B51-1191	MC4100 $\Delta acrAB$-scar Δara714	pACYC184-AcrAB$_{S1043C,\,His\,(Cys\,less)}$		This study
B51-1192	MC4100 $\Delta acrAB$-scar Δara714	pACYC184-AcrAB$_{\Delta L1,\,S1043C,\,His\,(Cys\,less)}$		This study
B51-1193	MC4100 $\Delta acrAB$-scar Δara714	pACYC184-AcrAB$_{\Delta L1,\,Q737L,\,His\,(Cys\,less)}$		This study
B51-1194	MC4100 $\Delta acrAB$-scar Δara714	pACYC184-AcrAB$_{PAL1/L2,\,S1043C,\,His\,(Cys\,less)}$		This study
B51-1195	MC4100 $\Delta acrAB$-scar Δara714	pACYC184-AcrAB$_{AANAA\,L1/PAL2,\,His\,(Cys\,less)}$		This study
B51-1196	MC4100 $\Delta acrAB$-scar Δara714	pACYC184-AcrAB$_{AAAAD\,L1/PAL2,\,His\,(Cys\,less)}$		This study
B51-1197	RAM1009 $lamB+$ Linked with Tn10 (62.3%)			This study
B51-1198	MC4100 $\Delta acrAB$-scar Δara714	pACYC184-AcrAB$_{\Delta L1,\,Q737L,S1043C,\,His\,(Cys\,less)}$		This study
B51-1199	MC4100 $\Delta acrAB$-scar Δara714	pACYC184-AcrAB$_{AANAA\,L1/PAL2,\,S1043C,\,His\,(Cys\,less)}$		This study
B51-1200	MC4100 $\Delta acrAB$-scar Δara714	pACYC184-AcrAB$_{AAAAD\,L1/PAL2,\,S1043C,\,His\,(Cys\,less)}$		This study
B51-1201	C43			Miroux and Walker, 1996
B51-1202	C43			Miroux and Walker, 1996
B51-1203	JM109	pET24d (+)		This study
B51-1204	BL21(DE3) $\Delta acrAB$::Km^r	pLysS		This study
B51-1205	BL21(DE3) $\Delta acrAB$::Km^r	pLysS		This study
B51-1206	C43 $\Delta acrAB$::Km^r			This study
B51-1207	C43 $\Delta acrAB$::Km^r			This study
B51-1208	BL21(DE3) $\Delta acrAB$::Km^r			This study

B51-1209	BL21(DE3) Δ*acrAB*::Km^r		This study
B51-1210	C43 Δ*acrAB*-scar		This study
B51-1211	C43 Δ*acrAB*-scar		This study
B51-1212	BL21(DE3) Δ*acrAB*-scar		This study
B51-1213	BL21(DE3) Δ*acrAB*-scar		This study
B51-1214	BL21(DE3) Δ*acrAB*-scar	pLysS	This study
B51-1215	BL21(DE3) Δ*acrAB*-scar	pLysS	This study
B51-1216	JM109	pET16b-AcrB$_{His}$	Martin Pos
B51-1217	JM109	pET16b-AcrB$_{His}$	Martin Pos
B51-1218	JM109	pET24a-AcrB$_{His}$	Martin Pos
B51-1219	JM109	pET24a-AcrB$_{His}$	Martin Pos
B51-1220	BL21(DE3) Δ*acrAB*-scar	pET16b-AcrB$_{His}$	This study
B51-1221	BL21(DE3) Δ*acrAB*-scar	pET16b-AcrB$_{His}$	This study
B51-1222	C43 Δ*acrAB*-scar	pET16b-AcrB$_{His}$	This study
B51-1223	C43 Δ*acrAB*-scar	pET16b-AcrB$_{His}$	This study
B51-1224	BL21(DE3) Δ*acrAB*-scar	pET24a-AcrB$_{His}$	This study
B51-1225	BL21(DE3) Δ*acrAB*-scar	pET24a-AcrB$_{His}$	This study
B51-1226	C43 Δ*acrAB*-scar	pET24a-AcrB$_{His}$	This study
B51-1227	C43 Δ*acrAB*-scar	pET24a-AcrB$_{His}$	This study
B51-1228	JM109	pET24a-AcrB$_{His, C493S, C887S}$	This study
B51-1229	JM109	pET24a-AcrB$_{His, C493S, C887S}$	This study
B51-1230	JM109	pET24a-AcrB$_{His, C493S, C887S}$	This study
B51-1231	JM109	pET24a-AcrB$_{His, C493S, C887S}$	This study
B51-1232	MC4100 Δ*tolC*-scar Δ*acrAB*::Km^r Δ*ara*714	pACYC184-AcrAB	This study
B51-1233	MC4100 Δ*tolC*-scar Δ*acrAB*::Km^r Δ*ara*714	pACYC184-AcrAB	This study
B51-1234	MC4100 Δ*tolC*-scar Δ*acrAB*::Km^r Δ*ara*714	pACYC184-AcrAB	This study
B51-1235	MC4100 Δ*tolC*-scar Δ*acrAB*::Km^r Δ*ara*714	pACYC184-AcrAB	This study

B51-1236	MC4100 Δ*acrAB*::Km[r] Δ*ara*714	pACYC184-AcrA	This study
B51-1237	MC4100 Δ*acrAB*::Km[r] Δ*ara*714	pACYC184-AcrA	This study
B51-1238	MC4100 Δ*tolC*-scar Δ*acrAB*::Km[r] Δ*ara*714	pACYC184-AcrA	This study
B51-1239	MC4100 Δ*tolC*-scar Δ*acrAB*::Km[r] Δ*ara*714	pACYC184-AcrA	This study
B51-1240	BL21(DE3) Δ*acrAB*-scar	pET24a-AcrB$_{His, C493S, C887S}$	This study
B51-1241	BL21(DE3) Δ*acrAB*-scar	pET24a-AcrB$_{His, C493S, C887S}$	This study
B51-1242	C43 Δ*acrAB*-scar	pET24a-AcrB$_{His, C493S, C887S}$	This study
B51-1243	C43 Δ*acrAB*-scar	pET24a-AcrB$_{His, C493S, C887S}$	This study
B51-1244	JM109	pET24a-AcrB$_{His, C/C ΔL1}$	This study
B51-1245	JM109	pET24a-AcrB$_{His, C/C ΔL1}$	This study
B51-1246	BL21(DE3) Δ*acrAB*-scar	pET24a-AcrB$_{His, C/C ΔL1}$	This study
B51-1247	BL21(DE3) Δ*acrAB*-scar	pET24a-AcrB$_{His, C/C ΔL1}$	This study
B51-1248	C43 Δ*acrAB*-scar	pET24a-AcrB$_{His, C/C ΔL1}$	This study
B51-1249	C43 Δ*acrAB*-scar	pET24a-AcrB$_{His, C/C ΔL1}$	This study
B51-1250	JM109	pET24a-AcrB$_{His, C/C ΔL1, Q737L}$	This study
B51-1251	JM109	pET24a-AcrB$_{His, C/C ΔL1, Q737L}$	This study
B51-1252	BL21(DE3) Δ*acrAB*-scar	pET24a-AcrB$_{His, C/C ΔL1, Q737L}$	This study
B51-1253	BL21(DE3) Δ*acrAB*-scar	pET24a-AcrB$_{His, C/C ΔL1, Q737L}$	This study
B51-1254	C43 Δ*acrAB*-scar	pET24a-AcrB$_{His, C/C ΔL1, Q737L}$	This study
B51-1255	C43 Δ*acrAB*-scar	pET24a-AcrB$_{His, C/C ΔL1, Q737L}$	This study
B51-1256	JM109	pET24a-AcrB$_{His, C/C PAL1/L2}$	This study

168

B51-1257	JM109	pET24a-AcrB$_{His, C/C}$ PAL1/L2	This study
B51-1258	BL21(DE3) Δ*acrAB*-scar	pET24a-AcrB$_{His, C/C}$ PAL1/L2	This study
B51-1259	BL21(DE3) Δ*acrAB*-scar	pET24a-AcrB$_{His, C/C}$ PAL1/L2	This study
B51-1260	C43 Δ*acrAB*-scar	pET24a-AcrB$_{His, C/C}$ PAL1/L2	This study
B51-1261	C43 Δ*acrAB*-scar	pET24a-AcrB$_{His, C/C}$ PAL1/L2	This study
B51-1262	JM109	pET24a-AcrB$_{His, C/C}$ AANAA L1/PAL2	This study
B51-1263	JM109	pET24a-AcrB$_{His, C/C}$ AANAA L1/PAL2	This study
B51-1264	BL21(DE3) Δ*acrAB*-scar	pET24a-AcrB$_{His, C/C}$ AANAA L1/PAL2	This study
B51-1265	BL21(DE3) Δ*acrAB*-scar	pET24a-AcrB$_{His, C/C}$ AANAA L1/PAL2	This study
B51-1266	C43 Δ*acrAB*-scar	pET24a-AcrB$_{His, C/C}$ AANAA L1/PAL2	This study
B51-1267	C43 Δ*acrAB*-scar	pET24a-AcrB$_{His, C/C}$ AANAA L1/PAL2	This study
B51-1268	JM109	pET24a-AcrB$_{His, C/C}$ AAAAD L1/PAL2	This study
B51-1269	JM109	pET24a-AcrB$_{His, C/C}$ AAAAD L1/PAL2	This study
B51-1270	BL21(DE3) Δ*acrAB*-scar	pET24a-AcrB$_{His, C/C}$ AAAAD L1/PAL2	This study
B51-1271	BL21(DE3) Δ*acrAB*-scar	pET24a-AcrB$_{His, C/C}$ AAAAD L1/PAL2	This study
B51-1272	C43 Δ*acrAB*-scar	pET24a-AcrB$_{His, C/C}$ AAAAD L1/PAL2	This study
B51-1273	C43 Δ*acrAB*-scar	pET24a-AcrB$_{His, C/C}$ AAAAD L1/PAL2	This study

B51-1274	MC4100 Δ*acrAB*-scar Δ*ara*714	pACYC184-AcrA$_{L222Q}$ AcrB$_{\Delta L1, \text{His (Cys less)}}$	1	This study
B51-1275	MC4100 Δ*acrAB*-scar Δ*ara*714	pACYC184-AcrA$_{L222Q}$ AcrB$_{\Delta L1, \text{His (Cys less)}}$	2	This study
B51-1276	MC4100 Δ*acrAB*-scar Δ*ara*714	pACYC184-AcrA$_{K58C, L222Q}$ AcrB$_{\Delta L1, \text{His (Cys less)}}$	1	This study
B51-1277	MC4100 Δ*acrAB*-scar Δ*ara*714	pACYC184-AcrA$_{K58C, L222Q}$ AcrB$_{\Delta L1, \text{His (Cys less)}}$	2	This study
B51-1278	MC4100 Δ*acrAB*-scar Δ*ara*714	pACYC184-AcrA$_{S196C, L222Q}$ AcrB$_{\Delta L1, \text{His (Cys less)}}$	1	This study
B51-1279	MC4100 Δ*acrAB*-scar Δ*ara*714	pACYC184-AcrA$_{S196C, L222Q}$ AcrB$_{\Delta L1, \text{His (Cys less)}}$	2	This study
B51-1280	MC4100 Δ*tolC*::Km^r Δ*acrA*-scar Δ*ara*714	pSF4000-*hlyCABD*		This study
B51-1281	MC4100 Δ*tolC*::Km^r Δ*acrA*-scar Δ*ara*714	pSF4000-*hlyCABD*	pTrc99a-	This study
B51-1282	MC4100 Δ*tolC*::Km^r Δ*acrA*-scar Δ*ara*714	pSF4000-*hlyCABD*	pTrc99a- TolC (BspHI clone)	This study
B51-1283	MC4100 Δ*tolC*::Km^r Δ*acrA*-scar Δ*ara*714	pSF4000-*hlyCABD*	pTrc99a- TolC$_{147AGSG150}$	This study
B51-1284	MC4100 Δ*tolC*::Km^r Δ*acrA*-scar Δ*ara*714	pSF4000-*hlyCABD*	pTrc99a- TolC$_{147AGSG150, A128V}$	This study
B51-1285	MC4100 Δ*tolC*::Km^r Δ*acrA*-scar Δ*ara*714	pSF4000-*hlyCABD*	pTrc99a- TolC$_{147AGSG150, I133S}$	This study
B51-1286	MC4100 Δ*tolC*::Km^r Δ*acrA*-scar Δ*ara*714	pSF4000-*hlyCABD*	pTrc99a- TolC$_{147AGSG150, D153E}$	This study
B51-1287	MC4100 Δ*tolC*::Km^r Δ*acrA*-scar Δ*ara*714	pSF4000-*hlyCABD*	pTrc99a- TolC$_{147AGSG150, S350A}$	This study
B51-1288	MC4100 Δ*tolC*::Km^r Δ*acrA*-scar Δ*ara*714	pSF4000-*hlyCABD*	pTrc99a- TolC$_{147AGSG150, R390C}$	This study

[a] Genotype of MC4100 is F- *araD139* D(*argF-lac*)*U139 rpsL150 flbB5301 ptsF25 deoC1 thi-1 rbsR relA* (Casadaban, 1976).

[b] If no plasmid is listed, the strain does not contain a plasmid. Antibiotic resistance markers for plasmids are as follows: pTrc99a (Ap^r; Pharmacia), pACYC184 (Tc^r, Cm^r; Chang and Cohen, 1978); pCP20 (Ap^r, Cm^r, *ts* replicon, thermal induction of FLP synthesis; Datsenko and Wanner, 2000); pKD46 (Ap^r; Lambda-red recombinase; Datsenko and Wanner, 2000); pKD4 (Km^r; Datsenko

and Wanner, 2000); pSF4000-*hlyCABD*+ (Cm^r, expresses Haemolysin proteins Welch *et al.*, 1981); pACYC184-*acrA* (Cm^r; expresses wild type AcrA); pBAD33 (Cm^r; Guzman *et al.*, 1995)

Table 9. List of primers used in this study

Primer Name	Gene	SEQuence[a]	Purpose[b]
TolC147DEL F	*tolC*	CCAACGTTTTAACGTGGCTGGTAGCGATCACCG	SDM
TolC147DEL R	*tolC*	CGGTGATCGCTACCAGCCACGTTAAAACGTTGG	SDM
TolCA147G1 F	*tolC*	CAACGTTTTAACGTGGGGGGTAGCGGCATCACC	SDM
TolCA147G1 R	*tolC*	GGTGATGCCGCTACCCCCCACGTTAAAACGTTG	SDM
TolC147DEL/150ins F	*tolC*	CCAACGTTTTAACGTGGCTGGTAGCGGCATCACCGACGTGCAGAACG	SDM
TolC147DEL/150ins R	*tolC*	CGTTCTGCACGTCGGTGATGCCGCTACCAGCCACGTTAAAACGTTGG	SDM
TolCG148L F	*tolC*	CCAACGTTTTAACGTGGGGCTGAGCGGCATCACCGACGTGC	SDM
TolCG148L R	*tolC*	GCACGTCGGTGATGCCGCTCAGCCCCACGTTAAAACGTTGG	SDM
TolCL148S F	*tolC*	CCAACGTTTTAACGTGGGCTCCGTAGCGATCACCGACGTGC	SDM
TolCL148S R	*tolC*	GCACGTCGGTGATCGCTACGGAGCCCACGTTAAAACGTTGG	SDM
TolCV149S F	*tolC*	CGTTTTAACGTGGGCCTGTCAGCGATCACCGACGTGCAG	SDM
TolCV149S R	*tolC*	CTGCACGTCGGTGATCGCTGACAGGCCCACGTTAAAACG	SDM
TolCA150G F	*tolC*	CGTTTTAACGTGGGCCTGTCAGGGATCACCGACGTGCAGAACGC	SDM
TolCA150G R	*tolC*	GCGTTCTGCACGTCGGTGATCCCTGACAGGCCCACGTTAAAACG	SDM
#1	*tolC*	CTACAAACAAGCCGTAGTTTGCGCTCAAAGCTCATTAGACG	SDM
#2	*tolC*	CGTCTAATGAGCTTTGAGCGCAAACTACGGCTTGTTTGTAG	SDM
R367E Top	*tolC*	GGCTACTCGGTCGGTACGGAAACCATTGTTGATGTGTTGG	SDM
R367E R	*tolC*	CCAACACATCAACAATGGTTTCCGTACCGACCGAGTAGCC	SDM
TolC-F1	*tolC*	TTGATCCTTCAACACCGCGACCG	SEQ
TolC-F2	*tolC*	TTGGCCTGAGCTTCTCGCTGCC	SEQ
TOLC-R1	*tolC*	ACATTCAGCGCAGCCAGTTCCG	SEQ
TOLCF	*tolC*	GAATGCCCATGGGGAAATTGCTCCCCATTC	CL
TOLC BSPHI	*tolC*	CAGGAAACAGATCATGAGGAAATTGCTCCC	CL
TOLC-M-BSPHI	*tolC*	GAGCCAGGTCATGAACCTGATGC	CL
XBAI-TOLC FWD.	*tolC*	GCTCTAGAGGAAACAGACCATGAAGAAATTG	CL
TOLCBGL	*tolC*	TCGTCGAGATCTGTTACGGAAAGGGTTATGACCG	PCR
TOLC-	*tolC*	ACGTAAGGCAACGTAAAGATACGGGTTATCTGTAG	PCR

MARKER FWD		GCTGGAGCTGCTTCG	
TOLC-MARKER REV	*tolC*	TTCCGGGACCAGTGGTAAATACCCATCAGACATATGAATATCCTCCTTAG	PCR
TOLRX	*tolC*	CTTACGTCTAGACGGGGCCGAAGCC	PCR
TOLCR	*tolC*	GCGGCAGATAACCCGAAGCTTTACGTTGCC	PCR
TolC Q142C F	*tolC*	CCGTCAATTAGATCAAACCACCtgtCGTTTTAACGTG	SDM
TolC Q142C R	*tolC*	CACGTTAAAACGacaGGTGGTTTGATCTAATTGACGG	SDM
TolC-1C Q142C F	*tolC*	GCGATCTACCGTCAATTAGATtgtACCACCCAACGTTTTAACGTG	SDM
TolC-1C Q142C R	*tolC*	CGCTAGATGGCAGTTAATCTAacaTGGTGGGTTGCAAAATTGCAC	SDM
TolC R390E F	*tolc*	GCAAGAGCTGGCGAATGCGgaaTATAACTACCTGATTAATC	SDM
TolC R390E R	*tolC*	GATTAATCAGGTAGTTATAttcCGCATTCGCCAGCTCTTGC	SDM
TolC 2Ala T1 FWD	*tolC*	CCAACGTTTTAACGTGGGCgcGGcAGCGATCACCGACGTGCAGAACGC	SDM
TolC 2Ala T1 REV	*tolC*	GCGTTCTGCACGTCGGTGATCGCTgCCgcGCCCACGTTAAAACGTTGG	SDM
TolC PA T1 FWD	*tolC*	CCACCCAACGTTTTAACGTGGcCgcGGcAGCGATCACCGACGTGCAGAACGC	SDM
TolC PA T1 REV	*tolC*	GCGTTCTGCACGTCGGTGATCGCTgCCgcGgCCACGTTAAAACGTTGGGTGG	SDM
TolC G147A FWD	*tolC*	CCCAACGTTTTAACGTGGcCCTGGTAGCGATCACCG	SDM
TolC G147A REV	*tolC*	CGGTGATCGCTACCAGGGCCACGTTAAAACGTTGGG	SDM
TolC G147C FWD	*tolC*	CCACCCAACGTTTTAACGTGtGCCTGGTAGCGATCACCGACG	SDM
TolC G147C REV	*tolC*	CGTCGGTGATCGCTACCAGGCACACGTTAAAACGTTGGGTGG	SDM
TolC G365C FWD	*tolC*	GCGGGCTACTCGGTCtGTACGCGTACCATTGTTGATG	SDM
TolC G365C REV	*tolC*	CATCAACAATGGTACGCGTACAGACCGAGTAGCCCGC	SDM
TolC A128C F	*tolC*	CGCTTATTTCAACGTGTTGAATGCTATTGACGTTCTTTCCTATACAC3	SDM
TolC A128C R	*tolC*	GTGTATAGGAAAGAACGTCAATAcaATTCAACACGTTGAAATAAGCG	SDM
TolC 6HXHR	*tolC*	GCTCTAGAAGCTTAGTGATGGTGATGGTGATGGTTACGGAAAGGGTTATGACC	CL
TolCB-R	*tolC*	GTTCAGACGGATCCGAAGCCCCGTCG	CL
TolC G147C FWD	*tolC*	CCAACGTTTTAACGTGTGCCTGGTAGCGATCACC	SDM
TolC G147C REV	*tolC*	GGTGATCGCTACCAGGCACACGTTAAAACGTTGG	SDM
TolC G365C FWD	*tolC*	GAAGCGGGCTACTCGGTCTGTACGCGTACCATTGTTG	SDM

173

TolC G365C REV	*tolC*	CAACAATGGTACGCGTACAGACCGAGTAGCCCGCTTC	SDM
TolC FS1 FWD	*tolC*	CTACCGGGATTTCTGACACTCTTATAGCGGTTCGAAAAC	SDM
TolC FS1 REV	*tolC*	GTTTTCGAACCGCTATAAGAGTGTCAGAAATTAAGAGTGTCAGAAATCCCGGTAG	SDM
DtolC FWD	*tolC*	ATCGCGCTAAATACTGCTTCACCACAAGGAATGCAATGTAGGCTGGAGCTGCTTCG	DEL
DtolC REV	*tolC*	TTATGACCGTTACTGGTGGTAGTGCGTGCGGATGTTCATATCAATATCCTCCTTAG	DEL
TolC Promoter	*tolC*	CCGCACCTCATGACTCATTTGC	PCR
TolC BsphI hybrid Fwd	*tolC*	CAGGAAACAGATCATGAGGAAATTGCTCCC	PCR
TolC External	*tolC*	GTAACGGGCAGGTTGTCTGGC	PCR
TestingDELta-acrEF-F	*acrEF*	ACGTCGGTGAACCGCAGGTTACC	PCR
TestingDELta-acrEF-R	*acrEF*	TGGTTCCTGGCGCGGCTTCC	PCR
TestingDELta-acrEF-2R	*acrEF*	TCATCAGGATAGGACGCAGACGC	PCR
TolC L169C FWD	*tolC*	CCGTGCTGGCGAACGAAtgtACCGCgCGTAATAACCTTGATAACGC	SDM
TolC L169C REV	*tolC*	GCGTTATCAAGGTTATTACGCGCGGTACATTCGTTCGCCAGCACGG	SDM
TolC A269C FWD	*tolC*	CGAAAACCCGTGGTtgCGCTGGTACCCAGTATGACG	SDM
TolC A269C REV	*tolC*	CGTCATACTGGGTACCAGCGCAACCACGGGTTTTCG	SDM
TolC T272C FWD	*tolC*	CCCGTGGTGCCGCTGGTtgCCAGTATGACGATAGC	SDM
TolC T272C REV	*tolC*	GCTATCGTCATACTGGCAACCAGCGGCACCACGGG	SDM
TolC Ext 2 fwd	*tolC*	CGCCAACCTTTTGCGGTAGCGGC	PCR
TolC Ext 2 rev	*tolC*	GGAAGAATGCGGCAGATAACCCG	PCR
pBAD33_Rev	pBAD33	5'-ATCAGACCGCTTCTGCGTTC-3'	SEQ
pACYC184(SalI)R	pAcyc184	5'-GAAGGCTCTCAAGGGCATCGG-3'	SEQ
AcrB FWD NcoI for pET24d	*acrB*	gaCCATGgCTAATTTCTTTATCGATCGCCCG	CL
AcrB FWD BspHI for pET24d	*acrB*	gaTCATGaCTAATTTCTTTATCGATCGCCCG	CL
AcrA Cryst FWD	acrA	atccatggctGTCAAAACTGAACCTCTGCAGATCACAACCG	CL
AcrA Cryst Rev	acrA	gctcgagGCCCTGTTGCGGGACTAAAATAGCG	CL
AcrA	acrA	GTGACCCAGTCCAGCAACGACaTgaTGCGCCTGAAA	SDM

174

FL223-224MM FWD		CAGGAACTGGC	
AcrA FL223-224MM REV	acrA	GCCAGTTCCTGTTTCAGGCGCATCATGTCGTTGCTGGACTGGGTCAC	SDM
AcrA LL287-288MM FWD	acrA	CGGATCACACTaTGaTGCCGGGTATGTTCGTGCGC	SDM
AcrA LL287-288MM REV	acrA	GCGCACGAACATACCCGGCATCATAGTGTGATCCG	SDM
AcrA-PCR-F-KpnI	*acrA*	GACCAGGTACCAATTTGAAATCGGACACTCGAGG	PCR
AcrB-F-D795A	*acrB*	GGTATGTTCGTGCTGCTGCGGGTCAGATGGTGCC	SDM
AcrB-R-D795A	*acrB*	GGCACCATCTGACCCGCAGCAGCACGAACATACC	SDM
AcrB-F-D256A	*acrB*	GCTGAAAGTGAATCAGGCAGGTTCCCGCGTGC	SDM
AcrB-R-D256A	*acrB*	GCACGCGGGAACCTGCCTGATTCACTTTCAGC	SDM
acrBL1-malE_Bam	*acrB*	ACGATCTCCGGATCCTACC	PCR
acrBL1-malE_Hin	*acrB*	GAGGATGAAAGCTTAGACCAGCG	PCR
AcrB-BsphI-F	*acrB*	CCGTTAAGTCATGACTAATTTTCTTTATCGAT	PCR
AcrB-F1	*acrB*	CCATTATCATCATGTTGGCAGG	SEQ
AcrB-F2	*acrB*	CGTTATCAACACCGATGGC	SEQ
AcrB-F3	*acrB*	TCGAAGATTGAGCTGGGTGG	SEQ
AcrB-F4	*acrB*	CCATCGGCCTGTTGGTGG	SEQ
AcrB-F5	*acrB*	GCACCACTACACCGACAGC	SEQ
AcrB-F6	*acrB*	GCAATCGTGGAACTGGGTAC	SEQ
AcrB-F7	*acrB*	CGTTGGGAGTACGGTTCG	SEQ
AcrB-F8	*acrB*	GACGTTTACTTCCAGGTAGG	SEQ
AcrB-R1	*acrB*	CCAGACTCAAAGGTCAGG	SEQ
AcrB-R2	*acrB*	CCACCAACAGGCCGATGG	SEQ
AcrA-F1	*acrA*	CCGCAACAGGGCGTAACCCGT	SEQ
AcrA-F2	*acrA*	GTATGTACCATAGCACGACG	SEQ
AcrA-F3	*acrA*	GGTAGCGACATCGAAGCAGG	SEQ
AcrA-F4	*acrA*	CATTGGTACAGAACGGTCAG	SEQ
AcrA-R1	*acrA*	CATCAGAACGACCGCCAGAGG	SEQ
acrA rev	*acrA*	GTCTTAACGGATCCTGTTTAAGTTAAG	PCR
RacrAB-HindIII	*acrAB*	CTCCTTAAGCTTCGTAGGTTATGC	CL
FacrAB-BspHI	*acrAB*	AGATCTCATGAACAATCCGACTTGTC	CL
acrB fwd	*acrB*	CTTAACTTAAACAGGATCCGTTAAGAC	CL

175

AcrB-PCR-F-SphI	*acrB*	CTTAAGCATGCCAGGAGCCGTTAAGACATGCC	CL
AcrB-his-R-HindIII	*acrB*	GCTCTAGAAGCTTAATGGTGATGGTGATGATGATCGACAGTATGGCTGTGCTCG	CL
DacrAfwd	*acrA*	GACCAATTTGAAATCGGACACTCGAGGTTTACATTGTAGGCTGGCGCTGCTTCG	DEL
DacrArev	*acrA*	GCAAAAATCGGGCGATCGATAAAGAAATTAGGCATATGAATATCCTCCTTAG	DEL
Matt1	*acrB*	AGTCCAAGTCTTAACTTAAACAGGAGCCGTTAAGACTGTAGGCTGGAGCTGCTTCG	DEL
Matt2	*acrB*	AGGCCGCTTACGCGGCCTTAGTGATTACACGTTGTACATATGAATATCCTCCTTAG	DEL
Stidham1	*acrA*	TCAGATGGATCCGCGACCTATCAG	PCR
Stidham2	*acrA*	GGTTTACTCATGAACAAAAACAGAGGG	PCR
Stidham3	*acrA*	GCTCTAGAAGCTTAGTGATGGTGATGGTGATGAGACTTGGACTGTTCAGGCTGAGC	PCR
AcrB-R-D795C	*acrB*	CGAGAATGGCACCATCTGACCGCAAGCAGCACGAACATACC	SDM
AcrB-F-D795C	*acrB*	GGTATGTTCGTGCTGCTTGCGGTCAGATGGTGCCATTCTCG	SDM
AcrB-R-Q255C	*acrB*	CAGCACGCGGGAACCATCGCAATTCACTTTCAGCAGGATTTTGC	SDM
AcrB-F-Q255C	*acrB*	GCAAAATCCTGCTGAAAGTGAATTGCGATGGTTCCCGCGTGCTG	SDM
AcrAL222Q-F	*acrA*	GCAAAGCCAAAGTGTCACAGATCACCAGTGACGGC	SDM
AcrAL222Q-R	*acrA*	GCCGTCACTGGTGATCTGTGACACTTTGGCTTTGC	SDM
AcrEPCRFwdBspHI	*acrE*	CACCTCATGACTATTTATACGAGAGGC	PCR
AcrEPCRRevBamHI	*acrE*	GTCAGGATCCCTTACTTCGATGCAGTATCTGC	PCR
acrE_int_r	*acrE*	GCGAACTTCGGCTATACGATAAGC	PCR
dacrE-fwd	*acrE*	GTAAATAACGCGCTTTTGGTTTTTTGAGGAATAGTATGTAGGCTGGAGCTGCTTCG	DEL
AcrA A79C F	*acrA*	CCTGCGACCTATCAGtgtACATACGACAGTGCG	SDM
AcrA A79C R	*acrA*	CGCACTGTCGTATGTacaCTGATAGGTCGCAGG	SDM
acrA rev (His-tagXbaI/HindIII)	*acrA*	GCAAGCTTCTAGATTAGTGATGGTGATGGTGATGAGACTTGGACTGTTCAGGCTGAGC	CL
acrB-XbaI-Forward	*acrB*	ACGGTCTAGACAGGAGCCGTTAAGACATG	CL
AcrB correct A738 Fwd	*acrB*	GGAAAAAGCGCAGGCGCTGGGTGTTTCTATC	SDM
AcrB correct A738 Rev	*acrB*	GATAGAAACACCCAGCGCCTGCGCTTTTTCC	SDM
AcrA correct D244 Fwd	*acrA*	CTGACGTTACCGTTGATCAGACCACTGGGTC	SDM
AcrA	*acrA*	GACCCAGTGGTCTGATCAACGGTAACGTCAG	SDM

176

correct D244 Rev			
AcrB R259A Fwd	*acrB*	CAGGATGGTTCCgcCGTGCTGCTGCGTG	SDM
AcrB R259A Rev	*acrB*	CACGCAGCAGCACGgcGGAACCATCCTG	SDM
AcrB DEL H1 Fwd	*acrB*	CGGCAAAATCCTGCTGGGTTCCCGCGTGCTG	SDM
AcrB DEL H1 Rev	*acrB*	CAGCACGCGGGAACCCAGCAGGATTTTGCCG	SDM
AcrB poly A H1 Fwd	*acrB*	CGGCAAAATCCTGCTGgcAGcGgcTgcgGcgGGTTCgC GCGTGCTGC	SDM
AcrB poly A H1 Rev	*acrB*	GCAGCACGCGcGAACCcgCcgcAgcCgCTgcCAGCAGG ATTTTGCCG	SDM
pACYC DEL AcrA Fwd	*pACYC*	ccaatttgaaatcggacactcgaggtttacatATGCCTAATTTCTTTAT CGATCGCCCGATTTTTGCG	SDM
pACYC DEL AcrA Rev	*pACYC*	CGCAAAAATCGGGCGATCGATAAAGAAATTAGGC ATatgtaaacctcgagtgtccgatttcaaattgg	SDM
AcrB DEL H2 Fwd	*acrB*	CGGCGACTGGTATGTTCGTATGGTGCCATTCTCGG CG	SDM
AcrB DEL H2 Rev	*acrB*	CGCCGAGAATGGCACCATACGAACATACCAGTCGC CG	SDM
AcrB poly A H2 Fwd	*acrB*	GGTATGTTCGTGCTGCTGcTGcTgctATGGTGCCATTC TCGGCG	SDM
AcrB poly A H2 Rev	*acrB*	CGCCGAGAATGGCACCATagcAgCAgCAGCAGCACG AACATACC	SDM
AcrA S83G FWD	*acrA*	CCTATCAGGCGACATACGACgGTGCGAAAGGTGAT CTGGCG	SDM
AcrA S83G REV	*acrA*	CGCCAGATCACCTTTCGCACcGTCGTATGTCGCCTG ATAGG	SDM
AcrA T111P FWD	*acrA*	GTTATCAGAAACTGCTCGGTcCTCAGTACATCAGTA AGCAAG	SDM
AcrA T111P REV	*acrA*	CTTGCTTACTGATGTACTGAGgACCGAGCAGTTTCT GATAAC	SDM
AcrA A135T FWD	*acrA*	GCTGCGGTAACTaCGGCGAAAGCTGCC	SDM
AcrA A135T REV	*acrA*	GGCAGCTTTCGCCGtAGTTACCGCAGC	SDM
AcrA N146T FWD	*acrA*	GAAACTGCGCGGATCAcTCTGGCTTACACC	SDM
AcrA N146T REV	*acrA*	GGTGTAAGCCAGAgTGATCCGCGCAGTTTC	SDM
AcrB KAAAA H1 FWD	*acrB*	CGGCAAAATCCTGCTGaaAGcGgcTgcgGcgGGTTCg	SDM
AcrB KAAAA H1 REV	*acrB*	CGAACCCGCCGCAGCCGCTTTCAGCAGGATTTTGC CG	SDM
AcrB	*acrB*	CGGCAAAATCCTGCTGgcAGcGaaTgcgGcgGGTTCaC	SDM

AANAA H1 FWD		GCGTGCTGC	
AcrB AANAA H1 REV	*acrB*	GCAGCACGCGTGAACCCGCCGCATTCGCTGCCAGC AGGATTTTGCCG	SDM
AcrB AAAQA H1 FWD	*acrB*	CCTGCTGgcAGcGgcTcagGcgGGTTCgCGCGTGCTGC	SDM
AcrB AAAQA H1 REV	*acrB*	GCAGCACGCGCGAACCCGCCTGAGCCGCTGCCAGC AGG	SDM
AcrB AAAAD H1 FWD	*acrB*	CCTGCTGgcAGcGgcTgcgGatGGTTCgCGCGTGCTGC	SDM
AcrB AAAAD H1 REV	*acrB*	GCAGCACGCGCGAACCATCCGCAGCCGCTGCCAGC AGG	SDM
AcrB AAAAK H1 FWD	*acrB*	CGGCAAAATCCTGCTGgcAGcGgcTgcgaagGGcTCaCG CGTGCTGC	SDM
AcrB AAAAK H1 REV	*acrB*	GCAGCACGCGTGAGCCCTTCGCAGCCGCTGCCAGC AGGATTTTGCCG	SDM
AcrB AADAA H2 FWD	*acrB*	GGTATGTTCGTGCTGCTGaTGcTgctATGGTGCCATTC TCGGCG	SDM
AcrB AADAA H2 REV	*acrB*	CGCCGAGAATGGCACCATAGCAGCATCAGCAGCA CGAACATACC	SDM
AcrB AAAAQ H2 FWD	*acrB*	GTTCGTGCTGCTGcTGcTcagATGGTGCCATTCTCGG CG	SDM
AcrB AAAAQ H2 REV	*acrB*	CGCCGAGAATGGCACCATCTGAGCAGCAGCAGCA CGAAC	SDM
AcrB AAACA H1 FWD	*acrB*	CGGCAAAATCCTGCTGgcAGcGgcTtgcGggGGTTCaCG CGTGCTGC	SDM
AcrB AAACA H1 REV	*acrB*	GCAGCACGCGTGAACCCCCGCAAGCCGCTGCCAGC AGGATTTTGCCG	SDM
AcrB AACAA H2 FWD	*acrB*	GTTCGTGCTGCTtgTGcTgctATGGTGCCATTCTCGGC G	SDM
AcrB AACAA H2 REV	*acrB*	CGCCGAGAATGGCACCATAGCAGCACAAGCAGCA CGAAC	SDM
AcrB D407A FWD	*acrB*	CCATCGGCCTGTTGGTGGcTGACGCgATCGTTGTGG TAG	SDM
AcrB D407A REV	*acrB*	CTACCACAACGATCGCGTCAGCCACCAACAGGCCG ATGG	SDM
AcrB	*acrB*	CGCTTGATGCGGTGCGcATGgcTTTACGTCCGATCC	SDM

R971A FWD		TGATG	
AcrB R971A REV	*acrB*	CATCAGGATCGGACGTAAAGCCATGCGCACCGCAT CAAGCG	SDM
AcrA G248E FWD	*acrA*	CCGTTGATCAGACCACTGaGTCTATCACCCTACGCG	SDM
AcrA G248E REV	*acrA*	CGCGTAGGGTGATAGACTCAGTGGTCTGATCAACG G	SDM
AcrA K58C FWD	*acrA*	GGATTATCCTGAAGCGTAATTTCtgcGAAGGTAGCG ACATCGAAGCAGG	SDM
AcrA K58C REV	*acrA*	CCTGCTTCGATGTCGCTACCTTCGCAGAAATTACG CTTCAGGATAATCC	SDM
AcrA K58C REV	*acrA*	CCTGCTTCGATGTCGCTACCTTCGCAGAAATTACG CTTCAGGATAATCC	SDM
AcrA S196C FWD	*acrA*	GATGTGACCCAGTCCtGCAACGACTTCCTGC	SDM
AcrA S196C REV	*acrA*	GCAGGAAGTCGTTGCAGGACTGGGTCACATC	SDM
AcrB C493S FWD	*acrB*	GATCCTGACTCCAGCTCTTaGTGCCACCATGCTGAA ACCG	SDM
AcrB C493S REV	*acrB*	CGGTTTCAGCATGGTGGCACTAAGAGCTGGAGTCA GGATC	SDM
AcrB C887S FWD	*acrB*	GATTGTCGTGTTCCTGaGTCTGGCGGCGCTG	SDM
AcrB C887S REV	*acrB*	CAGCGCCGCCAGACTCAGGAACACGACAATC	SDM
AcrB F136A FWD	*acrB*	GCGTTGAGAAATCATCCAGtAGCgcgCTGATGGTTG TCGGCGTTATC	SDM
AcrB F136A FWD	*acrB*	GCGTTGAGAAATCATCCAGtAGCgcgCTGATGGTTG TCGGCGTTATC	SDM
AcrB F136A REV	*acrB*	GATAACGCCGACAACCATCAGCGCGCTACTGGATG ATTTCTCAACGC	SDM
AcrB F610A FWD	*acrB*	GAACAACGTTGAGTCGGTGgcgGCgGTTAACGGCTT CGGC	SDM
AcrB F610A REV	*acrB*	GCCGAAGCCGTTAACCGCCGCCACCGACTCAACGT TGTTC	SDM
AcrB F610A REV	*acrB*	GCCGAAGCCGTTAACCGCCGCCACCGACTCAACGT TGTTC	SDM
AcrB F615A FWD	*acrB*	GTTCGCCGTTAACGGggcaGGCTTTGCGGGACGTGG	SDM
AcrB F615A REV	*acrB*	CCACGTCCCGCAAAGCCTGCCCCGTTAACGGCGAA C	SDM
EmrA DEL Forward	*emrA*	taagaagatcgtggagaacaatatgagcgcaaatgcggagTGTAGGCTG GAGCTGCTTCG	DEL
EmrB DEL Reverse	*emrB*	aaatgaactggcttagttgtacttagtgcgcaccgcctccCATATGAATAT CCTCCTTAG	DEL
EmrA PCR Forward	*emrA*	TGACTGGCCAGCATCGCAAC	PCR
EmrB PCR Reverse	*emrB*	GGAACTGCACATCTAGTCAG	PCR
AcrA L252R	*acrA*	GACCACTGGGTCTATCACacgcCGCGCTATCTTCCCG AACCCGG	SDM

FWD			
AcrA L252R REV	*acrA*	5'-CCGGGTTCGGGAAGATAGCGCGGCGTGTGATAGACCCAGTGGTC-3'	SDM
AcrB AAACA H1 FWD	*acrB*	5'-CGGCAAAATCCTGCTGGcAGcGgcTtgcGcgGGTTCaCGtGTGCTGC-3'	SDM
AcrB AAACA H1 REV	*acrB*	5'-GCAGCACACGTGAACCCGCGCAAGCCGCTGCCAGCAGGATTTTGCCG-3'	SDM
AcrB AAAGA H2 FWD	*acrB*	5'-GTTCGTGCTGCTGcTGgTgctATGGTGCCATTCTCGGCG-3'	SDM
AcrB AAAGA H2 REV	*acrB*	5'-CGCCGAGAATGGCACCATAGCACCAGCAGCAGCACGAAC-3'	SDM
AcrB Q255C-FWD	*acrB*	CAAAATCCTGCTGAAAGTGAATTGTGATGGTTCCCGCGTGCTGCTG	SDM
AcrB Q255C-REV	*acrB*	CAGCAGCACGCGGGAACCATCACAATTCACTTTCAGCAGGATTTG	SDM
AcrB D795C-FWD	*acrB*	CTGGTATGTTCGTCCTGCTTGTGGTCAGATGGTGCCATTC	SDM
AcrB D795C-REV	*acrB*	GAATGGCACCATCTGACCACAAGCAGCACGAACATACCAG	SDM
AcrA S83C FWD	*acrA*	CAGGCGACATACGACtGTGCGAAAGGTGATCTG	SDM
AcrA S83C REV	*acrA*	CAGATCACCTTTCGCACaGTCGTATGTCGCCTG	SDM
AcrB Q737L FWD	*acrB*	CGACCAGGAAAAAGCGCtcGCGCTGGGTGTTTCTATC	SDM
AcrB Q737L REV	*acrB*	GATAGAAACACCCAGCGCGAGCGCTTTTTCCTGGTCG	SDM
0	*acrB*	CGTTGAGTCGGTGTTCGCgGTTAACGGCTTCGGC	SDM
AcrB A610F REV	*acrB*	GCCGAAGCCGTTAACCGCGAACACCGACTCAACG	SDM
acrBfor pET24a	*acrB*	GGATCCCATATGCCTAATTTCTTTATCGATC	CL
acrBrev pET24a	*acrB*	AAGCTTCTCGAGATGATGATCGACAGTATGGCTG	CL
DELta acrEF FWD	*acrEF*	GCTTATCGTATAGCCGAAGTTCGCCCACAGTGTAGGCTGGAGCTGCTTCG	DEL
DELta acrEF REV	*acrEF*	ATACACCCAATGTGAAGTGGTAAAGGCCGACATATGAATATCCTCCTTAG	DEL
DELta acrEF REV2	*acrEF*	GTTTTTGGCCGACAAGCCAATTGTCGTTAGCATATGAATATCCTCCTTAG	DEL
N-terminal 6His Tag bamHI AcrB	*acrB*	gcatacGGATCCGTTAAGACATGcatcaccatcaccatcacCCTAATTTCTTTATCGATCGCCCG	CL

<hr>

a All sequences are listed from 5' to 3'.

References:

Andersen C., Koronakis E., Bokma E., Eswaran J., Humphreys D., Hughes C., and Koronakis V. (2002) Transition to the open state of the TolC periplasmic tunnel entrance. *Proc Natl Acad Sci U S A* **99:** 11103-11108.

Augustus A.M., Celaya T., Husain F., Humbard M., and Misra R. (2004) Antibiotic-sensitive TolC mutants and their suppressors. *J Bacteriol* **186:** 1851-1860.

Bagai I., Rensing C., Blackburn N.J., and McEvoy M.M. (2008) Direct metal transfer between periplasmic proteins identifies a bacterial copper chaperone. *Biochemistry* **47:** 11408-11414.

Bagai I., Liu W., Rensing C., Blackburn N.J., and McEvoy M.M. (2007) Substrate-linked conformational change in the periplasmic component of a Cu(I)/Ag(I) efflux system. *J Biol Chem* **282:** 35695-35702.

Bai J., Mosley L., and Fralick J.A. (2010) Evidence that the C-terminus of OprM is involved in the assembly of the VceAB-OprM efflux pump. *FEBS Lett* **584:** 1493-1497.

Bavro V.N., Pietras Z., Furnham N., Pérez-Cano L., Fernández-Recio J., Pei X.Y.*, et al.* (2008) Assembly and channel opening in a bacterial drug efflux machine. *Molecular Cell* **30:** 114-121.

Bohnert J.A., Karamian B., and Nikaido H. (2010) Optimized nile red efflux assay of AcrAB-TolC multidrug efflux system shows competition between substrates. *Antimicrob Agents Chemother* **54:** 3770-3775.

Bokma E., Koronakis E., Lobedanz S., Hughes C., and Koronakis V. (2006) Directed evolution of a bacterial efflux pump: Adaptation of the *E. coli* TolC exit duct to the *Pseudomonas* MexAB translocase. *FEBS Lett* **580:** 5339-5343.

Brandenburg K., Garidel P., Schromm A.B., Andra J., Kramer A., Egmond M., and Wiese A. (2005) Investigation into the interaction of the bacterial protease OmpT with outer membrane lipids and biological activity of OmpT:Lipopolysaccharide complexes. *Eur Biophys J* **34:** 28-41.

Bratu S., Landman D., George A., Salvani J., and Quale J. (2009) Correlation of the expression of *acrB* and the regulatory genes *marA, soxS* and *ramA* with antimicrobial resistance in clinical isolates of *Klebsiella pneumoniae* endemic to New York City. *J Antimicrob Chemother* **64:** 278-283.

Casadaban M.J. (1976) Transposition and fusion of the lac genes to selected promoters in *Escherichia coli* using bacteriophage lambda and mu. *J Mol Biol* **104:** 541-555.

Cascales E., Buchanan S.K., Duche D., Kleanthous C., Lloubes R., Postle K*., et al.* (2007) Colicin biology. *Microbiol Mol Biol Rev* **71:** 158-229.

Chang A.C., and Cohen S.N. (1978) Construction and characterization of amplifiable multicopy DNA cloning vehicles derived from the P15A cryptic miniplasmid. *J Bacteriol* **134:** 1141-1156.

Dastidar V., Mao W., Lomovskaya O., and Zgurskaya H.I. (2007) Drug-induced conformational changes in multidrug efflux transporter AcrB from *Haemophilus influenzae*. *Journal of Bacteriology* **189:** 5550-5558.

Datsenko K., and Wanner B. (2000) One-step inactivation of chromosomal genes in *Escherichia coli* K-12 using PCR products. *Proc Natl Acad Sci U S A* **97:** 6640-6645.

Deol, S. S., Bond, P. J., Domene, C., Sansom, M. (2004) Lipid-protein interactions of integral membrane proteins: a comparative simulation study. *Biophys. J.* **87:**3737-3749.

Duplay P., Bedouelle H., Fowler A., Zabin I., Saurin W., and Hofnung M. (1984) Sequences of the *malE* gene and of its product, the maltose-binding protein of *Escherichia coli* K12. *J Biol Chem* **259:** 10606-10613.

Elkins C.A., and Nikaido H. (2003) Chimeric analysis of AcrA function reveals the importance of its C-terminal domain in its interaction with the AcrB multidrug efflux pump. *J Bacteriol* **185:** 5349-5356.

Eswaran J., Hughes C., and Koronakis V. (2003) Locking TolC entrance helices to prevent protein translocation by the bacterial type I export apparatus. *J Mol Biol* **327:** 309-315.

Fabrega A., Roca I., and Vila J. (2010) Fluoroquinolone and multidrug resistance phenotypes associated with the overexpression of AcrAB and an orthologue of MarA in *Yersinia enterocolitica*. *Int J Med Microbiol* **300:** 457-463.

Federici, L., Walas, F., and Luisi, B. (2004) The structure and mechanism of the TolC outer membrane transport protein. *Curr. Sci.* **87:** 190-196.

Fernandez-Recio J., Walas F., Federici L., Venkatesh Pratap J., Bavro V.N., Miguel R.N.*, et al.* (2004) A model of a transmembrane drug-efflux pump from gram-negative bacteria. *FEBS Lett* **578:** 5-9.

Fischer N., and Kandt C. (2011) Three ways in, one way out: Water dynamics in the trans-membrane domains of the inner membrane translocase AcrB. *Proteins* **79:** 2871-2885.

Fralick J. (1996) Evidence that TolC is required for functioning of the Mar/AcrAB efflux pump of *Escherichia coli*. *J Bacteriol* **178:** 5803-5805.

Ge Q., Yamada Y., and Zgurskaya H. (2009) The C-terminal domain of AcrA is essential for the assembly and function of the multidrug efflux pump AcrAB-TolC. *J Bacteriol* **191:** 4365-4371.

German, G. J., **Misra, R.**, and Kropinski, A. (2006). The T1-like bacteriophages. *In The Bacteriophages. R. Calender (ed).* 211-224.

Gerken H., and Misra R. (2004) Genetic evidence for functional interactions between TolC and AcrA proteins of a major antibiotic efflux pump of *Escherichia coli*. *Mol Microbiol* **54:** 620-631.

Harwood J.L., and Russell N.J. (1984) Lipids in plants and microbes. London; Boston: G. Allen & Unwin.

Herrera C.M., Hankins J.V., and Trent M.S. (2010) Activation of PmrA inhibits LpxT-dependent phosphorylation of lipid A promoting resistance to antimicrobial peptides. *Mol Microbiol* **76:** 1444-1460.

Husain F., and Nikaido H. (2010) Substrate path in the AcrB multidrug efflux pump of *Escherichia coli*. *Mol Microbiol* **78:** 320-330.

Husain F. (2006) Characterization of AcrAB-TolC antibiotic efflux complex of *Escherichia coli*. .

Husain F., Humbard M., and Misra R. (2004) Interaction between the TolC and AcrA proteins of a multidrug efflux system of *Escherichia coli*. *J Bacteriol* **186:** 8533-8536.

Ip H., Stratton K., Zgurskaya H., and Liu J. (2003) pH-induced conformational changes of AcrA, the membrane fusion protein of *Escherichia coli* multidrug efflux system. *J Biol Chem* **278:** 50474-50482.

Jane A. Colmer, Joe A. Fralick, Abdul N. Hamood. (1998) Isolation and characterization of a putative multidrug resistance pump from *Vibrio cholerae*. *Molecular Microbiology* **27:** 63-72.

Kim H.M., Xu Y., Lee M., Piao S., Sim S.H., Ha N.C., and Lee K. (2010) Functional relationships between the AcrA hairpin tip region and the TolC aperture tip region for the formation of the bacterial tripartite efflux pump AcrAB-TolC. *J Bacteriol* **192:** 4498-4503.

Kim S., Yum S., Jo W.S., Lee B.L., Jeong M.H., and Ha N.C. (2008) Expression and biochemical characterization of the periplasmic domain of bacterial outer membrane porin TdeA. *J Microbiol Biotechnol* **18:** 845-851.

Knowles T.J., Browning D.F., Jeeves M., Maderbocus R., Rajesh S., Sridhar P.*, et al.* (2011) Structure and function of BamE within the outer membrane and the beta-barrel assembly machine. *EMBO Rep* **12:** 123-128.

Koronakis V. (2003) TolC--the bacterial exit duct for proteins and drugs. *FEBS Lett* **555:** 66-71.

Koronakis V., Eswaran J., and Hughes C. (2004) Structure and function of TolC: The bacterial exit duct for proteins and drugs. *Annu Rev Biochem* **73:** 467-489.

Koronakis V., Sharff A., Koronakis E., Luisi B., and Hughes C. (2000) Crystal structure of the bacterial membrane protein TolC central to multidrug efflux and protein export. *Nature* **405:** 914-919.

Krishnamoorthy G., Tikhonova E.B., and Zgurskaya H.I. (2008) Fitting periplasmic membrane fusion proteins to inner membrane transporters: Mutations that enable *Escherichia coli* AcrA to function with *Pseudomonas aeruginosa* MexB. *J Bacteriol* **190:** 691-698.

Lobedanz S., Bokma E., Symmons M.F., Koronakis E., Hughes C., and Koronakis V. (2007) A periplasmic coiled-coil interface underlying TolC recruitment and the assembly of bacterial drug efflux pumps. *Proc Natl Acad Sci U S A* **104:** 4612-4617.

Lugtenberg E.J.J., and Peters R. (1976) Distribution of lipids in cytoplasmic and outer membranes of *Escherichia coli* K12. *Biochimica Et Biophysica Acta (BBA) - Lipids and Lipid Metabolism* **441:** 38-47.

Masi M., Vuong P., Humbard M., Malone K., and Misra R. (2007) Initial steps of colicin E1 import across the outer membrane of *Escherichia coli*. *J Bacteriol* **189:** 2667-2676.

Mikolosko J., Bobyk K., Zgurskaya H.I., and Ghosh P. (2006) Conformational flexibility in the multidrug efflux system protein AcrA. *Structure* **14:** 577-587.

Misra R., and Bavro V.N. (2009) Assembly and transport mechanism of tripartite drug efflux systems. *Biochimica Et Biophysica Acta (BBA) - Proteins & Proteomics* **1794:** 817-825.

Morona and Reeves. 1981. Molecular cloning of the tolC locus of escherichia coli K-12 with the use of transposon Tn10. *Mol Gen Genet* **184:** 430-433.

Murakami S., Nakashima R., Yamashita E., Matsumoto T., and and Yamaguchi A. (2006) Crystal structures of a multidrug transporter reveal a functionally rotating mechanism. *Nature* **443:** 173-179.

Nehme D., and Poole K. (2007) Assembly of the MexAB-OprM multidrug pump of *Pseudomonas aeruginosa*: Component interactions defined by the study of pump mutant suppressors. *J Bacteriol* **189:** 6118-6127.

O'Keeffe, A. H., East, J. M., Lee, A. G. (2000) Seletivity in lipid binding to the bacterial outer membrane protein OmpF. *Biophys J* **79:** 2066-2074.

Pages J.M., and Amaral L. (2009) Mechanisms of drug efflux and strategies to combat them: Challenging the efflux pump of gram-negative bacteria. *Biochim Biophys Acta* **1794:** 826-833.

Pei X.Y., Hinchliffe P., Symmons M.F., Koronakis E., Benz R., Hughes C., and Koronakis V. (2011) Structures of sequential open states in a symmetrical opening transition of the TolC exit duct. *Proc Natl Acad Sci U S A* **108:** 2112-2117.

Raetz C.R. (1990) Biochemistry of endotoxins. *Annu Rev Biochem* **59:** 129-170.

Raetz C.R., and Whitfield C. (2002) Lipopolysaccharide endotoxins. *Annu Rev Biochem* **71:** 635-700.

Ramakrishnan M., Pocanschi C.L., Kleinschmidt J., and Marsh D. (2004) Association of spin-labeled lipids with β-barrel proteins from the outer membrane of *Escherichia coli*. *Biochemistry (N Y)* **43:** 11630-11636.

Sansom M.S., Bond P.J., Deol S.S., Grottesi A., Haider S., and Sands Z.A. (2005) Molecular simulations and lipid-protein interactions: Potassium channels and other membrane proteins. *Biochem Soc Trans* **33:** 916-920.

Seeger M.A., Schiefner A., Eicher T., Verrey F., Diederichs K., and Pos K.M. (2006) Structural asymmetry of AcrB trimer suggests a peristaltic pump mechanism. *Science* **313:** 1295-1298.

Seeger M.A., von Ballmoos C., Eicher T., Brandstatter L., Verrey F., Diederichs K., and Pos K.M. (2008) Engineered disulfide bonds support the functional rotation mechanism of multidrug efflux pump AcrB. *Nat Struct Mol Biol* **15:** 199-205.

Srikumar R., Kon T., Gotoh N., and Poole K. (1998) Expression of *Pseudomonas aeruginosa* multidrug efflux pumps MexA-MexB-OprM and MexC-MexD-OprJ in a multidrug-sensitive *Escherichia coli* strain. *Antimicrob Agents Chemother* **42:** 65-71.

Su C.C., Long F., Zimmermann M.T., Rajashankar K.R., Jernigan R.L., and Yu E.W. (2011) Crystal structure of the CusBA heavy-metal efflux complex of *Escherichia coli*. *Nature* **470:** 558-562.

Swick M.C., Morgan-Linnell S.K., Carlson K.M., and Zechiedrich L. (2011) Expression of multidrug efflux pump genes *acrAB-tolC*, *mdfA*, and *norE* in *Escherichia coli* clinical isolates as a function of fluoroquinolone and multidrug resistance. *Antimicrob Agents Chemother* **55:** 921-924.

Symmons M.F., Bokma E., Koronakis E., Hughes C., and Koronakis V. (2009) The assembled structure of a complete tripartite bacterial multidrug efflux pump. *Proc Natl Acad Sci U S A* **106:** 7173-7178.

Takatsuka Y., and Nikaido H. (2006) Threonine-978 in the transmembrane segment of the multidrug efflux pump AcrB of escherichia coli is crucial for drug transport as a probable component of the proton relay network. *J Bacteriol* **188:** 7284-7289.

Takatsuka Y., Chen C., and Nikaido H. (2010) Mechanism of recognition of compounds of diverse structures by the multidrug efflux pump AcrB of *Escherichia coli*. *Proc Natl Acad Sci U S A* **107:** 6559-6565.

Takeuchi Y., and Nikaido H. (1984) Physical interaction between lipid A and phospholipids: A study with spin-labeled phospholipids. *Rev Infect Dis* **6:** 488-492.

Tamura N., Murakami S., Oyama Y., Ishiguro M., and Yamaguchi A. (2005) Direct interaction of multidrug efflux transporter AcrB and outer membrane channel TolC detected via site-directed disulfide cross-linking. *Biochemistry (N Y)* **44:** 11115-11121.

Thanassi, D. G., Cheng, L. W., Nikaido, H. (1997) Active efflux of bile salts by *Escherichia coli*. *J Bacteriol* **179:** 2512-2518.

Tikhonova E.B., Yamada Y., and Zgurskaya H.I. (2011) Sequential mechanism of assembly of multidrug efflux pump AcrAB-TolC. *Chem Biol* **18:** 454-463.

Tikhonova E.B., Dastidar V., Rybenkov V.V., and Zgurskaya H.I. (2009) Kinetic control of TolC recruitment by multidrug efflux complexes. *Proc Natl Acad Sci U S A* **106:** 16416-16421.

Tikhonova E.B., and Zgurskaya H.I. (2004) AcrA, AcrB, and TolC of *Escherichia coli* form a stable intermembrane multidrug efflux complex. *J Biol Chem* **279:** 32116-32124.

Touzé T., Eswaran J., Bokma E., Koronakis E., Hughes C., and Koronakis V. (2004) Interactions underlying assembly of the *Escherichia coli* AcrAB–TolC multidrug efflux system. *Mol Microbiol* **53:** 697-706.

Trepout S., Taveau J.C., Benabdelhak H., Granier T., Ducruix A., Frangakis A.S., and Lambert O. (2010) Structure of reconstituted bacterial membrane efflux pump by cryo-electron tomography. *Biochim Biophys Acta* **1798:** 1953-1960.

Vaccaro L., Scott K.A., and Sansom M.S.P. (2008) Gating at both ends and breathing in the middle: Conformational dynamics of TolC. *Biophys J* **95:** 5681-5691.

Vaccaro L., Koronakis V., and Sansom M.S.P. (2006) Flexibility in a drug transport accessory protein: Molecular dynamics simulations of MexA. *Biophys J* **91:** 558-564.

Vakharia H., German G.J., and Misra R. (2001) Isolation and characterization of *Escherichia coli tolC* mutants defective in secreting enzymatically active alpha-hemolysin. *J Bacteriol* **183:** 6908-6916.

Vediyappan G., Borisova T., and Fralick J.A. (2006) Isolation and characterization of VceC gain-of-function mutants that can function with the AcrAB multiple-drug-resistant efflux pump of *Escherichia coli*. *J Bacteriol* **188:** 3757-3762.

Vuong P., Bennion D., Mantei J., Frost D., and Misra R. (2008) Analysis of YfgL and YaeT interactions through bioinformatics, mutagenesis, and biochemistry. *J Bacteriol* **190:** 1507-1517.

Weeks J.W., Celaya-Kolb T., Pecora S., and Misra R. (2010) AcrA suppressor alterations reverse the drug hypersensitivity phenotype of a TolC mutant by inducing TolC aperture opening. *Mol Microbiol* **75:** 1468-1483.

Welch A., Awah C.U., Jing S., van Veen H.W., and Venter H. (2010) Promiscuous partnering and independent activity of MexB, the multidrug transporter protein from *Pseudomonas aeruginosa*. *Biochem J* **430:** 355-364.

Welch R.A., Dellinger E.P., Minshew B., and Falkow S. (1981) Haemolysin contributes to virulence of extra-intestinal *E. coli* infections. *Nature* **294:** 665-667

Xu Y., Sim S.H., Song S., Piao S., Kim H.M., Jin X.L.*, et al.* (2010) The tip region of the MacA alpha-hairpin is important for the binding to TolC to the *Escherichia coli* MacAB-TolC pump. *Biochem Biophys Res Commun* **394:** 962-965.

Xu Y., Sim S., Nam K.H., Jin X.L., Kim H., Hwang K.Y.*, et al.* (2009) Crystal structure of the periplasmic region of MacB, a noncanonic ABC transporter, *Biochemistry (N Y)* **48:** 5218-5225.

Xu Y., Lee M., Moeller A., Song S., Yoon B., Kim H.*, et al.* (2011) Funnel-like hexameric assembly of the periplasmic adapter protein in the tripartite multidrug efflux pump in gram-negative bacteria. *Journal of Biological Chemistry* **286:** 17910-17920.

Yu, E. W., McDermott, G., Zgurskaya, H. I., Nikaido, H., Koshland, D. E., Jr. (2003) Structural basis of multiple drug-binding capacity of the AcrB multidrug efflux pump. *Science* **300:** 976-980.

Yum, S., Xu, Y., Piao, S., Sim, S. H., Kim, H. M., Jo, W. S., Kim, K. J., Kweon, H. S., Jeong, M. H., Jeon, H., Lee, K., Ha, N. C. (2009) Crystal structure of the periplasmic component of a tripartite macrolide-specific efflux pump. *J Mol Biol* **387:** 1286-1297.

Zgurskaya H.I., Yamada Y., Tikhonova E.B., Ge Q., and Krishnamoorthy G. (2009) Structural and functional diversity of bacterial membrane fusion proteins. *Biochimica Et Biophysica Acta (BBA) - Proteins & Proteomics* **1794:** 794-807.